

10

**Quantification of Receptor - Ligand Interactions on Bioengineered Autocrine Cell System - A Comparison of Theory and Experiments**

by

Gregory Todd Oehrtman

B.S., Chemical Engineering  
University of Texas at Austin, 1991

M.S., Chemical Engineering  
University of Illinois - Champaign, Urbana, 1995

Submitted to the Department of Chemical Engineering  
in Partial Fulfillment of the Requirements for the Degree of

Doctor of Philosophy in Chemical Engineering

at the

Massachusetts Institute of Technology

September 1997

© 1997 Massachusetts Institute of Technology  
All rights reserved

Signature of Author .....  
..... Department of Chemical Engineering  
..... July 31, 1997

Certified by.....  
..... Douglas A. Lauffenburger  
..... J. R. Mares Professor of Chemical Engineering  
..... Thesis Supervisor

Accepted by .....  
..... Robert E. Cohen  
..... St. Laurent Professor of Chemical Engineering  
..... Chairman, Committee for Graduate Students

APR 13 1998

LIBRAIRIE

# Quantification of Receptor - Ligand Interactions on Bioengineered Autocrine Cell System - A Comparison of Theory and Experiments

by

Gregory Todd Oehrtman

Submitted to the Department of Chemical Engineering on August 28, 1997  
in Partial Fulfillment of the Requirements for the Degree of  
Doctor of Philosophy in Chemical Engineering

## ABSTRACT

A model autocrine cell system was constructed by transfecting the genes for transforming growth factor alpha (TGF $\alpha$ ) and its receptor (epidermal growth factor receptor, EGFR) into a cell line normally lacking both, mouse B82 fibroblasts. The human TGF $\alpha$  gene was transfected into both EGFR-positive and EGFR-negative B82s cells using a two-plasmid tetracycline inducible vector, permitting both autocrine and paracrine cell systems. The full-length TGF $\alpha$  transmembrane protein was correctly transported to the cell surface and 99% of the TGF $\alpha$  cleaved and secreted into the extracellular media as the mature 5.5 kDa TGF $\alpha$  protein. A 100-fold range in TGF $\alpha$  secretion expression is achieved by altering medium's tetracycline concentrations.

Validation of anchorage-dependent autocrine cell computer modelling was achieved experimentally for both extracellular bulk ligand concentrations and receptor / ligand complex levels. High ligand expression rates enabled extracellular ligand accumulations, measured by TGF $\alpha$  ELISAs, to remain independent of cell density and addition of anti-receptor blocking antibodies. At lower secretion rates, both cell density and blocking antibody additions were important parameters in receptor-mediated ligand uptake.

The autocrine model was also validated by development of a novel assay to quantify receptor ligand complexes. Molecular Devices Cytosensor measurements of cellular metabolic rates were correlated to receptor complexes via free EGF in  $I^{125}$  EGF binding experiments and Cytosensor experiments. Using the Cytosensor enabled precise measurements of TGF $\alpha$  induction in autocrine cells, complex levels as a function of TGF $\alpha$  secretion rates and inhibition of receptor complexes as a function of competing antibodies. It was determined experimentally and mathematically that blocking antibody inhibited autocrine receptor complex formation around 1 nM and was a 1000x more effective inhibitor than decoy antibodies. An indication of intracellular receptor / ligand binding was found in B82R<sup>+</sup> / secreted mature EGF as addition of blocking antibodies could not inhibit receptor complex signalling compared to autocrine B82R<sup>+</sup> / transmembrane TGF $\alpha$ .

Further investigations using these engineered cell systems should help yield an improved understanding in regulation of wound healing, tissue regeneration, and cancer progression facilitated by autocrine factors.

Thesis Supervisor: Douglas A. Lauffenburger  
Title: J. R. Mares Professor of Chemical Engineering

## Acknowledgments

This research was funded by NSF Biotechnology Program, Engineering Directorate, Division of Biological and Critical Systems.

I would like to thank my advisor, Doug Lauffenburger, for his advice, support, and insight during the course of this work. Also, I would like to thank him for the opportunity to travel to various research labs for the advancement of this research and my expertises.

I would like to thank the Lauffenburger lab for their support and suggestions throughout this research. A special thanks goes to Lily Chu and Cartikeya Reddy as my "links to the engineering world" for keeping me up-to-date, giving advice, sending forms and supplies, dealing with administrative problems, and being "surrogate Greg" to Laura while I was in Utah. I can not thank you both enough.

I would also like to thank Steve Wiley, Lee Opresko, Patrick Burke, Becky Worthylake, Birgit Will-Simmons, and Maggie Woolf along with the rest of the University of Utah Pathology Department. The Wiley lab's support, advice, and help have been immeasurable towards completing this thesis. Allowing me to use their lab space, materials, and time has been greatly appreciated. Little did Steve realize when accepting me into his lab for "a half of a semester," it would become 30 months over several years. Thank you very much.

Also, I would like to thank Laura Walker, undergraduate at MIT, working with me on my thesis. Her time, effort, and organization was immeasurably in completion of this thesis in the development of the Cytosensor assays. Her dedication to the project while I was away in Utah greatly enhanced the scope of this research.

Last, but not least, I would like to thank my parents for a lifetime of love, encouragement, and support, for without, I would have never succeeded.

## Table of Contents

Chapter 1:	Introduction and Background.....	11
1.1	Growth Factors and Cell Function.....	11
1.2	Transforming Growth Factor Alpha (TGF $\alpha$ ).....	13
1.3	Epidermal Growth Factor Receptor.....	15
1.4	Control of Autocrine Systems.....	17
1.5	Mathematical Modelling of Autocrine Systems.....	18
1.6	Expression System for Autocrine Ligand.....	20
1.7	Cell Microphysiometer Assay for Autocrine Ligand Binding.....	22
1.8	Thesis Overview.....	24
	Figures.....	26
Chapter 2:	Modelling Autocrine Cell Receptor / Ligand / Antibody Interactions.....	48
2.1	Revising Anchorage-Independent to -Dependent Model.....	48
2.2	Computer Modelling Predictions.....	49
	Tables.....	52
	Figures.....	55
Chapter 3:	Experimental Methods - Ligand Characterization.....	59
3.1	Materials.....	59
3.2	Making pUHD10.3 / TGF $\alpha$ .....	60
3.3	Transfection of DNA into B82 Cells.....	61
3.4	Selection of TGF $\alpha$ Secreting Clones.....	61
3.5	Detection of TGF $\alpha$ .....	62
3.6	Determining Cellular Processing of TGF $\alpha$ Protein.....	63
3.7	TGF $\alpha$ Secretion Time Course from Paracrine Clones.....	64
3.8	Tetracycline Concentration Effect on TGF $\alpha$ Secretion.....	65
3.9	Cell Density Effect on TGF $\alpha$ Secretion.....	66
3.10	Creation of sEGF Clones.....	66
	Tables.....	68
	Figures.....	70

Chapter 4:	Results - Ligand Characterization .....	76
4.1	Overview of Experiments .....	76
4.2	Making pUHD10.3 / TGF $\alpha$ .....	76
4.3	Selection of TGF $\alpha$ Secreting Clones .....	77
4.4	Determining Cellular Processing of TGF $\alpha$ Protein .....	78
4.5	TGF $\alpha$ Secretion Time Course from Paracrine Cells .....	78
4.6	Tetracycline Concentration Effects on TGF $\alpha$ Secretion .....	79
4.7	Cell Density Effects on TGF $\alpha$ Secretion .....	80
4.8	Creation of B82R <sup>+</sup> normal and mutated / sEGF autocrine clones.....	81
	Tables .....	82
	Figures.....	86
Chapter 5:	Methods for Ligand - Receptor Complex Characterization.....	93
5.1	General Protocol for Testing Cells on the Cytosensor.....	93
5.2	B82R <sup>+</sup> ECAR Response as a Function of mAb225 and mEGF .....	94
5.3	Correlating Cytosensor's ECAR to Receptor / Ligand Complex Levels.....	95
5.3a.	I <sup>125</sup> Binding - Receptor / Ligand Complexes.....	95
5.3b.	Cytosensor ECAR Output.....	95
5.3c.	Equating ECAR to Receptor / Ligand Complexes.....	96
5.4	Measuring B82R <sup>+</sup> / TGF $\alpha$ Induction .....	96
5.5	Tetracycline Gradient on Autocrine B82R <sup>+</sup> / TGF $\alpha$ Cells.....	97
5.6	Antibody Inhibition of Receptor / Ligand Complex on B82R <sup>+</sup> / TGF $\alpha$ .....	97
5.7	Blocking Antibody Inhibition of Receptor Complexes on B82R <sup>+</sup> / sEGF.....	98
Chapter 6:	Results - Ligand / Receptor Complex Characterization .....	99
6.1	Overview of Experiments .....	99
6.2	General Cytosensor Runs .....	99
6.3	B82R <sup>+</sup> ECAR Response as a Function of mAb225 and mEGF .....	100
6.4	Correlating Cytosensor's ECAR to Receptor / Ligand Complex Levels.....	101
6.4a.	I <sup>125</sup> Binding - Receptor / Ligand Complexes.....	102
6.4b.	Cytosensor ECAR Output.....	102
6.4c.	Equating ECAR to Receptor / Ligand Complexes.....	104
6.5	Measuring B82R <sup>+</sup> / TGF $\alpha$ Induction .....	104
6.6	Tetracycline Gradient on Autocrine B82R <sup>+</sup> / TGF $\alpha$ Cells.....	106

6.7	Antibody Inhibition of Receptor / Ligand Complex on B82R <sup>+</sup> / TGF $\alpha$ .....	107
6.8	Blocking Antibody Inhibition of Receptor Complexes on B82R <sup>+</sup> / sEGF.....	109
	Figures.....	111
Chapter 7:	Discussion and Future Study .....	134
7.1	Overview .....	134
7.2	Summary of Results .....	134
7.3	Discussion.....	137
7.4	Future Study .....	138
Appendix A	.....	141
Appendix B	.....	144
Appendix C	.....	146
Appendix D	.....	157
References	.....	170

## List of Tables

Chapter 2:	Modelling Autocrine Cell Receptor / Ligand / Antibody Interactions	
Table 2.1	Autocrine model equations - Blocker Antibody .....	52
Table 2.2	Autocrine model equations - Decoy Antibody .....	53
Table 2.3	Autocrine model nomenclature and parameters values.....	54
Chapter 3:	Experimental Methods - Ligand Characterization	
Table 3.1	Molecular weight standards used for G-50 fine column.....	68
Table 3.2	Time course points for TGF $\alpha$ secretion from paracrine B82 cells ...	69
Chapter 4:	Results - Ligand Experiments	
Table 4.1	Comparison of autocrine TGF $\alpha$ / EGFR cells.....	82
Table 4.2	Detection of secreted and membrane bound TGF $\alpha$ .....	83
Table 4.3	Mutant B82 EGFR trafficking and affinity parameters .....	84
Table 4.4	Artificially engineered cell systems .....	85

## List of Figures

Chapter 1:	Introduction and Background	
Figure 1.1	Ligand secretion pathways.....	26
Figure 1.2	TGF $\alpha$ precursor .....	27
Figure 1.3	Amino acid relationship between members of the EGF family....	28
Figure 1.4	Schematic representation of hTGF $\alpha$ structure.....	29
Figure 1.5	Epidermal growth factor ligands and receptors family .....	30
Figure 1.6	EGF receptor domains .....	31
Figure 1.7	Receptor tyrosine kinases.....	32
Figure 1.8	Inhibition of phosphorylation by anti-receptor monoclonal antibodies .....	33
Figure 1.9	Relationship between EGF receptor occupancy and mitogenic response.....	34
Figure 1.10	Experimental data on ligand decoy's and receptor blocker's affect on autocrine cell stimulation.....	35
Figure 1.11	Autocrine cell model schematic - decoy antibody .....	36
Figure 1.12	Autocrine cell model schematic - blocker antibody .....	37
Figure 1.13	Decoy receptor effects on cell receptor complex levels.....	38
Figure 1.14	Receptor antibody effects on cell receptor complex levels .....	39
Figure 1.15	pUHD15.1.....	40
Figure 1.16	pUHD10.3.....	41
Figure 1.17	Two plasmid schematic .....	42
Figure 1.18	Schematic of ligand - receptor signalling detection by Molecular Devices Cytosensor .....	43
Figure 1.19	Schematic drawing of Cytosensor .....	44
Figure 1.20	Representation of Cytosensor measurement and output.....	45
Figure 1.21	Predicted metabolic response of paracrine and autocrine cells....	46
Figure 1.22	Artificially engineered B82 TGF $\alpha$ family.....	47
Chapter 2:	Modelling Autocrine Cell Receptor / Ligand / Antibody Interactions	
Figure 2.1	Autocrine computer models with blocker antibodies .....	55
Figure 2.2	Modelling predictions - Varying ligand secretion rates.....	56
Figure 2.3	Modelling predictions - Blocker versus Decoy antibodies .....	57
Figure 2.4	Modelling predictions - Bulk ligand concentrations .....	58



Chapter 3:	Experimental Methods - Ligand Characterization	
Figure 3.1	pMTE4 .....	70
Figure 3.2	pXER.....	71
Figure 3.3	Bluescript II KS+ Plasmid.....	72
Figure 3.4	pREP8.....	73
Figure 3.5	pBS/TGF $\alpha$ wt.....	74
Figure 3.6	pUHD10.3 / TGF $\alpha$ .....	75
Chapter 4:	Results - Ligand Characterization	
Figure 4.1	pUHD10.3 / TGF $\alpha$ Digest .....	86
Figure 4.2	EGFR / TGF $\alpha$ expression at similar cell density .....	87
Figure 4.3	TGF $\alpha$ molecular weight .....	88
Figure 4.4	TGF $\alpha$ time course .....	89
Figure 4.5	Effect of tetracycline concentration on TGF $\alpha$ secretion.....	90
Figure 4.6	Tetracycline gradient on autocrine clone #1.....	91
Figure 4.7	Experimental bulk ligand concentrations.....	92
Chapter 6:	Results -Ligand / Receptor Complex Characterization	
Figure 6.1	Experimental raw and rate data.....	111
Figure 6.2	B82R <sup>+</sup> control cells - Cytosensor EGF response curve .....	112
Figure 6.3	Cytosensor measurements - B82R <sup>+</sup> with EGF and mAb225 .....	113
Figure 6.4	Overview ECAR to Complex - B82R <sup>+</sup> / 1st plasmid .....	114
Figure 6.5	Overview ECAR to Complex - uninduced B82R <sup>+</sup> / TGF $\alpha$ .....	115
Figure 6.6	Overview ECAR to Complex - induced B82R <sup>+</sup> / TGF $\alpha$ .....	116
Figure 6.7	I <sup>125</sup> Binding - B82R <sup>+</sup> / 1st plasmid.....	117
Figure 6.8	I <sup>125</sup> Binding - uninduced B82R <sup>+</sup> / TGF $\alpha$ .....	118
Figure 6.9	I <sup>125</sup> Binding - induced B82R <sup>+</sup> / TGF $\alpha$ .....	119
Figure 6.10	Cytosensor - B82R <sup>+</sup> / 1st plasmid .....	120
Figure 6.11	Cytosensor - uninduced B82R <sup>+</sup> / TGF $\alpha$ .....	121
Figure 6.12	Cytosensor - induced B82R <sup>+</sup> / TGF $\alpha$ .....	122
Figure 6.13	ECAR to Complex Correlation - B82R <sup>+</sup> / 1st plasmid.....	123
Figure 6.14	ECAR to Complex Correlation - uninduced B82R <sup>+</sup> / TGF $\alpha$ .....	124
Figure 6.15	ECAR to Complex Correlation - induced B82R <sup>+</sup> / TGF $\alpha$ .....	125
Figure 6.16	Induction of B82R <sup>+</sup> / TGF $\alpha$ cells on Cytosensor.....	126
Figure 6.17	B82R <sup>+</sup> / TGF $\alpha$ induction measured on the Cytosensor .....	127

Figure 6.18	Tetracycline gradient affects on B82R <sup>+</sup> / TGF $\alpha$ cell ECAR .....	128
Figure 6.19	Representative Cytosensor run - induced B82R <sup>+</sup> / TGF $\alpha$ with blocking antibodies .....	129
Figure 6.20	Compilation of B82R <sup>+</sup> / TGF $\alpha$ competing antibody additions ....	130
Figure 6.21	Control experiment - mAb225 and cell stimulation .....	131
Figure 6.22	Control experiment - TGF $\alpha$ neutralization with anti-TGF $\alpha$ antibody .....	132
Figure 6.23	Comparison of autocrine cell systems - TGF $\alpha$ vs. sEGF .....	133

## Chapter 1: Introduction and Background

Cell functions such as proliferation and migration are important in physiological and pathological situations, including wound healing, cancer, and tissue regeneration. Cellular interactions in these processes are often regulated by growth factor receptors and their ligands (Bennett and Schultz 1993; ten Dijke and Iwata 1989; Kumar *et al.* 1992). When the receptor and its ligand are produced by the same cell, it is called an autocrine cell. This situation is found in many different cell lines, such as lymphocytes, fibroblasts, and primary tumors. (Derynck 1992; Morishige *et al.* 1991; Sporn and Roberts 1992; Sporn and Todaro 1980). Mathematical analysis of the autocrine network have identified key molecular and cellular parameters governing the dynamics of receptor / ligand complexes as well as cell signaling. Important parameters include autocrine ligand secretion rate, cellular density, receptor binding and receptor trafficking rate constants (Forsten and Lauffenburger 1992a). These parameters can be systematically altered with cells accessible to the manipulation of the receptor and ligand genes. The research in this thesis deals with the development and characterization of this sort of model autocrine system, for the purposes of testing the importance of key parameters and elucidating control mechanisms governing cell responses to autocrine factors.

### 1.1 Growth Factors and Cell Functions

Metabolic processes in the cell can be maintained through the uptake of amino acids, essential vitamins, nutrients and salts in serum free media, however, only upon the addition of growth factors will quiescent cells begin cell division or mitosis (Bennett and Schultz 1993). Growth factors are produced and secreted from a variety of cells including platelets, keratinocytes and fibroblasts. Although a multitude of cells express growth factors (ligands), the growth factors interact with their high affinity receptors via only four pathways (Figure 1.1). The endocrine and paracrine pathways involve the production and transport of the secreted ligand to either distant or adjacent cells, respectively. The juxtacrine pathway is similar to a paracrine system, but the ligand binds adjacent cells while remaining membrane-bound. In the last pathway, the autocrine system, the ligand is secreted and bound by the same cell. Note that if a subset of the autocrine cells' receptors become internalized (down-regulated) or are inhibited from binding the ligand, autocrine cells become paracrine cells.

Upon growth factor / receptor binding, a cascade of events occur leading to the uptake of  $Ca^{2+}$ , phosphorylation of proteins, and eventually, the synthesis of DNA and cell proliferation (Carraway and Cerione 1993; Gill *et al.* 1987; Kumar *et al.* 1992). Overproduction of the receptor and / or its ligand in an autocrine pathway could lead to over-

stimulation of the cell and runaway cell proliferation. One growth factor, transforming growth factor alpha (TGF $\alpha$ ) and its receptor, epidermal growth factor receptor (EGFR) has been found over-expressed in several cancers. Over half of the mammary carcinomas and most squamous, hepatomas, melanomas, glioblastomas and renal carcinomas express this enhanced synthesis autocrine pathway (Derynck 1992).

Because growth factors are important in cell proliferation and migration, clinical strategies that modulate growth factor activities have been receiving attention as methods for promoting wound healing and inhibiting cancer. Treatment of chronic wounds increase health care costs because it requires extended hospital stays and half of the amputations in the United States are a result of ulceration (Meyer-Ingold 1993; Roberts 1993). Thus, the use of growth factors to promote cell proliferation and migration could speed healing, decrease patient's discomfort, shorten hospital stays and reduce amputations. These growth factors could be added exogenously or via gene therapy. One particular study used transfected insulin-like factor-I (IGF-I) keratinocytes, promoting increased epithelium growth *in vivo* (Eming *et al.* 1996). While secretion of IGF-I in epithelia is normally paracrine (fibroblast to keratinocytes), this study created an autocrine growth system to show IGF-I role in epidermal proliferation. Other autocrine studies utilizing TGF $\alpha$  and TGF $\beta$  have been performed in transgenic mice (Sellheyer *et al.* 1993; Vassar and Fuchs 1991), showing these cytokines are also important autocrine mediators of epidermal homeostasis.

At the opposite end are attempts to inhibit cancer cell proliferation. As mentioned, some cancer cell lines over-express growth factors and / or growth factor receptors. High levels of human epidermal growth factor receptor or HER1, has been found in a significant fraction of epidermoid head and neck carcinomas, breast cancer, and epidermal carcinomas (Fabricant *et al.* 1977; Filmus *et al.* 1985; Hendler *et al.* 1985). Some of these carcinomas, A431 and MDA MB-468, also have been shown to produce TGF $\alpha$ , classifying them as autocrine (Derynck *et al.* 1987; Ennis *et al.* 1989). Over-expression of a related receptor, *Neu* / HER2, is associated with poor prognosis in breast cancer, ovarian cancer, and lung carcinoma (Kern *et al.* 1990; Kraus *et al.* 1987; Slamon *et al.* 1987; Slamon *et al.* 1989; Varley *et al.* 1987; van der Vijver *et al.* 1987). When a growth factor and its receptor are produced by the same cell, at abnormally high levels, there is the potential for loss of regulation. While, several clinical trials have attempted to affect wound healing and tumor progression by modulating growth factor activities, their results have been unclear (Meyer-Ingold 1993; Mulshine *et al.* 1992). In most of these studies, the protein (ligand or antibody) was used without an understanding of half-lives, secretion rates, ligand / receptor dynamics, and effective concentrations at the target site. Experimental studies in this

thesis as well as computer modelling should help increase our understanding of autocrine cell systems and aid in the design of related clinical treatments.

## 1.2 Transforming Growth Factor Alpha (TGF $\alpha$ )

Epidermal growth factor (EGF) was first discovered by Stanley Cohen (Cohen 1962) when studying a nerve growth promoting protein of the mouse submaxillary gland. This protein promoted precocious eyelid opening and teeth eruption of newborn mice. Later isolation and characterization of the protein established that EGF is synthesized as a large precursor of 1207 amino acids (160 kD), containing eight EGF-like repeats and one full length EGF sequence which is cleaved into the secreted 53 amino acid (6 kD) protein (Bell *et al.* 1986; Scott *et al.* 1983). EGF has been shown to be an effective inhibitor of gastric acid and pepsin secretions with high levels of protein detected in the urine, mammary fluids, saliva, and prostatic fluids (Carpenter and Wahl 1990).

EGF's sister protein was discovered when analyzing polypeptides from mouse sarcoma virus-transformed cell medium which induced anchorage independent growth of normal rat kidney (NRK) cells on soft agar, a characteristic of transformed cells (DeLarco and Todaro 1978; Todaro *et al.* 1980). Upon further purification of the medium, two proteins were isolated, transforming growth factor alpha (TGF $\alpha$ ) and beta (TGF $\beta$ ). TGF $\alpha$  is able to bind epidermal growth factor's receptor (EGFR), but can only transform NRK cells in the presence of TGF $\beta$ , which cannot bind EGFR (Anzano *et al.* 1982). Thus, it is the synergistic effect of these two proteins that leads to the reversible transformation of the NRK cells. Since its discovery, TGF $\alpha$  has been found in many cancer cells, but also in several "normal" cells like epithelial and gastric intestinal mucosa cells (Beauchamp *et al.* 1989; Valverius *et al.* 1989), macrophages (Madtes *et al.* 1988; Rappolee *et al.* 1988a), in the brain (Wilcox and Derynck 1988b), and in the pituitary (Kobrin *et al.* 1988).

TGF $\alpha$  is a 50 amino acid protein (5.6 kDa) derived from a 160 amino acid glycosidic transmembrane precursor (25 kDa) (Carpenter and Wahl 1990; Feild *et al.* 1992). Shown in Figure 1.2, the transmembrane precursor consists of a 39 amino acid N-terminal signal sequence with an Asn<sub>24</sub> N-glycosylation site, the mature TGF $\alpha$  protein and a 71 amino acid carboxyl terminal transmembrane tail. The TGF $\alpha$  protein is a member of the epidermal growth factor (EGF) family (Figure 1.3) which besides EGF (Cohen 1962), includes heparin - binding EGF (Higashiyama *et al.* 1992), amphiregulin (Shoyab *et al.* 1989), betacellulin (Shing *et al.* 1993), and heregulin (Holmes *et al.* 1992; Wen *et al.* 1992). The EGF family is characterized by the CX<sub>7</sub>CX<sub>4,5</sub>CX<sub>10-13</sub>CXCX<sub>8</sub>C motif where X is any non-cysteine amino acid. (Carpenter and Wahl 1990). TGF $\alpha$  shares about 40% homology with EGF, but within its own TGF $\alpha$

family, there is up to 90% amino acid homology between human and rat TGF $\alpha$  (Carpenter and Wahl 1990). Nuclear magnetic resonance studies along with homology and site-directed mutagenesis studies suggest that the TGF $\alpha$  structure is similar to EGF.

A schematic representation of TGF $\alpha$  is shown in Figure 1.4. The mature TGF $\alpha$  protein is composed of several anti-parallel  $\beta$  sheets and a tight turn in the middle of the protein. These  $\beta$  sheets and tight turn align the two terminals to opposite sites of the protein and has been suggested to construe the binding domain for the EGF family (Campbell *et al.* 1990; Hoeplich *et al.* 1989). However, chimeric TGF $\alpha$ /EGF studies with chicken EGF receptor (cEGFR) indicate that the B-loop  $\beta$ -sheet is not only a structural motif, but may be a binding site for the TGF $\alpha$ -cEGFR complex (Richter *et al.* 1995). Analysis of site-directed mutagenesis on TGF $\alpha$  and EGF proteins show that the six cysteines along with Gly19, Val33, Tyr38, and Gly40 are highly conserved structural amino acids while Phe15, Phe17, Arg42 and Leu48 appear to be important EGF receptor binding sites (Feild *et al.* 1992). Site directed mutagenesis with these amino acids result in a decrease of ligand-receptor affinity, ranging over three orders of magnitude.

The ligand-receptor affinity is a function of the binding and dissociation rate constants for ligand binding to its receptor, commonly referred to as  $K_d$  (equilibrium dissociation constant). Human EGF's and TGF $\alpha$ 's affinity for the human EGF receptor is 1 nM (Ebner and Derynck 1991). While, both TGF $\alpha$  and EGF have similar affinities for human EGFR, TGF $\alpha$  is a 100x fold better agonist for chicken EGFR than EGF ligand (Lax *et al.* 1988a). This preference for TGF $\alpha$  is likely due to a bulky hydrophobic amino acid between the fourth and fifth cysteines (valine 33) at the "hinge" site, compared to EGF's hydrogen bond donor (asparagine 33). Betacellulin and heparin-binding EGF also have hydrophobic residues (isoleucine 33) with comparable affinity for chicken EGFR as TGF $\alpha$ , while amphiregulin and heregulin are more similar to EGF (lysine 33). This suggests a sub-grouping of EGF family proteins into TGF $\alpha$  and EGF-like sub-classifications (Puddicombe *et al.* 1996).

A major difference between TGF $\alpha$  and EGF is the presence of five histidine amino acids in TGF $\alpha$  and two histidines in EGF making the isoelectric points (pI) 4.6 for EGF versus 5.9 for TGF $\alpha$ . The isoelectric point difference may explain ligand-receptor trafficking dynamic changes resulting in reduced receptor degradation and constant ligand recycling rate in the presence of TGF $\alpha$ , especially at lower intercellular complex levels. (Ebner and Derynck 1991; French *et al.* 1995). This difference may also explain why TGF $\alpha$  is a more potent agonist for migration and monolayer formation in keratinocytes (Barrandon and Green 1987), increased arterial blood flow (Gan *et al.* 1987), bone resorption (Stern *et al.* 1985), and hepatocyte growth (Brenner *et al.* 1989).

### 1.3 Epidermal Growth Factor Receptor

Members of EGF-like ligand family discussed earlier all bind to receptors in the EGF family. These receptors are labeled HER1 (Cohen and Ushiro 1980; Cohen *et al.* 1982), HER2 (King *et al.* 1985), HER3 (Kraus *et al.* 1989), and HER4 (Plowman *et al.* 1993a) for Human Epidermal growth factor Receptor. As seen in Figure 1.5, all the ligands except heregulin bind to HER1 while heregulin binds to HER3 and 4. Over-expression of HER2 is a poor prognosis of cancer, leading to an intensive search for its ligand. During this search, heregulin was discovered and originally thought to be HER2's ligand as ligand addition causes HER2 phosphorylation (Holmes *et al.* 1992; Wen *et al.* 1992). Later, it was determined that heregulin initiated heterodimerization between HER3 or 4 with HER2, resulting in HER2 phosphorylation and activation (Carraway and Cantley 1994; Carraway *et al.* 1995; Plowman *et al.* 1993b).

While HER2, 3, and 4 are structurally homologous to HER1, there are subtle differences between the receptors: i.e. to date, no ligand has been found for HER2; HER3 and 4 have closer extracellular homology (~65%) to each other than to the other receptors (~43%); HER3 does not have intrinsic kinase activity, but binds several different SH2 proteins which do not interact with the other three receptors (Carraway and Cantley 1994); and all receptors except HER1 are endocytosis impaired (Baulida *et al.* 1996). Also, heregulin-induced mitogenesis will occur in NIH 3T3 cells transfected with HER3 or HER4. However, heregulin-induced cell transformation was achieved only upon co-transfection of HER1 or HER2 with HER3 or HER4. This transformation correlated with receptor transphosphorylation (Zhang *et al.* 1996).

The EGF receptor, HER1, is a 170 kDa transmembrane glycoprotein with intrinsic protein tyrosine kinase activity (Carpenter and Wahl 1990). The receptor, shown in Figure 1.6, is composed of four domains: the extracellular, transmembrane, juxtamembrane and cytoplasmic domains. The extracellular domain consists of 621 amino acids and has two dominant structural features: 51 cysteine residues (compared with only nine cysteines in the cytoplasmic domain) and twelve potential N-linked glycosylation sites. The cysteines are predominantly located in two regions (134-313, 446-612) (Ullrich *et al.* 1984) which appear to cooperate in forming a single high-affinity EGF binding site (Gill *et al.* 1987). The transmembrane region of the receptor spans residues 622-644 and may function in transmitting the ligand binding signal to the cytoplasmic domain (Gill *et al.* 1987). Controversy exists as to whether the signal is transmitted intramolecular through the transmembrane or intermolecular with EGFR dimerization (Yarden and Schlessinger 1987). However, several studies have shown that EGF / EGFR protein signaling can occur in the absence of EGFR dimerization (Carraway and Cerione 1993). The juxtamembrane region directly following the

transmembrane region contains thirteen highly basic amino acids and has an important regulatory site, threonine 654, which upon phosphorylation decreases the receptor's affinity for its ligand (Davis 1988; Lund *et al.* 1990).

The 539 amino acid cytoplasmic domain contains the catalytic domain and several regulatory domains. The tyrosine kinase domain from residues 663 to 957 is similar to several other receptor tyrosine kinases, Figure 1.7 (Czech *et al.* 1990; Pawson and Schlessinger 1993). An important amino acid in this domain is Lysine 721 which is required for ATP binding. Mutations of this amino acid results in failure to mediate phosphatidyl inositol turnover,  $\text{Ca}^{2+}$  intake,  $\text{Na}^+/\text{H}^+$  exchange, DNA synthesis, EGF-stimulated tyrosine kinase activity, receptor autophosphorylation and internalization (Czech *et al.* 1990; Moolenaar *et al.* 1988; Wiley *et al.* 1991). Another important amino acid in the kinase domain is residue 743. A single nucleotide mutation changing the amino acid from valine to glycine diminishes the ability of the EGFR to phosphorylate itself and other proteins by 5 fold and 90%, respectively (Fowler *et al.* 1995; Luetkeke *et al.* 1994). The phenotype of this mutation in mice is very similar to  $\text{TGF}\alpha$  deficient mice exhibiting skin and eye abnormalities. The domain which regulates ligand induced internalization is residues 993-1022. Sequential truncation of amino acids from this region reduces EGFR internalization down to the basal rate of normal membrane turnover (Chang *et al.* 1993; Chen *et al.* 1989). The carboxyl terminal residues 1022-1186 function as the autoregulatory domain and contains four of the five tyrosine autophosphorylation sites - residues 1068, 1086, 1148 and 1173 (Chang *et al.* 1993). The effect of autophosphorylation on receptor kinase activity is controversial, but site-directed mutations of 1068, 1148, and 1173 had only a minor effect on kinase activity (Bertics and Gill 1985; Downward *et al.* 1984; Honegger *et al.* 1987). The domain containing residues 984-996 is the actin binding domain which mediates interactions believed to be responsible for high affinity binding (den Hartigh *et al.* 1992). Occupancy-induced lysosomal targeting of the EGF receptor has been isolated to the 945-991 region where the sequence YLVI, at residues 954-958, as been previously proposed as a lysosomal targeting motif (Guarnier *et al.* 1993; Opresko *et al.* 1995). The EGFR lysosomal targeting region was recently used in a yeast two-hybrid expression library to find EGFR's lysosomal sorting protein named sorting nexin-1 (SNX1). SNX1 contained a region of homology to yeast vacuolar sorting protein and its over-expression decreased EGFR surface concentrations (Kurten *et al.* 1996).

The importance of EGFR in embryonic development is dramatically demonstrated in EGFR knockout mice. One group developed two strains of knockout mice. The first strain died at mid-gestation due to placental defects and the other strain lived to 3 weeks with skin, kidney, brain, liver, and gastrointestinal tract abnormalities (Threadgill *et al.* 1995). Also



determined was the important role played by EGFR in trophectoderm development (the first epithelial layer to form in mammalian embryos), blastocoel formation by the trophectoderm, and implantation (Wiley *et al.* 1995). A review of EGF / TGF $\alpha$  and their receptor can also be found in Boonstra or Carpenter (Boonstra *et al.* 1995; Carpenter and Wahl 1990).

#### 1.4 Control of Autocrine Systems

As described earlier, the autocrine pathway occurs in many different cell lines ranging from primary human tumors such as multiple myeloma (Kawano *et al.* 1988), adult T-cell leukemia (Niitsu *et al.* 1988), colon and esophageal carcinomas (Sun *et al.* 1994; Yoshida *et al.* 1990) to normal cells such as macrophages, lymphocytes, and fibroblasts (Heldin and Westermark 1990; Wong and Wahl 1991). Normal autocrine cells transformed by transfection of SV40 large T antigen remain pathologically similar to parental cells (Tsao *et al.* 1996). It required the further mutation / mis-regulation of cell mechanisms by additional transfection of v-Ha-ras into cells to become highly tumorigenic (Valverius *et al.* 1989).

With this slight change in cellular regulation, an autocrine cell changes from responding to wound healing signals to unbridled proliferation. This connection between two extremes is summarized by two reciprocal quotes (Sporn and Roberts 1992): “‘a wound is a tumor that heals itself’ (Haddow 1972) , and ‘tumors are wounds that do not heal’” (Dvorak 1986). Thus, while autocrine factors have been associated with cancer, these growth factors are important in tissue repair and wound healing to breakdown collagen, fibroblast migration, and formation of new collagen and vessels (Sporn and Roberts 1986). To quote: “The difference between the involvement of these peptides in carcinogenesis and tissue repair appears to depend more strongly on the context and degree of their expression and activity, rather than on their mere presence or absence. Only when regulation is lost, does pathology result (Sporn and Roberts 1992).”

One method to inhibit the autocrine ligand-receptor signaling pathway and restore equilibrium to a misregulated autocrine system is addition of antibodies against the EGF receptor (Gill and Lazar 1981; Modjtahedi *et al.* 1993a; Modjtahedi *et al.* 1993b; van de Vijver *et al.* 1991). In Figure 1.8a, van de Vijver shows the addition of 20 nM (~3  $\mu$ g/ml) monoclonal anti-EGFR 528 or 225 antibodies to A431 cells decreases EGFR tyrosine phosphorylation to 30% +/- 10% basal level. As seen in Figure 1.8b, the receptor mass remains constant, thus the phosphorylation decrease resulted from blocking TGF $\alpha$  / EGFR binding with antibodies and not degradation of protein. Note, that the TGF $\alpha$ -EGFR  $K_d$ , a measure of ligand-receptor affinity, is about 1 nM, therefore, they were using a twenty fold excess of antibody. Modjtahedi's group also showed they could completely inhibit TGF $\alpha$  / EGFR binding in neck

carcinoma and breast carcinoma cells using 100 nM of rat monoclonal anti-EGFR antibodies. An important finding from van de Vijver's paper, is that exogenously added antibodies can inhibit the binding of TGF $\alpha$  to its EGFR receptor, suggesting that TGF $\alpha$ -EGFR binding does not occur during receptor / ligand biosynthesis, intracellular processing, and vesicular secretion.

In Vijver's paper, addition of anti-receptor antibodies reduced receptor phosphorylation due to the inhibition of receptor-ligand binding. As prolonged phosphorylation leads to DNA synthesis and proliferation, the question should be "what is the relationship between receptor occupancy and mitogenic response?" One group calculated there was a linear relationship between steady-state EGF receptor occupancy and the mitogenic response in fibroblast cells (Knauer *et al.* 1984). Knauer's graph, Figure 1.9, shows low EGF receptor occupancy can induce a mitogenic response, and in fact, maximum mitogenic response is achieved with less than 25% of total receptor occupancy. Other researchers have studied the effects of autocrine cell proliferation upon the addition of anti-receptor blocking and anti-ligand decoy antibodies (Rodeck *et al.* 1990; Yamada and Serrero 1988). Some of their key findings are presented in Figure 1.10. In Figure 1.10a, the proliferation of a series of carcinoma cell lines was completely inhibited upon addition of 30 nM anti-EGFR monoclonal antibody 425, interrupting the cell's EGF / TGF $\alpha$  autocrine loop. Figure 1.10b shows the addition of micromolar anti-ligand decoy antibody concentrations resulted in the decreased cell growth of autocrine insulin-dependent teratoma cells to sixty percent normal. Although system parameters were not determined in these experiments, the overall trends in receptor phosphorylation, ligand binding, and cell proliferation indicate the feasibility of using antibodies to inhibit the formation of receptor / ligand complexes. Therefore, in order to attain complete inhibition of EGFR signaling and mitogenic response, an analysis of the parameters affecting ligand-receptor binding should be performed.

### **1.5 Mathematical Modelling of Autocrine Systems**

Mathematical modeling is an ideal technique to determine which cellular parameters are important for interrupting the autocrine pathway. An early model analyzed cellular and environmental parameters', such as inoculum cell density and carrier beads versus culture dishes, importance on regulating mammalian autocrine cell growth. To obtain similar cell growth rates with increasing microsphere radius required a linearly proportional increase in initial number of autocrine cells seeded. A second observation was greater inoculum cell density / unit area was required to achieve similar growth rates for spherical microcarriers versus flat tissue culture dishes (Lauffenburger and Cozens 1989). This model was based on autocrine platelet-derived growth factor (PDGF) cells, modelling ligand production, diffusion,

binding, and cell proliferation. Some differences between this model and current experimental system is the assumption of infinite bulk medium (therefore, no extracellular bulk ligand concentration variable) and no competing antibodies. Another disadvantage is the use of cell proliferation as the dependent variable. Experimentally, cell proliferation must be recorded periodically over several days and the increasing cell density's effect on other cellular parameters would be difficult to quantitate.

A second group evaluated the antibody concentration required to neutralize gastrin-releasing peptide (GRP) autocrine growth factor's effect on small cell lung cancer (Mulshine *et al.* 1992). It was determined that 160 mg anti-GRP decoy antibody would reduce receptor occupancy below 10% for a 1 kg tumor *in vivo*. Some problems with this model are steady state calculations (thus, no difference between autocrine cells and receptor cells "bathed" in ligand), assumption of no proliferation below 10% receptor occupancy (see Knauer *et al.*, 1984), no difference between local cell environment versus bulk medium and based on *in vivo* whole body assay versus *in vitro* culture dish experiments.

Another model analyzed competition between decoy antibodies and surface receptors (Goldstein *et al.* 1989). The experimental system used 2,4-dinitrophenyl (DNP) aminocaproyl-L-tyrosine (DCT) as the ligand. Monoclonal anti-DNP antibodies were used as a decoy antibody and a cell receptor by anchoring the antibody to rat basophilic leukemia cell's high affinity Fc<sub>ε</sub> receptor. Experimental data and computer modelling indicated that 2.4 μM decoy antibody was required to inhibit DCT rebinding to cells containing 6x10<sup>5</sup> receptors. Deficiencies with this model include: not an autocrine system (ligand exogenously added), quasi-steady state equilibrium assumptions, no internalization and degradation of receptor / ligand complexes or normal receptor trafficking. They do have an implied screening length, separating receptor / ligand binding at the cell surface from ligand in the bulk medium. An advantage with this system is using the same antibody as both decoy and receptor plus the ability to easily manipulate receptor concentrations by varying amount of anti-DNP antibody bound to cells.

Computation work based on the interleukin 2 (IL2) system, a well studied autocrine T lymphocyte system (Duprez *et al.* 1985; Smith 1990) has been performed by Forsten and Lauffenburger (Forsten and Lauffenburger 1992a; Forsten and Lauffenburger 1992b; Forsten and Lauffenburger 1994a). Forsten's papers perform mathematical calculations on autocrine ligand binding using solution decoys and receptor blocking antibodies as competitors to receptors / ligand binding. In Kim Forsten's computer model shown in Figure 1.11 (decoy) and Figure 1.12 (blocker), known IL2 values for the ligand and receptor secretion rates, ligand and receptor binding kinetics, diffusion rates, and degradation rates were used. By varying the

parameters values for cell density, ligand secretion, diffusion, ligand-receptor affinity and solution decoys, she was able to analyze their effects on receptor complex numbers.

Computer modelling indicate two inhibition regimes exist when using competing soluble receptor decoys on autocrine cells (Figure 1.13a). The first stage of inhibition occurs at low decoy concentrations and is a function of the ligand's diffusion limitations into the bulk medium. The second plateau of inhibition results from the diffusion limitations of the soluble receptor decoy into the cell receptor's binding "domain." At this point, the cell receptor and soluble receptor compete directly for freshly synthesized and receptor-released ligand. The location of these plateaus with respect to soluble receptor concentration is a function of the cell density and ligand secretion rates. According to the model, every 10 fold increase in cell density requires a similar 10 fold increase in soluble decoy receptor concentration to achieve the same inhibition level of receptor complex numbers. Also, increasing secretion rates means a similar increase in decoy receptor concentrations to maintain similar receptor complexes levels (Figure 1.13a and b).

A second method for inhibiting receptor - ligand binding uses blocking antibodies against the receptor as mentioned in section 1.4. In Figure 1.14a, receptor-ligand complex levels were predicted as a function of cell density and anti-receptor blocking antibodies concentrations (Forsten and Lauffenburger 1992b). When comparing this figure against Figure 1.13a, there are a few noticeable differences such as the lack of a second plateau and inhibition of receptor complexes at different inhibitor concentrations. Interruption of the receptor complex is preempted in the soluble decoy model compared to the receptor blocking model due to the depletion of soluble decoys by ligand binding as they diffuse into the proximal secretion layer. This diffusion and "effective" proximal ligand decoy concentration causes the second plateau and orders of magnitude increase in antibodies required to achieve complete ligand binding inhibition when compared to receptor blocking antibodies (Figure 1.14b). A possible problem with this model besides anchorage-independence and IL2 versus EGF / TGF $\alpha$  / EGFR cell systems is the lack of intercellular receptor / ligand sorting between degradation and recycling pathways upon internalization of complexes. However, these computer models reflect the need for an experimental understanding into cellular parameters such as cell density and ligand secretion rates to prevent unregulated proliferation of cancerous cells.

## **1.6 Expression System for Autocrine Ligand**

DNA expression vectors are utilized to promote the expression of a foreign gene in a transfected cell under constitutive or inducible control. A review of different enhancers and promoters controlling / promoting the expression of proteins from expression vectors can be

found in *Gene Transfer and Expression - A Laboratory Manual* by Michael Kriegler (Kriegler 1990). There are several promoters and enhancers used in expression vectors which constitutively express the desired gene, some of the more common ones include SV40 and hCMV. SV40 enhancer was the first enhancing DNA sequence discovered, derived from the viral DNA SV40 (Banerji *et al.* 1981; Moreau *et al.* 1981). However, the SV40 enhancer is very complex (three functional units) and subject to positional effects and has cell type specific dependencies on cellular factors. The second enhancer is human cytomegalovirus (hCMV) which is about 400 base pairs long, has little cell-type or species preference and several fold more active than SV40 (Boshart *et al.* 1985).

In contrast to the number of constitutive promoters and enhancers, there are very few which regulate gene expression. Two of the most common ones are metallothionein (Palmiter *et al.* 1982) and mouse mammary tumor virus (Huang *et al.* 1981; Lee *et al.* 1981). Metallothionein promoter is induced by the addition of heavy metals or phorbol esters. Typically, these vectors have high basal expression in the absence of metal and modest induction of gene expression upon addition of metal (Palmiter *et al.* 1982). An adjustment of the ratio between metal-responsive elements and basal-level elements had a best case 200 fold induction (McNeall *et al.* 1989). Mouse mammary tumor virus promoter has glucocorticoid-responsive elements which are induced by addition of dexamethasone. Utilization of this promoter resulted in low protein expression (unpublished observation).

To obtain a high and controllable protein expression from cells, a two plasmid transactivator expression system under tetracycline control was used (Gossen and Bujard 1992). This plasmid system was constructed so that protein expression levels could be gradually induced from low to high expression with the adjustment of tetracycline concentrations. The first plasmid (pUHD 15.1), shown in Figure 1.15, contains a gene sequence which fuses the *tet* repressor protein to the activating domain of herpes simplex virus virion protein 16. The fused protein, tetracycline-controlled transactivator (tTA), is constitutively expressed using the human cytomegalovirus (hCMV) promoter / enhancer regulatory region. The second plasmid, (pUHD 10.3), shown in Figure 1.16, has a hCMV minimal promoter created by removing the enhancer region via PCR from the normal hCMV DNA sequence. In addition, seven inserts of the 19 bp inverted repeat sequence for the *tet* operator from Tn10 were added upstream of the hCMV minimal promoter, creating the fused protein's binding site. The 19 bp repeat sequence is 5'- TCTCTATCACTGATAGGGA-3'. Following the *tet* operators and hCMV region is the polylinker and SV40 polyadenylation regions. A schematic of the two plasmid system is shown in Figure 1.17. The tTA protein from the first plasmid is sensitive to low tetracycline concentrations and in the presence of

tetracycline can not stimulate mRNA transcription on the second plasmid. However, in the absence of tetracycline, the tTA protein promotes RNA polymerase binding, leading to RNA transcription and protein synthesis.

### 1.7 Cell Microphysiometer Assay for Autocrine Ligand Binding

A method for observing autocrine receptor / ligand complex levels can be achieved by measuring extracellular acidification rates (ECAR) using Molecular Devices Microphysiometer / Cytosensor and correlating its data to receptor complex numbers obtained from  $I^{125}$  EGF binding experiments. The production of acidic metabolites occurs via glycolysis of glucose to lactic acid or glucose oxidization to  $CO_2$  by respiration. At physiological pH, these weak acids dissociate, yielding two to six  $H^+$  per glucose molecule. Normal cultured fibroblast cells have a very active glycolysis rate, accounting for about 80% of the secreted protons or around  $10^8$  protons per second (McConnell *et al.* 1992). The Cytosensor can also detect intracellular pH regulation via the sodium-hydrogen exchange pump independent of glucose pathways. Chemicals inhibiting this ion exchange pump are choline (increases intracellular proton concentration) and amiloride (inhibitor of  $Na^+ - H^+$  exchange system). The secondary signalling pathway is another contributor to extracellular pH changes and can be interrupted using genistein (inhibit tyrosine kinase activity), forskolin and cholera toxin (increase cAMP), or staurosporine (inhibits protein kinase C). Both the sodium-hydrogen exchange pump and secondary signalling pathway are regulated by receptor / ligand signalling, thus, changes in complex levels affect cell metabolic rates in shown in Figure 1.18.

The Cytosensor detects small changes in extracellular hydrogen proton concentration (rms error < 0.001 pH units) using a light-addressable potentiometric sensor (LAPS) (Owicki *et al.* 1990). A schematic of the LAPS is shown in Figure 1.19a. The surface of the silicon nitride insulator contains silanol and silamine groups which titrate as a function of pH (zero charge at pH 3.5). Using an amplitude-modulated light-emitting diode (LED), a charge separation results in a compensatory capacitatively coupled movement at the sensor's insulator surface which is detected by the ammeter. As increasing potential is applied to the solution, the depletion layer collapses, inhibiting the photocurrent. Thus, a plot of photocurrent ( $I_p$ ) versus applied potential ( $\Psi$ ) is obtained with a characteristic inflection point ( $d^2 I_p / d\Psi^2 = 0$ ) defined as ( $\Psi_{PIP}$ ). As the sensor's surface potential depends on solution pH, changes in the inflection point correlates to extracellular pH changes. The instrument's pH response to surface potential is 61 mV per pH unit at 37 °C, sweeping over 1000 mVs. Shown in Figure 1.19b, medium is pumped by peristaltic pump through a debubbler-degasser to the sensor chamber. Cells are pre-attached to a membrane insert and in diffusive contact with the LAPS sensor.

The pH change is ascertained over defined time periods by briefly halting the flow of medium over cells to generate the  $I_p - \Psi$  graph (Figure 1.20a). Measuring  $\Psi_{pip}$  once a second for 20 seconds when the pump is off creates a  $\Psi_{pip}$  versus time graph from which a linear best fit line gives the cell's  $H^+$  secretion rate (Figure 1.20b). The medium's flow is resumed and the entire pump cycle repeated every few minutes. A plot of cells' acidification rate over time shows the response of cells to additives (Figure 1.20c).

Original Cytosensor applications include measuring cellular apoptosis as a function of chemotherapeutic drugs, metabolic poisons (i.e. carbonylcyanide chlorophenylhydrazone), and various irritants (i.e. dimethyl sulfoxide, acetone, benzalkonium Cl) (Parce *et al.* 1989). Receptor-mediated responses were measured as a function of growth factor additions and competing antibodies (Owicki *et al.* 1990) along with secondary pathway transduction elucidation via probes for G proteins (i.e. cholera toxins, forskolin, protein kinase C inhibitors (staurosporine), tyrosine kinase inhibitors (genistein)) (Molecular Devices Corp. 1994). More recent Cytosensor applications are variations of the same experiments including anti-infective saponins on fungi and bacteria (Okunji *et al.* 1996), different agonists on dopamine D2 and D3 receptors (Boyfield *et al.* 1996), peptide ligands or anti-idiotypic antibody on B-lymphoma cells (Renschler *et al.* 1995), or HER2 / HER3 metabolic response upon heregulin additions (Chan *et al.* 1995). Hypothesizing that extracellular acidification should correlate directly with receptor / ligand complex levels, it was believed that Cytosensor utilization could be expanded to studying receptor complexes quantitatively.

Having described the Cytosensor inner workings and previous applications, predictions on autocrine cell responses to varying ligand concentrations and inhibitors can be formulated. Shown in Figure 1.21a, it is predicted that autocrine B82R<sup>+</sup> / TGF $\alpha$  autocrine cells' extracellular acidification rates will increase as a function of increasing ligand expression as receptor / ligand signalling complexes correspondingly increase. Addition of antibodies to cells stimulated by ligand, exogenously added or endogenously secreted, would decrease cell's ECAR as shown in Figure 1.21b. Experiments can be performed on two different types of autocrine cells, this thesis's autocrine B82R<sup>+</sup> / TGF $\alpha$  cell system (TGF $\alpha$  synthesized as transmembrane precursor and cleaved into a mature protein) and an autocrine B82R<sup>+</sup> / sEGF (sEGF is synthesized as a mature protein). B82R<sup>+</sup> / sEGF's ECAR should be higher than autocrine TGF $\alpha$  cells, because TGF $\alpha$  must be cleaved at the surface before it can diffuse and bind to the EGF receptor, allowing more chances for antibody inhibition, whereas sEGF could bind before surface expression. Autocrine ligands and receptors are secreted in close proximity, increasing their effective concentrations, whereas, exogenously added ligands and antibodies must diffuse through the bulk medium before competing for receptor binding. Thus, both

TGF $\alpha$  and EGF autocrine cell's advantage should result in a higher ECAR versus non-autocrine cells in the presence of antibody.

As Cytosensor's output is a metabolic rate and experimental values in terms of ligand concentrations / receptor-ligand complexes / free receptor levels, an experiment relating Cytosensor's data to these variables must be performed. A calibration between Cytosensor output and receptor / ligand complexes can be obtained using radioactive ligand equilibrium binding data. Two experiments would be performed, one with radiolabelled ligand data (bound ligand versus free ligand) and one with Cytosensor data (extracellular acidification rate versus free ligand). The Scatchard equation from equilibrium binding data (Scatchard 1949) can be solved from its more common form (Eq. 2.1) for free ligand concentration as shown in equation 2.2.

$$C / L = - C / K_d + R_t / K_d \quad \text{Equation 2.1}$$

$$L = C * K_d / (R_t - C) \quad \text{Equation 2.2}$$

After determining the constants,  $K_d$  and  $R_t$ , Equation 2.2 can be substituted into an analogous fit of the Cytosensor's ECAR versus free ligand graph. The combined equation eliminates free ligand, leaving bound ligand (complexes), metabolic rate and grouped constants.

By combining these techniques, the Cytosensor can be utilized to quantify an antibody's ability to interrupt an autocrine loop. Autocrine receptor / ligand complex formation may be inhibited by addition decoy and blocking antibody concentrations. Since ECAR is proportional to receptor complex levels, Cytosensor's data can be replotted as receptor complex levels versus antibody concentrations. Cytosensor data would be compared to computer model data depicted in Figure 1.14b predicting blocking antibody superiority over decoy antibody in receptor / ligand complex inhibition. Thus, a relationship between Cytosensor data and receptor complex levels will allow analysis of computer models and experimental results.

## 1.8 Thesis Overview

Computer modelling has indicated methods for inhibiting the autocrine signalling pathway; however, only a few uncontrolled experiments have been performed on this system. Some of the experimental problems are cell systems which make more than one ligand for the EGF receptor or a single, constitutive, ligand production rate. In order to examine methods for interrupting the autocrine pathway, I have developed an artificial autocrine and paracrine TGF $\alpha$  cell system using mouse B82 L cells, which do not have endogenous EGF receptors nor EGF family ligands.

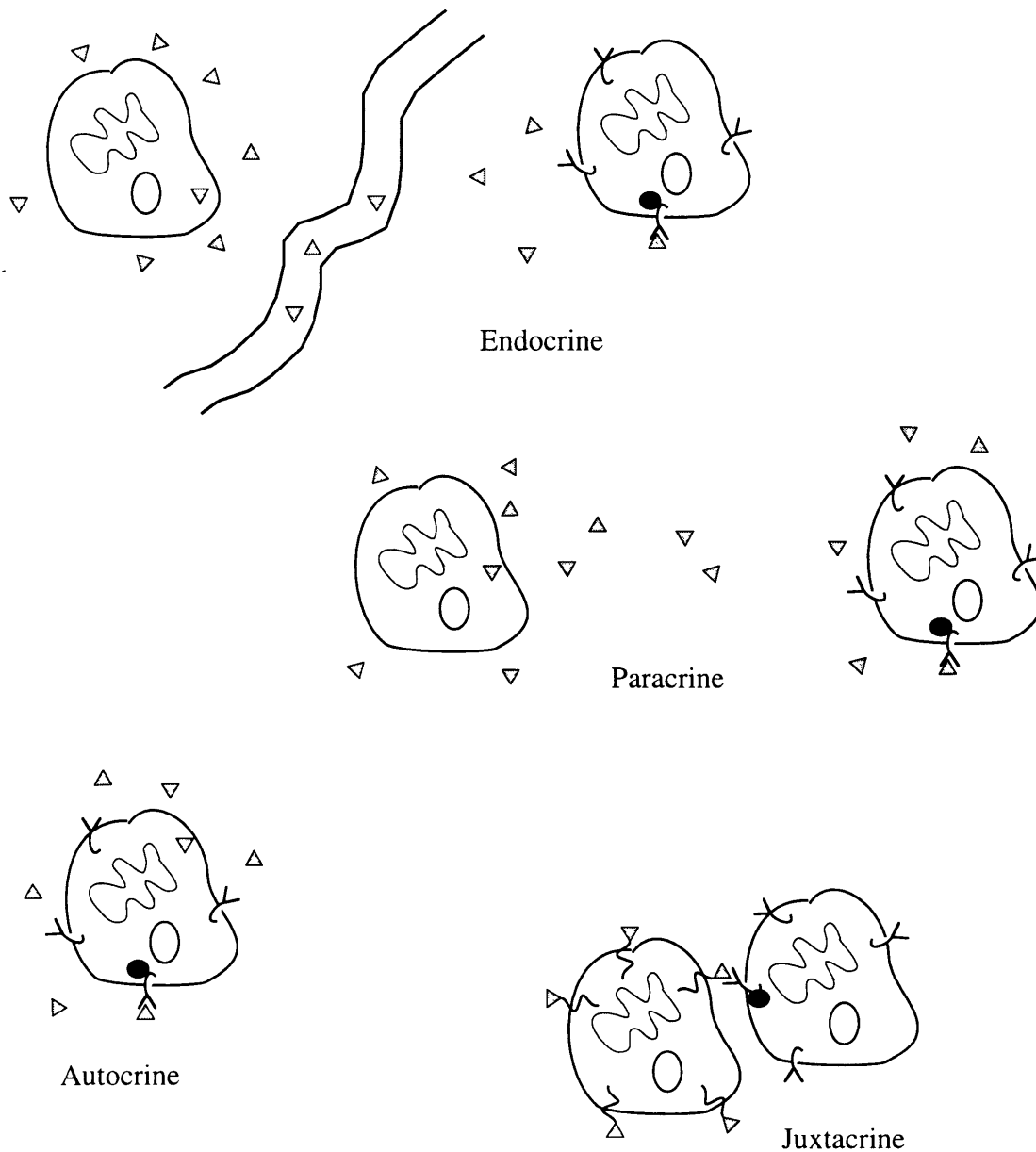
The transmembrane TGF $\alpha$  gene sequence was spliced into the second plasmid of the two plasmid tetracycline system and transfected into EGF receptor-positive and -negative cells



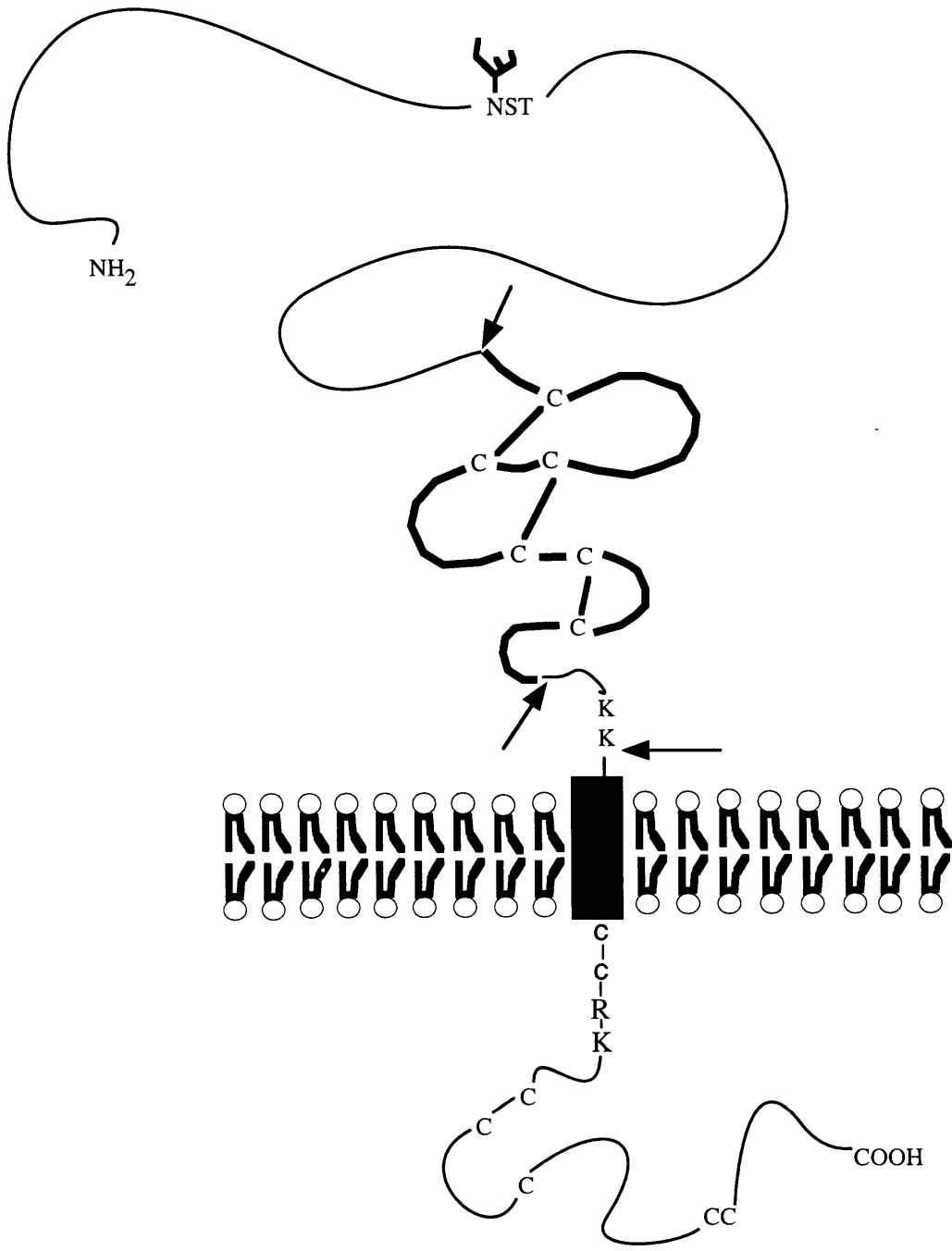
via calcium precipitation. TGF $\alpha$  secreting cells were isolated using histidinol selection, subcloning and ELISAs. With the successful transfection of TGF $\alpha$  into these cells, I obtain single ligand-receptor dynamics. Figure 1.22 shows how the cells were developed and which plasmids were utilized to construct an B82 EGF receptor-positive and -negative TGF $\alpha$  expression system. Nomenclature throughout the thesis will refer to autocrine and paracrine cells using EGF / TGF $\alpha$  ligands with and without their receptor, EGFR. B82R<sup>+</sup> / TGF $\alpha$  autocrine cells refer to the normal, same cell, receptor / ligand expression as defined in Figure 1.1. While a true paracrine cell system has ligand expressing cells and ligand receiving receptor cells, all further references to a paracrine cell refer only to the ligand expressing cell, B82 EGFR negative (R<sup>-</sup>) / TGF $\alpha$ .

The two plasmid system enables the regulation of TGF $\alpha$  expression levels before, during and after experiments. Studies in which tetracycline concentrations were varied demonstrate the ability to incrementally and precisely adjust TGF $\alpha$  expression. TGF $\alpha$  was characterized using Sephadex column separation and membrane extraction, showing that the transfected B82 cells secrete mature TGF $\alpha$ . Having characterized the TGF $\alpha$  expression system, experiments were performed on the cells to test model predictions on bulk ligand concentrations as a function of cell density and receptor / ligand complexes as a function of competing antibodies. Bulk ligand measurement as a function of cell density and ligand secretion rates indicated the importance of cell density and blocking antibodies when performing ligand accumulation / secretion experiments to obtain a “true” measurement of ligand secretion rates. The effect of ligand secreting rates verifies predictions that at high secretion, bulk TGF $\alpha$  concentrations would be independent of ligand uptake by its receptor, while dependent at lower secretion rates.

To quantify autocrine receptor / ligand complex accurately, an experimental system was developed using a modified I<sup>125</sup> binding assay and Molecular Devices Cytosensor. These measurements validated model predictions indicating blocking antibody’s superiority over decoy antibodies for inhibiting autocrine receptor / ligand complexes. Further experiments between autocrine cells expressing either transmembrane TGF $\alpha$  or mature EGF indicate the possibility of intracrine signalling in EGFR / EGF autocrine cells. Finally, the effect of increasing ligand expression levels in autocrine cells on receptor down-regulation and desensitization were studied. Thus, the bioengineered, experimental, autocrine cell system enabled a systematic study of cellular parameters which regulate cell signaling, gaining insights into the mechanisms of cancerous cell growth.



**Figure 1.1: Ligand secretion pathways.** Endocrine secretion: The ligand is secreted from the source cell and travels via the bloodstream to a target cell. Paracrine secretion: The source and target cells are in close proximity. Autocrine secretion: The target cells secretes its own ligand. Juxtacrine secretion: The source cell secretes membrane-bound ligand and by the adjacent target cell. (Adapted from Forsten and Lauffenburger, 1992a)



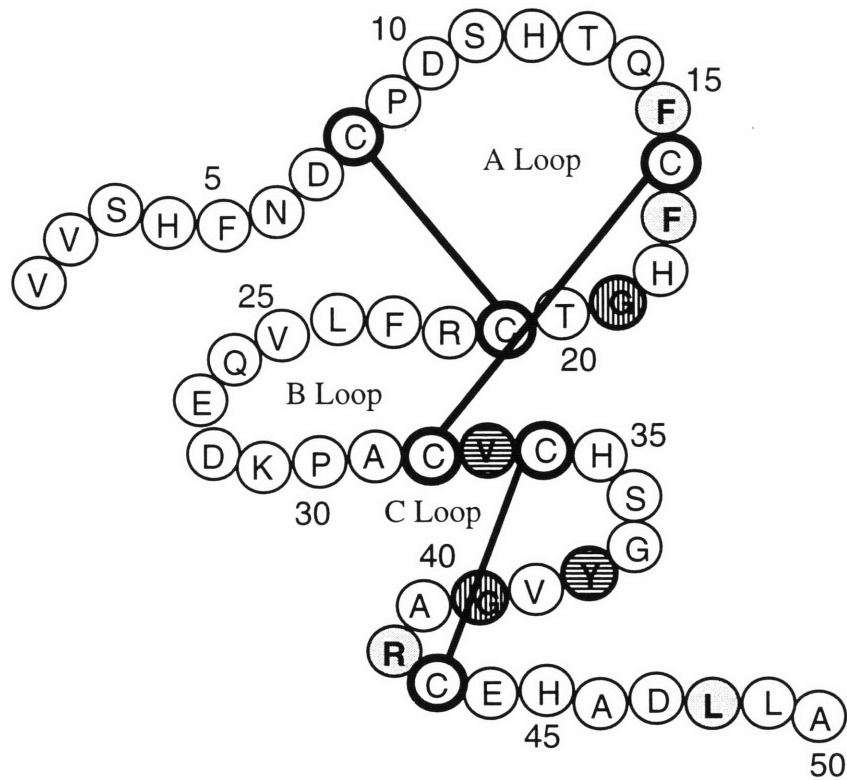
**Figure 1.2: TGF $\alpha$  precursor.:** The arrows indicate the cleavage sites used to excise the 50 amino acid mature TGF $\alpha$  protein from the 160 amino acid precursor. The mature protein is shown in bold. Glycosylation occurs on the asparagine residue of the NST triplet. (Adapted from Brackmann *et al.*, 1989)

	NH <sub>2</sub>	1	10	20	30	40	50
A)	(1)	NSDSE <b>C</b> PLSHDGY <b>CL</b> HD <b>GVC</b> MYIEAL			DKYAC <b>NC</b> VV <b>GYIG</b> ERCQYRD <b>LK</b> WWE <b>L</b> R		
B)	(1)	NSYP <b>G</b> CPSSYDGY <b>CL</b> NG <b>GVC</b> MHIESL			DSY <b>T</b> NC <b>CVIG</b> YS <b>GDR</b> CQTRD <b>L</b> RWWE <b>L</b> R		
C)	(1)	VVSHFND <b>C</b> PDSHTQ <b>FC</b> FH <b>GTC</b> RFLVQE			DKPAC <b>V</b> CH <b>SGYV</b> GAR <b>CE</b> HAD <b>L</b> LA		
D)	(1)	VVSHFWK <b>C</b> PDSHTQ <b>FC</b> FH <b>GTC</b> RFLVQE			EKPQ <b>C</b> VCH <b>SGYV</b> GVR <b>CE</b> HAD <b>L</b> LA		
E)	(39)	NRKKKN <b>C</b> NAEFQ <b>NC</b> I <b>H</b> <b>GE</b> CKYIEHL			EAV <b>T</b> CK <b>CQ</b> QE <b>YF</b> GER <b>CE</b> KS <b>M</b> KT		
F)	(28)	LGKKRDP <b>C</b> LRYKDF <b>CI</b> H <b>GE</b> CKYVKEL			RAP <b>S</b> CI <b>CH</b> P <b>GYH</b> GER <b>CH</b> GL <b>S</b> LPV		
G)	(31)	VKTHFSR <b>C</b> PKQYKH <b>YCI</b> H <b>GRC</b> RFVVDE			QTP <b>S</b> CI <b>CE</b> K <b>GYF</b> GAR <b>C</b> ERVD <b>L</b> FY		
H)	(175)	GTSHLV <b>KCA</b> EKEK <b>TF</b> CVNG <b>GE</b> CFMVKDLSNPSRYL <b>CK</b> CQ <b>P</b> G <b>F</b> T <b>GARC</b> TEN <b>V</b> PMK					

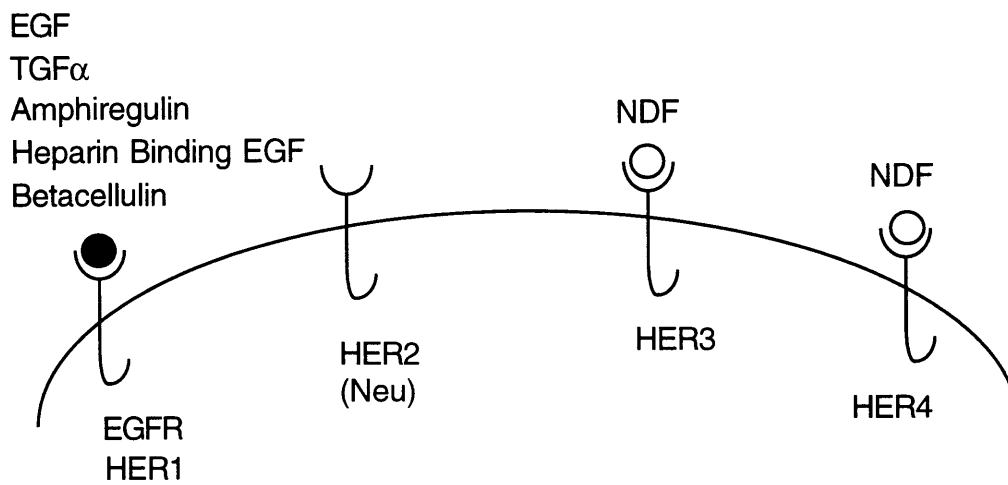
**Legend:**

A:	Human EGF (40%)	E:	Human Amphiregulin (26%)
B:	Mouse EGF (32%)	F:	Human Heparin Binding-EGF (32%)
C:	Human TGF $\alpha$ (-)	G:	Mouse Betacellulin (50%)
D:	Rat TGF $\alpha$ (90%)	H:	Human Heregulin $\alpha$ (30%)

**Figure 1.3: Amino acid relationship between members of the EGF family.** Heregulin sequence begins with amino acid 175 of the proHRG $\alpha$  protein, while the other polypeptide sequences are numbered relative to the mature form's NH<sub>2</sub> terminal. Conserved sequences between the proteins are denoted in bold highlight. Disulfide bonds are indicated by solid lines at the bottom. Residue numbering for EGF is shown at the top. Legend numbers in parentheses indicate percent homology with human TGF $\alpha$ . (Adapted from Shing *et al.*, 1993; Carpenter and Wahl, 1990)

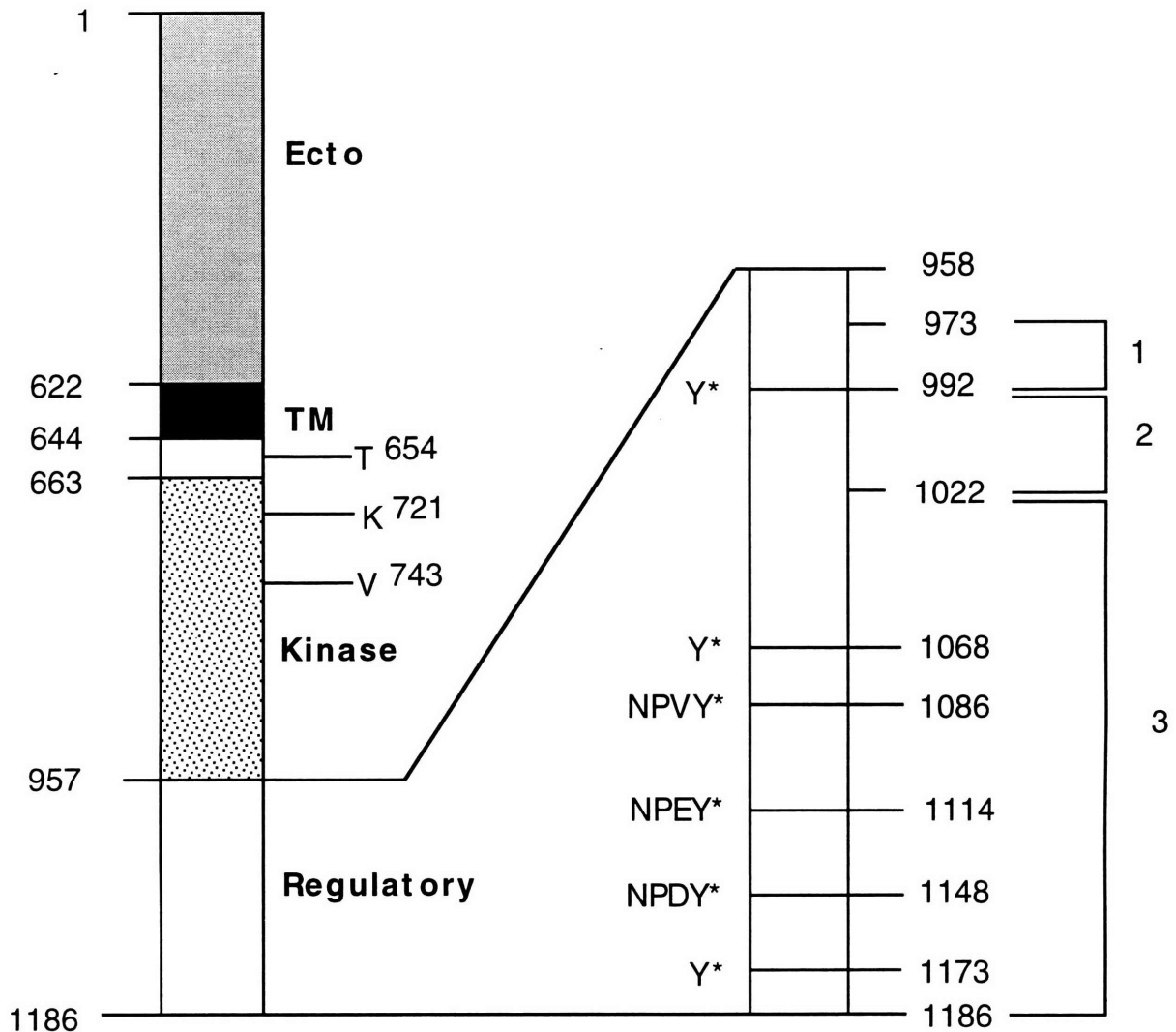


**Figure 1.4: Schematic representation of hTGF $\alpha$  structure.** Dot-filled circles are possible conserved EGF receptor binding sites. Hatch-filled circles are possible conserved TGF $\alpha$  structural amino acids. Conserved cysteines are shown with bold circles and linked via disulfide bridges indicated by solid lines. (Adapted from Feild *et al.*, 1992)

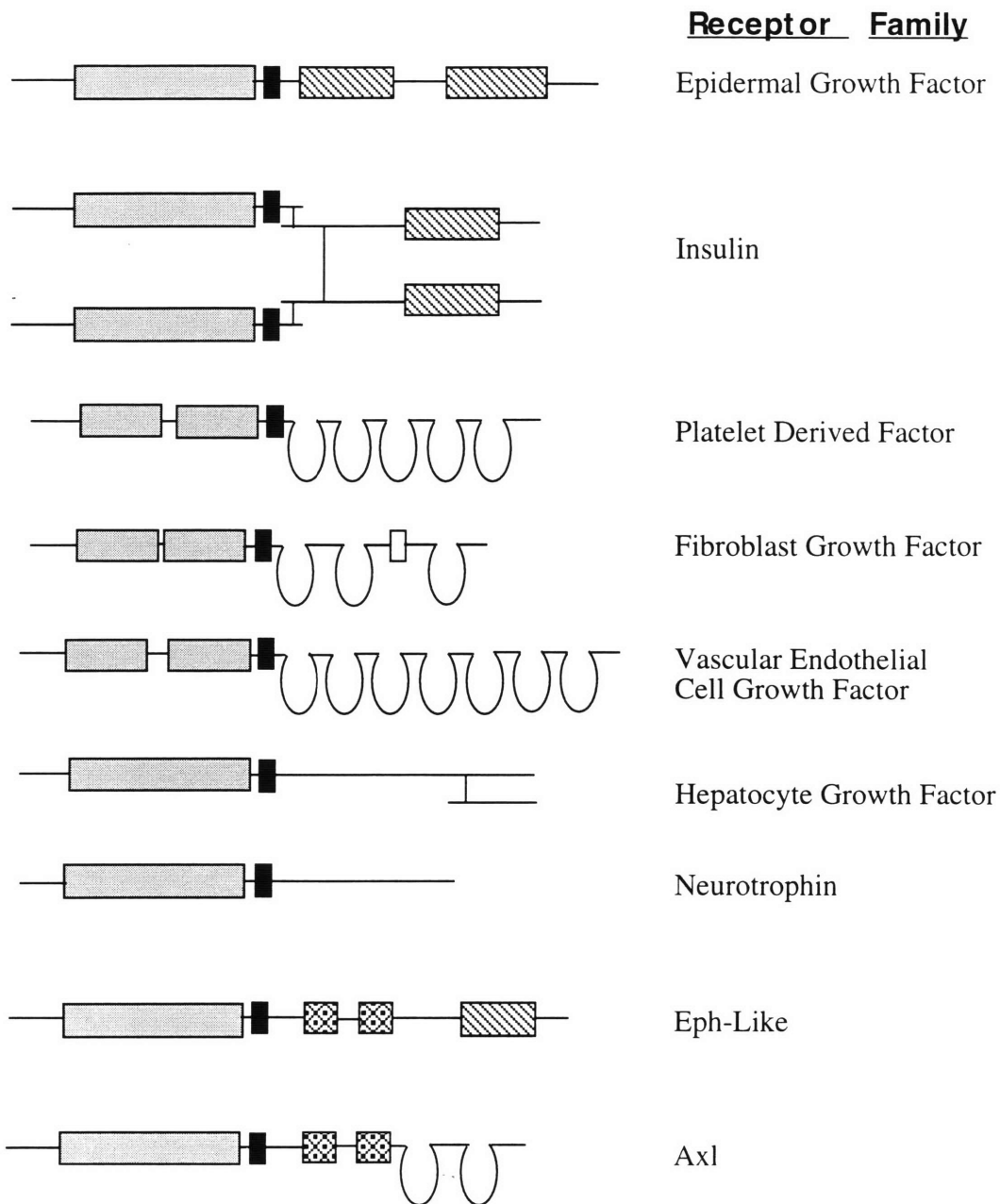


**Figure 1.5: Epidermal growth factor ligands and receptors family.**

Where EGF is epidermal growth factor, TGF $\alpha$  is transforming growth factor alpha, EGFR is epidermal growth factor receptor, HER is human EGFR, and NDF is *neu* differentiation factor (heregulin).

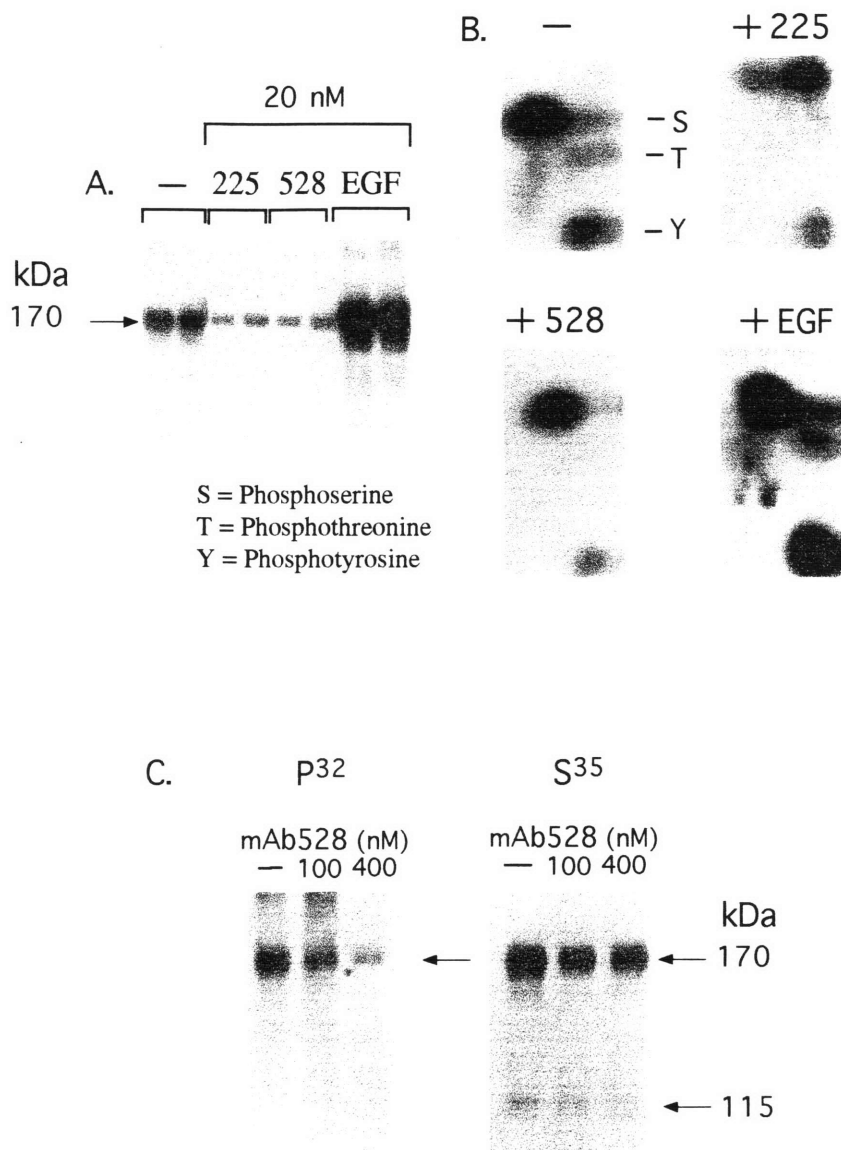


**Figure 1.6: EGF receptor domains.** Mutation of 721 to methionine abolishes kinase activity. Mutation of 654 to alanine decreases the affinity of EGFR for its ligands and 743 mutation to glycine results in wav-2 phenotype. Sequential deletion of the fragments 1, 2 and 3 from the COOH terminal results in the loss of endocytic function. NPXY motif is similar to the LDL receptor internalization code, where Y\* indicates tyrosine phosphorylation sites. (Adapted from Chang *et al.*, 1993 and Opresko *et al.*, 1995)



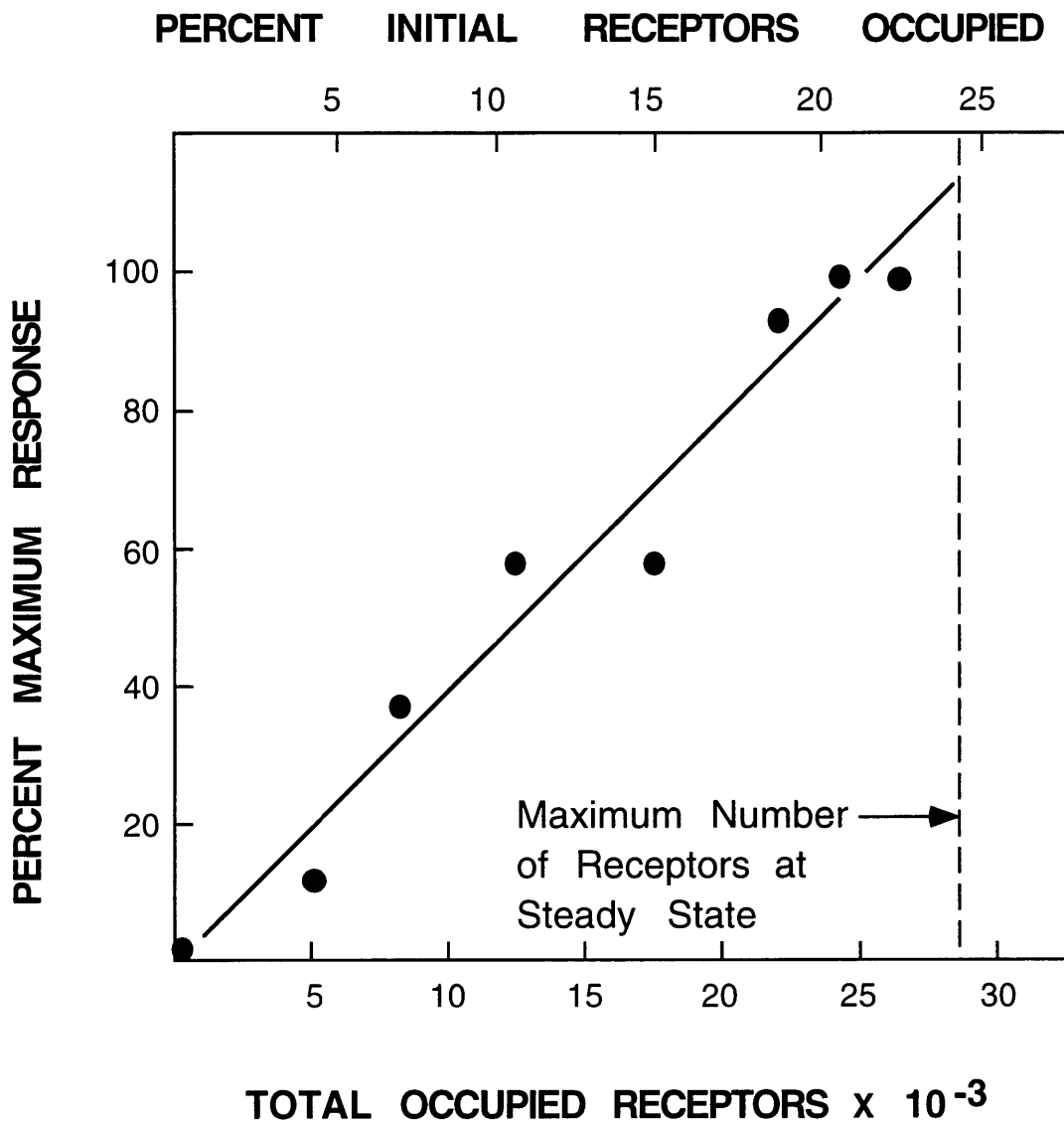
**Figure 1.7: Receptor tyrosine kinases.** Distinct families of receptor tyrosine kinase families as classified by Ullrich and Schlessinger, 1990. Identified structures are: tyrosine kinase domain (dotted boxes), transmembrane domain (solid box), cysteine-rich domains (stripped box), immunoglobulin-like domains (semi-circles), acid domain (open box), fibronectin III domain (checkered box). (Adapted from Fantl *et al.*, 1993)



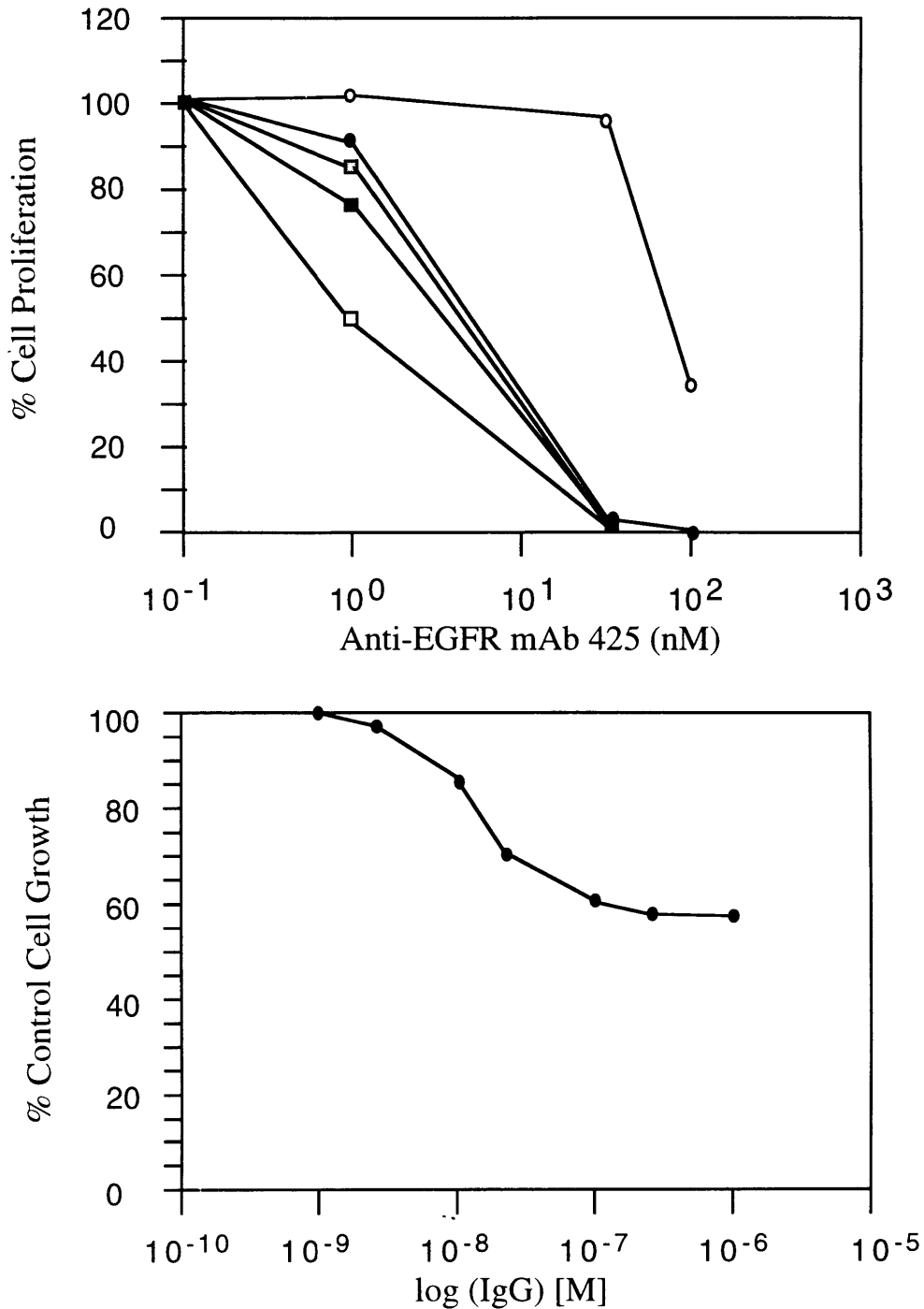


**Figure 1.8: Inhibition of phosphorylation by anti-receptor monoclonal antibodies.**

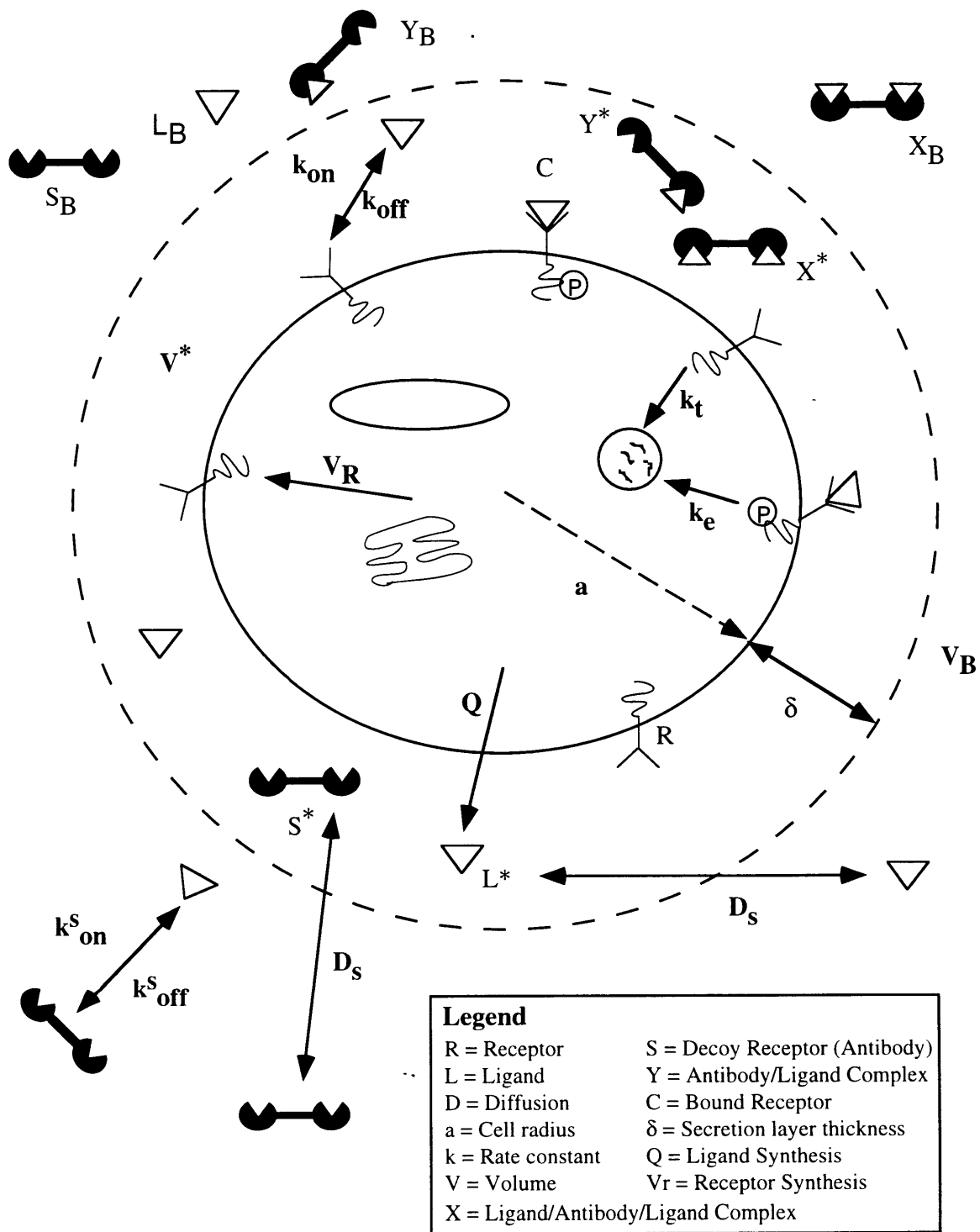
Graph A: A431 cells cultured in  $P^{32}$  for 16 hours with or with antibodies 225 and 528. Maximum phosphorylation response obtained with the culturing of A431 cells with EGF. Graph B: 170 kD bands excised from graph A and resolved on two-dimensional gel. Graph C: A431 cells cultured in  $P^{32}$  or  $S^{35}$  with or without antibody 528 for 16 hours. (Adapted from Van Der Vijver *et al.*, 1991)



**Figure 1.9: Relationship between EGF receptor occupancy and mitogenic response.** Dependence of maximum DNA synthesis rate on the number of total occupied receptors. (Adapted from Knauer *et al.*, 1994)

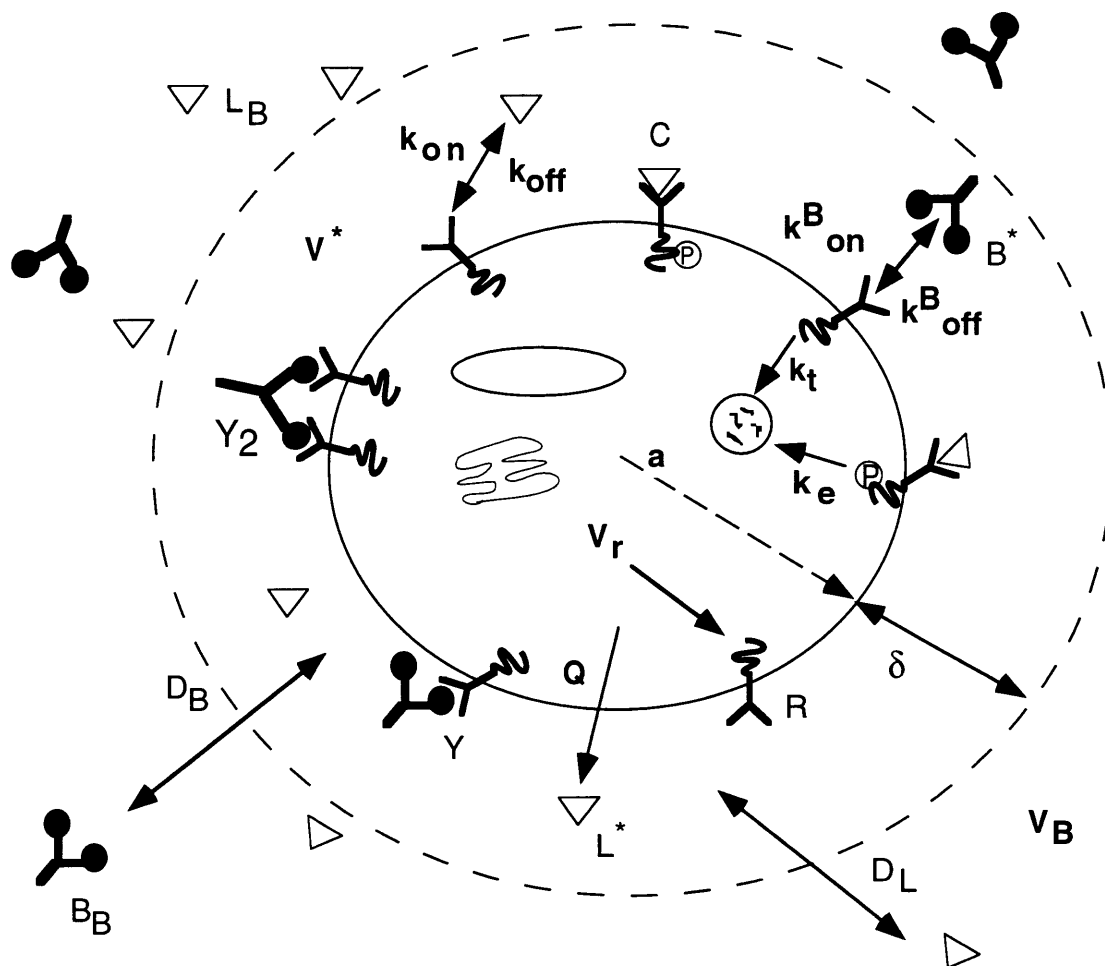


**Figure 1.10: Experimental data on ligand decoys' and receptor blocker's affect on autocrine cell stimulation.** Graph A: Inhibition of autocrine EGF/TGF $\alpha$  carcinoma cell proliferation in the presence of increasing receptor blocker antibody concentrations. Graph B: Inhibition of autocrine insulin-related factor teratoma cell proliferation in the presence of increasing ligand decoy antibodies. (Adapted from Rodeck *et al.*, 1990 and Yamada *et al.*, 1988)



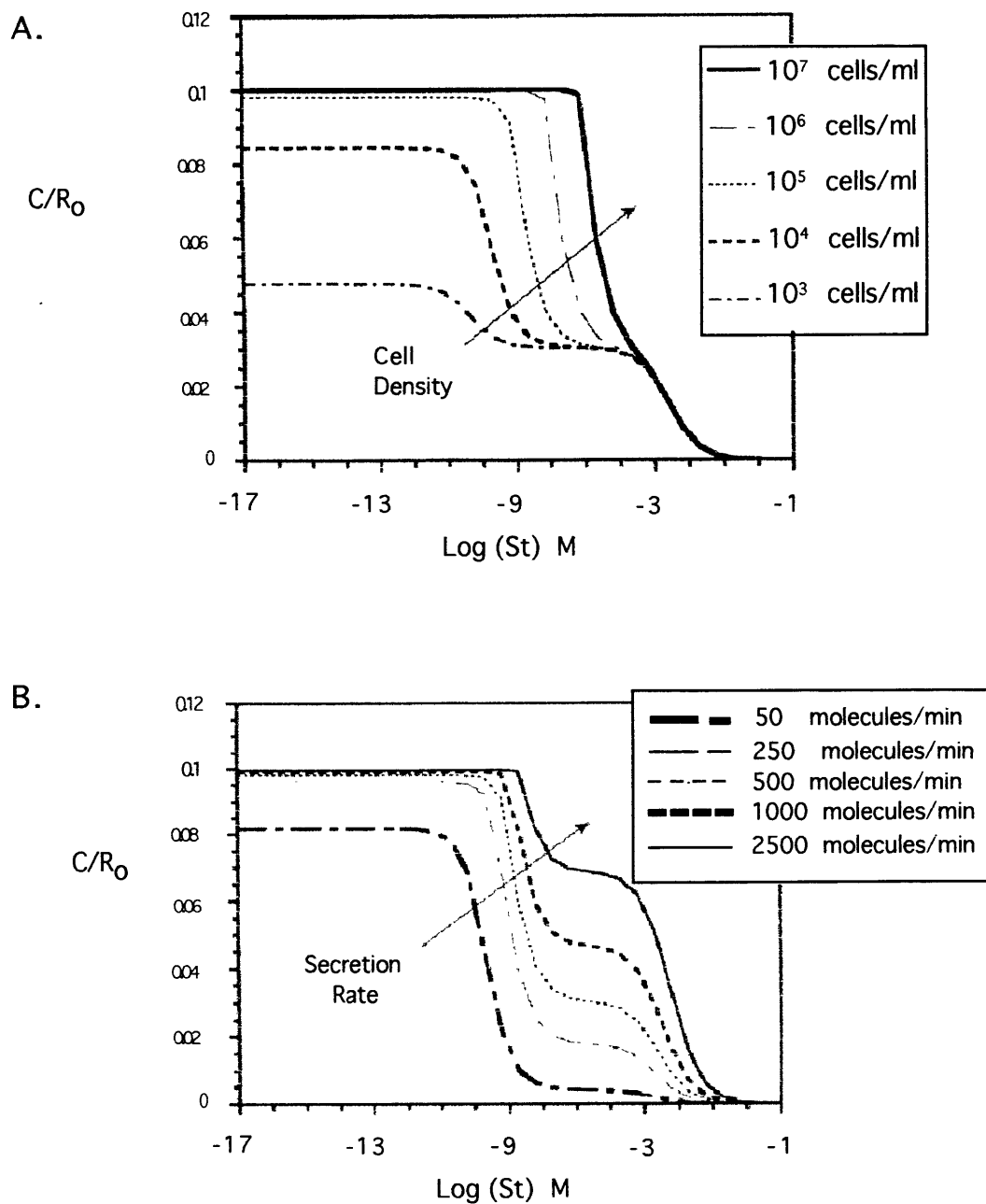
**Figure 1.11: Autocrine cell model schematic - decoy antibody.**

(Adapted from Forsten and Lauffenburger, 1992a)

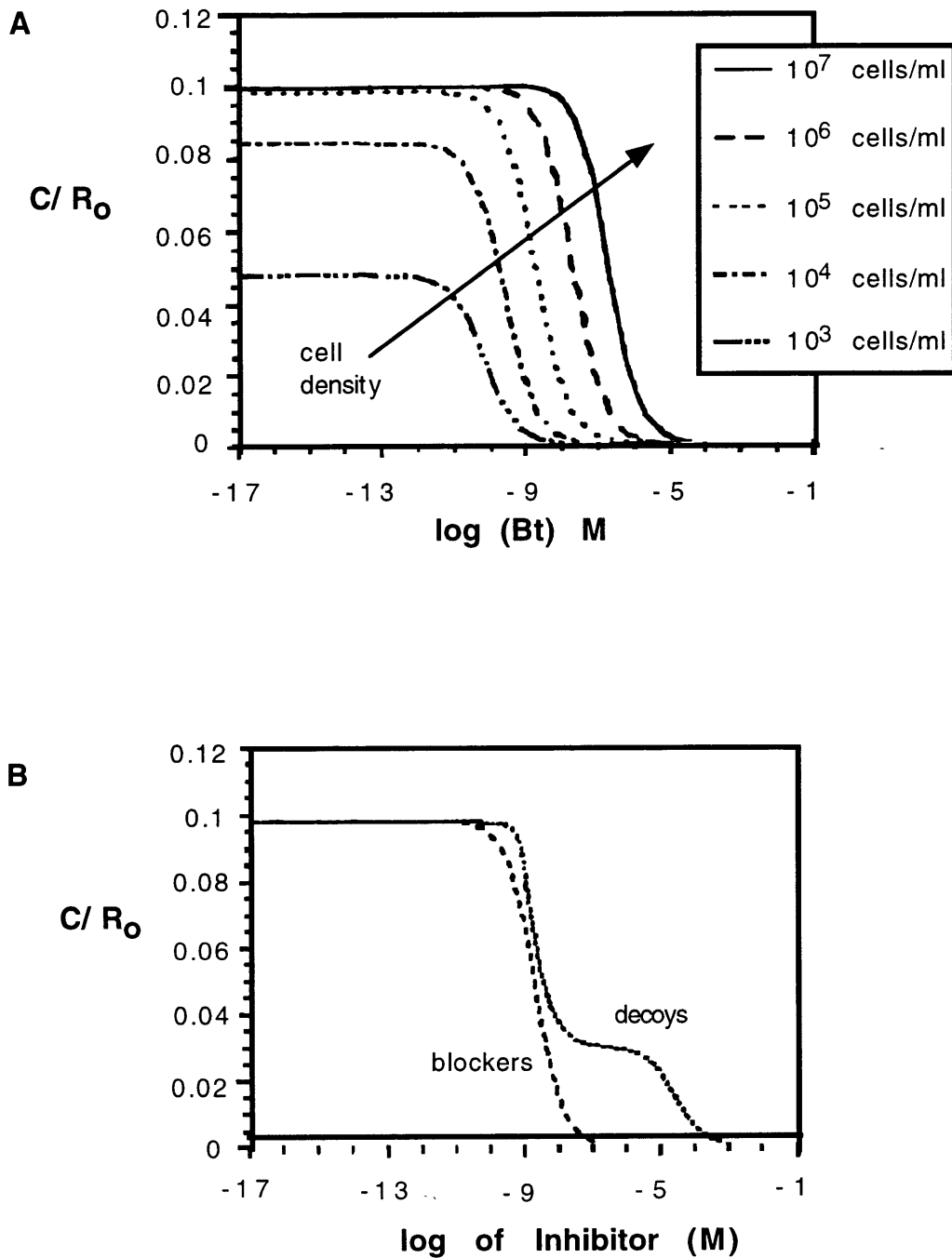


<b>Legend</b>	
<b>R</b> = Receptor	<b>B</b> = Free Blocker Antibody
<b>L</b> = Ligand	<b>Y</b> = Bound Blocker Antibody
<b>D</b> = Diffusion	<b>C</b> = Bound Receptor
<b>a</b> = Cell radius	$\delta$ = Secretion layer
<b>k</b> = Rate constant	<b>Q</b> = Ligand Synthesis
<b>V</b> = Volume	<b>V<sub>r</sub></b> = Receptor Synthesis
<b>Y<sub>2</sub></b> = Receptor / Antibody / Receptor Complex	

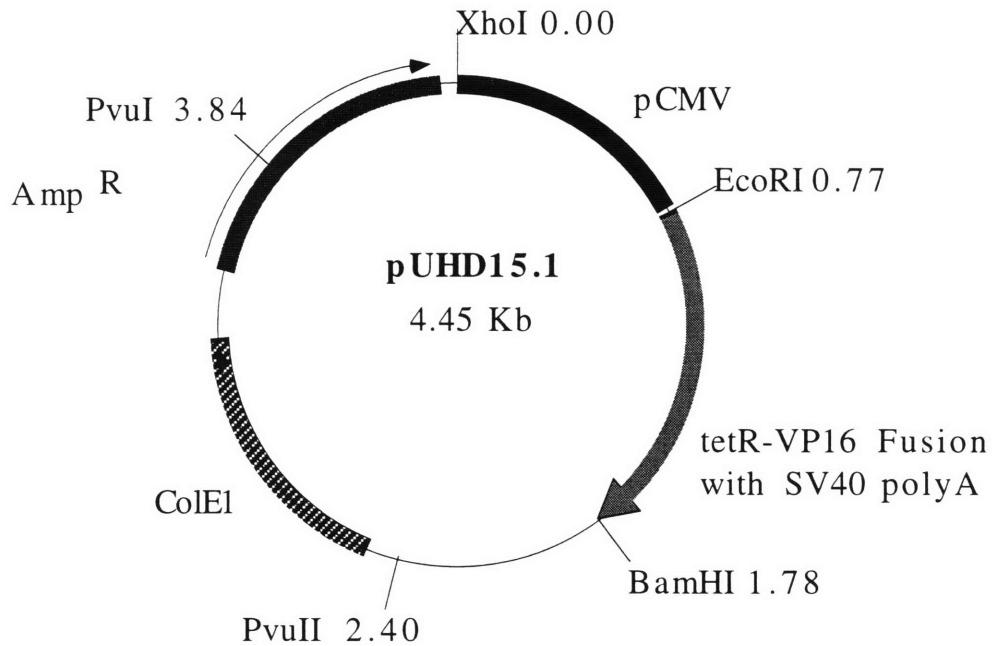
**Figure 1.12: Autocrine cell model schematic - blocker model.**  
 (Adapted from Forsten and Lauffenburger, 1992b)



**Figure 1.13: Decoy receptor effects on cell receptor complex levels.** Graph A: Effect of varying cell density on receptor - ligand complex levels. Graph B: Effect of varying ligand secretion on receptor - ligand complex levels. (Adapted from Forsten and Lauffenburger, 1992a)



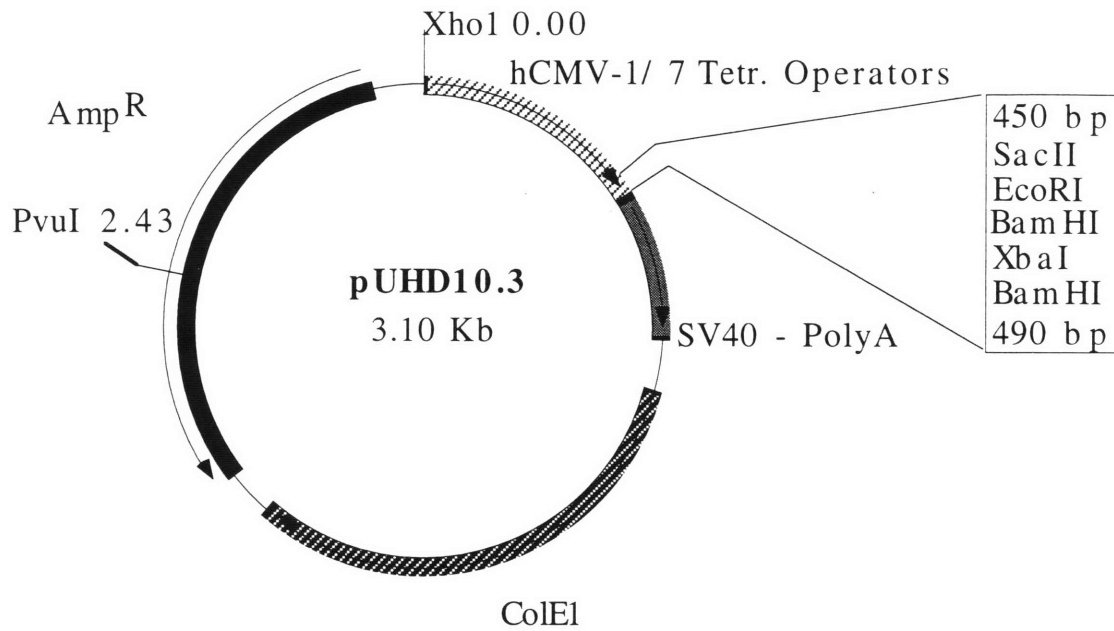
**Figure 1.14: Receptor antibody effects on cell receptor complex levels.** Graph A: Effect of varying cell density on receptor - ligand complex levels in the presence of receptor antibodies. Graph B: Comparison of receptor antibodies versus soluble decoy receptors at a cell density of  $10^5$  cells/ml. (Adapted from Forsten and Lauffenburger, 1992b)



Plasmid name: pUHD15.1  
 Plasmid size: 4.45 kb  
 Constructed by: M.Gossen  
 Construction date: 1991  
 Comments/References: PNAS **89**, 5547-5, 1992

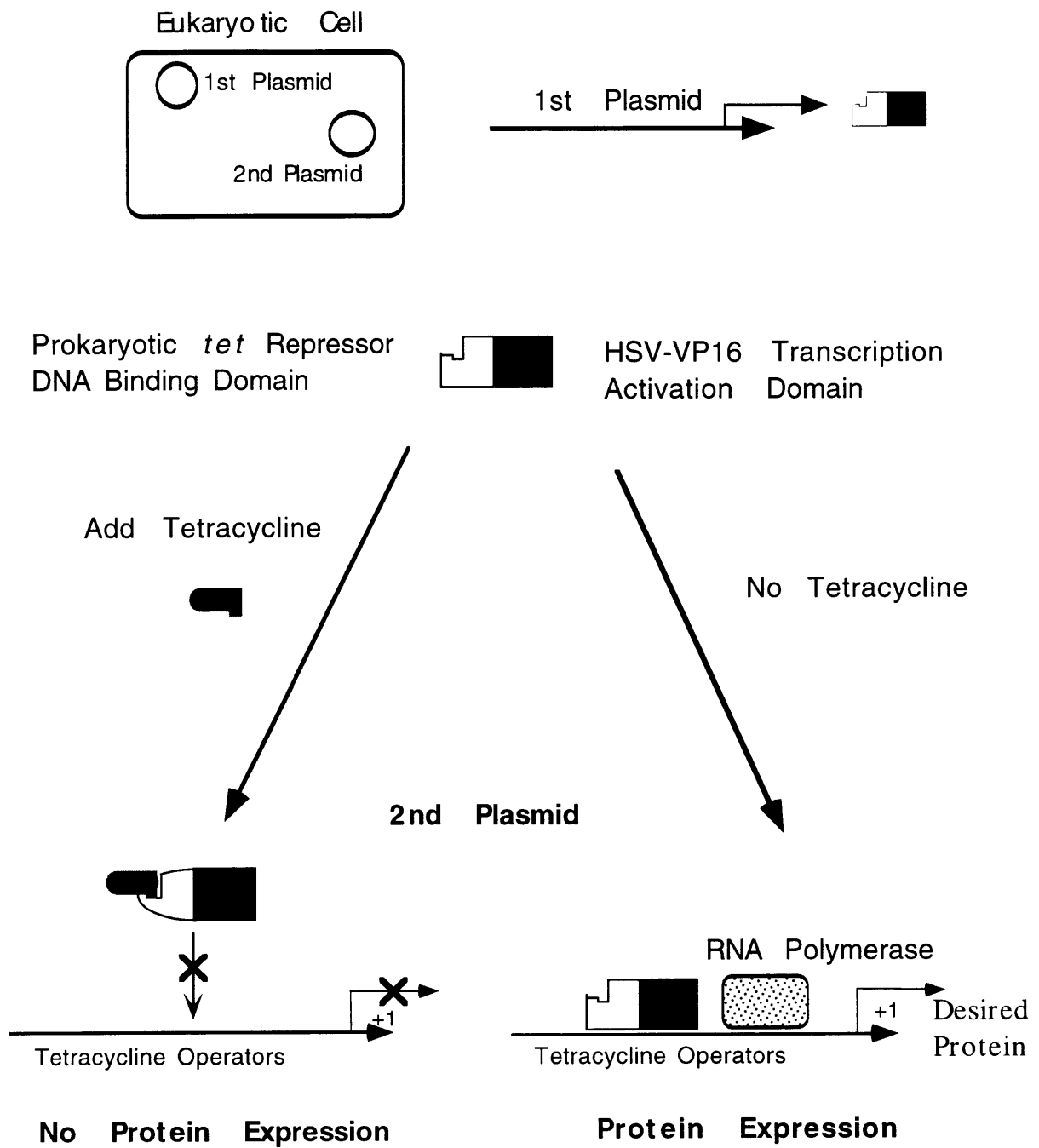
**Figure 1.15: pUHD15.1.** First plasmid of the tetracycline controlled two plasmid system.  
 (Adapted from Gossen and Bujard, 1992)



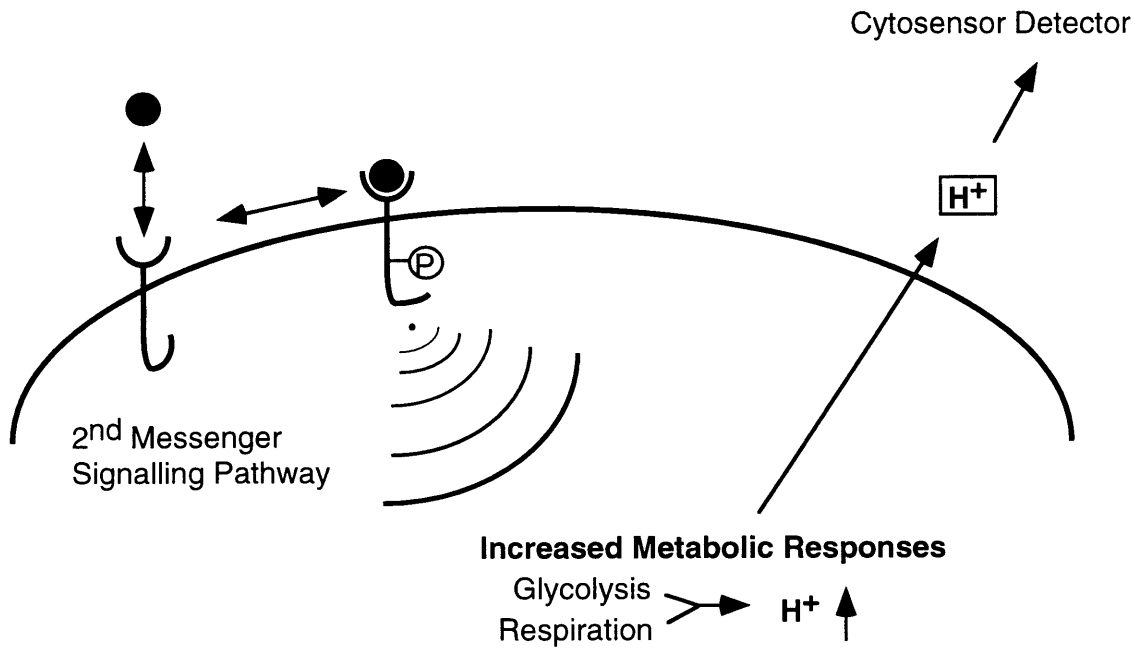


Plasmid name: pUHD10.3  
 Plasmid size: 3.10 kb  
 Constructed by: M. Gossen  
 Construction date: 1991  
 Comments/References: PNAS **89**, 5547-51, 1992

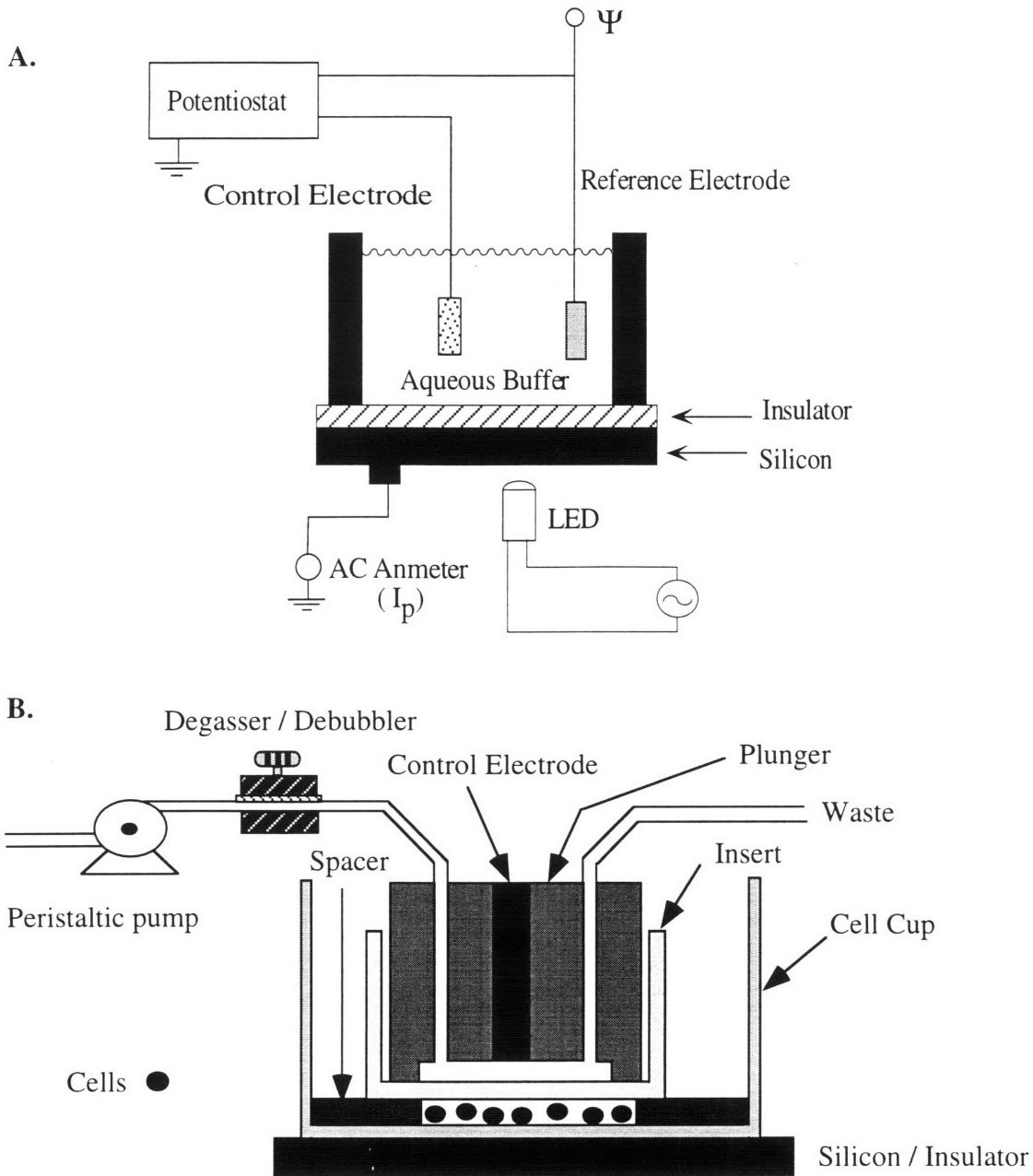
**Figure 1.16: pUHD10.3.** Second plasmid of the tetracycline controlled two plasmid system. (Adapted from Gossen and Bujard, 1992)



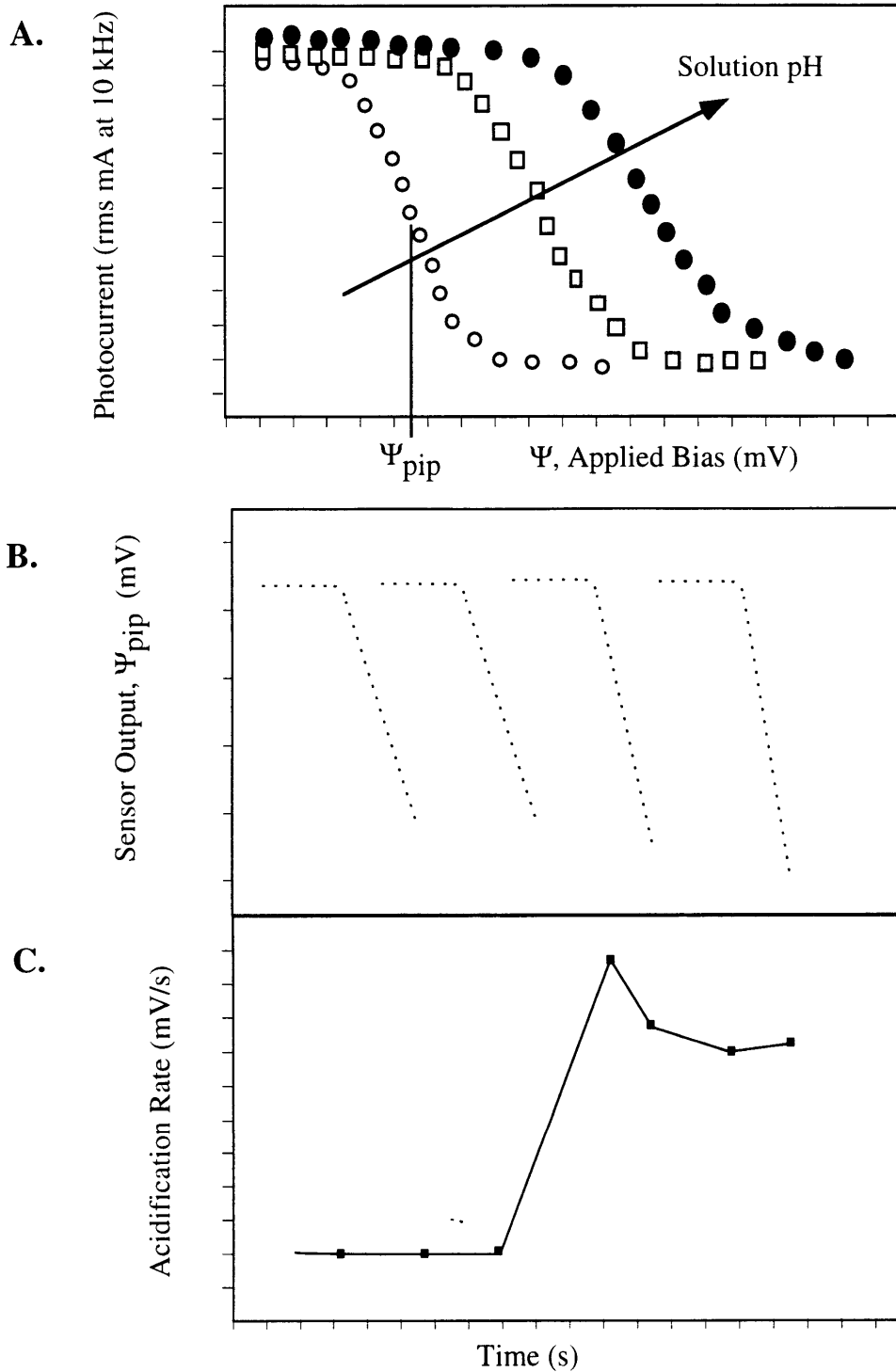
**Figure 1.17: Two plasmid schematic.** The removal of tetracycline allows the fused *tet* repressor / transcription activation protein to initiate transcription of mRNA.



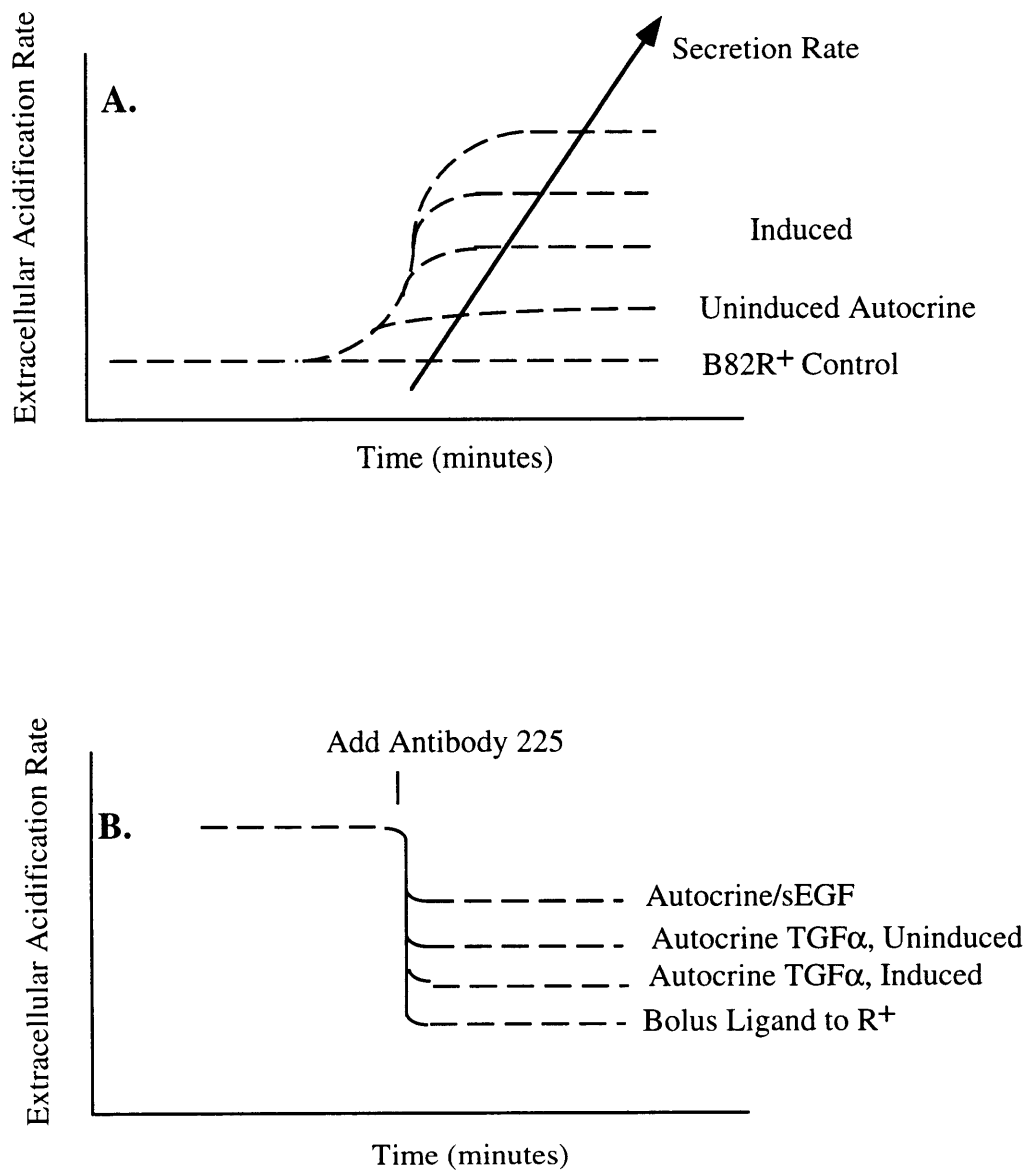
**Figure 1.18: Schematic of Ligand / Receptor signalling detection by Molecular Devices Cytosensor.**



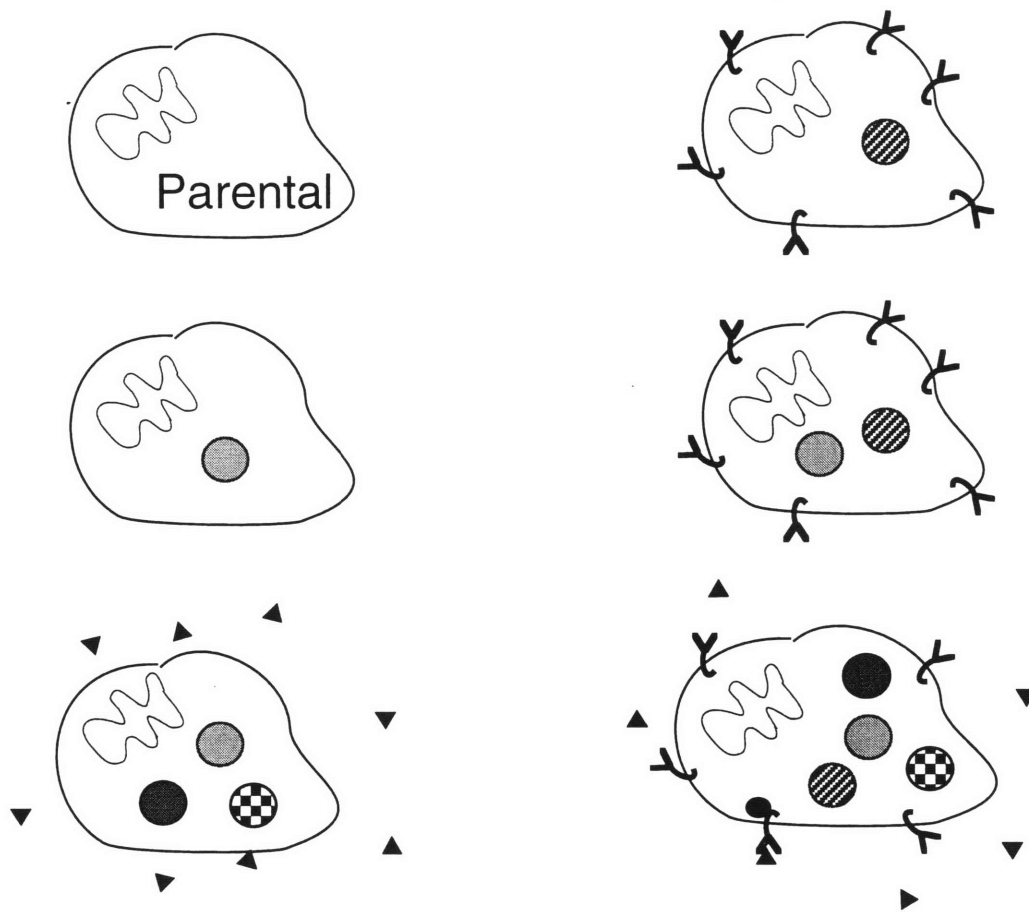
**Figure 1.19: Schematic drawing of Cytosensor.** Graph A) Schematic of light-addressable potentiometric sensor (LAPS) Graph B) Operational schematic of Cytosensor with peristaltic pump, degasser, sensor chamber and cells. (Adapted from McConnell, 1992).




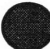


**Figure 1.20: Representation of Cytosensor measurement and output.** Graph A) Cytosensor's measurement of photocurrent resulting from applied potential. Graph B) Plot of  $\Psi_{pip}$  from Graph A as a function of time. Graph C) Rate data from Graph B determined by linear best fit line plotted versus time. (Adapted from Owicki, 1994).



**Figure 1.21: Predicted metabolic response of paracrine and autocrine cells.** Response rates are measured using Molecular Devices' Cytosensor. A) Effect of metabolic rate on autocrine cells upon addition of antibody. B) Metabolic response of autocrine cells as a function of tetracycline gradient/secretion rate gradient.



<b>Legend:</b>			
	pUHD15.1neo (1st Plasmid)		pXER (EGFR)
	pUHD10.3/TGF $\alpha$ (2nd Plasmid)		pR8 (Histidinol <sup>R</sup> )

**Figure 1.22: Artificially engineered B82 TGF $\alpha$  family.** A schematic of plasmids required to create a paracrine and autocrine TGF $\alpha$  cell system.

## Chapter 2: Modelling Autocrine Cell Receptor / Ligand / Antibody Interactions

### 2.1 Revising Anchorage-Independent to -Dependent Model

Described in chapter 1.5 was mathematical modeling work applied previously to IL-2 autocrine system for T-lymphocytes, which are anchorage-independent cells growing in suspension (Forsten and Lauffenburger 1992a; Forsten and Lauffenburger 1992b; Forsten and Lauffenburger 1994a). However, the B82R<sup>+</sup> / TGF $\alpha$  autocrine system is anchorage-dependent. Therefore, the existing model was modified from an anchorage-independent to -dependent cell situation. Figure 2.1 is a schematic illustration of the suspended autocrine cell with anti-receptor blocking antibodies (Forsten and Lauffenburger 1992b) while indicating important variables and parameters. Figure 2.1b is a schematic converting the anchorage-independent autocrine cell model to an anchorage-dependent cell situation with its additional relevant parameters indicated. The model equations for anchorage-dependent autocrine cells are listed in Table 4.1 (blocking antibody), Table 4.2 (decoy antibody), Table 4.3 (nomenclature). The anchorage-dependent LSODE programs are listed in Appendix C and D for blocking and decoy antibodies, respectively. Both models' parameter values were changed from IL-2 receptor system to EGF receptor system.

The secretion layer was determined to be the distance at which ligand flux becomes radial (Berg 1983), remains the same between suspension and anchored models. However, anchored cells have an advantage over suspended cells in that they are closer together in a 2D environment versus 3D environment. This close proximity of cells and cell-cell interactions suggests an intermediate boundary layer between the anchorage substratum and the bulk medium, represented by an intermediate volume parameter,  $V_i$ . Computer simulations with varying volume heights shows little effect on ligand concentrations and selected to be 25  $\mu\text{m}$  (Forsten and Lauffenburger 1992a). Thus, bulk volume,  $V_B$ , is the total volume minus cell, secretion, and intermediate layer volumes. As all calculations are based on volume per cell, the bulk volume and intermediate volumes need to be determined on a cell basis.  $\Psi$ , cell area ( $\text{cm}^2 / \text{cell}$ ), is a parameter based on assuming an evenly dispersed cell population on a defined surface area.  $V_i$  is calculated as intermediate boundary height times  $\Psi$ , minus cell and secretion layer volumes.  $V_B$  is equal to  $\Psi$  times the difference in medium height and intermediate boundary layer height in a culture dish. Extra diffusion terms are required for ligand and antibody trafficking between the intermediate boundary layer, secretion layer and bulk volumes. Thus, the following terms must be included in Equations 6, 7, 5, and 3 in Table 2.1 and similar substitution in Table 2.2:



$$\begin{array}{ll}
-\Delta_{\mathbf{L}}^i (L_{\mathbf{B}} - L_i) & \{1a\} \\
\Delta_{\mathbf{L}}^* (L_i - L^*) & \{1c\}
\end{array}
\qquad
\begin{array}{ll}
-\Delta_{\mathbf{B}}^i (B_{\mathbf{B}} - B_i) & \{1b\} \\
\Delta_{\mathbf{B}}^* (B_i - B^*) & \{1d\}
\end{array}$$

where:

$$\begin{array}{ll}
\Delta_{\mathbf{L}}^i = (\Pi D_{\mathbf{L}} \Psi^2) / \delta_{\text{int}} \{2a\} & \Delta_{\mathbf{B}}^i = (\Pi D_{\mathbf{B}} \Psi^2) / \delta_{\text{int}} \{2b\} \\
\Delta_{\mathbf{L}}^* = 2 \Pi D_{\mathbf{L}} (a + \delta) \{2c\} & \Delta_{\mathbf{B}}^* = 2 \Pi D_{\mathbf{B}} (a + \delta) \{2d\}
\end{array}$$

## 2.2 Computer Modelling Predictions

There are several different venues when analyzing B82R<sup>+</sup> / ligand autocrine cell signalling models; however, in this thesis, two directions were chosen: receptor / ligand complex levels and extracellular bulk ligand concentrations. The first is receptor / ligand complex levels. Figure 2.2 shows model predictions of cell receptor / ligand complex numbers as a function of anti-receptor blocking antibody concentration and ligand secretion rates for plated cells. Note that the receptor-ligand complex level are low compared to the total number of receptors available. However, only a small proportion of the total steady state receptors are required to initiate a mitogenic response (Knauer *et al.* 1984), at least in fibroblasts, as discussed in chapter 1.4 and shown in Figure 1.7. As seen and intuitively predicted, receptor / ligand complex levels increase with increasing ligand secretion rates, i.e. more ligand available allows formation of more complexes. Another important aspect of this graph is at what blocking antibody concentration completely inhibits receptor / ligand complexes. The model predicts a concentration of 1 nM blocking antibody will inhibit cell surface receptor / ligand complexes to essentially zero.

Figure 2.3 illustrates modelling predictions on the effect of anti-ligand decoy and anti-receptor blocking antibody additions to plated B82R<sup>+</sup> / ligand autocrine cells. As discussed in chapter 1.5 and Figure 1.11, blocking antibodies are predicted to be a superior inhibitor of receptor / ligand complexes compared to decoy antibody. Here again, it requires nearly 1,000 times more decoy antibody to completely inhibit receptor / ligand complexes. Changing the model from IL-2 to EGF also prominently affects decoy antibody's curve as to what level of inhibition will occur. In IL-2's curve, decoy antibodies started to inhibit complex as soon as blocking antibodies did, but had a second plateau over a large change in decoy antibody concentrations. In EGF autocrine cell model predictions, there was an offset in complex inhibition compared to blocking antibodies before complexes rapidly drop with a slope similar to blocking antibody's curve to zero. This difference in the curves is a result of ligand / receptor affinity and diffusion. IL-2's equilibrium dissociation constant,  $K_d$ , is 0.031 nM (Wang and

Smith 1987), while EGF's  $K_d$  is 1 nM. Both ligands have a  $k_{on}$  rate constant,  $0.1 \mu\text{M}^{-1} \text{sec}^{-1}$ ; however,  $k_{off}$  varies between the two by 1,000 fold. Thus, the antibodies are able to inhibit receptor / ligand complexes at an earlier concentration and mask the diffusion plateau when comparing differences between EGF and IL-2 receptor systems.

The next venue for modelling analysis is extracellular bulk ligand concentrations or the amount of ligand that escapes cell receptor binding and accumulates in the extracellular bulk medium. Extracellular bulk ligand concentration predictions on a per cell basis are plotted as a function of cell density in Figure 2.4a, for ligand synthesis rates of 30 and 6200 molecules / cell-minute and other parameter values given in the figure legend. These ligand secretion rates correspond to experimental data to be discuss in Chapter 4.7. One prediction is, at low cell densities, per-cell ligand levels should be similar regardless of blocking antibodies, but as cell density increases, per-cell ligand levels will decrease in the absence of antibody. This “clearance” is due to endocytic degradation mediated by binding to cell receptors (Will *et al.* 1995). Upon addition of blocking antibodies (at a concentration of  $20 \mu\text{g} / \text{ml}$ , or approximately 100 nM), ligand levels increase compared to cells without antibody. In the presence of blocking antibody, receptor-mediated ligand uptake is inhibited and extracellular bulk ligand concentrations remain constant regardless of cell density.

A second observation is a predicted difference in ligand clearance between low and high synthesis rates. At a low synthesis rate, ligand is rapidly lost from the medium at high cell densities. At a high ligand synthesis rate, ligand levels begin to decrease at the same cell density in the absence of antibody, but significantly less loss occurs at higher cell densities when compared to the low ligand secreting cells. This difference is due to competing ligand synthesis and receptor-mediated ligand degradation rates. At the higher ligand secretion rates, autocrine cells are simply creating more ligand than they can bind and degrade, becoming “pseudo-paracrine” cells (Will *et al.* 1995).

A common method of analyzing bulk ligand concentrations is to plot total ligand concentration per plate as shown in Figure 2.4b. Using this analysis, ligand accumulation increases linearly with increasing cell population in both the presence and absence of blocking antibodies at high ligand secretion rates. At lower secretion rates, ligand accumulation is also linear in the presence of antibody, due to the prevention of receptor-mediated ligand uptake and reaches an equilibrium between ligand uptake and secretion in the absence of blocking antibody. Both methods are valid, allowing the experimenter to analyze and interpret the data via two different methods.

These results underscore the necessity for measuring bulk ligand concentrations at defined (preferable low) cell densities and in the presence of sufficient blocking antibody in

order to reliably determine the ligand synthesis rate. Otherwise, one would obtain an incorrect ligand synthesis rate, underestimating the fraction of ligand taken up by cell receptors. This suggestion is consistent with the one previous examination of this topic, for the IL-2 T-lymphocyte system (Claret *et al.* 1992). In that work, it was found that 25-50 nM of anti-IL-2R blocking antibody was required to permit IL-2 to escape from secreting cells at maximal levels. The IL-2 synthesis rate can be estimated under these conditions to be approximately 300 molecules/cell-minute. These findings compare favorably with model predictions (Figure 2.2) that roughly 10-100 nM of an anti-receptor blocking antibody (possessing affinity on the order of 1 nM for the receptor) would be required, blocking a sufficient fraction of cell surface receptors and permitting a substantial amount of synthesized ligand to escape into the bulk extracellular medium. We note that this estimate depends on the cell density used by Claret *et al.* -- which was not reported in their study -- being sufficiently great (see Figure 2.4) that cell uptake of synthesized ligand in the absence of blocking antibody is indeed significant. Such an uncertainty reiterates the need to quantify key system parameters in order to properly interpret experimental findings.

This sort of mathematical modeling approach yields important insights concerning which molecular and cellular variables and parameters govern autocrine loop behavior. With an experimentally validated model, further detailed questions can be asked regarding regulation of autocrine signaling and consequent cell responses, not only allowing more rational design of therapeutic interventions but also deeper insight into fundamental biological mechanisms. A particularly intriguing issue, for instance, is the relationship between the level of autocrine ligand found in the extracellular environment and the functional significance of an autocrine loop. More precisely, it is typically considered that autocrine signaling is most important when a large concentration of autocrine ligand is found in the bulk medium, because this condition represents a "community" effect signal representing cell density (Alberts *et al.* 1994). However, it is alternatively conceivable that the most physiologically effective autocrine regulation occurs when very little ligand escapes into the extracellular medium. In this case, instead of reflecting information merely about cell density, the autocrine loop serves to give the secreting cell data about the molecular components present in its very local neighborhood; this can be termed a "sonar" effect. Thus, it will be crucial to be able to relate measurements of extracellular autocrine ligand concentration to other key parameters of the autocrine loop in order to properly understand the role of an autocrine loop in cell and tissue regulation.

**Table 2.1: Autocrine model equations - Blocker antibody**

1.  $dR / dt = -k_r R + V_r - k_{on} L^* R + k_{off} C - 2k_{on}^B B^* R + k_{off}^B Y - (k_c / sa) R Y + 2k_{coff} Y_2$
2.  $dC / dt = k_{on} L^* R - k_{off} C - k_e C$
3.  $V^* dB^* / dt = -2k_{on}^B B^* R + k_{off}^B Y + \Delta_B^* (B_i - B^*)$
4.  $dY / dt = 2k_{on}^B B^* R - k_{off}^B Y - k_1 Y + 2k_{coff} Y_2 - (k_c / sa) R Y$
5.  $V^* dL^* / dt = -k_{on} L^* R + k_{off} C + \Delta_L^* (L_i - L^*) + Q$
6.  $V_B dL_B / dt = -\Delta_L^1 (L_B - L_i)$
7.  $V_B dB_B / dt = -\Delta_B^1 (B_B - B_i)$
8.  $V_i dL_i / dt = -\Delta_L^* (L_i - L^*) + \Delta_L^1 (L_B - L_i)$
9.  $V_i dB_i / dt = -\Delta_B^* (B_i - B^*) + \Delta_B^1 (B_B - B_i)$
10.  $dY_2 / dt = (k_c / sa) R Y - 2k_{coff} Y_2 - k_2 Y_2$

where:

$$\Delta_L^* = 2\Pi D_L (a + \delta) \quad \Delta_B^* = 2\Pi D_B (a + \delta)$$

$$\Delta_L^1 = \pi D_L \Psi^2 / \delta_{int} \quad \Delta_B^1 = \pi D_B \Psi^2 / \delta_{int}$$

Initial Conditions:

$R / R_0 = 1.0$	Surface Receptors:	All receptor initially unbound
$C / R_0 = 0.0$	Surface Complexes:	No complexes
$B^* / B_i = 1.0$	Secretion Layer Antibody:	homogeneously distributed blocker concentration
$Y / R_0 = 0.0$	Bound Receptor / Antibody:	No initial binding
$L^* / K_d = 0.0$	Secretion Layer Ligand:	secretion has not begun
$L_B / K_d = 0.0$	Bulk Media Ligand:	secretion has not begun
$B_B / B_i = 1.0$	Bulk Media Antibody:	homogeneously distributed blocker concentration
$L_i / K_d = 0.0$	Intermediate Media Ligand:	secretion has not begun
$B_i / B_i = 1.0$	Intermediate Media Antibody:	homogeneously distributed blocker concentration
$Y_2 / R_0 = 0.0$	Receptor/Antibody/Receptor	No initial binding

where  $K_d$  is equilibrium dissociation constant and  $B_i$  is receptor blocker concentration

**Table 2.2 Autocrine model Equations - Decoy antibody**

1.  $dR / dt = -k_{on}L^*R + k_{off}C - k_tR + V_r$
2.  $dC / dt = k_{on}L^*R - k_{off}C - k_eC$
3.  $V^* dL^* / dt = -k_{on}L^*R + k_{off}C + 2k_{off}^sX^*V^* - 2k_{on}^sL^*S^*V^* - V^*k_{on}^sL^*Y^* + V^*k_{off}^sY^* + \Delta_L^*(L_1 - L^*) + Q$
4.  $V^* dS^* / dt = -2V^*k_{on}^sL^*S^* + V^*k_{off}^sY^* + \Delta_s^*(S_1 - S^*)$
5.  $V^*dY^* / dt = 2k_{on}^sS^*L^*V^* - k_{off}^sY^*V^* - k_{on}^sY^*L^*V^* + 2k_{off}^sX^*V^* + \Delta_s^*(Y_1 - Y^*)$
6.  $V^* dX^* / dt = V^*k_{on}^sL^*Y^* - 2V^*k_{off}^sX^* + \Delta_s^*(X_1 - X^*)$
7.  $V_B dL_B / dt = -2V_Bk_{on}^sL_B S_B + V_Bk_{off}^sY_B + 2k_{off}^sX_B V_B - k_{on}^sY_B L_B V_B - \Delta_L^*(L_B - L_1)$
8.  $V_B dS_B / dt = -2V_Bk_{on}^sL_B S_B + V_Bk_{off}^sY_B - \Delta_s^*(S_B - S_1)$
9.  $V_B dY_B / dt = 2k_{on}^sS_B L_B V_B - k_{off}^sY_B V_B - k_{on}^sY_B L_B V_B + 2k_{off}^sX_B V_B - \Delta_s^*(Y_B - Y_1)$
10.  $V_i dL_i / dt = 2k_{off}^sX_i V_i - 2k_{on}^sL_i S_i V_i - V_i k_{on}^sL_i Y_i + V_i k_{off}^sY_i - \Delta_L^*(L_1 - L^*) + \Delta_L^*(L_B - L_i)$
11.  $V_i dS_i / dt = -2k_{on}^sL_i S_i V_i + k_{off}^sY_i V_i - \Delta_s^*(S_1 - S^*) + \Delta_s^*(S_B - S_i)$
12.  $V_i dY_i / dt = 2k_{on}^sL_i S_i V_i - k_{off}^sY_i V_i - k_{on}^sY_i L_i V_i + 2k_{off}^sX_i V_i - \Delta_s^*(Y_1 - Y^*) + \Delta_s^*(Y_B - Y_i)$
13.  $V_i dX_i / dt = V_i k_{on}^sL_i Y_i - 2V_i k_{off}^sX_i - \Delta_s^*(X_1 - X^*) + \Delta_s^*(X_B - X_i)$
14.  $X_B = [S_t(V^* + V_1 + V_B) - (S^* + Y^* + X^*)V^* - V_i(S_1 + X_1 + Y_1) - V_B(S_B + Y_B)] / V_B$

where:

$$\Delta_L^* = 2\pi D_L(a + \delta) \quad \Delta_s^* = 2\pi D_s(a + \delta)$$

$$\Delta_L^1 = \pi D_L \Psi^2 / \delta_{int} \quad \Delta_s^1 = \pi D_s \Psi^2 / \delta_{int}$$

Initial Conditions:

$R / R_o = 1.0$	Surface Receptors:	All receptor initially unbound
$C / R_o = 0.0$	Surface Complexes:	No complexes
$L^* / K_d = 0.0$	Secretion Layer Ligand:	secretion has not begun
$S^* / S_t = 1.0$	Secretion Layer Antibody:	homogeneously distributed decoy conc.
$Y^* / S_t = 0.0$	Secretion Layer Bound L / Ab:	secretion has not begun
$X^* / S_t = 0.0$	Secretion Layer Bound L / Ab / L:	secretion has not begun
$L_B / K_d = 0.0$	Bulk Media Ligand:	secretion has not begun
$S_B / S_t = 1.0$	Bulk Media Antibody:	homogeneously distributed decoy conc.
$Y_B / S_t = 0.0$	Bulk Media Bound L / Ab:	secretion has not begun
$L_i / K_d = 0.0$	Intermediate Media Ligand:	secretion has not begun
$S_i / S_t = 0.0$	Intermediate Media Antibody:	homogeneously distributed decoy conc.
$Y_i / S_t = 0.0$	Intermediate Media L / Ab:	secretion has not begun
$X_i / S_t = 0.0$	Intermediate Media L / Ab / L:	secretion has not begun
$X_B / S_t = 0.0$	Bulk Media Bound L / Ab / L:	secretion has not begun

where  $K_d$  is equilibrium dissociation constant and  $S_t$  is ligand decoy concentration

**Table 2.3 Autocrine model nomenclature and parameter values**

Starbuck *et al.*, 1990

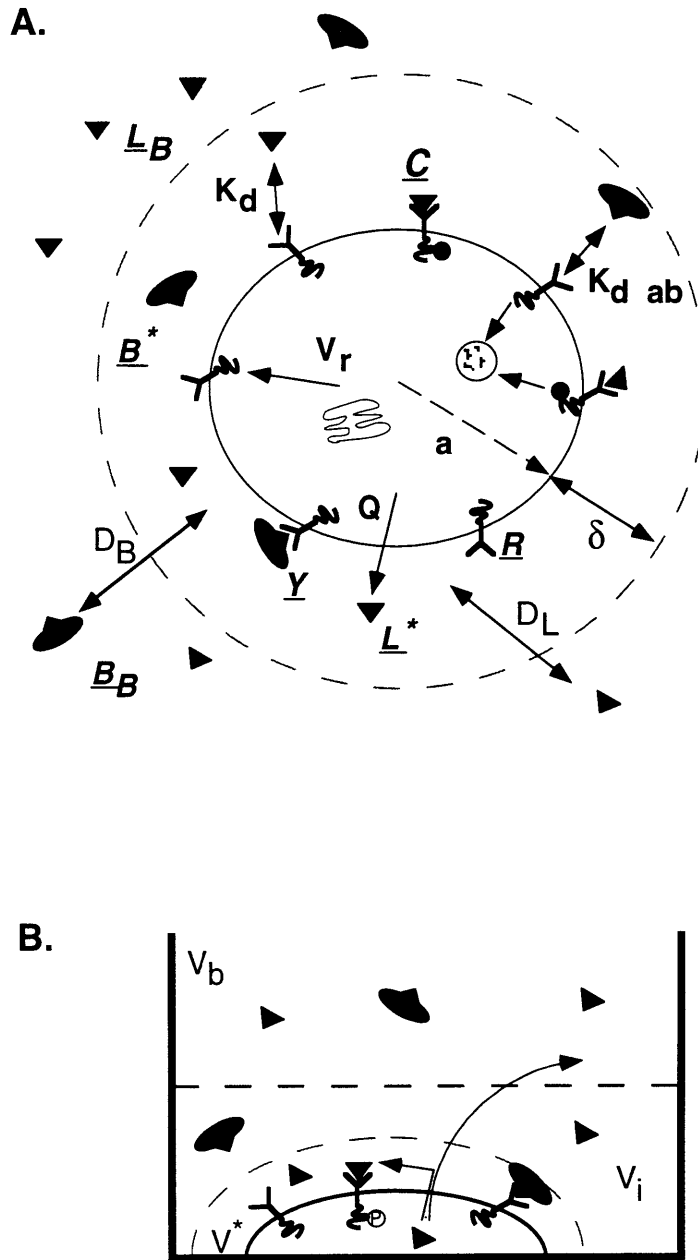
$K_d = 4.7 \text{ nM}$	Receptor / Ligand Equilibrium Dissoc. constant
$k_{on} = 0.34 \text{ min.}^{-1}$	Receptor / Ligand Dissociation rate constant
$k_{on} = 1.2e-13 \text{ cm}^3 / \text{ site-min.}$	Receptor / Ligand Association rate constant
$k_{on \text{ S,B}} = k_{on}$	Antibody - Antigen Dissociation rate constant
$k_{on \text{ S,B}} = k_{on}$	Antibody - Antigen Association rate constant
$R_o = 100,000 \text{ \# / cell}$	Initial receptor number
$k_t = 0.03 \text{ min.}^{-1}$	Constitutive internalization rate constant
$k_e = 0.3 \text{ min.}^{-1}$	Ligand-induced internalization rate constant

Forsten *et al.*, 1992a,b

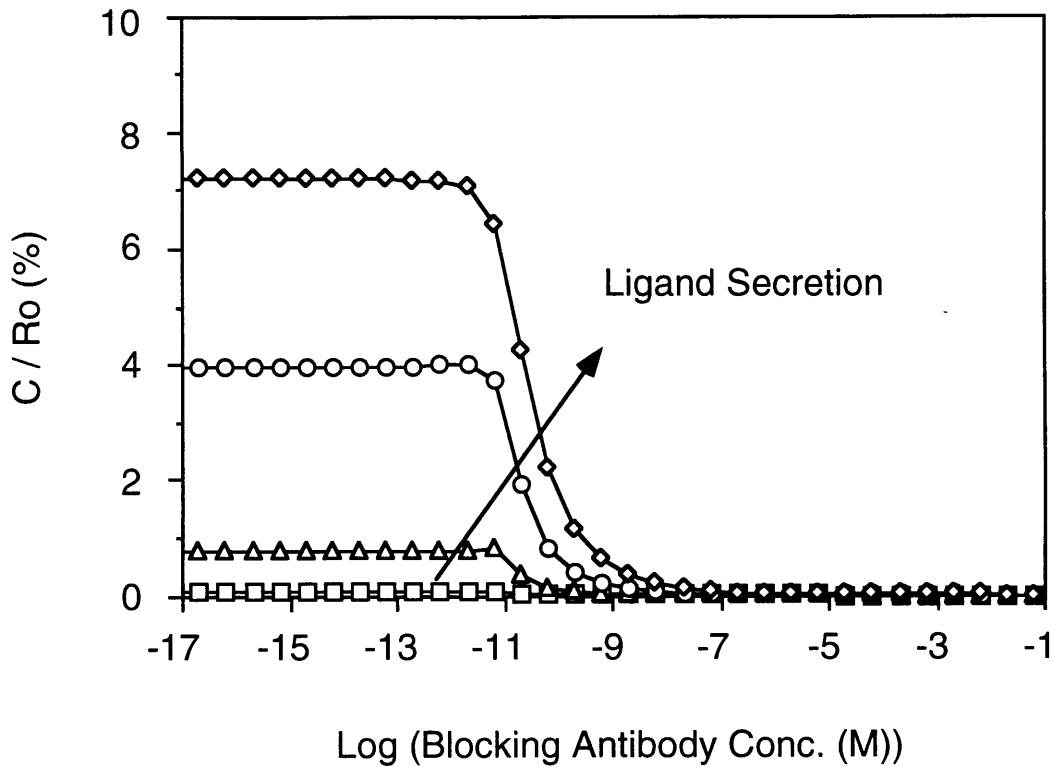
$k_1 = k_t$	Internalization rate const., Antibody / Receptor
$k_2 = k_e$	Induced internalization rate constant, Ab / Receptor / Ab
$\delta = 2e-5 \text{ cm}$	Secretion layer thickness
$\delta_{int} = 25e-4 \text{ cm}$	Intermediate layer thickness
$a = 5e-4 \text{ cm}$	Cell radius
$D_L = 9e-5 \text{ cm}^2 / \text{ min.}$	Ligand diffusion constant
$D_{S,B} = 2e-5 \text{ cm}^2 / \text{ min.}$	Antibody diffusion constant
$k_c = 480e-10 \text{ cm}^2 / \text{ min-molecule}$	Antibody / Receptor cell diffusion
$k_{coff} = 60 \text{ min}^{-1}$	Receptor / Antibody / Receptor dissociation

Experimental Conditions

$parea = 28.3 \text{ cm}^2$	60 mm dish plate area
$plvol = 5 \text{ cm}^3$	Media volume
$xheight = plvol / parea$	Height of media in plate
$\Psi = parea / \text{ cell density, cm}^2 - \text{ cell}$	Distance between cells - Homogeneously spread
$V_B = \Psi * (xheight - \delta_{int})$	Bulk volume
$V_{cell} = 5e-10 \text{ cm}^3 / \text{ cell}$	Cell volume
$V^* = 6.5e-11 \text{ cm}^3 / \text{ cell}$	Secretion layer volume
$V_1 = \Psi * \delta_{int} - V_{cell} - V^*$	Intermediate layer volume
$Q = 30 - 6,000 \text{ \# / cell - min.}$	Ligand secretion rate
$V_r = R_o * k_t$	Receptor secretion rate
$sa = 7.85e-7 \text{ cm}^2$	Cell surface area

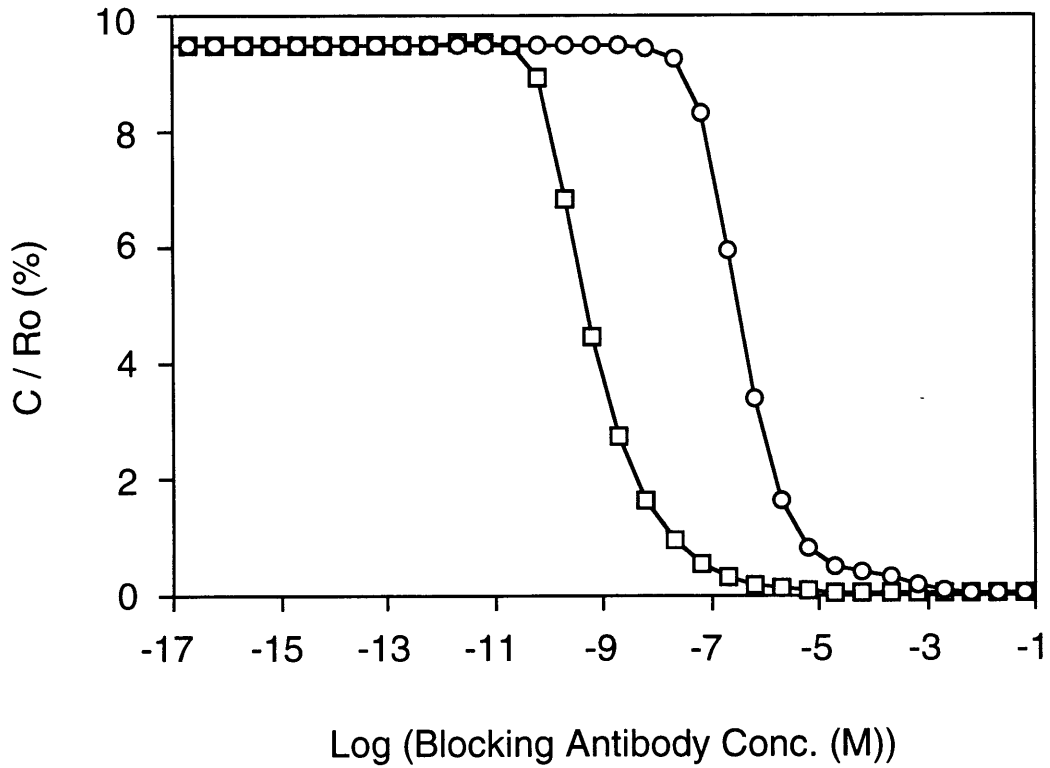


**Figure 2.1:** Autocrine computer model with blocker antibodies. Converting an autocrine suspension model (A) to a plated anchorage dependent model (B) with important variable indicated.

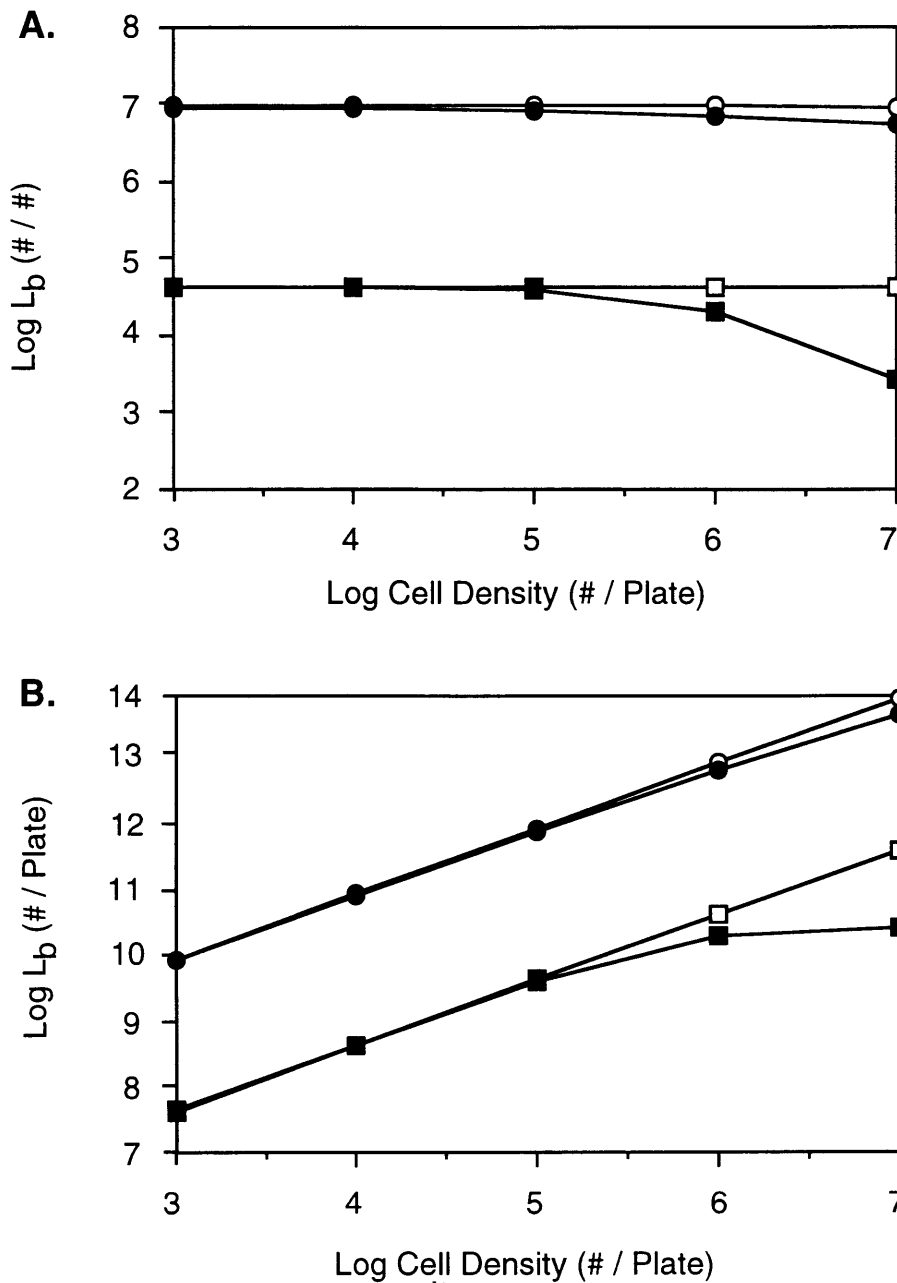


**Figure 2.2: Modelling predictions - Varying ligand secretion rates.** Effect of varying ligand secretion rate on receptor / ligand complex levels in the presence of anti-receptor blocking antibodies. Cell density is  $1e6$  cells / 60 mm plate. Ligand secretion rates: 30 (squares), 300 (triangles), 2000 (circles), and 6200 (diamonds) molecules / cell - minute.





**Figure 2.3: Modelling predictions - Blocker versus Decoy antibodies.** Comparison of receptor antibodies (squares) versus ligand decoy antibodies (circles) at a ligand secretion rate of 6,000 molecules / min. Cell density is  $10^7$  cells / plate.



**Figure 2.4: Modelling predictions - Bulk ligand concentrations.** Anchorage dependent autocrine cell model predictions of extracellular ligand concentrations as a function of cell density, ligand secretion rates, and blocking antibody concentrations. Ligand secretion rates are 30 (squares) and 6200 (circles) molecules / cell - minute. A. Bulk ligand concentrations as molecules / cell. B. Bulk ligand concentrations as molecules / plate. Antibody concentrations are 0 {-17 log} (solid) and 20 {-6.7} (open)  $\mu\text{g} / \text{ml}$ . Parameter values listed in Table 2.3.

## Chapter 3: Experimental Methods - Ligand Characterization

### 3.1 Materials

pUHD 15.1 and pUHD 10.3, shown in Figure 1.15 and 1.16, respectively, were made by Manfred Gossen and Hermann Bujard (University of Heidelberg, Heidelberg, Germany) and used with permission. pMTE4 (transmembrane TGF $\alpha$  cleavable protein), shown in Figure 3.1, was kindly provided by Dr. Rik Derynck (University of California-San Francisco, San Francisco, CA). The EGF receptor plasmid (pXER) in Figure 3.2 and B82 mouse fibroblast cells containing pXER were made and kindly provided by Dr. Gordon Gill (University of San Diego, San Diego, CA). The B82 EGF receptor and receptor minus cells containing pUHD15.1 (1st plasmid) was made and kindly provided by Dr. Birgit Will-Simmons (University of Utah, Salt Lake City, UT). The Bluescript II KS+ plasmid, Figure 3.3, was obtained from Strategene. pREP8 in Figure 3.4 was purchased from Invitrogen and modified into pR8 by Dr. Birgit Will-Simmons with the removal of the EBNA-1 and OriP (epstein barr virus origin of replication) segments to prevent episomal replication and allow for incorporation into chromosomal DNA.

The restriction enzymes and DNA modifying enzymes were purchased from Gibco BRL, New England Biolabs and Boehringer Mannheim. Bovine calf serum was purchased from Hyclone. Dulbecco-Volt Modified Eagle Media was purchased from Gibco BRL. Methotrexate, geneticin sulfate (G418) and histidinol were purchased from Sigma. The monoclonal antibodies 225 and 528 were produced and purified from hybridomas in Steve Wiley's lab. TriReagent (used for RNA isolation) was purchased from Molecular Research Center, Inc.

PBS/EDTA solution is 2.7 mM KCL, 1.5 mM KH<sub>2</sub>PO<sub>4</sub>, 137 mM NaCl, 8.1 mM Na<sub>2</sub>HPO<sub>4</sub>, 0.6 mM EDTA, 17 mg/liter phenol red. PBS/EDTA/trypsin is 90% PBS/EDTA and 10% of 0.5% trypsin solution in Ca/Mg free PBS.

B82 cells containing pUHD15.1 were selected and cultured in Dulbecco-Volt Modified Eagle Media with 10% bovine calf serum, 1 mM glutamine, 100 units/ml penicillin and 2.5  $\mu$ g/ml streptomycin. Selection was achieved and maintained with 600  $\mu$ g/ml G418. Medium for the B82 cells containing pXER (B82R<sup>+</sup>) used dialyzed bovine calf serum (6-8000 MWCO in PBS) and 1  $\mu$ M methotrexate to maintain selection on pXER.

B82 cells containing pUHD 15.1, pUHD10.3 / TGF $\alpha$  and pR8 were selected and cultured in a specially made medium containing a subset of amino acids (except histidine), salts, vitamins, 10% bovine calf serum, 1 mM glutamine, 100 units/ml penicillin and 2.5  $\mu$ g/ml streptomycin. See Appendix A for detailed listing of components and concentrations. Selection

was achieved and maintained with 600 µg/ml G418, and 800 µM histidinol. Suppression of TGFα secretion was achieved with 1-2 µg/ml of tetracycline. Medium for cells with pXER also contained dialyzed bovine calf serum and 1 µM methotrexate to maintain selection.

### 3.2 Making pUHD10.3 / TGFα

The 2nd plasmid, pUHD 10.3, contains pBR322 ColE1 and β-lactamase antibiotic resistance segments, a regulatory region with tetracycline operators, multiple cloning sites, and a SV40 polyadenylation sequence.

The TGFα plasmid, pMTE4, contains the signal sequence, mature TGFα protein sequence and TGFα cleavable transmembrane sequence. The plasmid uses the SV40/DHFR resistance segment for selection and a early SV40 promoter for constitutive TGFα expression. The entire TGFα sequence was removed from pMTE4 with a HindIII digest. The 800 bp fragment was placed into a unique HindIII site in Strategene's Bluescript II KS+ plasmid in the T7 to T3 orientation as shown in Figure 3.5.

The entire TGFα wild type sequence was cut from the Bluescript KS+ II/TGFα plasmid with XhoI and EcoRI. Before digesting the plasmid with EcoRI, the linear plasmid (cut with XhoI) was blunted with a Klenow enzyme fragment. The Klenow was disabled by heating at 75 ° C for 10 minutes before adding EcoRI restriction enzyme to remove the TGFα insert. pUHD10.3 was prepared by digesting the plasmid with BamHI, blunting with Klenow enzyme and finally digesting with EcoRI to provide a sticky end for the TGFα insert. The DNA fragments were isolated by running a 1% agarose gel, isolating the correct DNA segments and purified by Millipore filters. The concentration and molecular weight of the DNA was measured by running a 1% agarose gel. The DNA concentrations were determined to be 50 ng/µl for the 800 bp TGFα insert and 15 ng/µl for the 3 kbp pUHD10.3. One hundred ngs of the two DNA pieces were ligated together in a 6:1 molar ratio overnight at 16 ° C with 1 unit of T4 ligase.

The following morning, all of the ligated DNA was added to 100 µls of competent DH5α bacteria and stored on ice for 30 minutes in a 10 ml Falcon tube. The bacteria / DNA mixture was heat shocked for 90 seconds at 42 ° C before returning to ice for 2 minutes. Eight hundred µls of SOC media (2% bactotryptone, 0.5% yeast extract, 10 mM NaCl, 2.5 mM KCl, 10 mM MgCl<sub>2</sub>, 10 mM MgSO<sub>4</sub>, 20 mM glucose in ddH<sub>2</sub>O) was added to the bacteria and incubated for 45 minutes at 37 ° C before streaking the bacteria onto LB/ ampicillin (100 µg/ml) plates to grow overnight at 37 ° C. Three ml LB / ampicillin minipreps of individual bacteria colonies were grown overnight and the plasmid isolated using Promega's Wizard Miniprep. The purified plasmid was checked for the presence of the TGFα insert using PstI enzyme as the TGFα insert contains two sites, 50 bp apart, while pUHD10.3 does not contain a PstI

restriction site. A 1% agarose gel of the cut DNA showed that four of the twelve minipreps had the TGF $\alpha$  insert due to the less mobile linear plasmid running slower than the uncut supercoiled pUHD10.3 without the TGF $\alpha$  insert. The bacteria from miniprep #3 was grown in 200 mls LB / ampicillin and pUHD10.3 / TGF $\alpha$  (Figure 3.6) purified using Promega's Wizard Maxiprep.

### 3.3 Transfection of DNA into B82 Cells

The transfection of the B82 cells were accomplished using a CaPO<sub>4</sub> / DNA precipitate solution placed on a sparse cell population (Kriegler 1990; Wigler *et al.* 1979).

The day before DNA transfection, approximately one million B82R<sup>+</sup> / pUHD15.1 and B82R<sup>-</sup> / pUHD15.1 cells are plated into separate 60 mm Corning dishes containing normal medium. The next day, 30  $\mu$ g of pUHD 10.3 / TGF $\alpha$  and 10  $\mu$ g of pR8 were mixed into 250  $\mu$ ls of nanopure water. The DNA was sterilized with 250  $\mu$ l chloroform, mixed and then centrifuged at 10,000x g for 2 minutes. The top aqueous / DNA layer was combined with 500  $\mu$ ls of 2x HBS (HEPES Buffered Saline: 10 mM KCl, 11 mM Glucose, 1.4 mM Na<sub>2</sub>HPO<sub>4</sub>, 171 mM NaCl, and 42 mM HEPES), 200  $\mu$ ls of nanopure (sterile) water and 50  $\mu$ ls of 2.5 M CaCl<sub>2</sub>. After mixing and standing at room temperature for 30 minutes, 500  $\mu$ ls of the CaPO<sub>4</sub> / DNA precipitate solution was added to the B82R<sup>+</sup> / pUHD15.1 and B82R<sup>-</sup> / pUHD15.1 cells in normal medium.

After 24 hours, the CaPO<sub>4</sub> medium was removed and the cells rinsed with PBS/EDTA. Nonselective medium was added to the plates for 24 hours to allow the transfected cells to become histidinol resistant. On the second day, the medium was removed, the cells were rinsed with PBS/EDTA and trypsinized. All the cells from each transfection were passed at a 1:4 dilution into 60 mm Corning dishes containing selective medium (histidinol, G418, tetracycline and no histidine (His<sup>-</sup> media)). On the third day, the selective medium was removed and the cells washed with PBS/EDTA to remove dead cells before adding fresh selective medium to the plate. The selective medium was replaced about every three days until colonies appear (approximately 200-1000 cells per colony). The colonies were isolated using Bellco 8 x 8 mm glass cloning cylinders and transferred into an individual well of a Falcon 24 well plate containing selective medium. Cells found to produce secreted TGF $\alpha$  were maintained and cultured in the presence of selective medium.

### 3.4 Selection of TGF $\alpha$ Secreting Clones

The cells were grown from the Falcon 24 well plates into 3 wells of a 12 well Falcon plate - uninduced, induced and founder cells. Upon cell confluence, TGF $\alpha$  expression was induced by the removal of tetracycline-containing medium and replaced with tetracycline-free

medium. The following day, induced and uninduced cell medium was replaced, respectively, with fresh tetracycline-free medium and tetracycline medium, beginning the 24 hour secretion period. The tetracycline-free medium was added a day early to remove the tetracycline suppression, thus enabling the measurement of steady-state TGF $\alpha$  production. The B82R<sup>+</sup> / pUHD15.1 / pUHD10.3 - TGF $\alpha$  medium additionally contained 10  $\mu$ g/ml of anti-EGFR monoclonal antibody 528 to prevent receptor-mediated TGF $\alpha$  uptake.

At the end of the 24 hour period, one ml of medium was saved and the remaining volume recorded. The saved media was placed into a 1.6 ml centrifuge tube and spun at 17,000x g for 10 minutes to remove cell debris. The medium supernatant was stored at -70 ° C. Cell number was determined using a Coulter Counter Model ZBI010 with a 0.5 ml counting volume and threshold setting at 1 to 15  $\mu$ m.

### **3.5 Detection of TGF $\alpha$**

The detection of TGF $\alpha$  in the medium was performed using an Oncogene Science (OS) TGF $\alpha$  ELISA kit. The ELISA kit uses a sandwich enzyme immunoassay specific to TGF $\alpha$ , using pre-coated polyclonal goat anti-TGF $\alpha$  wells and goat anti-TGF $\alpha$  secondary biotinylated antibody. The binding of streptavidin-horseradish peroxidase to the secondary antibody allowed for the detection of TGF $\alpha$  by catalyzing the conversion of o-phenylenediamine dihydrochloride from a colorless chromophore to an amber chromophore. The 490 nm absorbance was measured using Molecular Devices spectrophotometer Model 250 and Biometallics, Inc  $\Delta$ Soft 1.8 Vmax software. Quantification of TGF $\alpha$  present was obtained using the six TGF $\alpha$  concentration standards in the ELISA kit.

Medium samples were removed from -70 ° C and thawed on ice before removing a 55  $\mu$ l aliquot and adding it to a 55  $\mu$ l aliquot of the 1:20 diluted OS secondary antibody. The OS ELISA wells were rinsed with 200  $\mu$ ls of 1x OS rinse buffer before adding 100  $\mu$ ls of the medium sample / antibody mixture. After a 3 hour room temperature incubation, the wells were washed three times with 1x OS wash buffer and rinsed twice with 1x OS rinse buffer. A 100  $\mu$ ls 1:100 dilution of streptavidin-horseradish peroxidase was added to each well and incubated for 30 minutes at room temperature. The wells were washed and rinsed again (as above) before adding 100  $\mu$ ls of the o-phenylenediamine solution. The reaction was incubated in the dark for 45 minutes before stopping with 100  $\mu$ ls of 4 N sulfuric acid and solution absorbance measured at 490 nm.

Medium samples, antibody, and streptavidin-horseradish peroxidase were diluted in assay buffer provided by Oncogene Science. The OS TGF $\alpha$  standards were diluted in unconditioned medium. The o-phenylenediamine tablet was diluted in substrate buffer provided

by Oncogene Science. Concentration and composition of buffers was not provided in the OS ELISA kit. The TGF $\alpha$  standards were 0, 50, 250, 500, 750 and 1000 pg/ml.

### **3.6 Determining Cellular Processing of TGF $\alpha$ Protein**

Twelve 100 mm Corning dishes were plated at a cell density of 1:10 with paracrine cells in tetracycline-free medium. After 24 hours, the medium was removed, cells washed with 1x PBS/EDTA and 5 mls of serum-free tetracycline-free medium added to each dish. After 6 days, all of the medium was collected and placed on ice. The medium was concentrated using an Amicon concentrator with a YM 3000 MWCO (molecular weight cut off) membrane filter. The medium was further concentrated in several 2 ml capacity Amicon centricons with 3000 MWCO by spinning at 7,000x g for four 2 hour periods. Both methods were performed on ice or at 4 °C. The medium volume was concentrated from 60 mls down to 1 ml using these two methods. The final concentration of TGF $\alpha$  was determined to be 160 ng/ml by Oncogene Science TGF $\alpha$  ELISA.

The molecular weight of the TGF $\alpha$  was determined using a meter G-50 fine Sephadex column, calibrated with the appropriate standards. 622  $\mu$ ls (100 ngs) of the concentrated TGF $\alpha$  was added to the mixture of protein standards in Table 2.1 and 59  $\mu$ ls of pure glycerol for a total volume of 1181  $\mu$ ls.

The protein/glycerol solution was added to a small PBS buffer head on top of the G-50 column. The protein was eluted into the beads before a larger buffer head was added. The column ran at 40 mls per hour with the effluent running through a spectrophotometer/chart recorder and into a fraction collector. The spectrophotometer/chart recorder was set at 280 nm absorbance, 6 cm/hr chart speed with a 0.5 absorbance range. The fractions were collected in 5 minute aliquots over 9 hours. Immediately after running the column, the fractions were assayed for TGF $\alpha$  protein using the Oncogene Science TGF $\alpha$  ELISA kit.

Cellular processing of the TGF $\alpha$  protein was also confirmed by determining the concentration of TGF $\alpha$  in the medium and cell membrane. Two Corning 60 mm dishes containing either autocrine or paracrine TGF $\alpha$  B82 cells were grown to 50% confluence before washing the cells with PBS/EDTA. Tetracycline-free medium was added to the cells and grown for 24 hours at 37 °C. The cells' medium was replaced with fresh tetracycline-free medium after washing the cells with PBS/EDTA to begin the 24 hour secretion period. As always, medium for the autocrine cells contained 10  $\mu$ g/ml of anti-EGFR monoclonal antibody 528 to prevent the uptake of TGF $\alpha$  by the EGFR receptor. At the end of the 24 hour secretion period, one ml of medium was saved from each cell type and the remaining volumes recorded. The

saved medium was placed into a 1.6 ml microcentrifuge tube and spun at 17,000x g for 10 minutes to remove cell debris. The medium supernatant was stored at -70 °C.

The membrane TGF $\alpha$  was extracted as follows. An extraction buffer was made with 800  $\mu$ ls 25 mM CHAPS, 10  $\mu$ ls of 400 mM sodium iodoacetate, 10  $\mu$ ls each of pepstatin, leupeptin, chymostatin, and aprotinin (all at 10 mg/ml) and diluted to 1 ml with ddH<sub>2</sub>O. The cells were rinsed three times with PBS / EDTA before adding 250  $\mu$ ls of extraction buffer to each plate. The cells were scraped off the dish and placed in a 1.6 ml microcentrifuge tube on ice. The dish was rinsed with 250  $\mu$ ls of extraction buffer and added to the microcentrifuge tube. After incubating for 15 minutes on ice, the samples were spun at 17,000x g for 15 minutes to remove debris. The supernatant was transferred to a new tube and stored at -70 °C.

Cell number was determined by counting a similarly plated cell dish using a Coulter Counter Model ZBI010 with a 0.5 ml counting volume and threshold setting at 1 to 15  $\mu$ m. The 0.5 mls of trypsinized cells were diluted in 1.5 mls of medium to inhibit further cell trypsinization and degradation before adding 18 mls of PBS to count the cells.

### **3.7 TGF $\alpha$ Secretion Time Course from Paracrine Cells**

Cells from three confluent 60 mm Corning dishes were plated into thirty 60 mm Corning dishes at a cell density of 1:10 in tetracycline-containing medium. The cells were allowed to settle and grow in the dishes for 24 hours before removing the medium and washing the cells with 1x PBS/EDTA. Five mls of tetracycline-free medium was added to all thirty plates to begin the time course experiment at time equal zero hours. A “pseudo” pulse/chase experiment was also performed by adding tetracycline-containing medium to half of the dishes after the cells were in tetracycline-free medium for 12 hours to induce the expression of TGF $\alpha$ .

At each time point, one dish was used for medium sampling and extracting RNA, while another dish were used to determine cell density. At the correct time, one ml of medium was collected from a dish, spun at 17,000x g for 10 minutes at 4 °C before storing the supernatant at -20 °C. One ml of TriReagent was added to the dish and cells lyzed for 10 minutes before collecting the TriReagent/cell extract in a 1.6 microcentrifuge tube and storing at -20 °C. Upon completion of time course experiment, the TriReagent and medium samples were transferred to -70 °C storage. Cell number was determined as described before using the Coulter Counter Model ZBI010. The time points for this experiment are shown in Table 2.2. Conditioned medium's TGF $\alpha$  concentration was determined later by Oncogene Science TGF $\alpha$  ELISA

The asterisk symbol (\*) and bold print denotes when fresh medium was added to cells for the next 24 hour period. The 24 hour replacement of fresh medium was done to maintain



cells in a constant, non-depleting environment of nutrients, growth factors, etc. and were applicable in a constant concentration of tetracycline.

### **3.8 Tetracycline Concentration Effect on TGF $\alpha$ Secretion**

The uninduced autocrine B82R<sup>+</sup> / TGF $\alpha$  and paracrine B82R<sup>-</sup> / TGF $\alpha$  cells were plated into a 6 well Falcon plate. The following day, cell medium were replaced with a tetracycline containing gradient to begin the induction of TGF $\alpha$ . 24 hours later, cell medium was replaced with fresh medium containing the same tetracycline gradient to start the 24 hour secretion experiment. The tetracycline gradient was 500  $\mu$ g/ml, 100 ng/ml, 10 ng/ml, 2 ng/ml, 1 ng/ml, 200 pg/ml. Normal suppression of TGF $\alpha$  secretion was achieved using 1  $\mu$ g/ml, therefore, these concentrations represent a 500/1, 1/10, 1/100, 1/500, 1/1000, 1/5000 gradient, respectively. Medium for autocrine cells also contained 10  $\mu$ g/ml of anti-EGFR monoclonal antibody 528 to prevent TGF $\alpha$  uptake by the EGF receptor.

At the end of the 24 hour period, one ml of medium was saved and the remaining volume recorded. The saved medium was placed into a 1.6 ml centrifuge tube and spun at 17,000x g for 10 minutes to remove cell debris. The medium supernatant was stored at -70 ° C. Conditioned medium's TGF $\alpha$  concentration was determined by Oncogene Science TGF $\alpha$  ELISA

Due to the low number of cells present, cell density was determined using a hemocytometer. The resuspended trypsinized cell solution was placed in the hemocytometer and cell number per 4-9 squares counted depending on cell concentration. The average number of cells per square multiplied by 10,000 gives cell concentration as number / ml.

This experiment was repeated by plating 250,000 autocrine B82R<sup>+</sup> / TGF $\alpha$  clone #1 cells into eighteen 60 mm Corning dish giving a 3 plate replicate with six different tetracycline concentrations. 24 h later, TGF $\alpha$  expression was pre-induced by addition of a tetracycline gradient to the cells. The tetracycline gradient was 10, 1, 0.1, 0.01, 0.001, and 0  $\mu$ g / ml. The next day, the 24 hour experiment was begun by replacing cell medium with fresh medium containing the tetracycline gradient and 10  $\mu$ g / ml blocking anti-EGFR antibody 225. At the end of the 24 hour period, one ml of medium was saved and the remaining volume recorded. The saved medium was placed into a 1.6 ml centrifuge tube and spun at 17,000x g for 10 minutes to remove cell debris. The medium supernatant was stored at -70 ° C. Conditioned medium's TGF $\alpha$  concentration was determined by Oncogene Science TGF $\alpha$  ELISA. Cell number was determined using a Coulter Counter Model S/STD IIA and Multisizer II with a 0.5 ml counting volume and threshold setting at 9.3  $\mu$ m to out. Trypsinized cells were diluted in

medium to inhibit further cell trypsinization and degradation before adding Isoton II solution to count cell number.

### **3.9 Cell Density Effect on TGF $\alpha$ Secretion**

B82R<sup>+</sup> (pXER) / pUHD15.1 / pUHD10.3 - TGF $\alpha$  / pR8 (autocrine clone #1) cells were serially diluted (two fold dilutions per point) into sixty 60 mm Corning dishes from 0.02-1 x 10<sup>6</sup> cells / dish as four sets (15 dishes / set). Triplicate cell density replicate points are done at 5e5, 6e4, and 8e3 cells / dish. On the next day, two sets were induced for the expression of TGF $\alpha$  by removal of tetracycline from the medium. Following an additional 24 h incubation, fresh medium containing tetracycline or tetracycline free medium was added to the cells with or without 20  $\mu$ g / ml monoclonal anti-receptor 225 as appropriate, giving the following experimental conditions: induced cells with mAb225, induced cells without mAb225, uninduced cells with mAb225 and uninduced cells without mAb225. The amount of antibody added was constant and not adjusted for cell density or receptor number.

24 hours later, one ml of conditioned medium was removed, spun at 17,000x for 10 minutes to remove cell debris and stored at -20 °C. Conditioned medium's TGF $\alpha$  concentration was determined by Oncogene Science TGF $\alpha$  ELISA

Cell number was determined using a Coulter Counter Model S/STD IIA and Multisizer II with a 0.5 ml counting volume and threshold setting at 9.3  $\mu$ m to out. Trypsinized cells were diluted in medium to inhibit further cell trypsinization and degradation before adding Isoton II solution to count cell number. Varying amounts of medium and Isoton II solution was used to dilute cell numbers at high cell density and maximize cell number at low cell densities during cell counting for counting on the Coulter Counter.

### **3.10 Creation of sEGF clones**

Creation of B82R<sup>+</sup> wild type / sEGF and B82R<sup>-</sup> / sEGF clones was performed by Dr. Birgit Will-Simmons (Will *et al.* 1995). Normal EGF is synthesized as a transmembrane protein (170 kDa) and the mature protein (6 kDa) is enzymatically cleaved into the medium upon surface expression. The EGF gene sequence used by Dr. Will-Simmons is the mature protein or secreted EGF, hence the term sEGF. The gene sequence was constructed by Niyogi's lab (Engler *et al.* 1988) for expression in *E. Coli*. To obtain mammalian expression, Dr. Will-Simmons switched EGF's bacteria signal sequence with EGFR's mammalian signal sequence. The new EGF construct was then placed into pUHD10.3, 2nd plasmid of the tetracycline controlled expression system, creating pUHD10.3 / sEGF. The plasmid was co-transfected with pR8 (histidinol resistance) into B82 EGFR positive and negative cells previously

transfected with pUHD15.1neo, the first plasmid of the tetracycline controlled expression system.

During this thesis work, pUHD10.3 / sEGF was transfected into several B82 cells containing mutated EGF receptors (A654, M721, M721A654,  $\Delta$ 647) (Lund *et al.* 1990; Wiley *et al.* 1991). These mutated EGFR B82 cells were previously transfected with pUHD15.1neo, allowing control of sEGF expression. All transfections done by Birgit and myself with pUHD10.3 / sEGF and pUHD15.1neo into B82 cells used the method of Wigler as described earlier in section 3.3

Detection of EGF was achieved by sandwich ELISA similar to TGF $\alpha$ 's. Monoclonal anti-EGF antibody HA (gift from Katsuzo Nishikawa, Kanazawa Medical University, Japan) in PBS / 0.02% sodium azide (PBSN) at 5-10  $\mu$ g / ml was used to coat the 96 well ELISA wells. ELISA wells were rinsed with 0.05% Tween-20 in PBSN after every addition. ELISA wells were blocked with 10% horse sera in PBSN (blocking buffer). A rabbit polyclonal sera directed against EGF was used as a secondary antibody diluted 1:100 in blocking buffer. Alkaline phosphatase-conjugated goat anti-rabbit antibody (Sigma) was used as the tertiary antibody at a dilution of 1:6000. Detection was achieved by using 1 mg / ml dinitrophenol (Sigma) in 10 mM diethanolamine and 0.5 mM MgCl<sub>2</sub>, pH 9.5. The reaction was quenched with 0.1 M EDTA after 4-10 minutes. Solution absorbance was read at 405 nm using Molecular Devices spectrophotometer Model 250 and Biometallics, Inc  $\Delta$ Soft 1.8 Vmax software. All solution volumes were 50  $\mu$ l except 200  $\mu$ l of blocking buffer was used to block ELISA plate. The ELISA plate was incubated overnight at room temperature to coat ELISA with monoclonal antibody HA and overnight again to block ELISA plate with 10% horse sera. The medium samples and antibody incubations were 2 hours at room temperature.

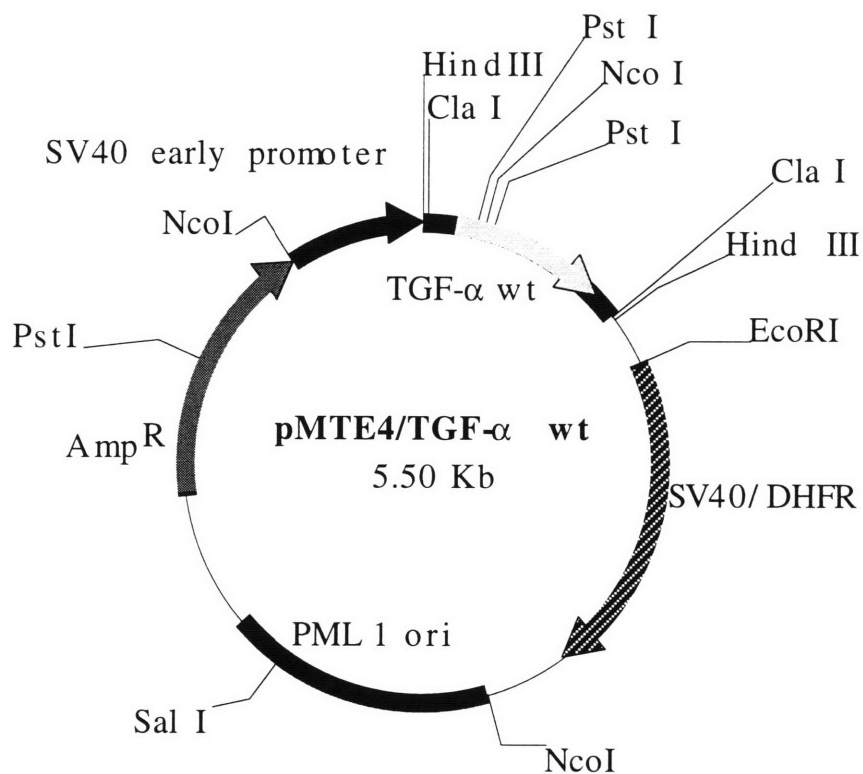
**Table 3.1: Molecular weight standards used for G-50 fine column.**

<b>Protein</b>	<b>MW Size (kDa)</b>	<b>Amount (mgs)</b>	<b>Volume (<math>\mu</math>ls)</b>
Albumin	66	2.5	100
Carbonic Anhydrase	29	1	100
Cytochrome C	12.4	1	100
Aprotinin	6.5	3	200

**Table 2.2: Time course points for TGF $\alpha$  secretion from paracrine B82 cells.**

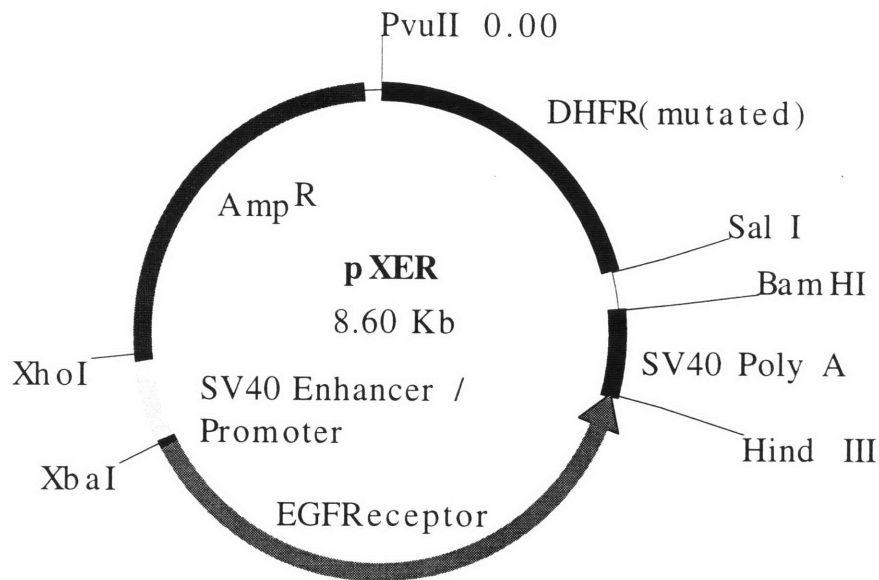
No Tetracycline	Pulse/Chase (Tetracycline added)
0 hour	
4 hours	
8 hours	
12 hours	0 hour (Addition of Tetr. Media)
18 hours	6 hours
<b>24 hours *</b>	12 hours
	18 hours
36 hours	<b>24 hours *</b>
<b>48 hours *</b>	36 hours
60 hours	<b>48 hours *</b>
	60 hours

The asterisk symbol (\*) and bold print denotes when fresh media was added to the cells for the next 24 hour period.



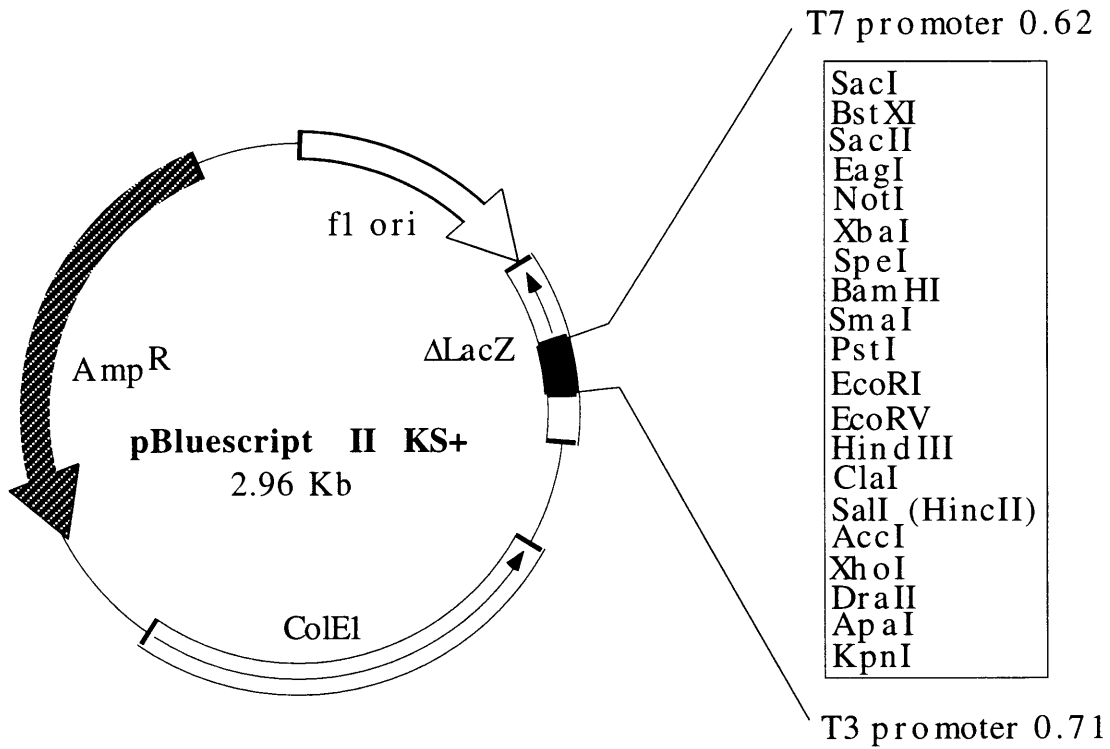
Plasmid name: pMTE4/ TGF- $\alpha$  wt  
 Plasmid size: 5.50 kb  
 Constructed by: Rik Derynck  
 Construction date:  
 Comments/References: Cell, **46**, 301-309, 1986

**Figure 3.1: pMTE4.** Cleavable prepro transmembrane TGF $\alpha$ . (Adapted from Derynck *et al.*, 1986)



Plasmid name: pXER  
 Plasmid size: 8.60 kb  
 Constructed by: Gordon Gill  
 Construction date: Unknown  
 Comments/References:

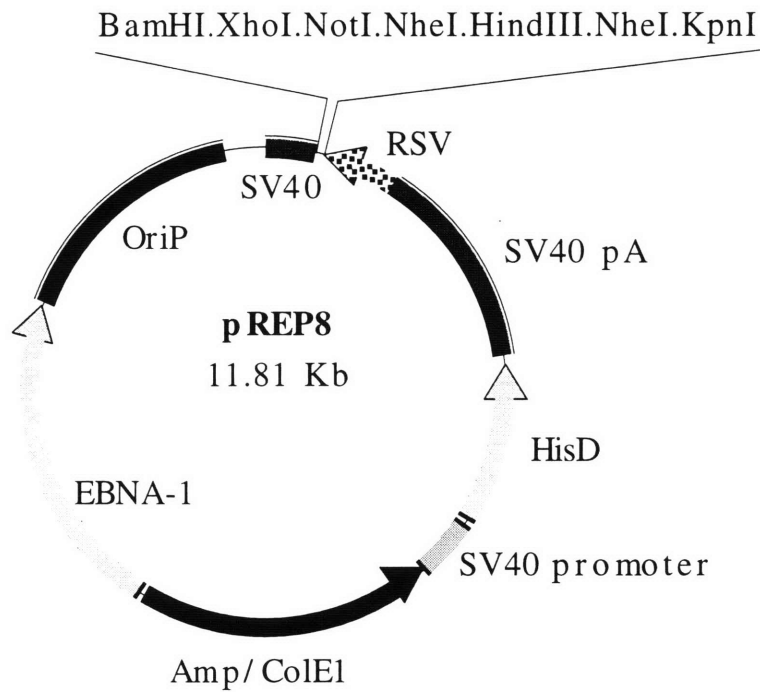
**Figure 3.2: pXER.** (pXER) The human EGF receptor plasmid. (Adapted from Chen *et al.*, 1987)



Plasmid name: pBluescript II KS+  
 Plasmid size: 2.96 kb  
 Constructed by: Unknown  
 Construction date: Unknown  
 Comments/References: From Strategene. Only an approximate map

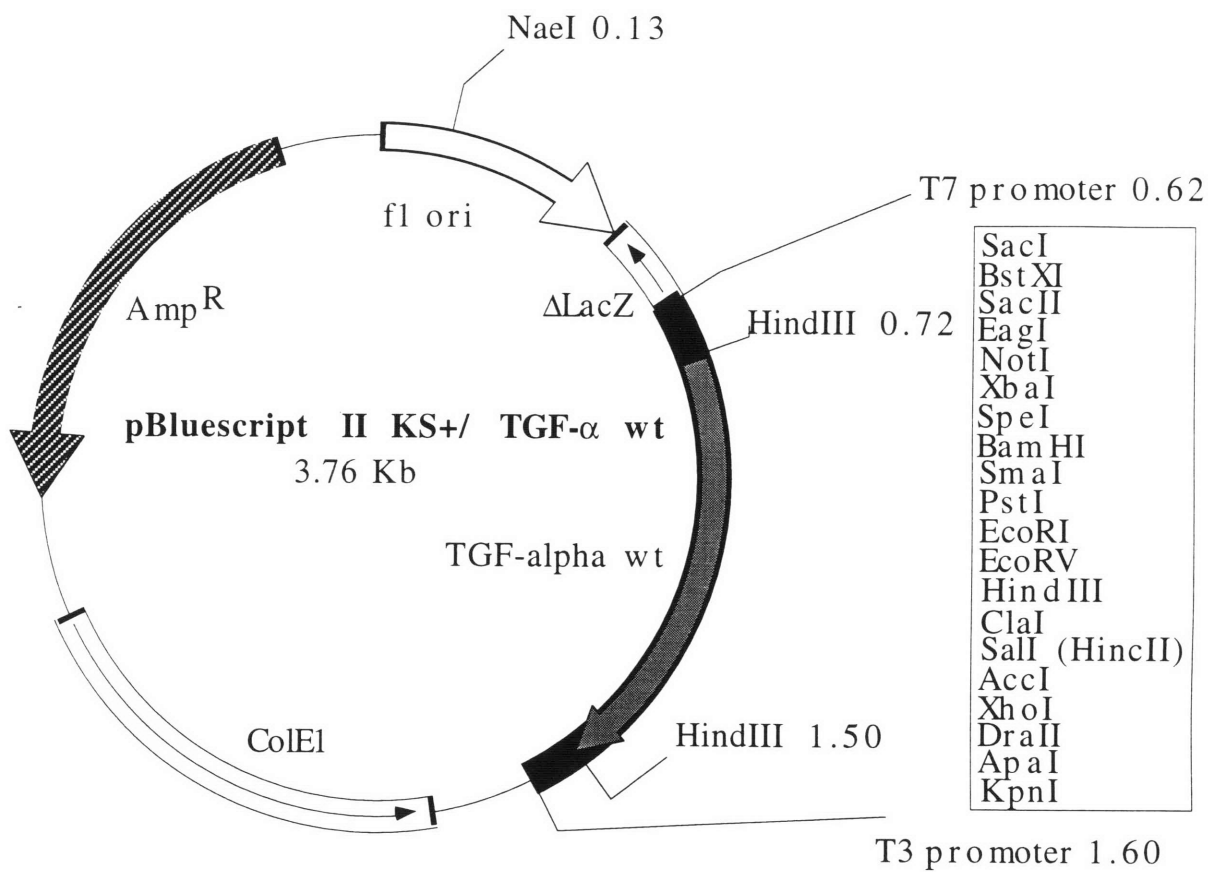
**Figure 3.3: Bluescript II KS+ Plasmid.** (Adapted from Strategene, 1995)





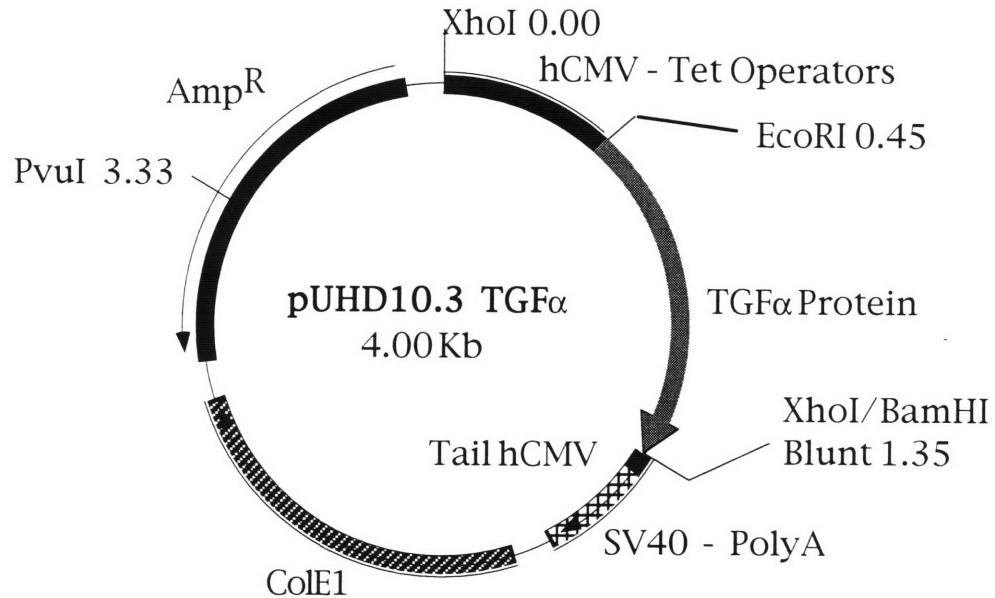
Plasmid name: pREP8  
 Plasmid size: 11.81 kb  
 Constructed by: Invitrogen  
 Construction date: Unknown  
 Comments/References:

**Figure 3.4: pREP8.** Plasmid from Invitrogen for histidinol resistance upon co-transfection with pUHD10.3 / sTGF $\alpha$  of the tetracycline controlled two plasmid system. (Adapted from Invitrogen, 1995)



Plasmid name: pBluescript II KS+/ TGF- $\alpha$  wt  
 Plasmid size: 3.76 kb  
 Constructed by: Greg Oehrtman  
 Construction date: 2/93  
 Comments/References:

**Figure 3.5: pBS /TGF $\alpha$  wt.** Cleavable prepro transmembrane TGF $\alpha$  in Bluescript II KS+.



Plasmid name: pUHD10.3 TGF $\alpha$   
 Plasmid size: 4.00 kb  
 Constructed by: Greg Oehrtman  
 Construction date: August 1994  
 Comments/References:

Original pUHD10.3 was constructed by H. Gossen, PNAS **89**, 5547-51, 1992. The full length cleavable transmembrane TGF $\alpha$  sequence was added by Greg Oehrtman from Bluescript II KS+/TGF $\alpha$  plasmid.

**Figure 3.6: pUHD10.3 / TGF $\alpha$ .** The prepro transmembrane TGF $\alpha$  inserted in the 2nd plasmid of the tetracycline controlled two plasmid system.

## Chapter 4: Results - Ligand Characterization

### 4.1 Overview of Experiments

The objective of this chapter was to develop an autocrine and paracrine TGF $\alpha$  - EGFR cell system. In order to achieve this goal, several sequential short term obstacles had to be overcome. These obstacles included placing the TGF $\alpha$  gene under the control of an inducible high expression, plasmid system, transfecting the plasmid into a TGF $\alpha$  negative cell line and characterizing the expression of the recombinant TGF $\alpha$ . The TGF $\alpha$  gene was obtained from Rik Derynck (University of California-San Francisco) and placed into the two plasmid tetracycline controlled expression system obtained from Gossen (University of Heidelberg). The two plasmid system was then transfected into mouse B82 L cells which do not have endogenous EGF receptors or TGF $\alpha$ . Transfection of the EGF receptor into B82 L cells by Gordon Gill (University of San Diego) enables the development of both an autocrine and paracrine cell system. TGF $\alpha$  expressed from these two cell systems were characterized by analyzing protein's molecular weight size, location, and secretion levels. A time course experiment tested the kinetics of TGF $\alpha$  expression from the two plasmid system. The utilization of these cells for testing theoretical models was determined by measuring the affect of tetracycline concentrations and cell densities on TGF $\alpha$  secretion levels.

### 4.2 Making pUHD10.3 / TGF $\alpha$

As stated in chapter 3.2, Bluescript II KS+ / TGF $\alpha$  wt was cut with XhoI, blunted with Klenow and the TGF $\alpha$  wt insert excised with EcoRI. pUHD10.3 was cut with BamHI, blunted with Klenow and cut with EcoRI to match the TGF $\alpha$  insert ends. The DNA pieces were gel isolated and ligated together to create pUHD10.3 / TGF $\alpha$  wt (Figure 3.6). After transforming bacteria, minipreps of individual colonies were grown up and the DNA isolated. The presence of the TGF $\alpha$  insert in the second plasmid was done by digesting the DNA with PstI. The PstI restriction site is not in the second plasmid while in the TGF $\alpha$  insert there are two sites, 50 bp apart. Therefore, a comparison between supercoiled and linear DNA can be made to determine the insert's presence.

Four bacteria colonies were determined to have the UHD10.3 / TGF $\alpha$  wt plasmid. Miniprep #3 was used to inoculate 200 mls of LB / ampicillin and the plasmid purified using Promega's Wizard Maxiprep. The DNA was checked to insure the insert's presence. A EcoRI, PstI, NcoI and SmaI digest compares a circular pUHD10.3 to a linearized pUHD10.3 / TGF $\alpha$ . A HindIII cut linearizes pUHD10.3 and removes the TGF $\alpha$  insert from pUHD10.3 / TGF $\alpha$ . Multiple RsaI sites in the TGF $\alpha$  insert and pUHD10.3 indicate the insert presence by comparing

size differences of the small DNA fragments. The 1% agarose gel is shown in Figure 4.1. It appears that not enough NcoI enzyme was added to the DNA to insure cutting, however, the remaining enzymes (EcoRI, HindIII, PstI and SmaI) gave the expected band sizes. A comparison of linearized DNA size by EcoRI and SmaI demonstrates that the second plasmid contains the insert. PstI and RsaI cut inside TGF $\alpha$  insert sequences and shows that the insert is TGF $\alpha$ . Excision of the TGF $\alpha$  insert using HindIII indicates that the TGF $\alpha$  fragment is the correct size.

### 4.3 Selection of TGF $\alpha$ Secreting Clones

After passing cells transfected with pUHD10.3 / TGF $\alpha$  and pR8 into selective histidine minus / histidinol medium, the cells were allowed to grow / die for several days with regular changing of selective medium. The surviving cells grew into colonies from an individual cell and were isolated using cloning rings. Seventy-two possible autocrine and paracrine clones were isolated by cloning rings and placed into 24 well plates. From these 72 clones, 28 paracrine clones and 12 autocrine clones continued to grow. Three paracrine clones were also isolated and grown up from a second pUHD10.3 TGF $\alpha$  / pR8 DNA transfection. The forty three successful clones were tested for expression of TGF $\alpha$  and determined that 9 clones were positive (5 autocrine and 4 paracrine).

The induction range of clones expressing TGF $\alpha$  was determined by measuring TGF $\alpha$  secretion rates at similar cell densities. Cells were grown in either the presence (repressed) or absence (induced) of tetracycline. B82R<sup>+</sup> / TGF $\alpha$  autocrine cell media also contained 20  $\mu$ g/ml anti-EGFR antibody 225 to prevent TGF $\alpha$  uptake by the EGF receptor. As shown in Figure 4.2, the autocrine clones displayed both high TGF $\alpha$  expression levels as well as a wide, dynamic, induction range. For example, the secretion rate of autocrine clone #9 increased from 0.14 to 41 ng/10<sup>6</sup> cells per 24 h (~10-3000 molecules/cell-minute) upon removal of tetracycline, roughly a 300-fold increase. The second highest expressor, autocrine clone #1, displayed a roughly 25-fold induction (from 1.5 to 36 ng/10<sup>6</sup> cells per 24 h (~100-2700 molecules/cell-minute)). The paracrine clones displayed a lower level of induced TGF $\alpha$  secretion (approximately 8 ng/10<sup>6</sup> cells per 24 h, or 600 molecules/cell-minute) and with only a 5-fold induction range. Shown in Table 4.1 is several other different cell lines expressing autocrine EGFR / TGF $\alpha$  ranging from 0.4 to 50 ng / million cells - day. Thus, not only does the newly created autocrine EGFR / TGF $\alpha$  cell system expresses TGF $\alpha$  within the range of other common autocrine cells, its expression of TGF $\alpha$  is regulated by tetracycline.

#### **4.4 Determining Cellular Processing of TGF $\alpha$ Protein**

Figure 4.3 shows the results of running paracrine's concentrated medium over a G-50 fine column with molecular weight standards. TGF $\alpha$  concentration in the fractions was determined by Oncogene Science TGF $\alpha$  ELISA. Elutions of the molecular weight standards monitored at 280 nm is re-plotted from the strip chart recorder data. The figure shows two TGF $\alpha$  peaks (6 kDa and 31 kDa) eluting off the column. The predicted molecular weight size for correctly processed, mature, secreted TGF $\alpha$  is 5.6 kDa. Therefore, within the resolution of this column, TGF $\alpha$  is correctly processed from the 25 kDa transmembrane TGF $\alpha$  into the mature protein. The 31 kDa TGF $\alpha$  peak could be derived from two different sources. This peak could be some secreted transmembrane TGF $\alpha$  which had not been cleaved or an aggregation of mature TGF $\alpha$  from the Amicon concentrating steps. A resolution between these two possibilities has not been pursued, but could be resolved by running a denaturing SDS polyacrylamide gel and protein detection by Western. If the peak was an aggregate, proteins would denature and run at 6 kDa. If the protein was transmembrane TGF $\alpha$ , the protein would run at 31 kDa. This avenue of experiments was not pursued as a clear majority of the protein was the correct molecular weight size, showing that TGF $\alpha$  was correctly processed.

After determined TGF $\alpha$  was correctly processed into its extracellular medium, it was questioned how much TGF $\alpha$  was secreted into the medium versus retained in the cell membrane after 24 hours. Samples from the cell membrane and media were analyzed for TGF $\alpha$  concentration using the Oncogene Science TGF $\alpha$  ELISA kit. As shown in Table 4.2, over 99% of TGF $\alpha$  is cleaved from the membrane and secreted into the medium. This secretion indicates that cleavage of TGF $\alpha$  from its membrane bound precursor is neither inhibited nor a rate limiting step in B82 cells. There could be another reason for low TGF $\alpha$  protein detection in membrane samples. The miscelle / TGF $\alpha$  sample would be sterically hindering one of the two anti-TGF $\alpha$  ELISA antibodies from binding, thus no TGF $\alpha$  would be detected. Western SDS-Page gels would refute or confirm this possibility. However, as this result was not central to the thesis, it was not pursued.

#### **4.5 TGF $\alpha$ Secretion Time Course from Paracrine Cells**

A time course experiment was performed to gain an understanding of TGF $\alpha$  secretion kinetics from paracrine cell lines. Figure 4.4 shows the secretion of TGF $\alpha$  from an induced paracrine cell line compared to a "pulse / chase" experiment from paracrine cells induced for 12 hours and then maintained in tetracycline medium for another 60 hours. There are two clear and interesting results from this experiment. The first result is the induction of paracrine cells. The cells quickly responded to removal of tetracycline, producing significant quantities of TGF $\alpha$

within 4 hours. Over the 60 hour period, the accumulative amount of TGF $\alpha$  in the medium was fairly constant with respect to time.

The second interesting result from this experiment was that TGF $\alpha$  production rate in the pulse / chase induced cells did not start to decrease when compared to fully induced cells until 48 hours after the re-introduction of tetracycline. This result would seem to indicate that TGF $\alpha$  mRNA might be fairly stable, allowing the production of TGF $\alpha$  protein long after new TGF $\alpha$  mRNA translation was inhibited by the addition of tetracycline. To check this explanation, would require running mRNA samples from each time point in a ribonuclease protection assay (RPA) and to determine if the TGF $\alpha$  mRNA remained constant after the addition of tetracycline for 48 hours. However, to ensure all future experiments with uninduced autocrine B82R<sup>+</sup> / TGF $\alpha$  cells are truly uninduced for the expression of TGF $\alpha$ , cells will be continuously cultured in tetracycline containing medium.

#### **4.6 Tetracycline Concentration Effects on TGF $\alpha$ Secretion**

As described in chapter 3.8, the cells were plated into individual wells of a 6 well plate. The cells were induced for a day before beginning the 24 hour secretion experiment. As always, autocrine cell medium contained 10  $\mu$ g/ml of monoclonal anti-EGFR 528 antibody for the 24 hour secretion period. The cell density was determined by Coulter Counter. TGF $\alpha$  concentrations were determined using a TGF $\alpha$  ELISA and stated on a per cell basis. The effect of tetracycline concentration on TGF $\alpha$  secretion for paracrine and autocrine cells is shown in Figure 4.5. The figure shows that the cells' TGF $\alpha$  secretion levels can be controlled by adjusting tetracycline concentrations in the medium. Also, it appears that the autocrine cell has a tighter "off" control, however, the autocrine cell density might have an affect as the autocrine's density is about an order of magnitude less than the paracrine's density. TGF $\alpha$  expression in the paracrine and autocrine cells ranged from 10 to 40 ng / million - 24 hours (500 to 3,200 molecules / cell-minute) and from 0.01 to 1.2  $\mu$ g / million - 24 hours (700 to 79,000 molecules / cell-minute), a 4 fold and 110 fold increase, respectively. This induction should give an experimenter an excellent range to measure what effect ligand secretion has on receptor downregulation and receptor-ligand complex levels with respect to cell density, ligand decoy and receptor blocking.

A review of secretion rates during this experiment and others, one realizes that TGF $\alpha$  expression is an order of magnitude higher than other experiments. This tetracycline experiment was performed in a 6 well Falcon plate with very few cells (autocrine cells contained around 10,000 cells / 35 mm dish - 1,000 cells / cm<sup>2</sup>) versus other experiments at 1,000,000+ cells / 60 mm dish (35,000 cells / cm<sup>2</sup>). The importance of cell density will be discussed in the next

section; however, another problem occurs when dividing TGF $\alpha$  concentration in the medium by a small cell numbers with possible large errors (counted by hemacytometer) to give a false, high, absolute number. Thus, while tetracycline can regulate TGF $\alpha$  expression, the absolute TGF $\alpha$  expression may be suspect.

The experiment was repeated at a later date with replicates to test tetracycline's regulation of TGF $\alpha$  expression and is shown in Figure 4.6. The experiment was performed as before on B82R<sup>+</sup> / TGF $\alpha$  autocrine clone #1 cells. Tetracycline concentration was varied from 10 to 0.001 and 0  $\mu\text{g} / \text{ml}$  in medium containing 10  $\mu\text{g} / \text{ml}$  blocking antibody 225. TGF $\alpha$  expression was inhibited down to 0.01  $\mu\text{g} / \text{ml}$  tetracycline. Expression began between 0.01 and 0.001  $\mu\text{g} / \text{ml}$  tetracycline, increasing 12 fold. The total expression range between uninduced to induced autocrine clone #1 cells was 70 fold. Also this time, the expression rate was in the "normal" regime of 100 to 6000 molecules / cell-minute versus the previous experiment. The error in the last experiment was most likely due to multiplying TGF $\alpha$  concentration by a low and inaccurate cell density.

#### **4.7 Cell Density Effects on TGF $\alpha$ Secretion**

Confirmation of theoretical predictions from chapter 2 is found in the experimental data shown in Figure 4.7a and b. Induced and uninduced TGF $\alpha$  expression was measured in autocrine clone #1 as a function of competing antibodies and cell density. As described in chapter 3.9, B82R<sup>+</sup> / TGF $\alpha$  autocrine clone #1 cells were serially diluted from 0.02-1 x 10<sup>6</sup> cells / 60 mm Corning dishes into four sets of 15 plates (9 dilutions with triplicates at 500,000, 62,500, and 7,812 cells / dish dilutions). The induction range in this experiment was 200 fold changing from 30 to 6200 molecules / cell-minute upon removal of tetracycline. At each cell density, half of the dishes received 20  $\mu\text{g}/\text{ml}$  anti-EGFR blocking antibody 225 to determine whether the inhibition of TGF $\alpha$  uptake would vary as a function of cell density.

As shown in Figure 4.7a, at a high ligand synthesis rate of ~6200 molecules/cell-minute, TGF $\alpha$  levels were not increased upon addition of blocking antibodies. This data contrasts with data obtained at the low ligand synthesis rate of ~30 molecules/cell-minute in uninduced cells. At lower ligand secretion rate, TGF $\alpha$  levels drop sharply to background levels in the absence of blocking antibody. Upon addition of EGFR blocking antibody, TGF $\alpha$  uptake is reduced and maintained a fairly constant level until higher cell density.

Figure 4.7b is plotted as total bulk ligand concentrations. As in Figure 2.5, ligand accumulation increases with increasing cell populations in the presence of antibody at the higher secretion rate. Upon removal of the antibody at the lower secretion rate, ligand accumulation does not occur, similar to Figure 2.5. Thus, experimental findings are both qualitatively and



quantitatively consistent with model predictions that the effectiveness of receptor-blocking antibodies is strongly dependent on both cell density and ligand synthesis rate.

#### **4.8 Creation of B82R<sup>+</sup> / sEGF Clones and Mutant Receptors**

As described earlier in Chapter 3.10 and Will *et al.*, 1995, Dr. Will-Simmons constructed a mature, secreted, form of EGF - termed sEGF. sEGF's expression plasmid is pUHD10.3 / sEGF in the two plasmid tetracycline-controlled expression system. She transfected the plasmid into B82 cells which already contained pUHD15.1neo and were EGFR wild type positive or negative, creating B82R<sup>+</sup> wild type / sEGF and B82R<sup>-</sup> / sEGF. Dr. Gordon Gill has also constructed several mutated EGFR plasmids and transfected them into B82R<sup>-</sup> cells (Chen *et al.* 1989). These receptors have different affinity and trafficking properties as shown in Table 4.3 (Lund *et al.* 1990; Wiley *et al.* 1991).

During the course of the thesis, there was an interest in looking at how these receptor affinity and trafficking changes would affect autocrine ligand / receptor interactions. Thus, pUHD15.1neo and pUHD10.3 / sEGF was transfected into several mutant EGFR cell lines. These mutated EGFR cell lines were A654, M721, A654M721, and Δ647. Shown in Table 4.4 is a compilation of all existing TGFα and sEGF expression systems in normal / mutated EGFR positive and negative B82 cells. The clones have a variety of TGFα and sEGF expression levels, however, ligand expression are all similar with nanogram expression. Also, the detection of ligand was not performed at similar cell density, but represents values obtained during clonal selections. Thus, a multiple of expression systems exist, allowing an unlimited number of hypotheses to be experimentally tested.

**Table 4.1 Comparison of Autocrine TGF $\alpha$  / EGFR cells**

Cell Type	Secretion Rate ng / million cells - day	Reference
Autocrine clone #1	1-40	
A431	10 * <sup>1</sup>	Rheiss <i>et al.</i> , 1991
MDA468	50	Hamburger and Pinnamaneni, 1992
MCF-7	5.2	Fontana <i>et al.</i> , 1992
Ishikawa	2.4	Gong <i>et al.</i> , 1992
MDCK / TGF $\alpha$ 1-16	0.4 * <sup>2</sup>	Dempsey and Coffey, 1994

Note: Referenced cells (except Dempsey and Coffey) did not use blocking antibodies to prevent ligand uptake by the receptor.

\*<sup>1</sup> TGF $\alpha$  concentration given as ng/ml, assumed a 10 ml volume.

\*<sup>2</sup> Assuming cell doubling every day from initial cell density given.

**Table 4.2: Detection of secreted and membrane bound TGF $\alpha$**

Cell Type	Source	pg/million cells	% Membrane/Media
Autocrine #1	Membrane Media	120 25400	0.47
Paracrine #22	Membrane Media	3 9160	0.04

**Table 4.3: Mutant B82 EGFR trafficking and affinity parameters**

<b>Cell Type</b>	<b>Control</b>	<b>+PMA</b>
Wt	I-Int., H-Aff.	L-Int., L-Aff.
A654	I-Int., H-Aff.	I-Int., L-Aff.
M721	L-Int., H-Aff.	L-Int., L-Aff.
A654M721	L-Int., H-Aff.	L-Int., L-Aff.
C'1022	I-Int., H-Aff.	L-Int., H-Aff.
C'1022A654	I-Int., H-Aff.	L-Int., H-Aff.
$\Delta$ 647	L-Int., L-Aff.	L-Int., L-Aff.

where:

I-Int. - High ligand induced receptor internalization

L-Int. - Low constitutive membrane turnover receptor internalization

H-Aff. - High receptor / ligand binding affinity

L-Aff. - Low receptor / ligand binding affinity

Source:

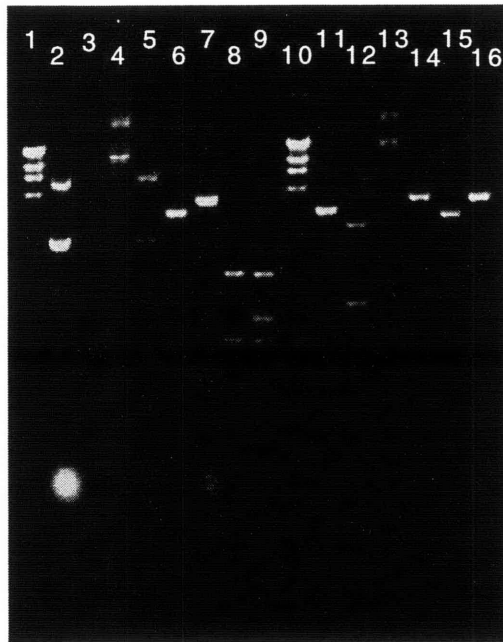
Lund *et al.*, 1990; Wiley *et al.*, 1991

**Table 4.4 Artificially engineered cell systems**

<u>Cell Type</u>	<u>Plasmids</u>	<u># of Clones</u>	<u>Induced</u>
EGFR <sup>+</sup> /TGF $\alpha$	pXER/pUHD15.1/pUHD10.3-TGF $\alpha$ /pR9	5	1 - 40
EGFR <sup>-</sup> /TGF $\alpha$	pUHD15.1/pUHD10.3-TGF $\alpha$ /pR9	4	.5 - 10
EGFR <sup>+</sup> /sEGF	pXER/pUHD15.1/pUHD10.3-EGF/pR9	2	5 - 200 <sup>(1)</sup>
EGFR <sup>-</sup> /sEGF	pUHD15.1/pUHD10.3-EGF/pR9	2	2 - 40 <sup>(1)</sup>
<u>EGFR<sup>+</sup> Mutations</u>			
A654/sEGF	pXER/pUHD15.1/pUHD10.3-EGF/pHyg.	6 <sup>(2)</sup>	5 - 8
M721/sEGF	pXER/pUHD15.1/pUHD10.3-EGF/pHyg.	12 <sup>(2)</sup>	1 - 10
M721A654/sEGF	pXER/pUHD15.1/pUHD10.3-EGF/pR9	15 <sup>(2)</sup>	1 - 140
$\Delta$ 647/sEGF	pXER/pUHD15.1/pUHD10.3-EGF/pHyg.	1	150

Induction is reported as ng/million cells/24 hours.

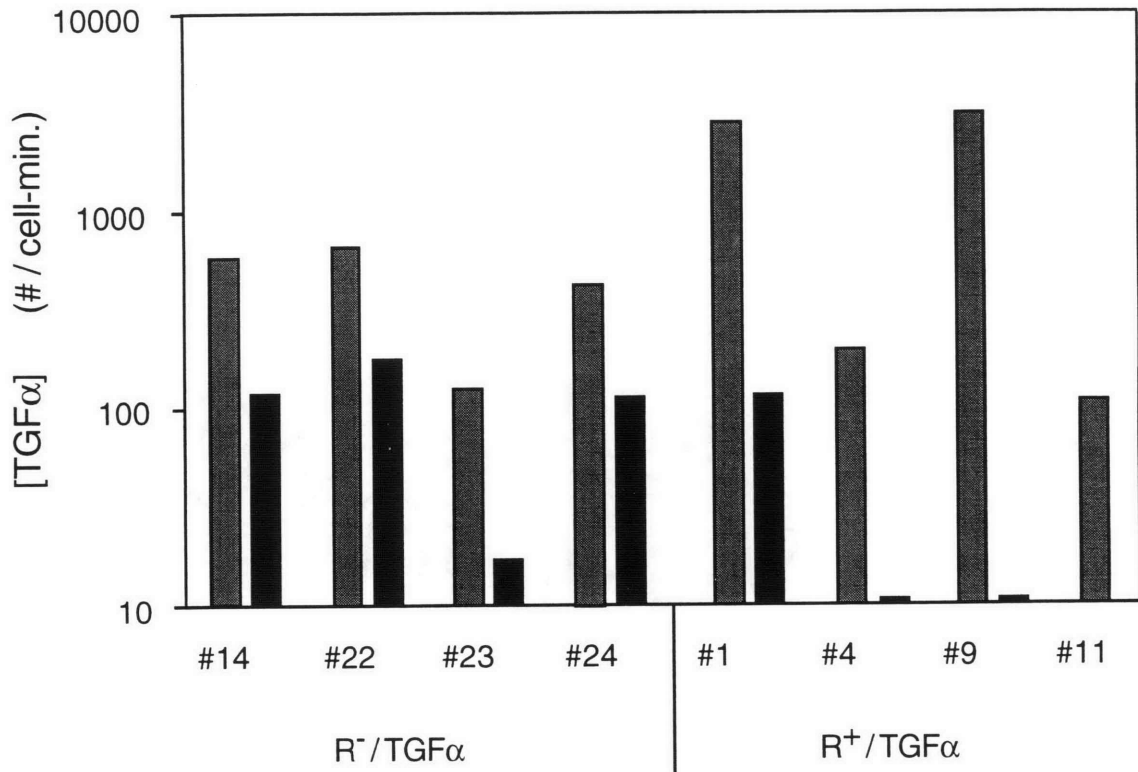
- (1) Will *et al.*, 1995  
(2) Not all clones tested at this time



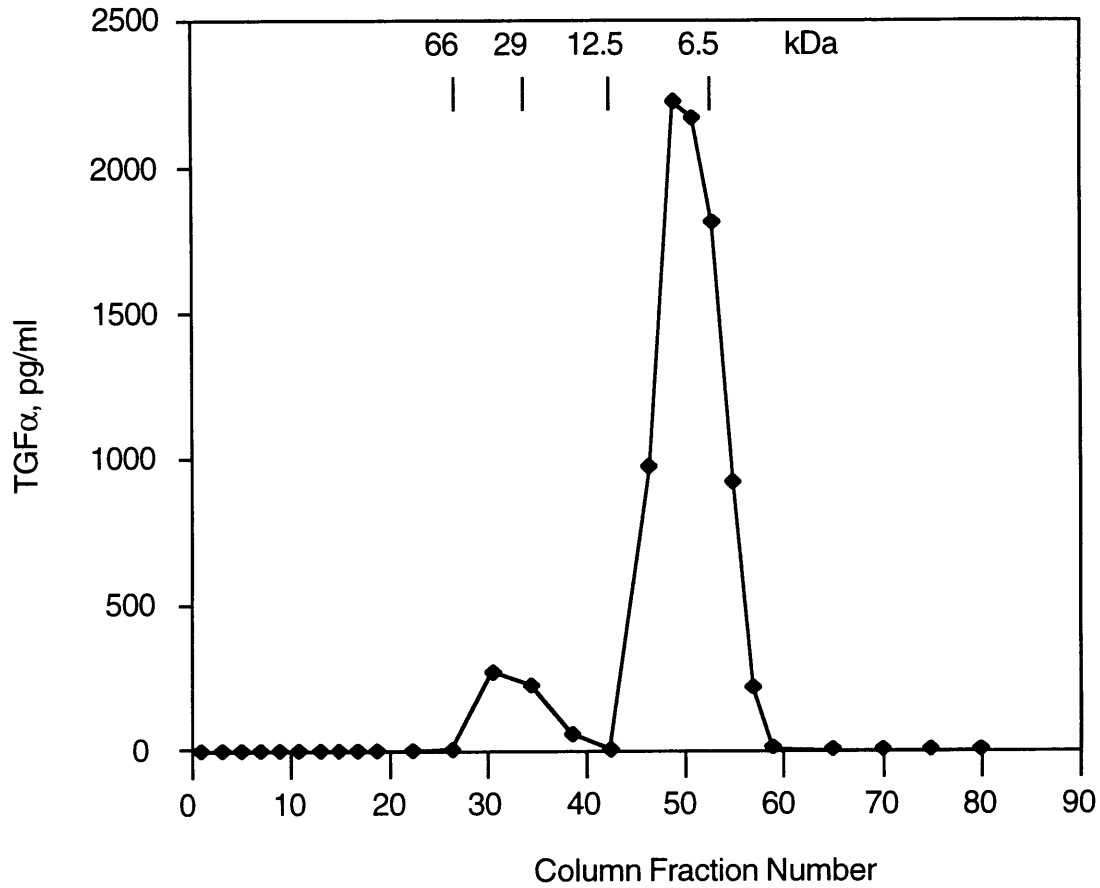
**Legend:**

Lane 1: MW Standards	Lane 9: pUHD10.3/TGF $\alpha$ w/RsaI
Lane 2: Uncut pUHD10.3/TGF $\alpha$	Lane 10: MW Standards
Lane 3: Blank	Lane 11: pUHD10.3 w/HindIII
Lane 4: pUHD10.3 w/NcoI	Lane 12: pUHD10.3/TGF $\alpha$ w/HindIII
Lane 5: pUHD10.3/TGF $\alpha$ w/ NcoI	Lane 13: pUHD10.3 w/PstI
Lane 6: pUHD10.3 w/EcoRI	Lane 14: pUHD10.3/TGF $\alpha$ w/PstI
Lane 7: pUHD10.3/TGF $\alpha$ w/EcoRI	Lane 15: pUHD10.3 w/SmaI
Lane 8: pUHD10.3 w/RsaI	Lane 16: pUHD10.3/TGF $\alpha$ w/SmaI

**Figure 4.1: pUHD10.3 / TGF $\alpha$  Digest.** Characterization of the TGF $\alpha$  2nd plasmid using several restriction digest enzymes.

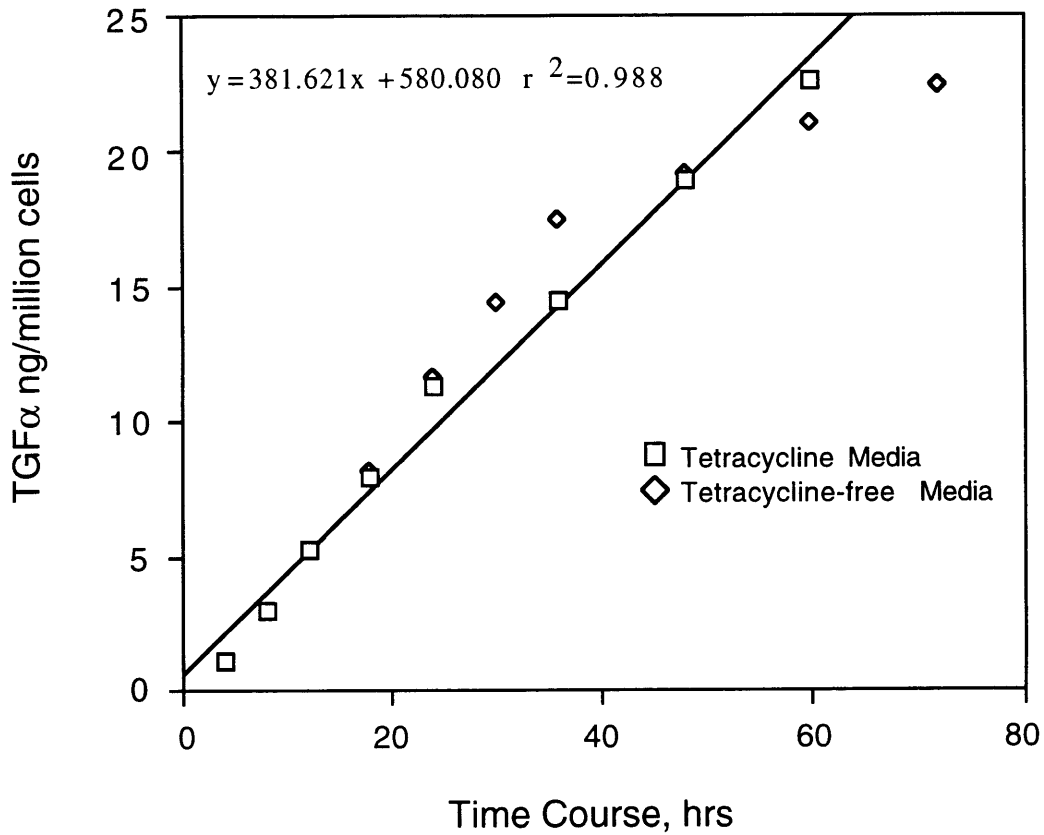


**Figure 4.2: EGFR / TGF $\alpha$  expression at similar cell density.** Induced TGF $\alpha$  expression by removal of tetracycline shown as shaded. Uninduced TGF $\alpha$  expression repressed by continuous tetracycline in cell medium shown as solid. Half of the plated cells were pre-induced for TGF $\alpha$  expression by removal of tetracycline from the medium. 24 hours later, tetracycline-containing and tetracycline-free media was added to the appropriate wells and TGF $\alpha$  concentrations were allowed to accumulate for 24 hours. In addition, autocrine medium contained 10  $\mu$ g / ml mAb 528 to prevent ligand uptake by EGFR. Cell density averaged 900,000 cells / 60 mm dish.

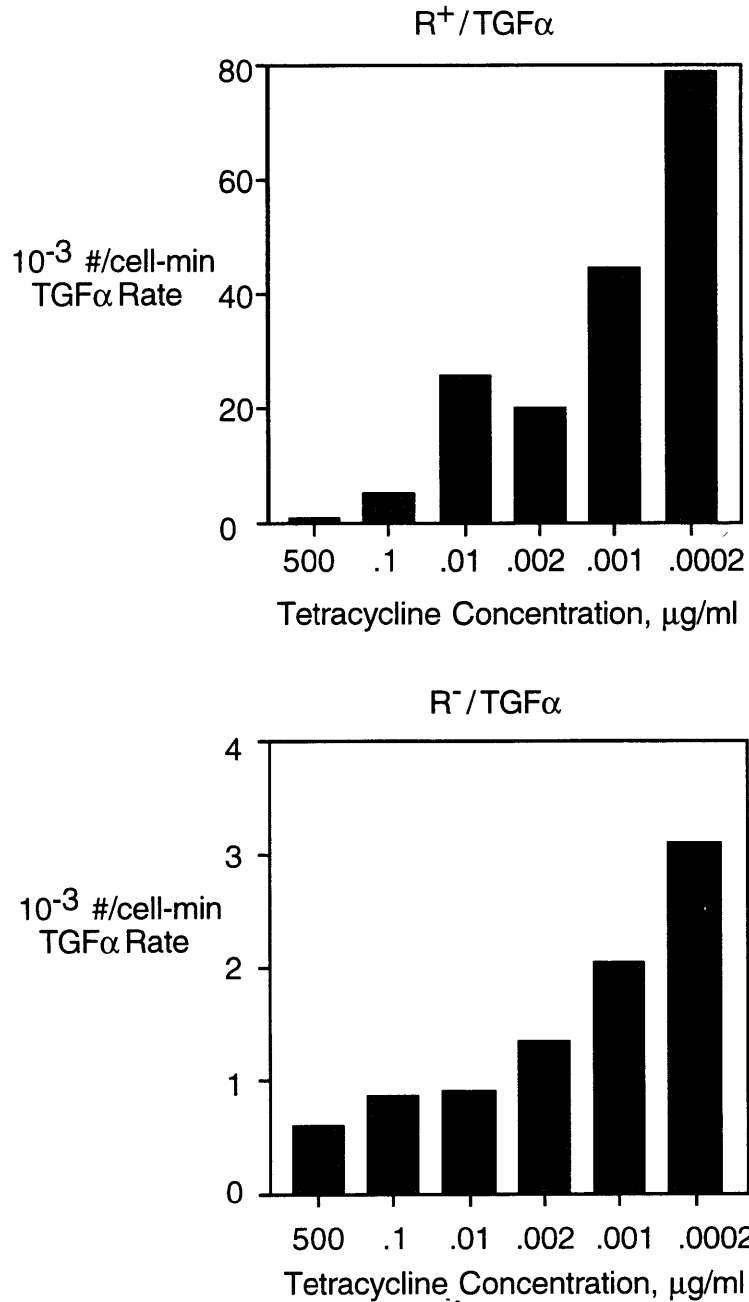


**Figure 4.3: TGF $\alpha$  Molecular Weight.** Determination of TGF $\alpha$ 's molecular weight in conditioned medium using a G-50 Sephadex column. Conditioned medium from B82R<sup>-</sup> / TGF $\alpha$  cells were concentrated using Amicon filters before adding to a 100x G-50 Sephadex column. Appropriate molecular standards were run simultaneously with the conditioned medium. Fractions were collected every 5 minutes and measured via A280 nm for total protein and TGF $\alpha$  ELISA.





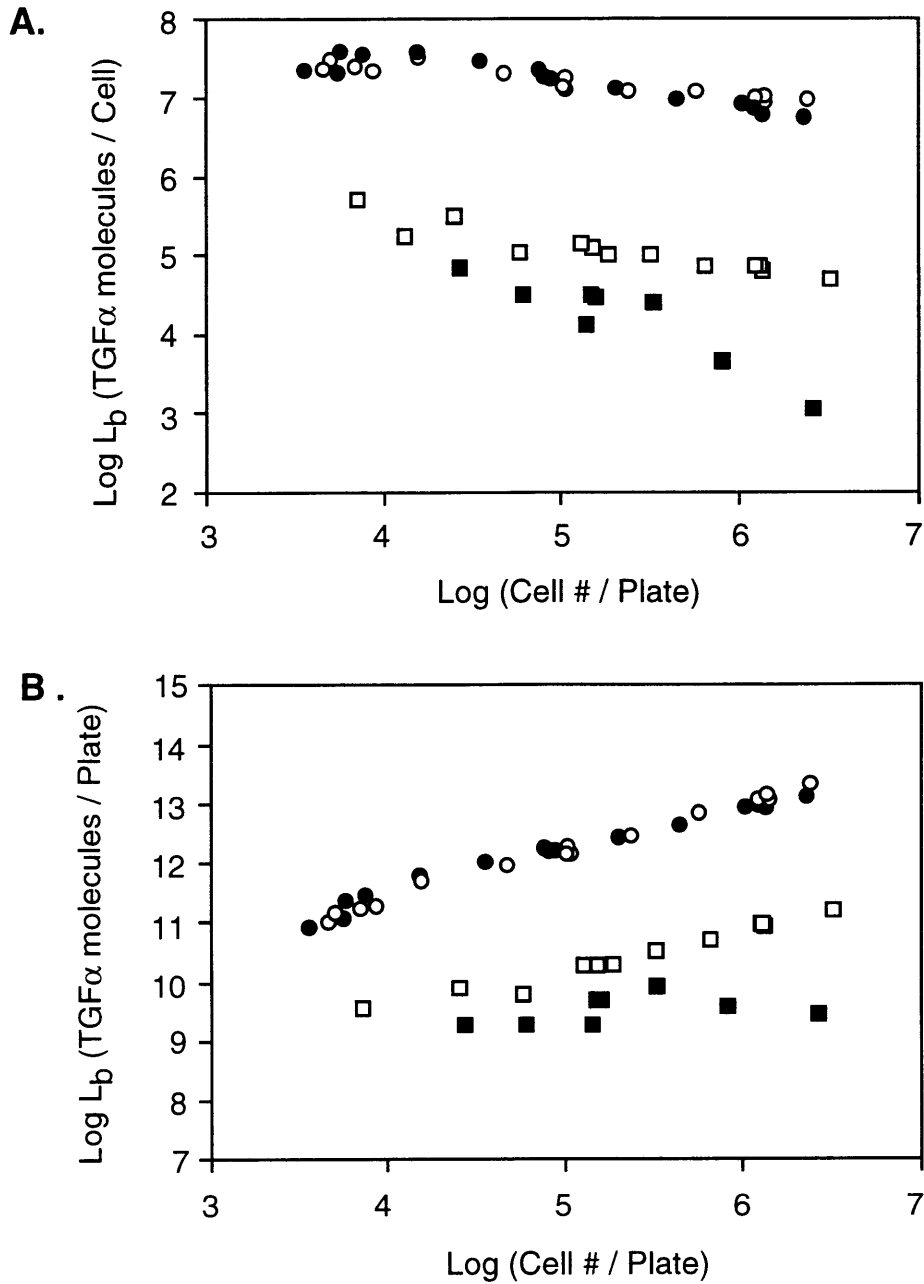
**Figure 4.4: TGFα time course.** Uninduced B82R<sup>-</sup> / TGFα clone #22 cells were plated and allowed to attach for 24 hours. TGFα expression was induced by replacing all of the cell plates' medium with tetracycline free medium (squares). Conditioned medium was removed at times indicated and cell number determined. Half of the cell plates medium were switched back to tetracycline containing media at 16 hours (diamonds)



**Figure 4.5: Tetracycline controlled TGFα expression.** Plated cells were pre-induced for TGFα expression by addition of fresh medium containing the tetracycline gradient for 24 h. The next day, fresh medium containing the tetracycline gradient was placed on the cells and TGFα concentration allowed to accumulate for 24 h. 10 μg / ml monoclonal antibody 528 was added to each well to prevent ligand uptake by EGFR. Autocrine cell density was ~10,000 cells / 35 mm dish. Paracrine cell density was ~120,000 cells / 35 mm dish.

PAGES (S) MISSING FROM ORIGINAL

91



**Figure 4.7: Experimental bulk ligand concentrations.** B82R<sup>+</sup> / TGFα clone #1 induced (circles) and uninduced (squares) ligand concentrations were tested as a function of cell density and ligand expression levels. TGFα expression occurred with 20 μg / ml anti-EGFR monoclonal antibody 225 (open) and without antibody (solid). A. Bulk ligand concentration as molecules/cell. B. Bulk ligand concentration as molecules/plate.

## **Chapter 5: Methods for Ligand-Receptor Complex Characterization**

The last two chapters characterized and examined B82R<sup>+</sup> / TGF $\alpha$  autocrine cells in terms of ligand expression. However, ligand expression is only half of the story. Binding of ligand to its receptor is an important cellular initiator and regulator of cell proliferation and migration as mentioned in chapter one. It has also been observed large fractions of carcinomas have an over-expressed autocrine loop. In these carcinomas, one or both of the ligand and receptor pair is over-expressed. How this over-expression affects cellular signalling and proliferation is not clearly understood. Does increased ligand and receptor lead to increased signalling? or does the cell regulatory machinery adjust to a new threshold? Previous research in the group analyzed several important parameters' affect on receptor / ligand complex inhibition as a function of blocking and decoy antibodies in a mathematical autocrine model. Having developed autocrine receptor / ligand expression cell lines, model predictions can be validated and new hypotheses tested. Autocrine cell parameters which may be varied experimentally are: ligand secretion rate (controlled by tetracycline concentrations), ligand secretion trafficking (synthesizing transmembrane precursors or mature protein), receptor trafficking rate (mutant EGFR receptor cells), receptor / ligand affinity (different ligands / mutated ligands). In these next two chapters, methods and results from Cytosensor experiments analyzing the first two parameters will be addressed as a function of blocking antibody and / or decoy antibody concentrations.

First, a method for measuring and quantifying ligand - receptor levels needed to be developed. Molecular Devices Cytosensor determines cells' metabolic rate by measuring changes in extracellular pH. The cells' metabolic rate can be increased by adding ligand to a cells' medium. Upon ligand binding to its receptor, signalling is initiated through the secondary pathway to increase cellular metabolic activities such as glycolysis and respiration. The ligand / receptor complex signal is amplified at each step in the secondary pathway, creating a large signal from a small initial source of complexes. For this detection method to work, the receptor / ligand binding step must be the rate-limiting step which would appear on a graph of metabolic rate vs. EGF as a dose dependent response to EGF concentrations.

### **5.1 General Protocol for Testing Cells on the Cytosensor**

Since B82 mouse fibroblast cells are an anchorage dependent cell line, the cells must be plated one day prior to running an experiment on the Cytosensor to allow for attachment of the cells to the transwell membrane. Quarter of a million (250,000) cells are seeded into each transwell (Corning Transwell #3402 - 3  $\mu$ m pore size, 12 mm diameter) in normal growth medium (See Chapter 2 for each cell type's appropriate media). Plating cells in serum free

conditions using D/H/B (Dulbecco-Volt Modified Eagle Media, 25 mM HEPES and 1 mg / ml BSA, all from Sigma) resulted in dead cells with little or no metabolic activity. One day after plating cells (experiment day), cell transwells are prepared for placement on the Cytosensor. First, a spacer (50  $\mu$ m high, 6 mm inner diameter, #R7026B - Molecular Devices) is placed in the transwell's medium directly over the cells. On top of the spacer is placed a transwell insert (3  $\mu$ m pore size, looks like a mini-transwell, fitting flush inside the original transwell, #R7025 - Molecular Devices). One ml running buffer to each insert cup completes assembly, creating a self-contained cell chamber of 1.4  $\mu$ ls. Cell / transwell assembly is placed in Cytosensor silicon sensor chambers and equilibrated for 2-3 hours in DV/cyto buffer (Dulbecco-Volt Modified Eagle Media with 2.59 gram / liter sodium chloride and 0.1 mg / ml BSA, no sodium bicarbonate) at a 100  $\mu$ ls / minute flowrate. Pump cycle with all experiments are 30 seconds on and 30 seconds off. ECAR is measured during the "pump off" period for 20 seconds, starting 8 seconds into the "pump off" period.

All protein samples are diluted in DV/cyto buffer to proper concentration before placing samples on the Cytosensor. Use of BSA in buffer prevents sample protein from sticking to the tubing's wall and loss of signal. Signal aberrations resulting from concentrated protein solutions and their buffers (high antibody concentrations at 100  $\mu$ g / ml) are eliminated by dialyzing protein in DV/s (DV/cyto without BSA) buffer for 24 hours. Protein concentration is re-measured using Sigma's BCA protein concentration determination assay (Procedure TPRO-562 using B9642 Bicinchoninic Acid and C2284 Copper (II) Sulfate Pentahydrate).

Once cell metabolic activity or extracellular acidification rate (ECAR) achieve a steady state baseline, the experiment is begun. Cells are exposed to EGF or TGF $\alpha$  additions until achieving maximal ECAR (about 10 minutes) after which the ligand is removed and cells allowed to acquire a new steady state baseline. In experiments with antibodies, cells are allowed to re-establish steady state ECAR before exposing them to a 30 minute challenge with competing antibodies.

## **5.2 B82R<sup>+</sup> ECAR Response as a Function of mAb225 and mEGF**

B82R<sup>+</sup> cells were seeded into transwells following the normal protocol and allowed to grow overnight. Cells were equilibrated in DV/cyto buffer on the Cytosensor before beginning the experiment as normal. Once cells reached steady state ECAR, each cell lane was re-equilibrated in the presence of 0, 0.01, 0.1 or 1  $\mu$ g/ml anti-receptor blocking antibody mAb225. Next, a stepwise gradient of mEGF was added to each lane with antibody and maximal ECAR peaks recorded. The mEGF gradient was 0.1, 1, 10, and 100 ng/ml. After each EGF addition,

cells were allowed to re-equilibrate their ECAR while in the continuous presence of anti-EGFR blocking antibody 225.

### **5.3 Correlating Cytosensor's ECAR to Receptor / Ligand Complex Levels**

#### **5.3a. I<sup>125</sup> Binding - Receptor / Ligand Complexes**

B82R<sup>+</sup> / 1st plasmid or B82R<sup>+</sup> / TGF $\alpha$  cells were seeded at approximately 100,000 cells / 35 mm Corning tissue culture dishes (#25000) in normal growth medium. Day 2, if induced B82R<sup>+</sup> / TGF $\alpha$  autocrine cells were required, induction was achieved by removal of tetracycline-containing medium and replacing it with tetracycline-free medium. Day 3, cell medium was switched from normal growth medium to D/H/B buffer 3 hours before beginning the experiment. The experiment was begun by removing D/H/B buffer and replacing it with I<sup>125</sup> EGF diluted in D/H/B buffer. Cells were placed in a 37 °C water bath incubator for 10 minutes to allow binding of I<sup>125</sup> EGF to EGFR. After 10 minutes, cells were placed on ice and I<sup>125</sup> EGF medium immediately removed. One half ml of cell medium was saved and counted in a Packard Bell (Cobra Model) Gamma Counter to determine free I<sup>125</sup> EGF concentration. Cells were then washed three times with 1x WHIPS (1 mg / ml PVP, 130 mM NaCl, 5 mM KCl, 0.5 mM MgCl<sub>2</sub>-6H<sub>2</sub>O, 1 mM CaCl<sub>2</sub>-2H<sub>2</sub>O, 20 mM HEPES) to remove excess free ligand. Bound ligand concentrations were determined by lysing cells with 1M NaOH for 10 minutes and determining radioactive counts of cell lysates plus a 1x WHIPS rinse in the Gamma Counter. The data was plotted as bound ligand (complexes, # / cell) versus free ligand (ng / ml).

#### **5.3b. Cytosensor ECAR Output**

B82R<sup>+</sup> / 1st plasmid or B82R<sup>+</sup> / TGF $\alpha$  cells were seeded at 250,000 cells per transwell in normal growth medium as usual. When measuring induced B82R<sup>+</sup> / TGF $\alpha$  autocrine cells, cells were plated into the transwell in tetracycline-free growth medium for overnight expression. Cells were equilibrated to steady state ECAR on the Cytosensor in DV/cyto buffer containing 1  $\mu$ g / ml tetracycline for uninduced autocrine cells and without tetracycline for induced autocrine cells. Equilibrated cells were exposed to a mEGF concentration gradient of 0.1, 0.3, 0.6, 1.2, 2.5, 5, 10, 25, 50 ng / ml. A method was devised to alternate EGF additions to a particular cell lane so that each lane "saw" a large increase in EGF concentrations to minimize receptor downregulation. Thus, additions were performed as follows:

- Lane A: 0.1, 1.2, 10 ng / ml EGF
- Lane B: 0.3, 2.5, 25 ng / ml EGF
- Lane C: 0.6, 5, 50 ng / ml EGF

Lane D: Blank - Background / Baseline

After each EGF addition, cells were allowed to re-equilibrate their ECAR to steady state before the next ligand addition. Exposure to EGF was minimized by immediate removal of EGF from cells as soon as peak ECAR was reached - determined by the “leveling” off of ECAR. Cytosensor data was plotted as peak ECAR (%) versus free ligand (ng / ml).

### 5.3c. Relating ECAR to Receptor / Ligand Complexes

A best fit line was determined for each curve ( $I^{125}$  EGF and Cytosensor) using KaleidaGraph™ 3.0 and Scatchard equation (Equation 5.1) (Scatchard 1949). Rearranging the equation and solving for  $I^{125}$  EGF (L) in terms of complexes (C) and two parameters (affinity constant,  $K_d$ , and total receptor number,  $R_t$ ) gave Equation 5.2.

$$C / L = - C / K_d + R_t / K_d \quad \text{Equation 5.1}$$

$$L = C * K_d / (R_t - C) \quad \text{Equation 5.2}$$

After determining the constants,  $K_d$  and  $R_t$ , Equation 5.2 was utilized for an analogous fit of the Cytosensor's ECAR versus free ligand graph, substituting  $L_{0.5}$  for  $K_d$  and  $ECAR_{max}$  for  $R_t$ . A relationship between ECAR and complexes was derived via two methods. The first method involved using discrete free ligand concentrations and calculating predicted ECAR and complex numbers from the best fit data. Plotting the two predicted variables together and using equation 5.2 for a best fit line (replacing  $R_t$  with m1, grouped variable 1, and  $K_d$  with m2, grouped variable 2) resulted in the desired correlation between ECAR and complexes. The second method involved mathematically solving equation 5.2, ECAR vs. free EGF and complexes vs. free EGF equations, for free EGF. Substituting one equation in the another and solving for ECAR vs. complexes, gave:

$$ECAR = [C * ECAR_{max} * K_d / (K_d - L_{0.5})] / [L_{0.5} * R_t / (K_d - L_{0.5}) + C] \quad \text{Equation 5.3}$$

### 5.4 Measuring B82R<sup>+</sup>/TGF $\alpha$ Induction

Uninduced B82R<sup>+</sup> / TGF $\alpha$  autocrine cells were seeded as normal at 250,000 cells per transwell in normal growth medium with 1  $\mu$ g / ml tetracycline and allowed to grow overnight. On Day 2, cells were equilibrated as normal on the Cytosensor in DV/cyto running buffer with 1  $\mu$ g / ml tetracycline medium. Upon obtaining steady-state ECAR baseline, the following conditions are imposed - one condition per lane:



- a. No tetracycline and no antibody 225 (Induced - Antibody)
- b. No tetracycline and 1  $\mu\text{g}$  / ml antibody 225 (Induced + Antibody)
- c. 1  $\mu\text{g}$  / ml tetracycline and no antibody (Uninduced - Antibody)
- d. 1  $\mu\text{g}$  / ml tetracycline and 1  $\mu\text{g}$  / ml antibody 225 (Uninduced + Antibody)

The experiment was run with these conditions for at least 7 hours, allowing TGF $\alpha$  to be synthesized, expressed, and captured by EGFR.

### **5.5 Tetracycline Gradient on Autocrine B82R<sup>+</sup>/TGF $\alpha$ Cells**

Uninduced B82R<sup>+</sup> / TGF $\alpha$  autocrine cells were seeded at 250,000 cells per transwell in normal tetracycline-free growth medium and allowed to grow overnight and induce TGF $\alpha$  expression. TGF $\alpha$  expression was repressed in two transwells by addition of 1  $\mu\text{g}$  / ml tetracycline. TGF $\alpha$  expression was partially inhibited in the third well by addition of 5 ng / ml tetracycline (0.5% of fully uninduced cells). The fourth well remained tetracycline free, allowing full induction of TGF $\alpha$  expression. On Day 2, the same tetracycline concentration was continued in DV/cyto running buffer and cells allowed to reach a steady-state ECAR as normal. Upon obtaining steady-state, 10 ng / ml mEGF was added to one of the two uninduced cells, semi-induced cells, and fully induced cells lanes (lanes B, C, and D). The other uninduced cell lane (A) was used as background / baseline. Upon reaching maximal ECAR, mEGF was removed and cells allowed to re-equilibrate their ECAR before adding 10  $\mu\text{g}$  / ml blocking Ab225 to lanes B, C, and D while lane A remained baseline ECAR. The antibody was left on the cells for a minimum of 30 minutes to ensure obtaining steady state ECAR.

### **5.6 Antibody Inhibition of Receptor / Ligand Complex on B82R<sup>+</sup> / TGF $\alpha$**

Uninduced B82R<sup>+</sup> / TGF $\alpha$  autocrine cells were seeded at 250,000 cells per transwell in normal growth medium and allowed to grow overnight. TGF $\alpha$  expression was induced during passage by plating the cells in tetracycline-free medium. On Day 2, cells were equilibrated as normal in DV/cyto running buffer without tetracycline on the Cytosensor before beginning the experiment. After reaching steady state ECAR, cells were exposed to 10 ng / ml mEGF in DV/cyto until maximum ECAR was reached, usually in 10 minutes. This EGF addition was to insure all cells responded similarly. After measuring peak ECAR, cell ECAR was re-equilibrated to steady state before adding an antibody gradient and ECAR decline recorded. Antibody / cell incubation proceeded for at least 30 minutes to insure reaching a new steady-state ECAR. Three antibody concentrations were tested at a time while the fourth lane received no antibody and served as the background / baseline lane.

### **5.7 Blocking Antibody Inhibition of Receptor Complexes on B82R<sup>+</sup> / sEGF**

The same procedure performed in section 5.6 were used with autocrine B82R<sup>+</sup> / sEGF cells constructed by Dr. Birgit Will-Simmons (Will *et al.* 1995). Again the procedure is:

Uninduced B82R<sup>+</sup> / sEGF autocrine cells were seeded at 250,000 cells per transwell in normal growth medium and allowed to grow overnight. sEGF expression was induced during passage by plating the cells in tetracycline-free medium. On Day 2, cells were equilibrated as normal in DV/cyto running buffer without tetracycline on the Cytosensor before beginning the experiment. After reaching steady state ECAR, cells were exposed to 10 ng / ml mEGF in DV/cyto until maximum ECAR is reached, usually in 10 minutes. This EGF addition was to insure all cells responded similarly. After measuring peak ECAR, cell ECAR was re-equilibrated to steady state before adding an antibody gradient and ECAR decline recorded. Antibody / cell incubation proceeded for at least 30 minutes to insure reaching a new steady-state ECAR. Three antibody concentrations were tested at a time while the fourth lane received no antibody and served as the background / baseline lane.

## **Chapter 6: Results - Ligand / Receptor Complex Characterization**

### **6.1 Overview of Experiments**

Having described methods for receptor - ligand complex detection and quantification in the previous chapter, the results of these experiments are discussed here. Cytosensor ECAR readings were shown to be EGF concentration-dependent, allowing a correlation between cellular metabolic rate as detected by the Cytosensor and receptor - ligand complexes as measured by  $I^{125}$  EGF binding studies. The successful correlation between ECAR and ligand / receptor complex and high signal to noise ratio on the Cytosensor is important because earlier work using anti-phosphotyrosine Westerns and ELISA incurred low signal to noise ratios, making complex level quantification difficult (data not shown). Having to perform cell lysates and multi-day preparations is another disadvantage with Westerns and ELISA, whereas Cytosensor data is real-time with living cells.

Using the Cytosensor, uninduced autocrine B82R<sup>+</sup> / TGF $\alpha$  were placed on the machine and its ECAR increased upon induction of TGF $\alpha$  expression over a seven hour period. This ECAR signal was reduced if cells were in the presence of competing anti-receptor blocking antibody. Finally, both autocrine B82R<sup>+</sup> / TGF $\alpha$  and B82R<sup>+</sup> / sEGF cells were exposed to various antibody concentrations and antigen specificity to determine the proteins' affect on cell ECAR. These studies prove the superiority of blocking antibodies over decoy antibodies on B82R<sup>+</sup> / TGF $\alpha$  cells, achieving receptor / ligand inhibition at 1,000 fold less concentration. However, anti-receptor antibodies were unable to inhibit autocrine B82R<sup>+</sup> / sEGF cells' signalling complexes as these cells express an intracrine signalling pathway.

### **6.2 General Cytosensor Runs**

The Molecular Devices Cytosensor measures the cells' extracellular pH every second during the experiment as described in section 1.7. Briefly, silanol and silamine groups on the surface of the silicon chip develop a surface potential as a function of pH. By applying an increasing external potential to the media, an amplitude-modulated light-emitting diode induced depletion layer collapses, inhibiting photocurrent electron flow in the silicon chip. A plot of current versus applied potential gives an inflection point characteristic of the solution's pH. Two regimes of extracellular pH detection and measuring occur in a Cytosensor experiment. When running buffer is continuously flowing over cells, changes in extracellular pH remains constant because the buffer's resonance time (1.7 seconds) is too short for cells to significantly acidify their buffer. However, once the buffer flow is stopped, cell acidification of extracellular buffer is detectable. The extracellular buffer acidification is measured over several seconds,

typically 20, before resuming buffer's flow. This on / off flow cycle is repeated every minute. By measuring the slope of pH reading versus time when the buffer is not flowing gives cell metabolic rate or extracellular acidification rate (ECAR). An example of the raw data measuring pH as a function of time is shown in Figure 6.1a.

Side products such as lactic acid and  $\text{HCO}_3^-$  are produced during cell breakdown of glucose to energy in glycolysis and energy utilization during respiration. At physiological pH, both lactic acid and  $\text{HCO}_3^-$  dissociate, yielding two to six  $\text{H}^+$  per glucose molecule. A cell's metabolic rate can be increased (addition of growth factors or phorbol esters) or decreased (addition of competing antibodies or chemicals inhibiting tyrosine kinase and protein kinase C activity). Figure 6.1b shows a typical response of B82 EGF receptor positive cells to an growth factor addition (EGF). The curve is normalized to extracellular acidification rates before addition of EGF and expressed as a percent change in baseline. Normalizing ECAR data is done because each cell lane has different absolute metabolic rates, but relative changes in normalized ECAR are similar.

After about 6 to 10 minutes, cells' metabolic rate peaks and starts dropping off. During the experiments, cells are switched off growth factors after reaching peak ECAR back to normal running buffer, minimizing receptor exposure to growth factors and allowing multiple growth factor exposure cycles. The data is analyzed by recording maximal ECAR per EGF addition and plotting ECAR as a function of EGF (Figure 6.2). This graph reveals that B82R<sup>+</sup> cell ECAR response has a dose dependent response to EGF. At low EGF concentrations, the slope of ECAR to EGF additions is fairly linear, however, at higher EGF concentrations, the ECAR response is saturating. The curve also indicates that EGF binding to its receptor is the rate limiting step and that the secondary signalling pathway is not rate limiting due to the dose dependent response to EGF. A further test proving the secondary signalling pathway was not rate limit was the addition of PMA (phorbol ester - activating protein kinase C). Cells' ECAR response was 6 times greater to 1  $\mu\text{M}$  PMA compared to 20 ng / ml EGF (data not shown).

### **6.3 B82R<sup>+</sup> ECAR Response as a Function of mAb225 and mEGF**

Presented in Figure 6.3 is B82 EGF receptor positive cells challenged with EGF and anti-receptor blocking antibody mAb225. Addition of monoclonal antibody 225 does not initiate receptor signalling (discussed later), but does compete for the same binding site on EGFR as EGF and TGF $\alpha$ . B82R<sup>+</sup> cells were equilibrated on the Cytosensor in the presence of varying blocking antibody concentrations until steady state ECAR. Next, varying concentrations of EGF were added until obtaining peak ECAR, upon which EGF was removed and cellular ECAR allowed to re-stabilize before adding a new EGF concentration. All buffers

and samples added to the cells contained blocking antibody, thus maintaining its concentration throughout the experiment.

The EGF response curve in the absence of antibody shows the dose dependent response of B82 EGFR positive cells to EGF as previously discussed. However, addition of blocking antibody inhibited EGF - EGFR binding and signalling, shifting the B82R<sup>+</sup> ECAR response curve rightward. The graph can also be analyzed by observing cellular response with 1 ng / ml EGF and as a function of increasing blocking antibody concentrations. B82R<sup>+</sup> cell response is near maximal without antibody, however, is inhibited upon addition of antibody. A hundred fold increase in antibody concentration, at a thousand fold greater concentration than EGF, completely inhibits EGF from binding to EGFR. Thus, the Cytosensor provides a method for measuring receptor / ligand complex inhibition as a function of antibody concentrations.

#### **6.4 Correlating Cytosensor's ECAR to Receptor / Ligand Complex Levels**

In the previous experiments, changes in receptor / ligand levels were detected as a function of ligand and antibody concentrations. However, Cytosensor output is in terms of extracellular acidification rate or ECAR. Computer models and predictions are in terms of receptor / ligand complexes. Thus, a correlation between ECAR and complexes was required. Published data indicated feasibility of measuring ligand dose-dependent responses on the Cytosensor (Pitchford *et al.* 1995) and recognizing that the same dose-dependent result occurs in I<sup>125</sup> EGF equilibrium binding experiments, it was hypothesized a correlation between ECAR and complex could be obtained. A compilation of data discussed in sections 6.4a, b, and c for B82R<sup>+</sup> / 1st plasmid, uninduced and induced autocrine B82R<sup>+</sup> / TGF $\alpha$  cells is presented in Figures 6.4, 6.5, and 6.6. The immediate observation is the dose dependent, saturating response to EGF in both Cytosensor and I<sup>125</sup> EGF data. With I<sup>125</sup> EGF, the only event measured is ligand binding to its receptor. In Cytosensor data, a multitude of events occur, affecting metabolic rates and Cytosensor output. These events include ligand binding to its receptor and a cascade of kinases interactions and signalling. A dose dependent EGF response on the Cytosensor indicates downstream secondary messenger signalling is not rate-limiting and solely dependent on complex numbers.

##### **6.4a. I<sup>125</sup> Binding - Receptor / Ligand Complexes**

Presented in Figures 6.7, 6.8, and 6.9 are the results from I<sup>125</sup> EGF binding experiments. Originally, I<sup>125</sup> EGF binding experiments were performed at 4 °C and free ligand allowed to incubate on the cells for 3 hours. To match Cytosensor experiments, the binding experiment was performed at 37 °C and allowed to incubate for 10 minutes. Cells were then

transferred immediately to ice and its medium removed. After washing cells multiple times with 1x WHIPS, they were lysed and total complexes measured. Cells were lysed because Cytosensor ECAR output represents both surface and internal signalling complexes. After converting I<sup>125</sup> binding data from radioactive counts (cpm) to complexes (molecules / cell) and free ligand (ng / ml), the data was plotted and a best - fit line determined using equation 6.1.

$$C = L * R_t / (K_d + L) \quad \text{Equation 6.1}$$

Two parameters were determined using this equation, receptor / ligand equilibrium constant,  $K_d$ , and total receptor number,  $R_t$ . The receptor number between cell lines were fairly similar, within 40,000 receptors, since B82R<sup>+</sup> / 1st plasmid are the parental strain of autocrine B82R<sup>+</sup> / TGF $\alpha$  cells. Thus, an abnormal clone, in receptor number, was not selected during TGF $\alpha$  plasmid transfection into B82R<sup>+</sup> / 1st plasmid cells. The gradual reduction in receptor number going from B82 R<sup>+</sup> / 1st plasmid cells to induced autocrine B82R<sup>+</sup> / TGF $\alpha$  cells may be indicative of increased ligand levels down-regulating receptor numbers. The difference between B82 R<sup>+</sup> / 1st plasmid and autocrine cells could be a clonal effect, but not between uninduced and induced autocrine cells as they are the same cell clone - only a difference of induction states.

The second parameter was  $K_d$ . This value was  $10.5 \pm 0.7$ ,  $11.4 \pm 1.1$ ,  $11.5 \pm 1$  ng / ml for B82 R<sup>+</sup> / 1st plasmid, uninduced autocrine and induced B82 R<sup>+</sup> / TGF $\alpha$  autocrine cells, respectively, or similar within experimental error. An average of 11.1 ng / ml equates to 1.84 nM binding affinity constant, within published EGF / EGFR  $K_d$  of 1-2 nM (Ebner and Derynck 1991).

#### 6.4b. Cytosensor ECAR Output

The second part to correlating complex number and ECAR is obtaining ECAR versus free ligand concentrations. This was accomplished by measuring changes in cell's ECAR as a function of free ligand concentrations. When working with induced autocrine cell, its medium was tetracycline-free overnight to induce TGF $\alpha$  expression. After equilibrating the cells to steady state ECAR on the Cytosensor, a gradient of EGF (similar range as performed with I<sup>125</sup> EGF) was added to each Cytosensor lane. Immediately after obtaining a peak ECAR or after 10 minutes of EGF exposure, the EGF was removed and cells allowed to return to baseline metabolic rates before beginning another EGF addition. Since EGF was sequentially added to cells, relatively large jumps in EGF concentrations were performed to minimize effects of previous EGF on later additions. Thus, cells saw a 10 fold increase in EGF versus doubling ligand concentrations at each measurement. The concentration jumps were accomplished by exposing a Cytosensor / cell lane to every third EGF concentration in the gradient profile.

Maximum ECAR was recorded at each EGF addition and plotted as ECAR versus EGF. The data was curve fit to equation 6.1 replacing  $R_t$  with  $ECAR_{max}$  and  $K_d$  with  $L_{0.5}$ .

Results from Cytosensor experiments are shown in Figures 6.10, 6.11, and 6.12. The data points are far more random compared to  $I^{125}$  EGF data. This variance is likely due to measuring a result through multiple secondary pathway signals, inaccuracies in ligand concentrations, and comparing experiments over several months. Cytosensor ligand concentrations were diluted down to predicted values. Whereas in  $I^{125}$  EGF experiments, EGF concentrations were measured and calculated based on radioactive counts. The worst fit data was with B82R<sup>+</sup> / 1st plasmid, however, it was caused mostly by one experimental series. If that series is removed, the fit improves from  $R^2 = 0.59$  to 0.75. The uninduced and induced curves were a fairly good fit with  $R^2 = 0.85$  and 0.79, respectively.

In this experiment, both parameters vary in interesting patterns. There is a large, 50%, drop in grouped  $ECAR_{max}$  upon TGF $\alpha$  expression induction. It is difficult to infer the decrease's significance.  $ECAR_{max}$  can be considered a function of receptor number or total signalling complexes similar to parameter  $R_t$  in  $I^{125}$  EGF data. It would be expected that R<sup>+</sup> / 1st plasmid cells, having no ligand expression, would have a similar  $ECAR_{max}$  value as low expressing, uninduced autocrine B82R<sup>+</sup> / TGF $\alpha$  cells. However, B82R<sup>+</sup> / 1st plasmid's  $ECAR_{max}$  is significantly different and smaller than uninduced autocrine cells. Eliminating the three high outliers in both R<sup>+</sup> / 1st plasmid and induced autocrine data shifts  $ECAR_{max}$  to 42 and 25, respectively (data not shown), thus, removal of the outliers only magnifies the differences between uninduced and R<sup>+</sup> / 1st plasmid cells.

The second parameter is ligand concentration at half maximally ECAR, or  $L_{0.5}$ . This parameter increases with increasing ligand expression. Since receptor / ligand affinity,  $K_d$ , was the same between cell lines (Section 6.3a), the increase in  $L_{0.5}$  could be a result of receptor desensitization. Therefore, higher concentrations of exogenous ligand are required to obtain similar signalling / metabolic responses with increasing ligand secretion rates. Removal of outliers discussed in the previous paragraph does not change this observed  $L_{0.5}$  differential. The numbers change from  $10.8 \pm 3.6$  to  $9.4 \pm 2.9$  in the induced autocrine data and doesn't change in R<sup>+</sup> / 1st plasmid data ( $2.1 \pm 1$  to  $2.1 \pm .81$ ) while uninduced autocrine cells  $L_{0.5}$  remains  $4.5 \pm 1$  (data not shown).

#### **6.4c. Relating ECAR to Receptor / Ligand Complexes**

After performing the  $I^{125}$  EGF and Cytosensor experiments and obtaining best fit equations, the equations were linked via variable free EGF to derive a correlation between

ECAR and complex numbers. This correlation can be derived by two methods as described in section 5.3c.

A best fit line using equation 5.3 was plotted for all three cell types in Figures 6.13, 6.14, and 6.15 with experimental data. To plot experimental data, free ligand concentrations from each experiment were converted into predicted ECAR or complexes via the corresponding graph's best fit equation. Thus, experimental free EGF concentrations from I<sup>125</sup> EGF experiments (experimental free EGF and experimental complexes) were converted to predicted ECAR using the equation from Cytosensor ECAR vs. free EGF data and plotted as predicted ECAR vs. experimental complexes.

The ECAR versus complexes graphs' curves become linear with increasing TGF $\alpha$  expression. This observation goes back to the Cytosensor data described in section 6.4b when receptor desensitization occurs with increasing TGF $\alpha$  expression. Thus, in a cell line which has not seen ligand, i.e. B82R<sup>+</sup> / 1st plasmid cells, short ligand exposure times to cells results in receptor / ligand signal saturation at high ligand concentrations. Compared to cells continuously in the presence of TGF $\alpha$  (i.e. autocrine), receptor desensitization has already occurred and apparently allows a linear signal response thereafter. One argument could be that exogenously added EGF concentrations is significantly smaller than autocrine TGF $\alpha$  secretion rates, masking the effect of EGF. However, 0.1 ng / ml exogenously added EGF corresponds to approximately 7,000 molecules per cell - minute. Induced autocrine TGF $\alpha$  cells express approximately 3,000 - 7,000 molecules per cell - minute. Calculations and Cytosensor chamber sizing parameters are in Appendix B.

Finally, an experimental system has been created to accurately, quantitatively, in real time, measure hard-to-detect receptor / ligand complexes. Also, Cytosensor output in terms of ECAR can be successfully correlated back to receptor / ligand complexes using correlation experiments with free ligand on both Cytosensor and I<sup>125</sup> binding experiments.

## 6.5 Measuring B82R<sup>+</sup> / TGF $\alpha$ Induction

The previous experiments discussed in Chapter 6 measured B82 EGFR cell responses to addition of blocking antibodies and / or EGF, however, the goal of this thesis was to measure receptor / ligand interactions in autocrine cells as a function of competing antibodies. Therefore, the following experiment was performed with autocrine B82R<sup>+</sup> / TGF $\alpha$  cells to demonstrate how well the Cytosensor could differentiate between varying TGF $\alpha$  secretion rates. Briefly, uninduced autocrine B82 R<sup>+</sup> / TGF $\alpha$  cells (medium containing 1  $\mu$ g/ml tetracycline) were plated onto transwells and allowed to attach overnight. The uninduced autocrine cells were placed on the Cytosensor and allowed to equilibrate their metabolic rates in normal DV / cyto running



buffer containing 1  $\mu\text{g}/\text{ml}$  tetracycline. After obtaining steady state ECAR, the following conditions were imposed:

1. Induced Autocrine cells: No tetracycline
2. Induced Autocrine cells: No tetracycline + 1  $\mu\text{g}/\text{ml}$  blocking antibody 225
3. Uninduced Autocrine cells: 1  $\mu\text{g}/\text{ml}$  tetracycline
4. Uninduced Autocrine cells: 1  $\mu\text{g}/\text{ml}$  tetracycline + 1  $\mu\text{g}/\text{ml}$  blocking antibody 225.

These experiments were run seven - eight hours, allowing TGF $\alpha$  expression into extracellular medium and binding to EGFR. Each cell chamber's ECAR was recorded at seven hours and normalized to uninduced autocrine cells with 1  $\mu\text{g}/\text{ml}$  blocking antibody 225. This baseline was chosen as it has smallest ECAR reading due to little ligand expression and receptor - ligand complex formation was inhibited. A typical TGF $\alpha$  induction experiment with autocrine B82 R<sup>+</sup> / TGF $\alpha$  cells is shown in Figure 6.16. As seen, induced cells' metabolic rate start increasing after about 5 to 6 hours, corresponding to the average time it takes for a cell to transcribe DNA to RNA, translation RNA to protein and secrete that protein in the extracellular medium (Bringman *et al.* 1987). After this initial ECAR increase, cells establish a new metabolic equilibrium.

The difference in ECAR response to TGF $\alpha$  induction and receptor / ligand complex inhibition can be quantitated more clearly in Figure 6.17. Induced autocrine cells' ECAR readings increased 16% compared to uninduced autocrine cells with blocking antibody. The induction is also significant between uninduced cells and induced cells (one standard deviation) and addition of blocking antibodies significantly reduced induced cells' ECAR levels by inhibiting TGF $\alpha$  from binding EGFR. Thus, this experiment showed that measurements of autocrine TGF $\alpha$  expression induction and inhibition autocrine signalling by blocking antibodies can be measured on the Cytosensor.

## 6.6 Tetracycline Gradient on Autocrine B82R<sup>+</sup>/TGF $\alpha$ Cells

One reason for using the tetracycline - controlled, two plasmid expression system is the ability to control TGF $\alpha$  expression levels between “off” and “on” by adjusting tetracycline concentrations in the medium. This induction “gradient” for TGF $\alpha$  expression was analyzed in section 3.5 by measuring extracellular ligand concentrations as a function of tetracycline concentrations. However, the Cytosensor provides an ability to measure receptor complex levels as a function of ligand expression. Briefly, uninduced autocrine cells were plated into Cytosensor transwells and allowed to attach overnight. A tetracycline gradient was added to

induce TGF $\alpha$  expression overnight and achieve steady state ligand expression for the experiment. Two transwells were designated as uninduced cells containing 1  $\mu$ g / ml tetracycline to its medium. One transwell was designated as semi-induced cells by addition of 5 ng / ml tetracycline to its medium (200 fold less tetracycline) and the last well designated as fully induced autocrine cells tetracycline - free medium.

A representative graph of these experiments is plotted in Figure 6.18a. Upon addition of 10 ng / ml EGF to each of the equilibrated autocrine cells, a difference in ECAR response can be observed. There was a slight decrease (5% difference) in peak ECARs between uninduced cells and semi-induced cells upon addition of EGF. A significant change in ECAR response occurs when induced autocrine cells received EGF, giving a 35% decrease compared to uninduced autocrine cells. This ECAR response differential between semi-induced and fully induced autocrine cells compared to uninduced autocrine cells highlights the receptor desensitization which occurs upon ligand induction. As seen in section 6.4a, autocrine cell receptor numbers were fairly similar between the two ligand expression levels (16% decrease), thus, at least half of the changes in ECAR must be due to desensitization of the EGF receptor.

Uninduced autocrine cells have very few receptor - ligand complexes compared to fully induced autocrine cells as uninduced cells produce little to no TGF $\alpha$  ligand. Thus, upon addition of high blocking antibody concentrations, one would expect a drop in ECAR corresponding to initial complex levels. As seen in Figure 6.18b, fully induced autocrine cells' ECAR dropped the most, due to the increased number of initial signalling complexes present compared to uninduced autocrine cells upon antibody addition. Since semi-induced autocrine cells' initial complex levels were in-between induced and uninduced cells, its ECAR drop naturally falls between fully induced and uninduced autocrine cell's ECAR in the presence of antibody. Thus, this experiment demonstrates receptor desensitization and initial receptor - ligand complex levels can be quantified on the Cytosensor.

### **6.7 Antibody Inhibition of Receptor / Ligand Complex on B82R<sup>+</sup>/TGF $\alpha$**

The next experiment tests the central hypothesis of this thesis that blocking antibodies are superior inhibitors of receptor / ligand complexes compared to decoy antibodies. Computer modelling indicates that blocking antibodies inhibit receptor / ligand complex formation at much lower antibody concentrations. One reason is unbound decoy antibody concentrations are "diluted" by binding to extracellular bulk ligand, decreasing the antibodies' effective diffusion gradient to the cell surface where it competes directly against EGFR for TGF $\alpha$ .

Briefly, uninduced autocrine B82R<sup>+</sup> / TGF $\alpha$  cells were plated in Cytosensor transwells overnight to allow cell attachment. TGF $\alpha$  expression was induced overnight to obtain steady

state ligand expression by removal of tetracycline from the medium. The induced autocrine cells were equilibrated on the Cytosensor in normal DV/cyto running buffer without tetracycline until their ECAR reached a steady state. Ten ng / ml mouse EGF was added to each lane and peak ECAR observed to ensure all cell lanes behaved similarly. Immediately upon reaching peak ECAR, EGF was removed from the cells and their ECAR allowed to re-adjust back to baseline. Upon establishing a baseline, varying concentrations of blocking antibody 225, decoy anti-TGF $\alpha$  antibody, or neutral rabbit IgG were added to each cell lane and decreases in ECAR measured for at least 30 minutes. An typical experiment is shown in Figure 6.19.

Shown in Figure 6.20 is a compilation of all antibody experiments on autocrine B82R<sup>+</sup> / TGF $\alpha$  cells. Blocking antibody concentrations were varied over five orders of magnitude resulting in no effect to total receptor / ligand binding inhibition. Inhibition of autocrine B82R<sup>+</sup> / TGF $\alpha$  binding was achieved at 1 nM blocking antibody, corresponding to predicted concentration in the mathematical model. Also predicted by the model was blocking antibody's superiority over decoy antibodies. Addition of high decoy antibody concentrations, around 900 nM, only slightly affected autocrine signalling, meaning nearly 7000 times more decoy antibody was required to achieved the same inhibition as blocking antibodies. Both antibodies have a  $K_d$  equal to EGF / EGFR's  $K_d$  of 1 nM (Mendelsohn *et al.* 1987; Technical Support 1995).

Several control experiments were performed to ensure these antibody effects were specific to receptor / ligand complex inhibition and not nonspecific events. Addition of nonspecific rabbit IgG at 100  $\mu$ g / ml did not affect cells' metabolic rate, indicating that reduction in ECAR upon addition of blocking antibodies is specific to the inhibition of autocrine receptor / ligand complex formation and not a random antibody effect. Another control experiment ensured that addition of blocking antibody 225 did not stimulate or inhibit cell signalling in control B82 R<sup>+</sup> or autocrine B82R<sup>+</sup> / TGF $\alpha$  cells. The experiment is shown in Figure 6.21. Antibody 225 was added to cells which did and did not receive a prior dosage of EGF. Antibody 225 did not stimulate cell metabolic rates through receptor binding and no decrease in ECAR occurred upon addition of blocking antibody after an EGF challenge. The second part of the experiment proved that the decrease in ECAR upon addition of antibody was not due blocking previously added exogenously bounded EGF (these complexes already disappeared), but by preventing autocrine ligand TGF $\alpha$  binding.

One possible explanation for experimental decoy antibody's inability to successfully inhibit receptor - ligand complex formation is the antibody could recognize and bind TGF $\alpha$  but not prevent it from binding to EGFR. In other words, it would be a recognition antibody, but not a neutralizing antibody. Two large molecules (170 kDa - receptor and 150 kDa - antibody) could successfully bind a small protein (5.5 kDa), the premise of sandwich ELISAs. Thus, an

experiment was performed to prove anti-TGF $\alpha$  decoy antibody was a neutralizing antibody. One Cytosensor transwell was plated with B82R<sup>+</sup> and three transwells were plated with induced autocrine B82R<sup>+</sup> / TGF $\alpha$  cells and allowed to attach overnight. The following day, ten  $\mu$ g / ml TGF $\alpha$  was added to each equilibrated cell lane and maximum ECARs recorded. Immediately, after obtaining peak ECAR, TGF $\alpha$  was removed and ECARs returned back to baseline. Next, the following conditions were applied:

1. B82R<sup>+</sup> - 10  $\mu$ g / ml decoy antibody + 10 ng / ml TGF $\alpha$
2. Induced Autocrine - 50  $\mu$ g / ml decoy antibody
3. Induced Autocrine - 50  $\mu$ g / ml blocking antibody
4. Induced Autocrine - blank

As seen in Figure 6.22b, addition of blocking antibody inhibited autocrine receptor / ligand binding while addition of decoy antibody did not. Addition of TGF $\alpha$  alone to B82R<sup>+</sup> cells increased ECAR (Figure 6.22a - triangles), however, complete inhibition of signalling was achieved upon addition of TGF $\alpha$  and decoy antibody (Figure 6.22b - triangles), proving that the decoy antibody is a neutralizing antibody.

A more nuanced comparison between experimental (Figure 6.20) and mathematical data (Figure 2.3) reveals a difference in initial receptor / ligand levels. Receptor / ligand complex levels are predicted to be around 6%, however, experimental calculations determined receptor complex levels are closer to 60%. A few potential explanations can be offered. First, one assumption when correlating receptor / ligand levels for autocrine cells is a one to one relationship exists between increasing ECAR upon addition of EGF and decreasing ECAR upon addition of competing antibodies. Since both proteins affect signalling pathway at the same point (receptor), the relationship should hold. If not, the data would suggest a 10 fold difference exists between signal induction and degradation.

A secondary possibility is cell density affecting receptor complex levels during the correlation experiments. During these experiments, cell density was around 350,000 cells / 35 mm dish for the I<sup>125</sup> EGF binding experiment and an estimated 400,000 cells / 12 mm transwell for the Cytosensor experiment. The difference in cell coverage is nearly an order of magnitude (~3 % and ~30%, I<sup>125</sup> and Cytosensor, respectively). At a higher cell density, receptor number could be further down-regulated and desensitized on the Cytosensor compared to I<sup>125</sup> cells. This desensitization would change the slope of ECAR versus complexes curve lower, meaning more complexes are required to achieve similar ECAR. However, there is an argument against this possibility upon analysis of uninduced and induced autocrine Cytosensor data (Figure 6.11

and 6.12). Assuming a ten fold increase in density was similar to a ten fold increase in ligand expression or at worst case nonlinear and greater, the autocrine ligand induction was 200 fold, yet the maximum ECAR only decreased by half upon ligand induction and receptor desensitization, not a 10 fold discrepancy.

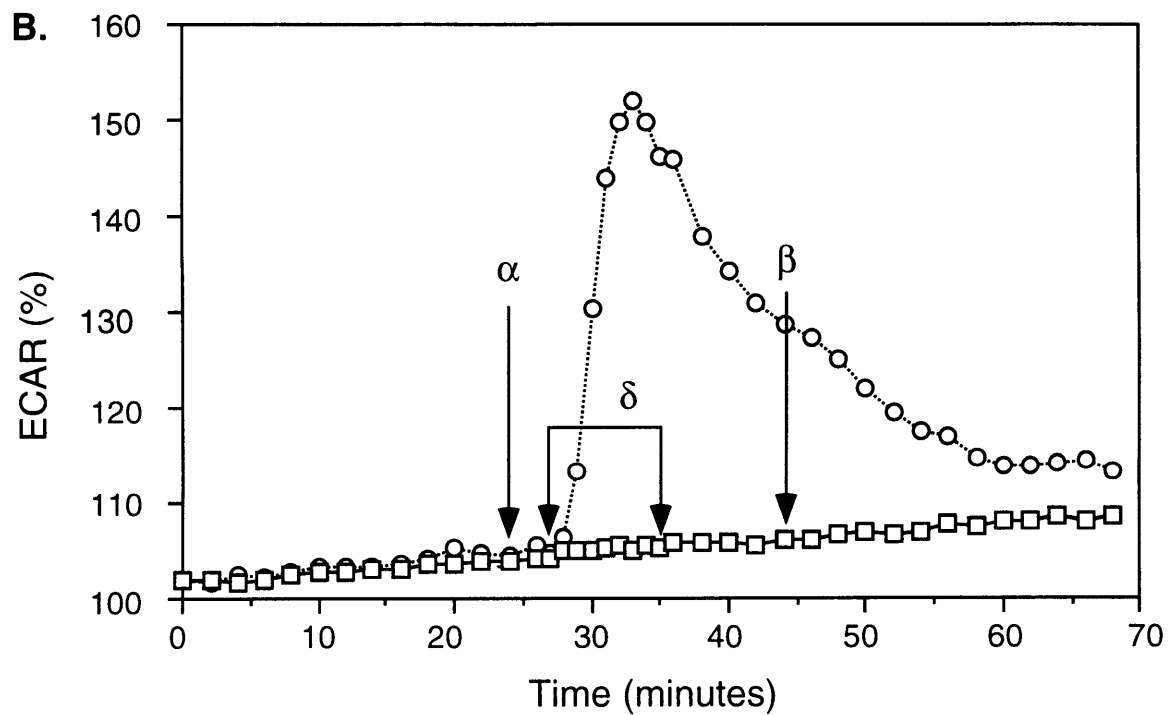
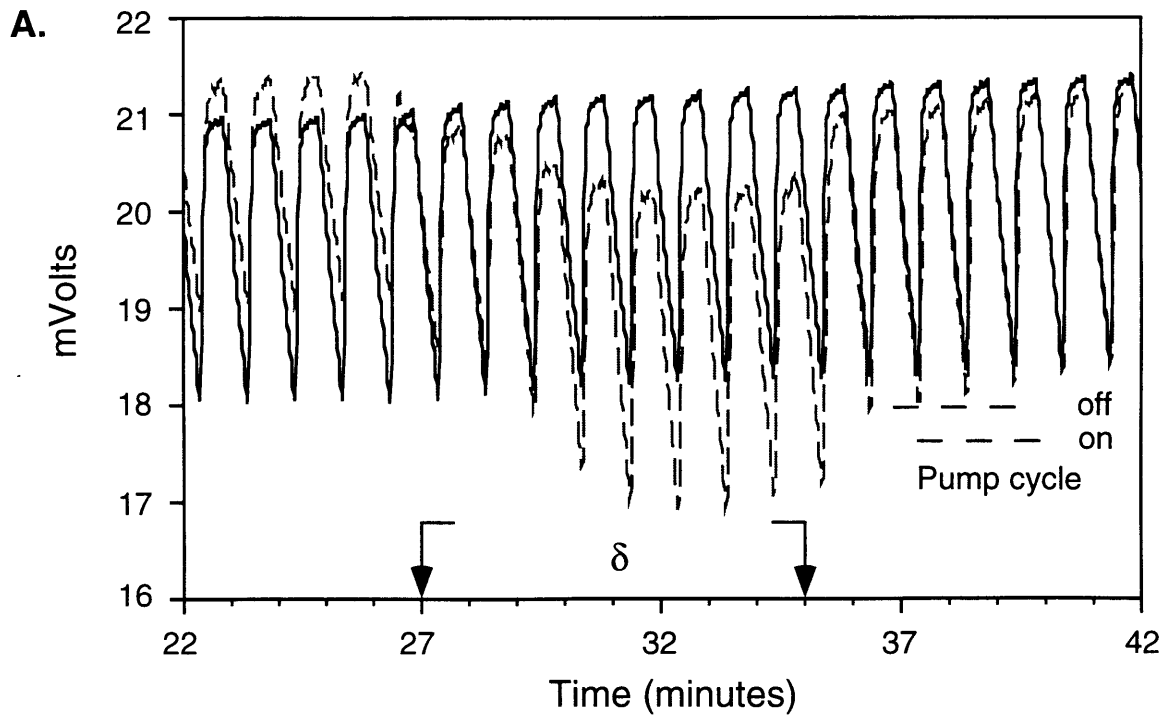
A third, and more likely, reason for the difference between experimental data and computer predictions is a subtle difference between EGF and TGF $\alpha$  proteins. Autocrine computer modelling assumes all receptor / ligand complexes are internalized and degraded in the lysosome. This is a valid assumption for EGF. But, while both proteins have similar  $K_d$ s at physiological pH, TGF $\alpha$  is more pH sensitive and dissociates from its receptor as pH decreases (TGF $\alpha$  - 6 nM to 400 nM and EGF - 3 nM to 80 nM as pH goes from 7.4 to 6.0). Thus, at endosomal pH, TGF $\alpha$  is mostly unbound, allowing receptor recycling back to the cell surface (Engler *et al.* 1988; French *et al.* 1995). Once, the receptors are back on the cell surface, they can quickly rebind ligand forming new signalling complexes. This recycling means less EGFR downregulation, faster recovery of binding following endocytosis, and therefore, increased receptor / ligand complex number along with enhanced mitogenic potency (Engler *et al.* 1988; Reddy *et al.* 1996). In addition, more ligand may be recycled as well at lower intercellular complex levels. Differences between EGF and TGF $\alpha$ 's endosomal trafficking could help explain why both bulk ligand concentrations and receptor / ligand complexes are higher than predicted by computer modelling.

### **6.8 Blocking Antibody Inhibition of Receptor Complexes on B82R<sup>+</sup>/sEGF**

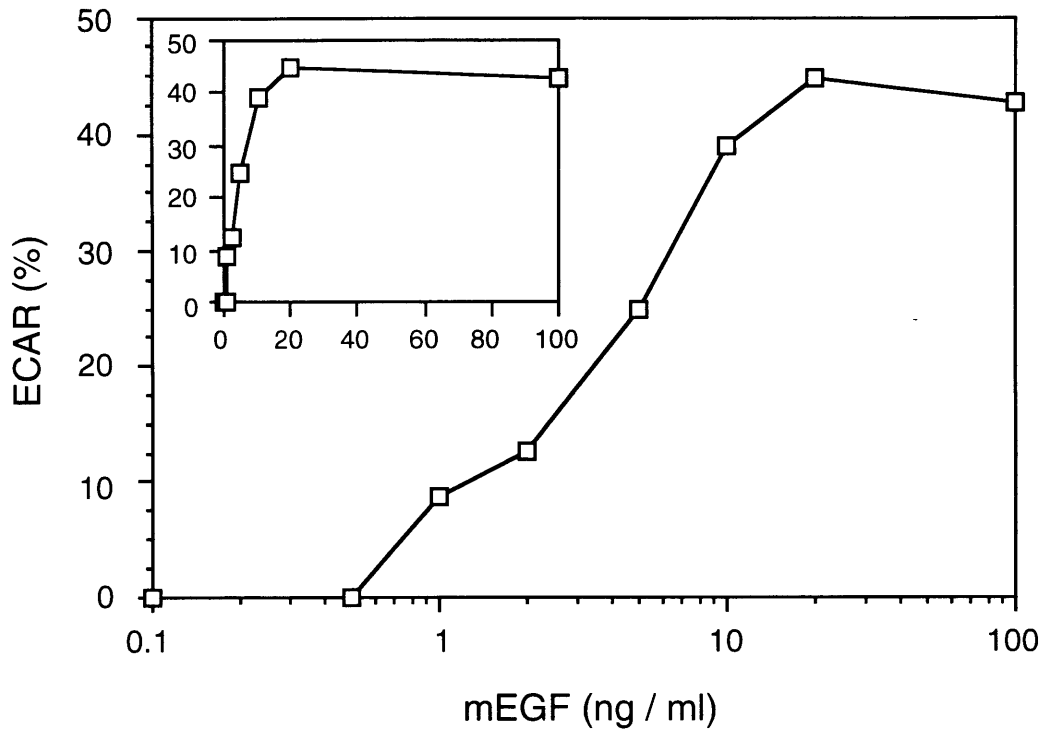
Autocrine B82R<sup>+</sup> / TGF $\alpha$ 's ligand is synthesized as a 25 kDa transmembrane precursor and expressed to the cell surface before the extracellular mature protein (5.5 kDa) is enzymatically cleaved into the medium. Autocrine B82R<sup>+</sup> / sEGF, constructed by Dr. Birgit Will-Simmons, is synthesized as a mature 6 kDa protein and secreted directly out to the medium. Studies in Dr. Steve Wiley's lab (University of Utah, Salt Lake City, Utah) and Dr. Jeff Morgan's lab (Shriners' Burn Institute, Cambridge, MA) indicate the inability of blocking antibodies to inhibit cell growth and migration in HMEC 184 and human keratinocytes cells upon transfection of sEGF into these EGFR positive cell lines (personal communications). It is hypothesized that sEGF and EGFR are secreted to the cell's surface in the same secretion vesicles and able to bind together before reaching the cell surface. To maintain normal receptor membrane turnover (0.03 min.<sup>-1</sup>) for 100,000 receptor would require synthesizing 3,000 new receptor / cell-minute. Both induced B82R<sup>+</sup> / TGF $\alpha$  and B82R<sup>+</sup> / sEGF autocrine clones can secrete over 6,000 ligand molecules / cell-minute. Thus, all of the receptors could be bound, signalling and immediately internalized upon reaching the cell's surface with an autocrine B82R<sup>+</sup>

/ sEGF cell. As transmembrane TGF $\alpha$  is bound to the secretory vesicle's surface and has a precursor NH<sub>2</sub> end, it would be sterically hindered from binding EGFR present in the secretory vesicles of autocrine B82R<sup>+</sup> / TGF $\alpha$  cells.

The inability of blocking antibody 225 to inhibit autocrine B82R<sup>+</sup> / sEGF receptor - ligand signalling is shown in Figure 6.23. Addition of 300  $\mu$ g / ml blocking antibody 225 to autocrine B82R<sup>+</sup> / TGF $\alpha$  cells would ensure complete and total inhibition of signalling; however, when added to autocrine B82R<sup>+</sup> / sEGF cells resulted in only a 4% change from baseline, similar to inhibition achieved with 0.02  $\mu$ g / ml (15,000 times less antibody) on autocrine B82R<sup>+</sup> / TGF $\alpha$  cells. Since both ligands bind similarly to EGFR, the difference would appear to be sEGF's ability to intracellularly bind EGFR before cell surface expression, thus preventing blocking antibody from binding extracellularly.

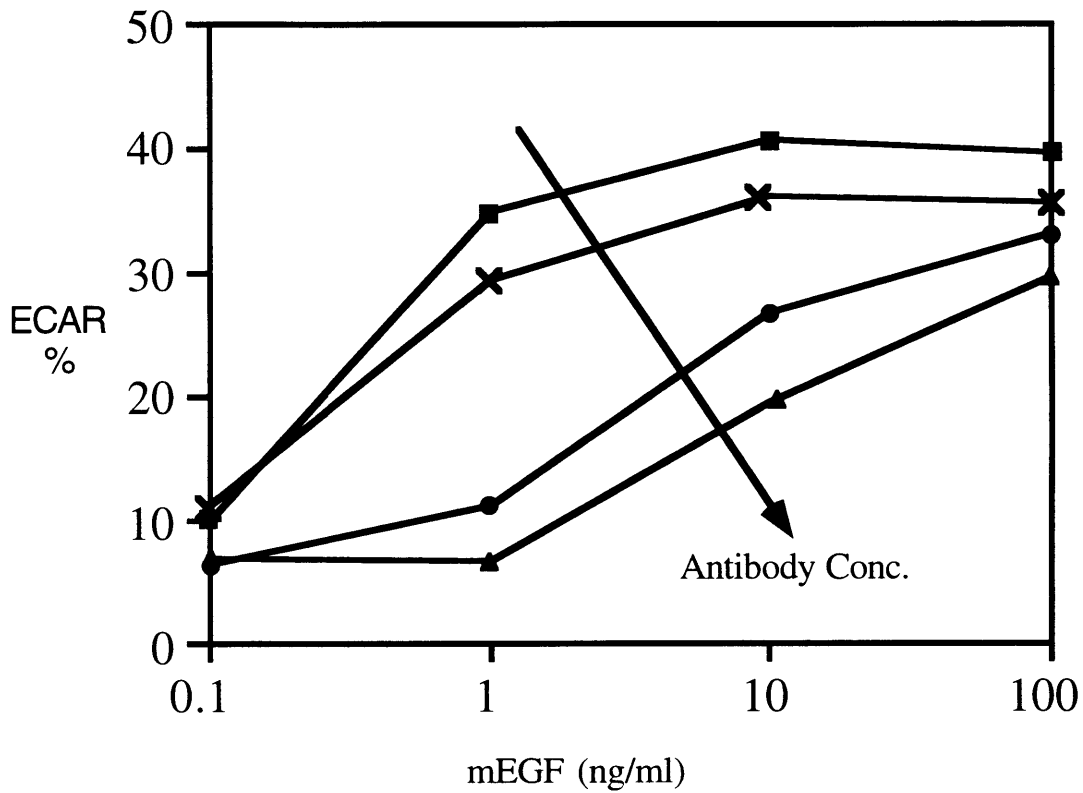


**Figure 6.1: Experimental raw and rate data.** Equilibrated B82R<sup>+</sup> were exposed to 20 ng / ml mEGF (circles / dotted line) or not (squares, solid line) for 8 minutes at  $\delta$ . Graph A. Raw data readings used to determine ECAR in graph B between points  $\alpha$  and  $\beta$ . Graph B. Rate data for B82R<sup>+</sup> cells.

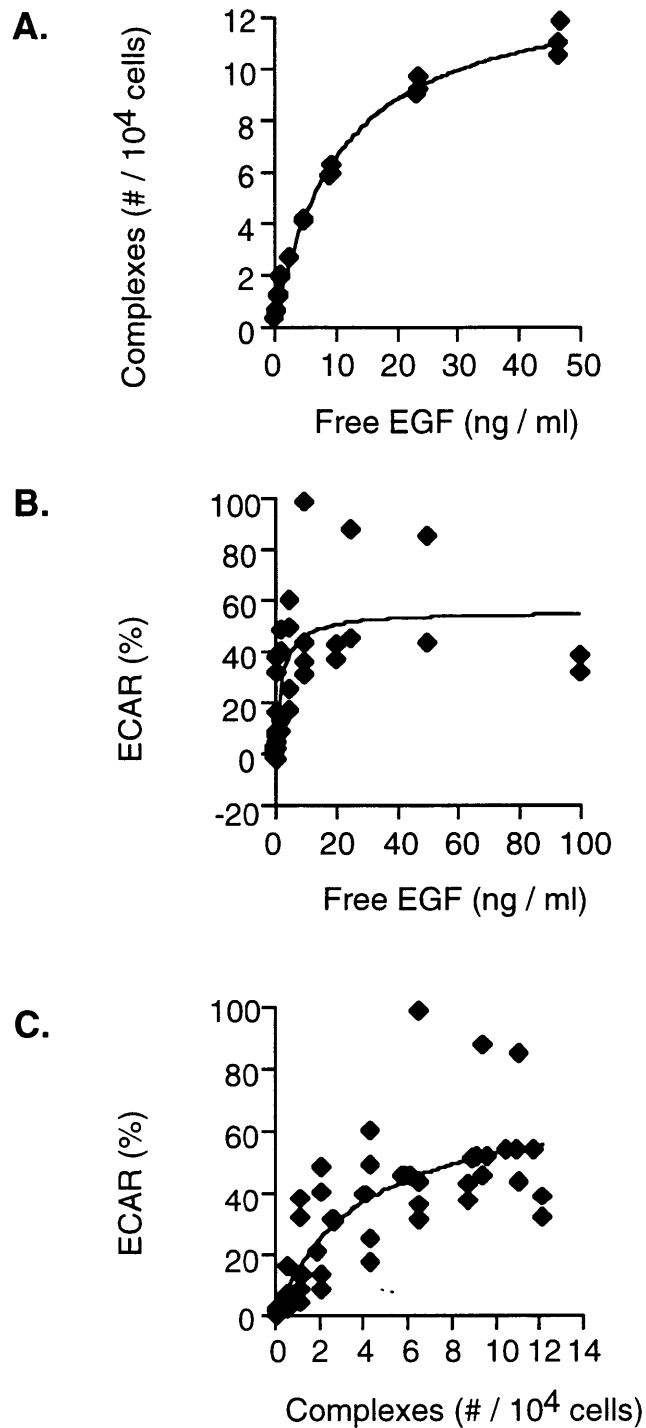


**Figure 6.2: B82R<sup>+</sup> control cells - Cytosensor EGF response curve.**  
 Equilibrated B82R<sup>+</sup> cells were exposed to a gradient of mEGF on Molecular Devices Cytosensor. Data plotted as log in the figure and linear in the insert.

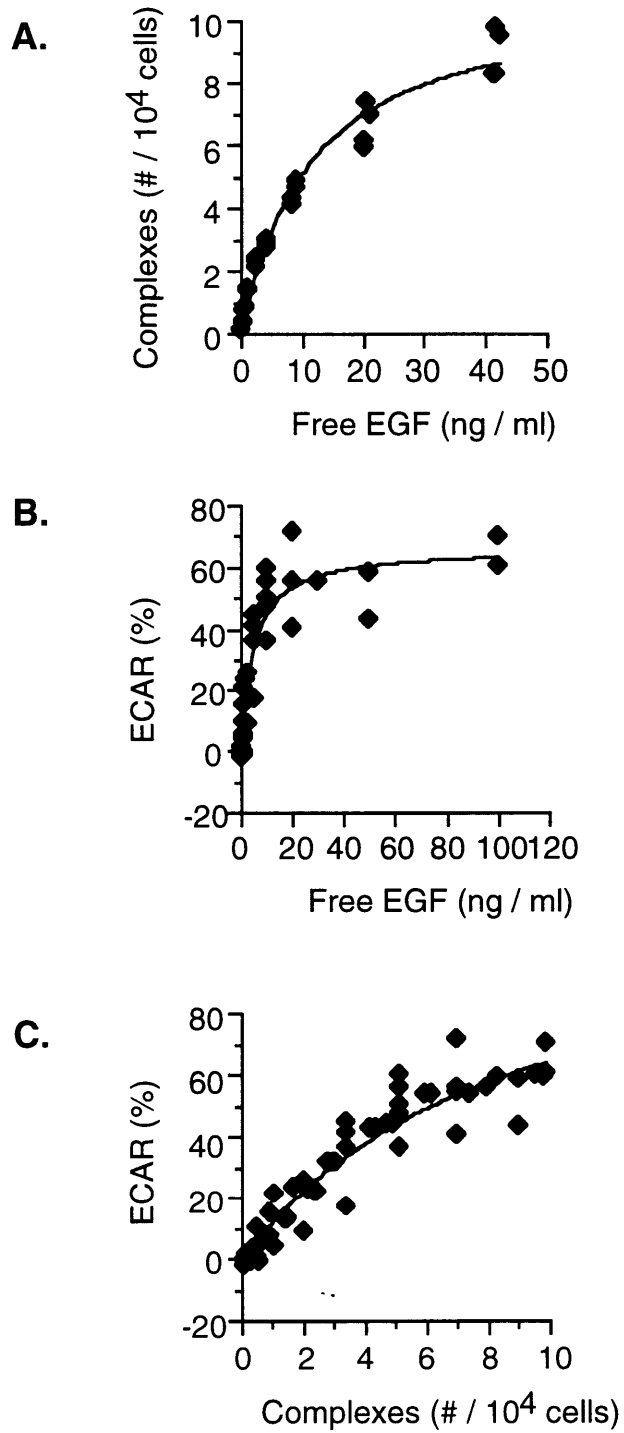




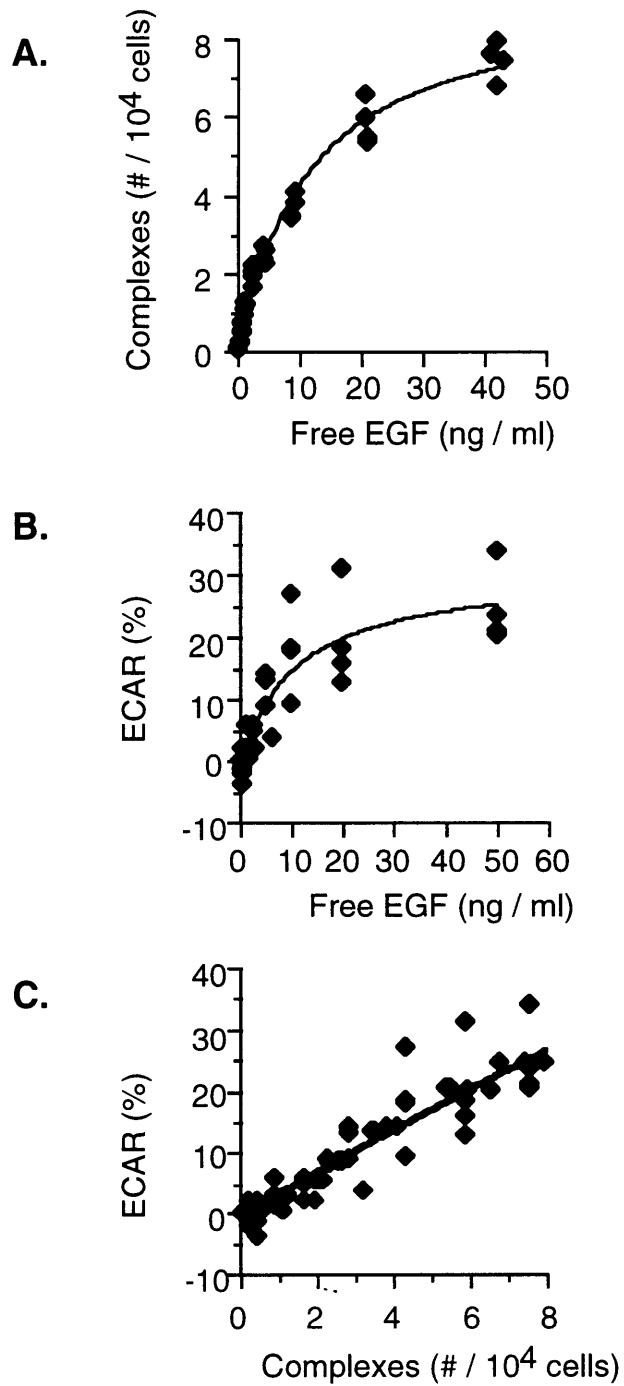
**Figure 6.3: Cytosensor measurement - B82R<sup>+</sup> with EGF and mAb225.** B82R<sup>+</sup> cells were equilibrated in the presence of 0 (squares), 0.01 (cross), 0.1 (circle), and 1 (triangle) µg / ml anti-EGFR antibody 225. Upon equilibration, the cells were exposed to indicated EGF gradient.



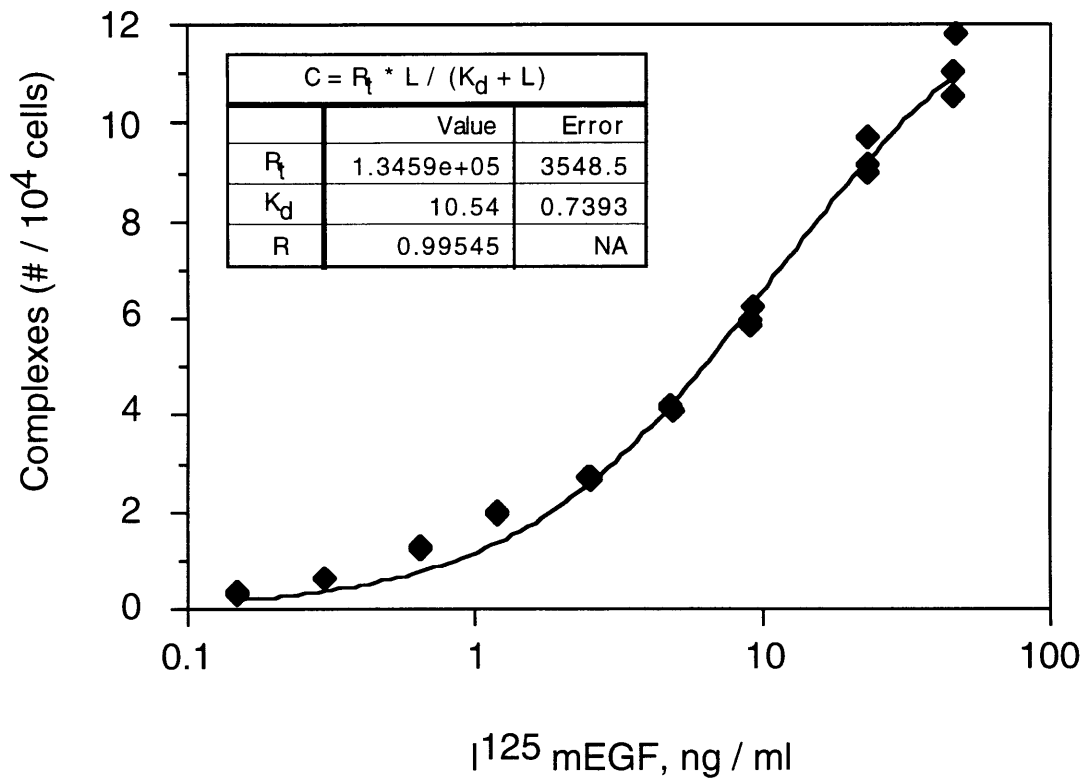
**Figure 6.4: Overview ECAR to Complex - B82R<sup>+</sup> / 1st plasmid.** Graph A. <sup>125</sup>I mEGF Gradient binding experiment. Graph B. mEGF Gradient on Cytosensor. Graph C. Correlation of ECAR to Complexes.



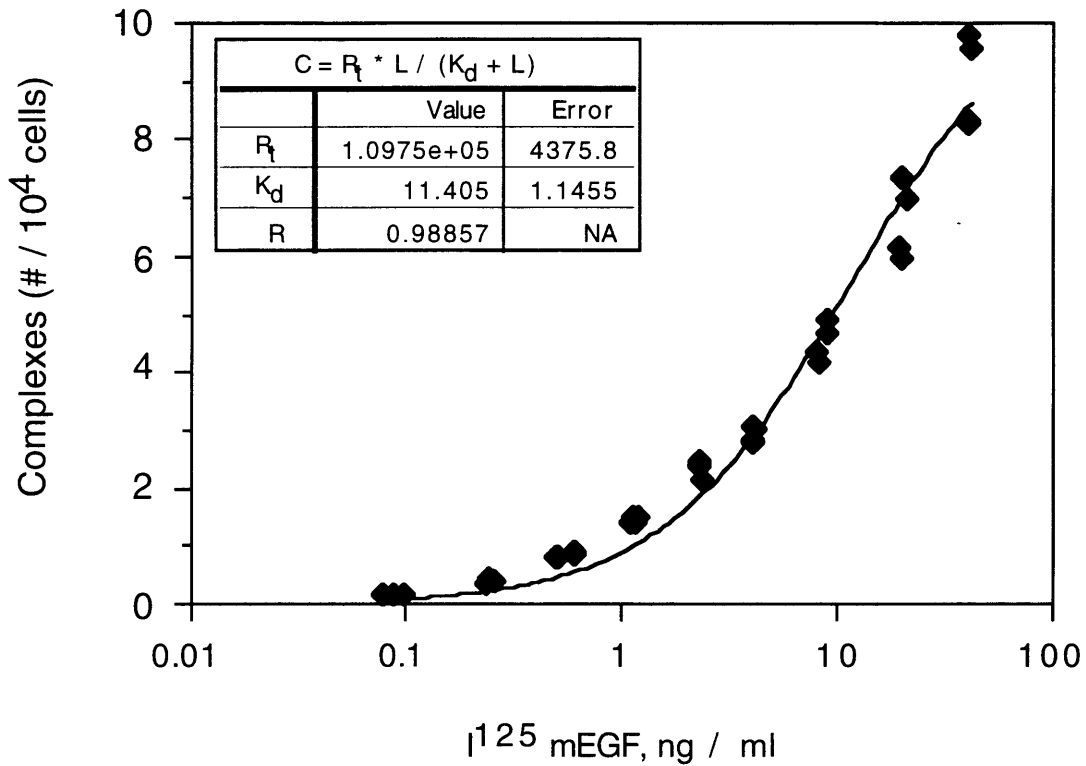
**Figure 6.5: Overview ECAR to Complex - uninduced B82R<sup>+</sup> / TGF $\alpha$ .** Graph A. [<sup>125</sup>mEGF Gradient binding experiment. Graph B. mEGF Gradient on Cytosensor. Graph C. Correlation of ECAR to Complexes.



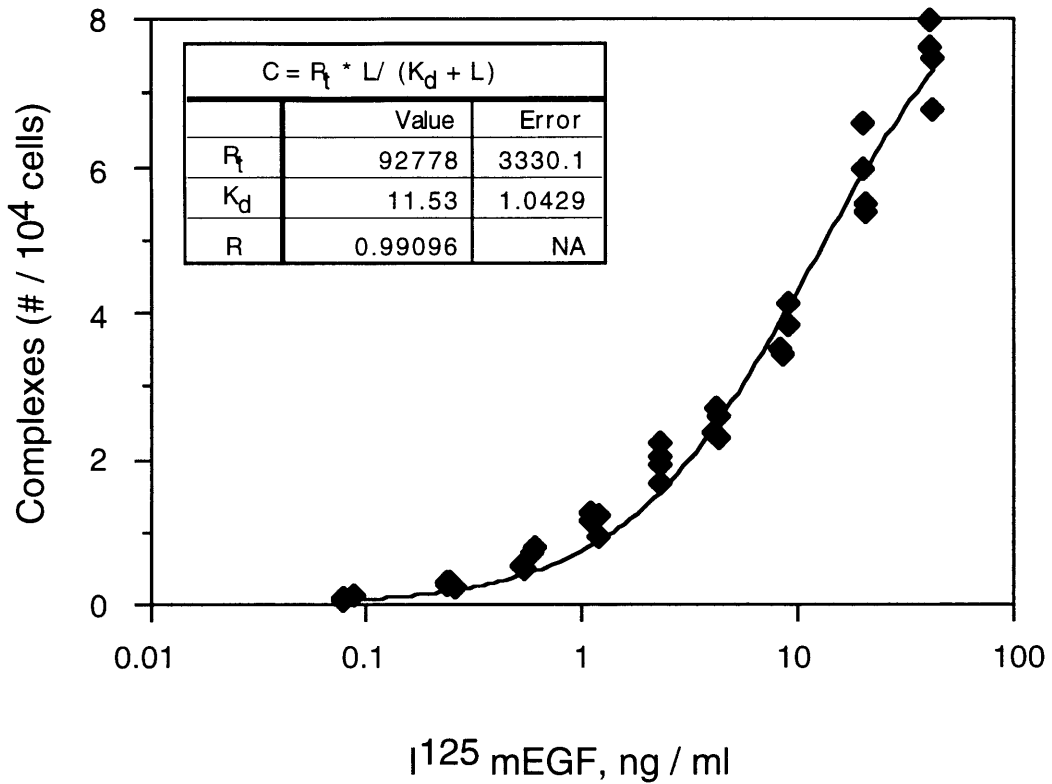
**Figure 6.6: Overview ECAR to Complex - Induced B82R<sup>+</sup> / TGF $\alpha$ .** Graph A. I<sup>125</sup> mEGF Gradient binding experiment. Graph B. mEGF Gradient on Cytosensor. Graph C. Correlation of ECAR to Complexes.



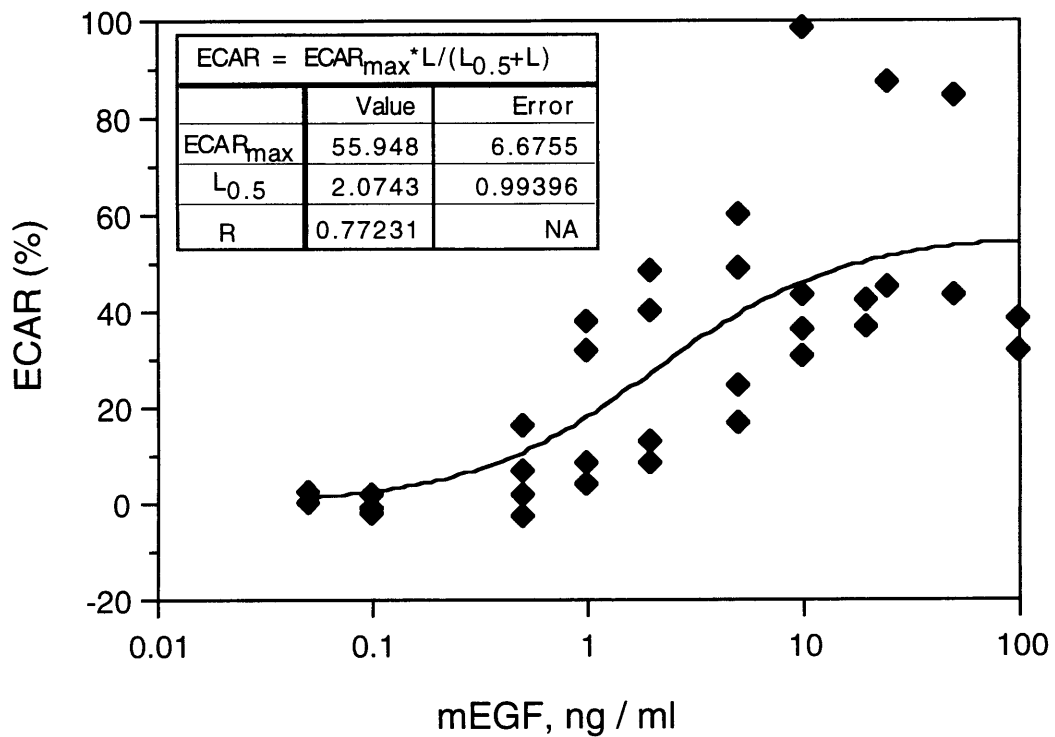
**Figure 6.7: <sup>125</sup>I Binding - B82R<sup>+</sup> / 1st plasmid.** After incubating cells with D/H/B media for 3 hours, cell were incubated with <sup>125</sup>I EGF for 10 minutes. Media was removed and cpm counts defined as free ligand. Cells were lysed with 1 M NaOH and cpm counts defined as bound ligand.



**Figure 6.8: I<sup>125</sup> Binding - Uninduced B82R<sup>+</sup> / TGF $\alpha$ .** Autocrine clone #1's TGF $\alpha$  expression was repressed by 1  $\mu$ g / ml tetracycline containing media. After incubating cells with D/H/B media for 3 hours, cell were incubated with I<sup>125</sup> EGF for 10 minutes. Media was removed and cpm counts defined as free ligand. Cells were lysed with 1 M NaOH and cpm counts defined as bound ligand.

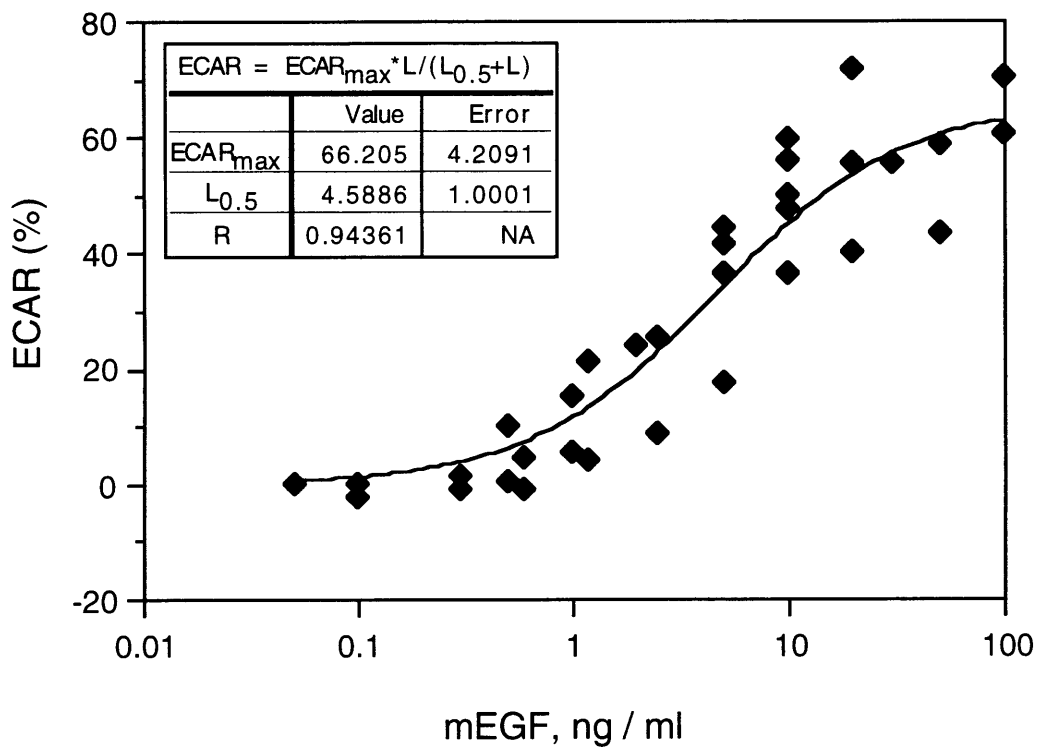


**Figure 6.9: <sup>125</sup>I Binding - Induced B82R<sup>+</sup> / TGF $\alpha$ .** Autocrine clone #1's TGF $\alpha$  expression was induced overnight by removal of tetracycline. After incubating cells with D/H/B media for 3 hours, cell were incubated with <sup>125</sup>I EGF for 10 minutes. Media was removed and cpm counts defined as free ligand. Cells were lysed with 1 M NaOH and cpm counts defined as bound ligand.

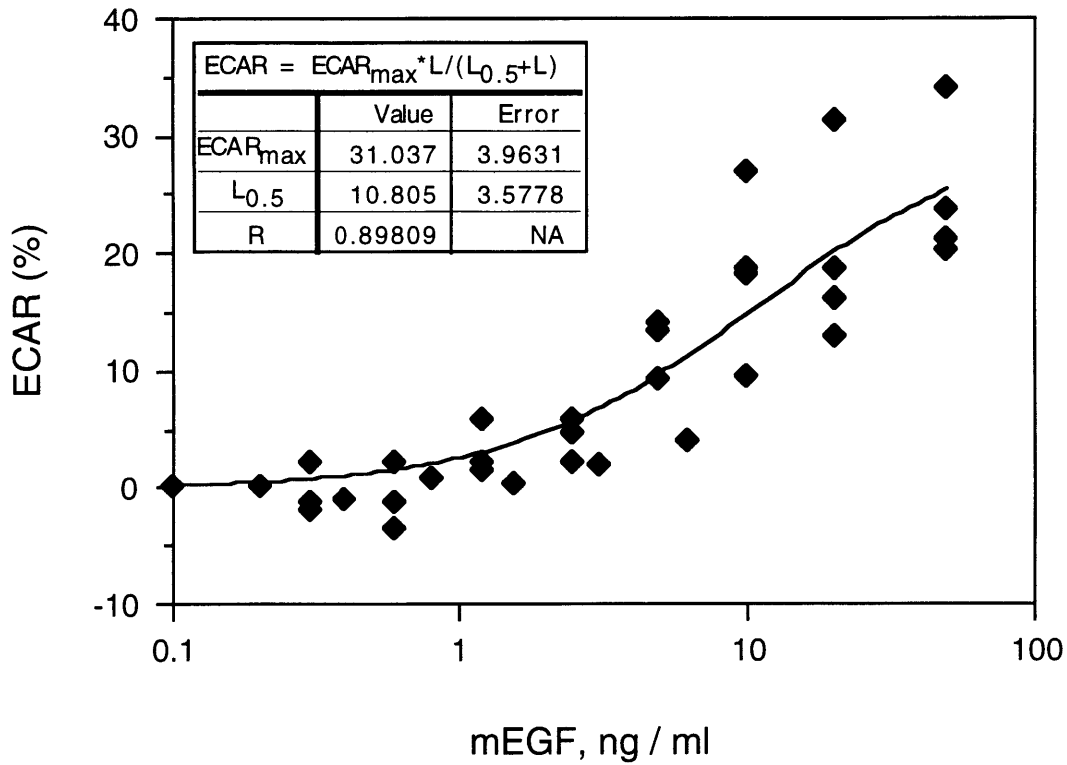


**Figure 6.10: Cytosensor - B82R<sup>+</sup> / 1st plasmid.** After equilibrating cells on the Cytosensor in DV / cyto running buffer for about 3 hours, cells were sequentially exposed to increasing concentration of a mEGF gradient.

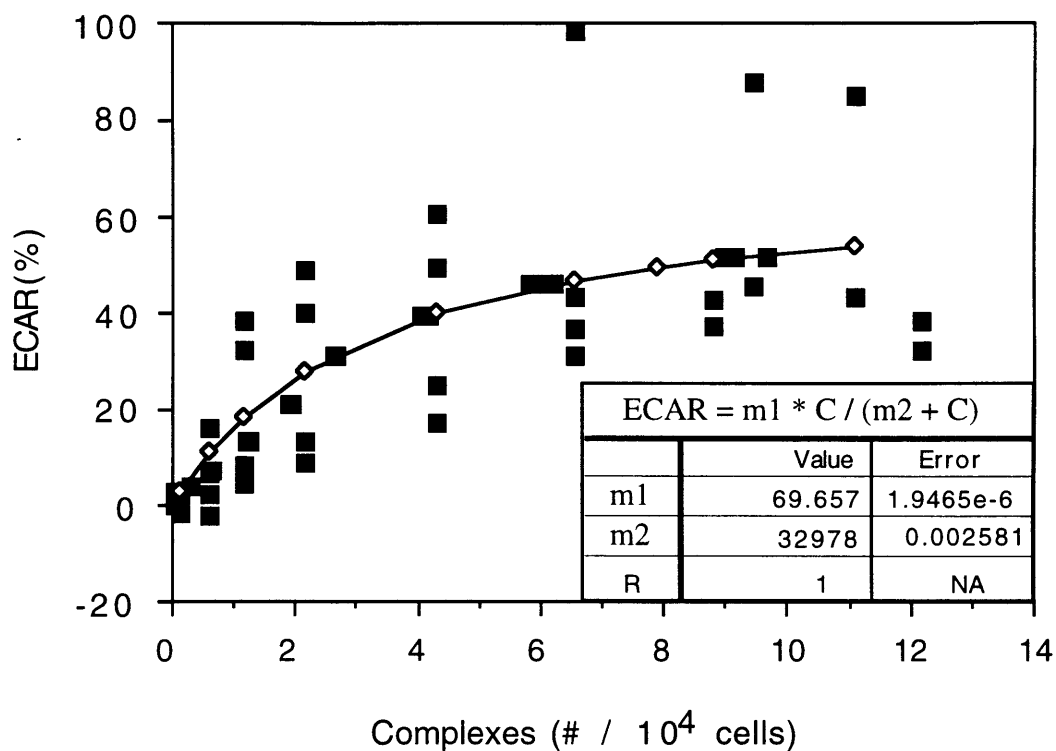




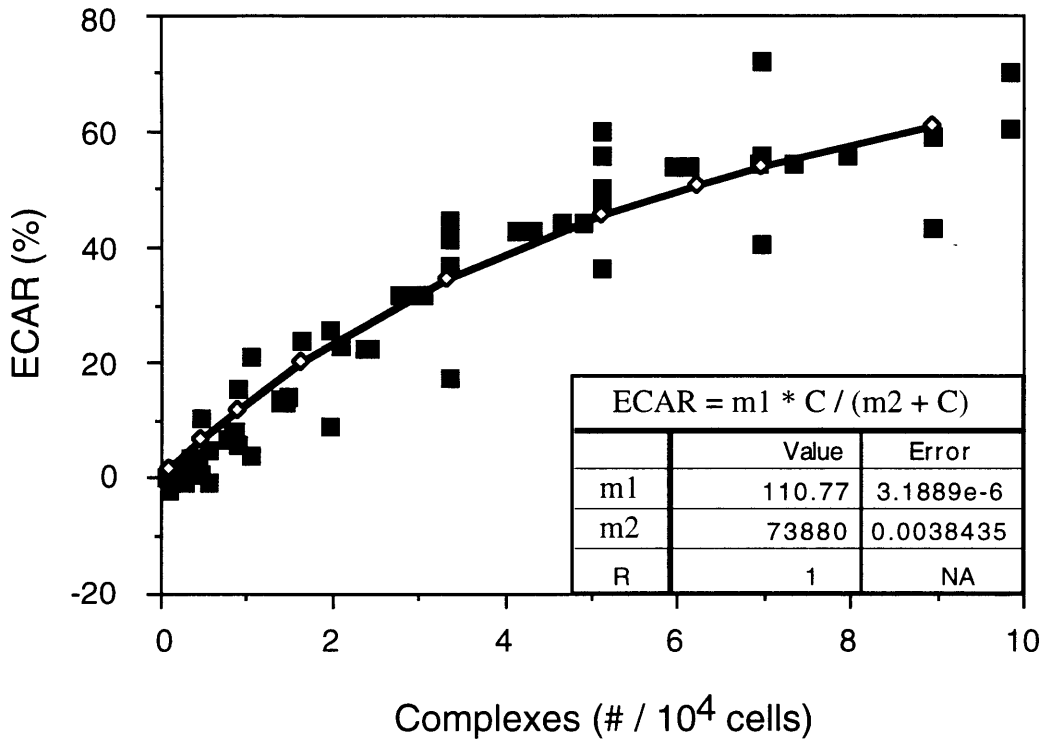
**Figure 6.11: Cytosensor - Uninduced B82R<sup>+</sup> / TGF $\alpha$ .** Autocrine clone #1's TGF $\alpha$  expression was repressed by 1  $\mu$ g / ml tetracycline containing media. After equilibrating cells on the Cytosensor in DV / cyto running buffer for about 3 hours, cells were sequentially exposed to increasing concentration of a mEGF gradient.



**Figure 6.12: Cytosensor - Induced B82R<sup>+</sup> / TGF $\alpha$ .** Autocrine clone #1's TGF $\alpha$  expression was induced overnight by removal of tetracycline. After equilibrating cells on the Cytosensor in DV / cyto running buffer for about 3 hours, cells were sequentially exposed to increasing concentration of a mEGF gradient.

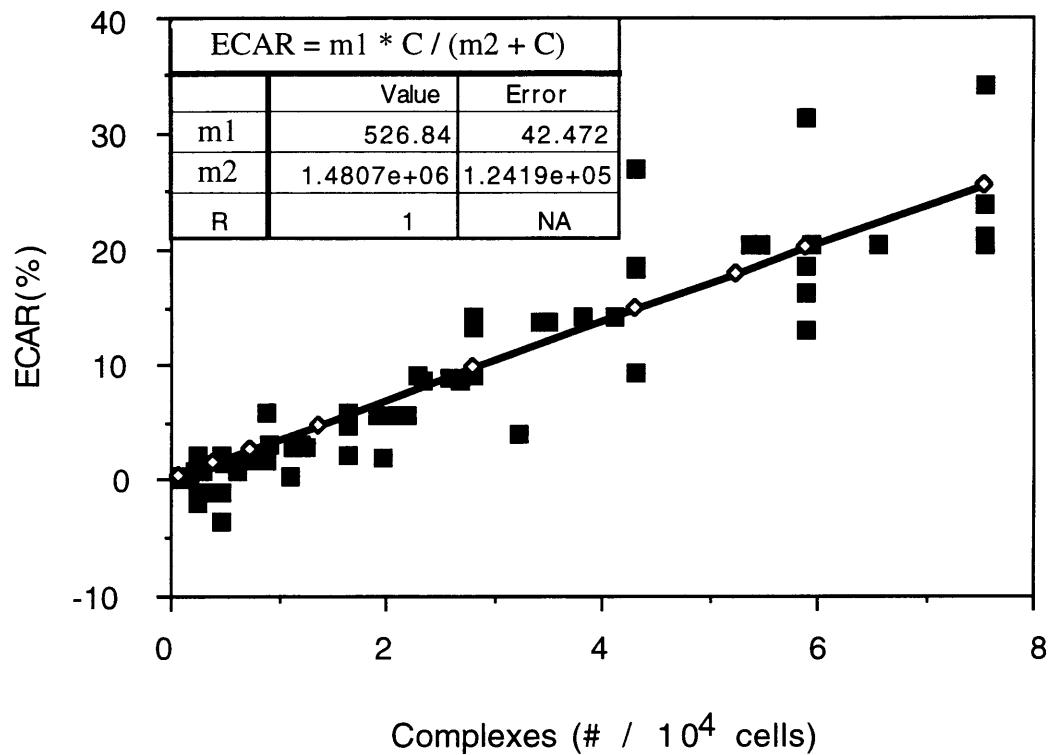


**Figure 6.13: ECAR to Complex Correlation - B82R<sup>+</sup> / 1st plasmid.** Correlation of B82R<sup>+</sup> / 1st plasmid cell data and equation plotted together. Line plot is obtained by combining best fit equations from Figures 6.7 and 6.10. Data obtained from same plots, free ligand concentration was converted into predicted ECAR or complexes and plotted against corresponding experimental ECAR or complexes.



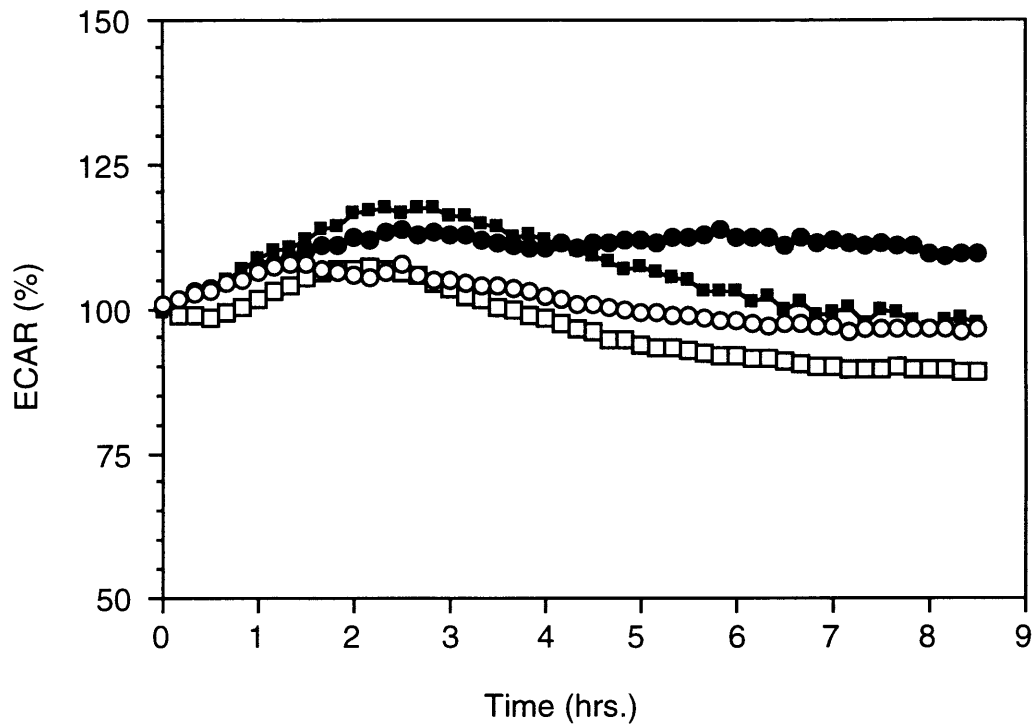
**Figure 6.14: ECAR to Complex Correlation. - Uninduced B2R<sup>+</sup> / TGF $\alpha$ .**

Correlation of uninduced autocrine clone #1 data and equation plotted together. Line plot is obtained by combining best fit equations from Figures 6.8 and 6.11. Data obtained from same plots, free ligand concentration was converted into predicted ECAR or complexes and plotted against corresponding experimental ECAR or complexes.

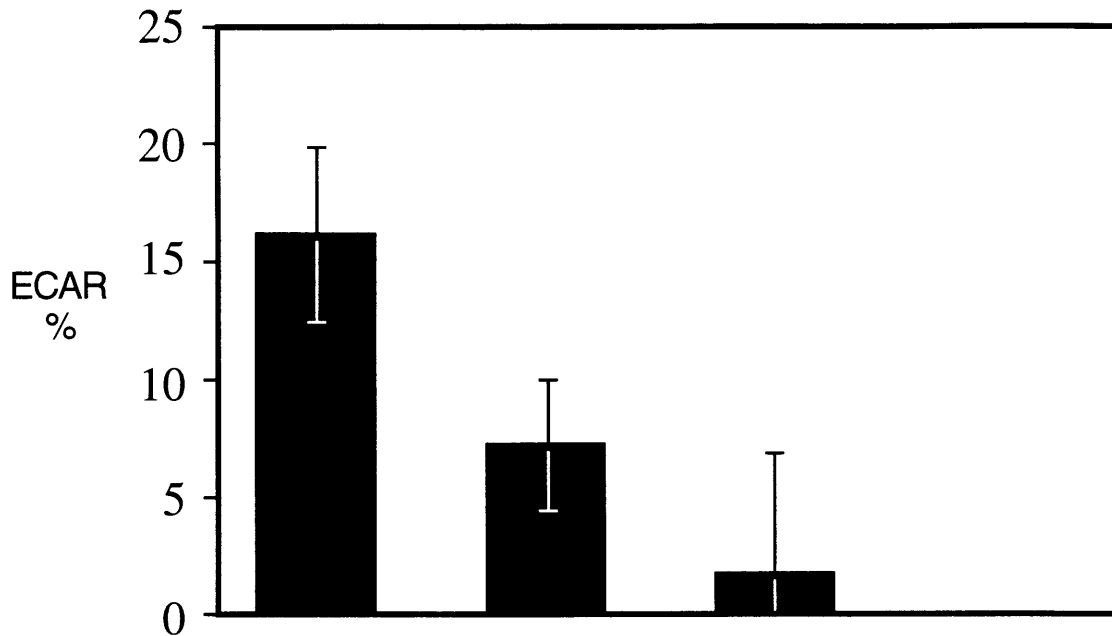


**Figure 6.15: ECAR to Complex Correlation - Induced B82R<sup>+</sup> / TGF $\alpha$  cells.**

Correlation of induced autocrine clone #1 data and equation plotted together. Line plot is obtained by combining best fit equations from Figures 6.9 and 6.12. Data obtained from same plots, free ligand concentration was converted into predicted ECAR or complexes and plotted against corresponding experimental ECAR or complexes.



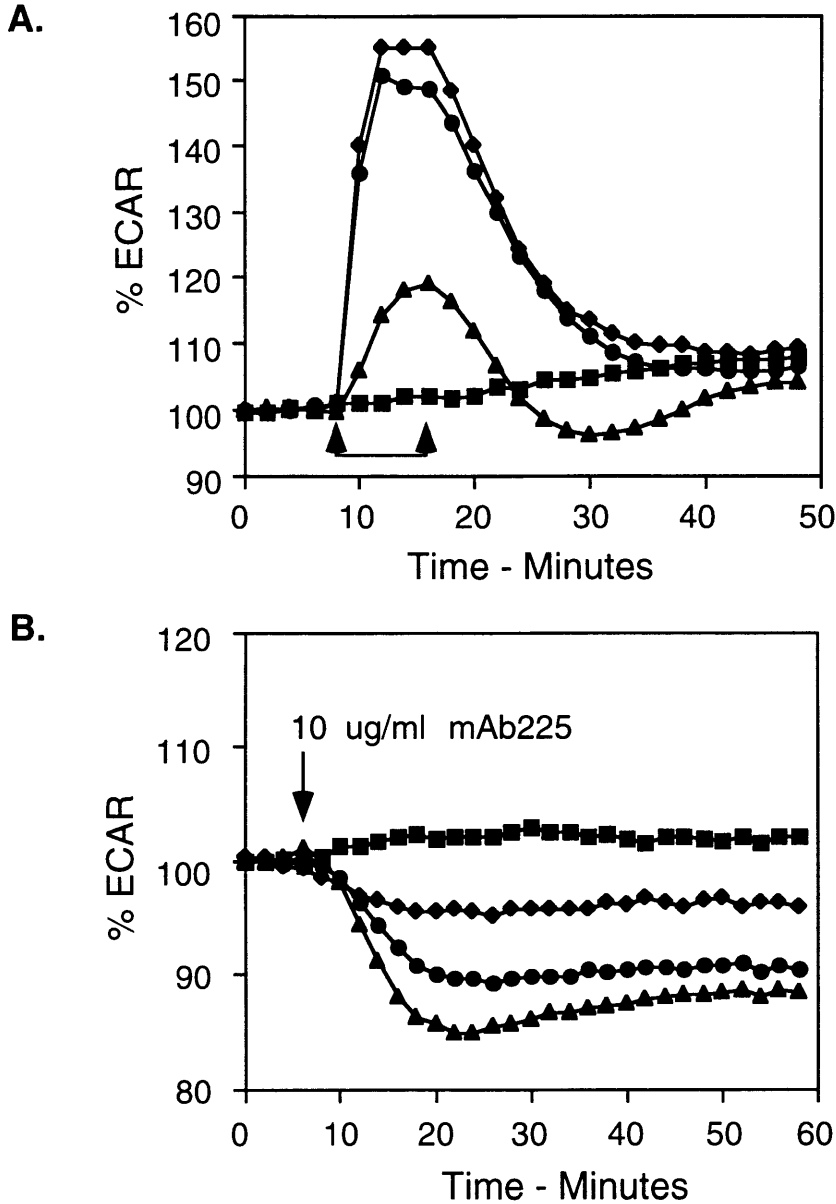
**Figure 6.16: Induction of autocrine B82R<sup>+</sup> / TGF $\alpha$  cells on Cytosensor.** Equilibrated autocrine clone #1 cells were induced (circle) or remained uninduced (squares) at time equal zero. Cells were also in the presence (open) or absence (solid) of 1  $\mu$ g / ml anti-EGFR 225 during the experiment. Only every 10 minute data point is plotted for clarity.



Induction:	+	-	+	-
Antibody:	-	-	+	+

**Figure 6.17: B82R<sup>+</sup> / TGF $\alpha$  induction measured on Cytosensor.**

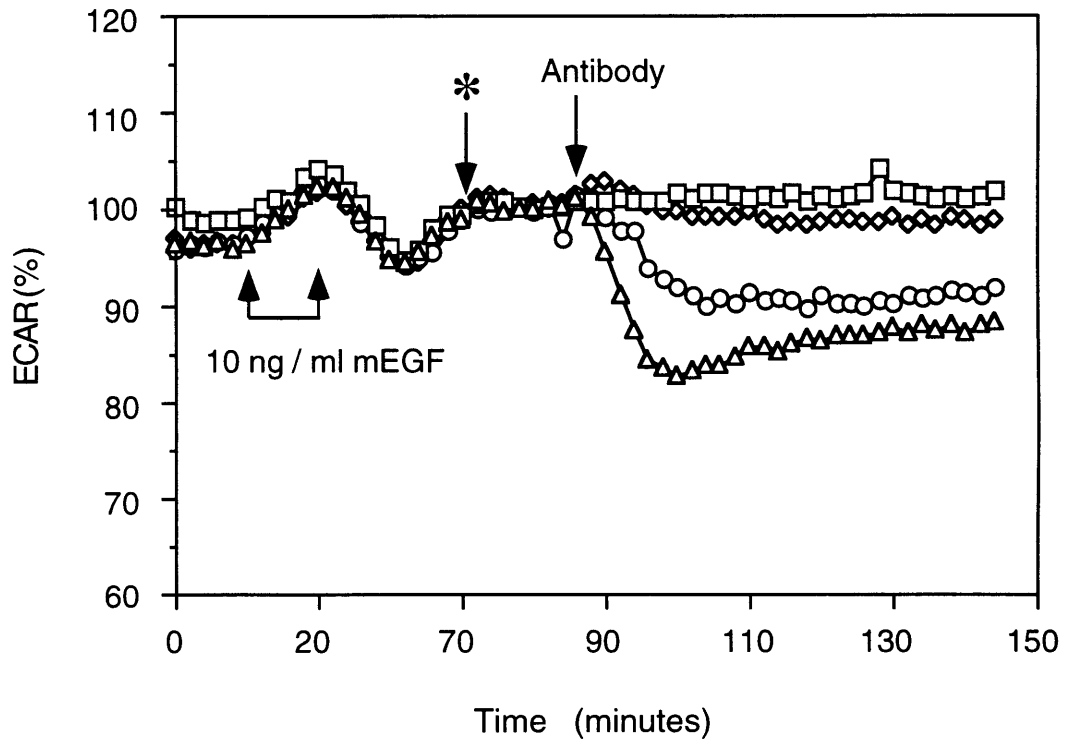
Uninduced B82R<sup>+</sup> / TGF $\alpha$  autocrine clone #1 cells were equilibrated on the Cytosensor before beginning experiment. Above indicated conditions were imposed on each cell lane and Cytosensor run for seven hours. ECAR readings at seven hours are recorded and shown. Data for each run is normalized to uninduced autocrine cell lane with blocking antibody. Anti-EGFR 225 blocking monoclonal antibody concentration was 1  $\mu$ g/ml.



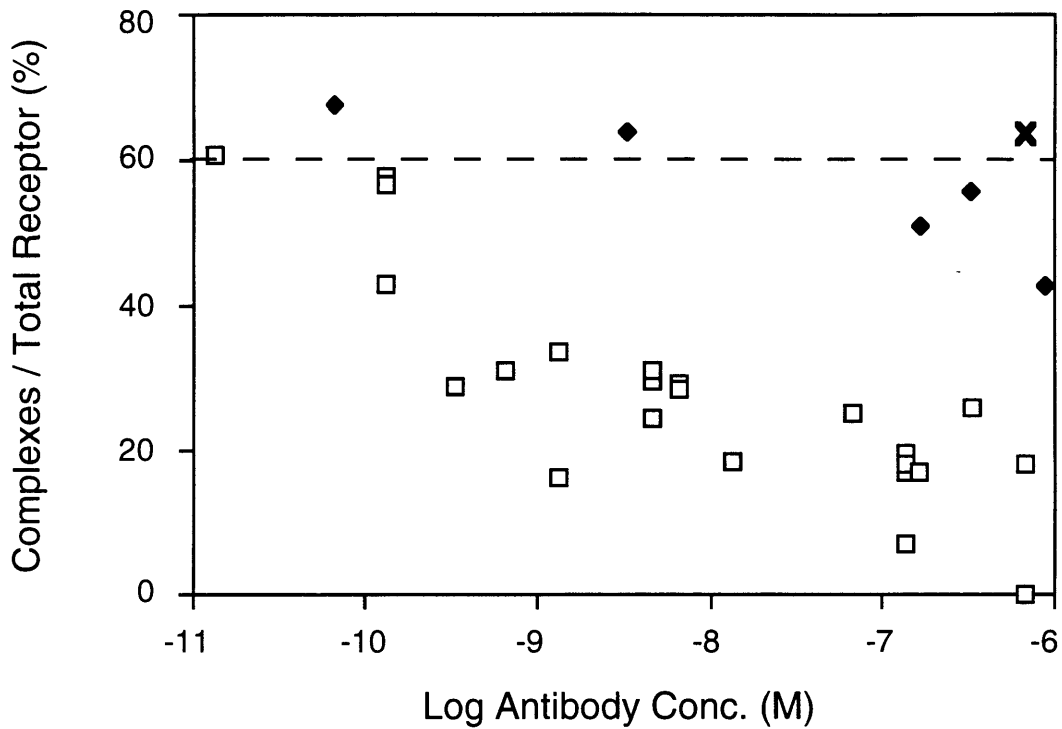
**Figure 6.18: Tetracycline gradient affects on B82R<sup>+</sup> / TGF $\alpha$  cell ECAR.**

Autocrine B82R<sup>+</sup> / TGF $\alpha$  clone #1 cells were plated onto Cytosensor transwells at varying tetracycline concentrations (ligand expression). Uninduced cells were at 1  $\mu$ g / ml tetracycline (squares and diamonds). Semi-induced cells were at 5 ng / ml tetracycline (circle) and fully induced tetracycline free (triangles). One uninduced cell line was control cells receiving no additions (squares). Graph A. Addition of 10 ng / ml mEGF. Graph B. Addition of 10  $\mu$ g / ml monoclonal anti-EGFR blocking antibody 225.

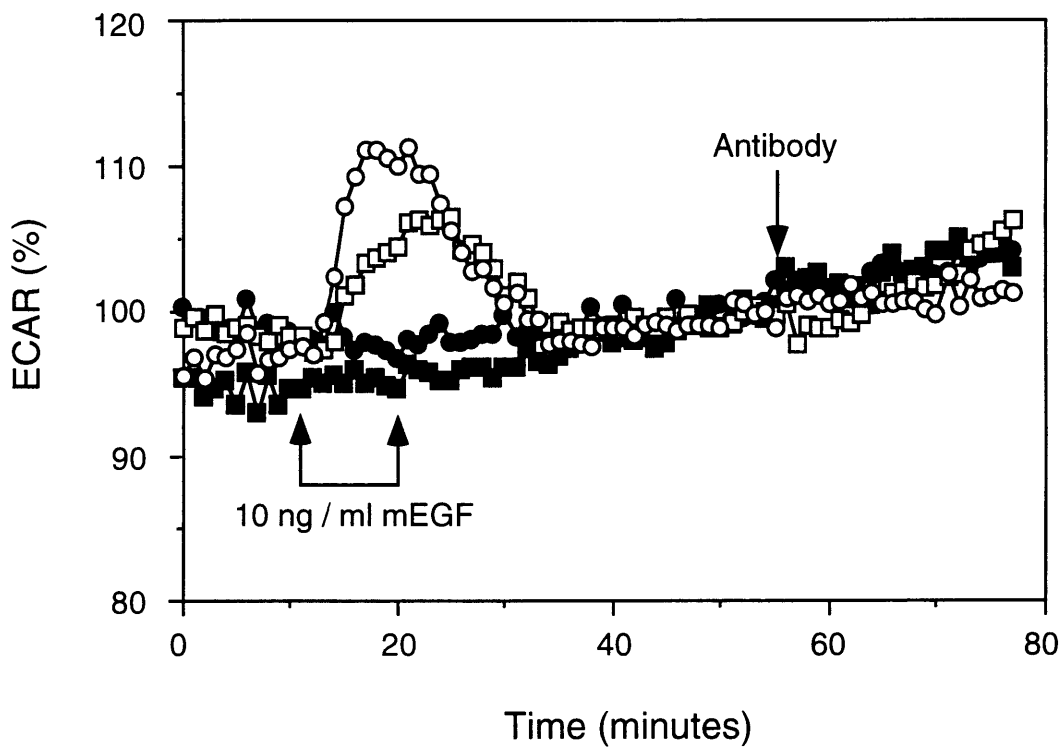




**Figure 6.19: Representative Cytosensor run - induced autocrine B82R<sup>+</sup> / TGF $\alpha$  with blocking antibodies.** Equilibrated autocrine clone #1 cells were exposed to 10 ng / ml mEGF for 10 minutes. After re-equilibration, the cells were challenged with 0.0 (squares), 0.02 (diamonds), 0.1 (circles), and 20 (triangles)  $\mu$ g / ml anti-EGFR blocking antibody 225. For clarity, a 30 minute span during re-equilibration was omitted (\*) and only every 2 minute Cytosensor data point is plotted.

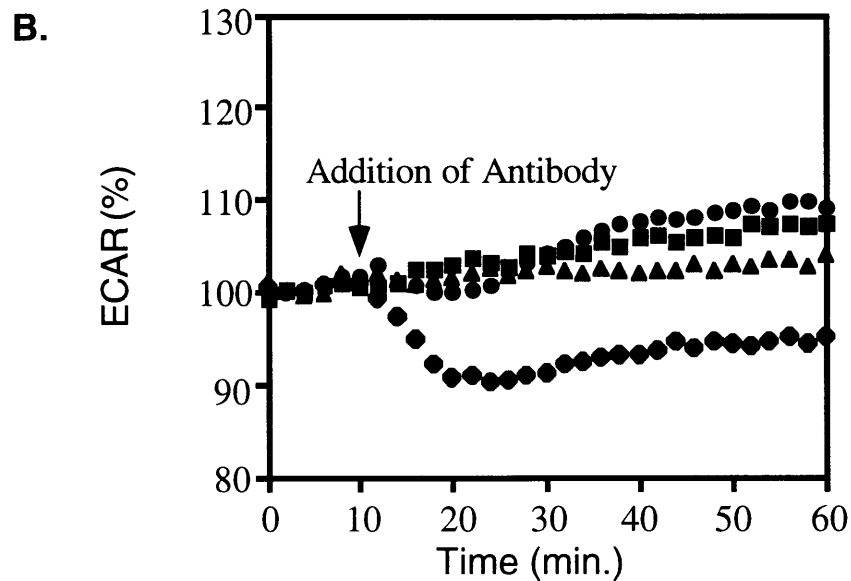
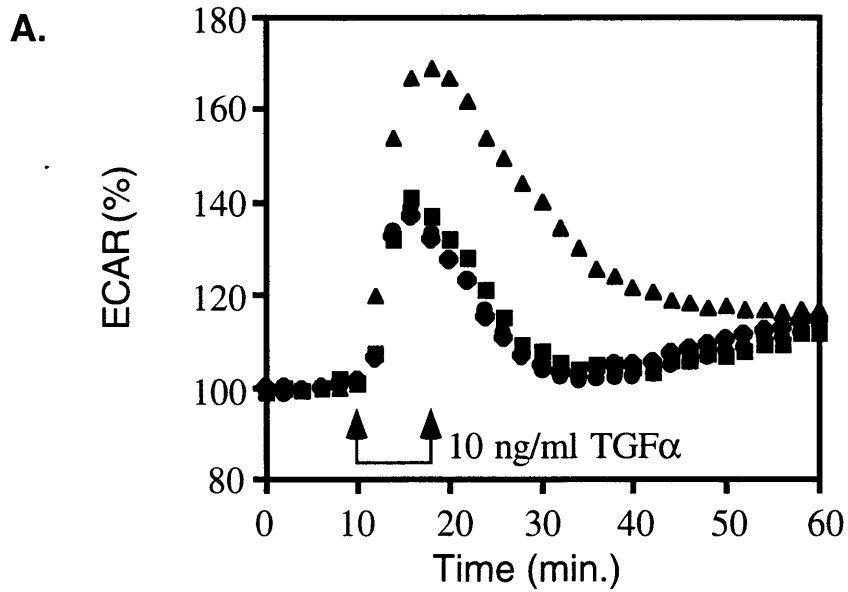


**Figure 6.20: Compilation of B82R<sup>+</sup> / TGF $\alpha$  competing antibody additions.** Equilibrated autocrine clone #1 cells were challenged by the addition of varying concentrations of anti-EGFR blocking antibody 225 (squares), anti-TGF $\alpha$  decoy antibody (diamonds), and non-specific rabbit IgG ("x"). Cytosensor ECAR was converted to complex number using correlation equation from Figure 6.15.

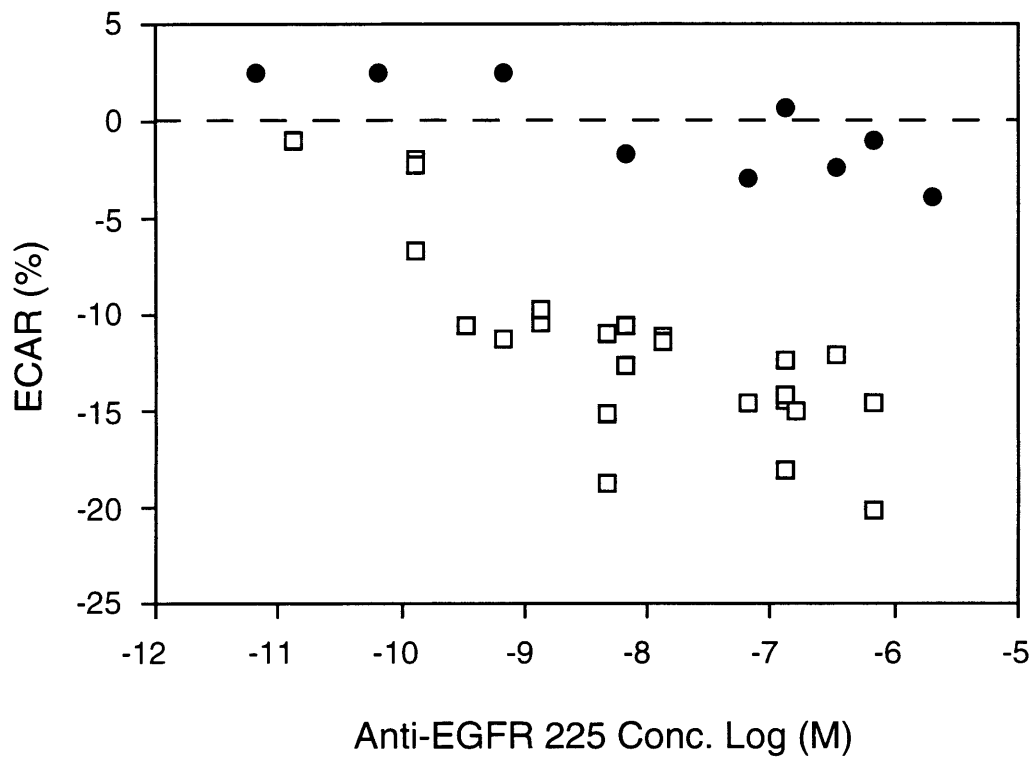


**Figure 6.21: Control experiment - mAb225 and cell stimulation.**

Equilibrated B82R<sup>+</sup> / 1st plasmid (circle) and B82R<sup>+</sup> / TGFα (square) autocrine clone #1 cells were challenged with 10 μg / ml anti-EGFR blocking antibody 225 after addition of 10 ng / ml mEGF (clear). One set of each cell type did not receive mEGF (solid).



**Figure 6.22: Control experiment - TGF $\alpha$  neutralization with anti-TGF $\alpha$  antibody.** B82R<sup>+</sup> (triangle) and autocrine B82R<sup>+</sup> / TGF $\alpha$  cells (square, circle, diamond) equilibrated on the Cytosensor. Graph A. All cells were exposed to 10 ng / ml TGF $\alpha$ . Graph B. 50  $\mu$ g / ml decoy antibody anti-TGF $\alpha$  was added to one autocrine cell lane (circle). 50  $\mu$ g / ml decoy antibody was also added in combination with 10 ng / ml TGF $\alpha$  to B82R<sup>+</sup>. 50  $\mu$ g / ml blocking monoclonal anti-EGFR antibody was added to one autocrine cell lane (diamond). Control autocrine received no additions (squares).



**Figure 6.23: Comparison of autocrine cell systems - TGF $\alpha$  vs. sEGF.**

Autocrine cells B82R<sup>+</sup> / TGF $\alpha$  (squares) and B82R<sup>+</sup> / sEGF (circles) equilibrated in the Cytosensor were challenged with a blocking anti-receptor antibody 225 concentration gradient.

## Chapter 7: Discussion and Future Study

### 7.1 Overview

The purpose of this thesis was to gain a quantitative understanding of receptor - ligand complex inhibition as a function of key cellular parameters in autocrine cells by addition of competing antibodies. This objective was accomplished by developing a B82R<sup>+</sup> / TGF $\alpha$  expression cell system, characterizing the TGF $\alpha$  expression system, and validating model predictions on extracellular ligand concentration and receptor / ligand complex numbers. To this end, the bioengineering autocrine EGFR / TGF $\alpha$  cell provided a 100 fold induction range (tens to thousands molecules / cell minute) via tetracycline control with constitutive EGFR expression. Testing of model predictions prove the importance of creating a protocol standard in the literature for measuring ligand secretion rates at one cell density in the presence of competing antibody. At high cell densities, it was found that addition of antibody was important at low ligand secretion rate, while less important at higher cell secretion rates. Measurement of receptor / ligand complexes using Molecular Devices Cytosensor showed blocking antibodies could inhibit receptor / ligand complexes at a thousand (1000x) fold less concentration than decoy antibodies. Finally, usage of Cytosensor indicated the possible existence of an intracrine signalling pathway in autocrine EGFR / sEGF cells as blocking antibodies were unable to inhibit receptor / ligand formation.

### 7.2 Summary of Results

Using a TGF $\alpha$  plasmid from Derynck (University of San Francisco) and the tetracycline-controlled two plasmid system (pUHD 15.1 and pUHD10.3) from Gossen and Bujard (University of Heidelberg), an inducible TGF $\alpha$  plasmid (pUHD10.3 / TGF $\alpha$ ) was constructed. The TGF $\alpha$  second plasmid was transfected into B82 receptor positive and negative cells already containing pUHD15.1. Under histidinol selection, clones were isolated and examined for TGF $\alpha$  protein secretion. Several clones were discovered to produce TGF $\alpha$ , resulting in the successful development of an inducible autocrine and paracrine TGF $\alpha$  cell system. The autocrine clones are composed of B82R<sup>+</sup> (pXER) / pUHD15.1 / (pR8) - pUHD10.3 TGF $\alpha$  wt, while the paracrine clones are B82R<sup>-</sup> / pUHD15.1 / (pR8) - pUHD10.3 TGF $\alpha$  wt (Figure 1.22). Autocrine clone #1 and paracrine clone #22 were chosen for further characterization as initial results indicated that these two cell lines had high TGF $\alpha$  expression. These two clones were found to have a broad protein expression range upon induction. The suppression of TGF $\alpha$  synthesis is obtained with the addition of tetracycline, a bacterial antibiotic, at low concentrations. Varying tetracycline concentration in the medium results in a

corresponding adjustment in TGF $\alpha$  secretory rates. TGF $\alpha$  protein expression was induced 4 (paracrine) to 100+ (autocrine) times higher than basal levels upon removal of tetracycline. Using high and low TGF $\alpha$  expressing clones and varying tetracycline controlled TGF $\alpha$  expression, an expression system spanning several orders of magnitude is attainable (Figure 4.2, 4.5 and 4.6). The ability to adjust TGF $\alpha$  levels enables one to determine the effect of ligand secretion rates on receptor complexes as modeled in Figure 2.2 and experimentally shown in Figure 6.18.

An experiment was done to verify the correct processing of TGF $\alpha$ . Paracrine medium was run over a Sephadex G-50 column and the fully processed, 5.5 kDa, mature TGF $\alpha$  protein was eluted from the column (Figure 4.3). This result indicates that the B82 cells have the elastase-like enzyme necessary for cleaving the mature TGF $\alpha$  from the transmembrane protein (Pandiella *et al.* 1992). Investigations revealed that 99% of TGF $\alpha$  is secreted into the medium, suggesting that the protein is correctly folded and processed through the ER and Golgi to the cell surface (Table 4.2). The experiment also shows that protein cleavage from the cell surface does not seem to be a rate-limiting step. TGF $\alpha$  accumulation rapidly increased in extracellular medium upon the removal of tetracycline (Figure 4.4). However, the slow inhibition of TGF $\alpha$  expression upon reintroduction of tetracycline indicates the presence of very stable messenger RNA, meaning that cells must be continuously grown in tetracycline containing medium to insure uninduced TGF $\alpha$  expression is truly repressed during experiments.

After characterizing TGF $\alpha$  expression in B82R<sup>+</sup> / TGF $\alpha$  cells, mathematical model predictions as to the effect of ligand secretion rates, cell density, and antibody additions on extracellular ligand concentrations were tested. Seen both experimentally and modeled (Figures 4.7 and 2.4), high ligand secretion rates renders extracellular ligand concentrations independent of cell density and blocking antibodies. The amount of ligand secreted overwhelms receptor-mediated uptake as ligand uptake is insignificant to the total amount secreted into the medium. However, at lower secretion rates, receptor-mediated ligand uptake becomes significant, resulting in large ligand loss from the medium. This data indicates the importance of measuring and reporting not only the “observed” ligand secretion rate, but important parameters such as cell density, plate size, and blocking antibody usage.

Original modelling predictions were done on receptor / ligand complexes as a function of several different autocrine parameters including ligand / receptor affinity, ligand secretion rates, and decoy anti-ligand antibodies versus blocking anti-receptor antibodies. Upon demonstrating that the bioengineered B82R<sup>+</sup> / TGF $\alpha$  autocrine cell system could test model predictions on ligand concentrations, the next step was to experimentally test receptor / ligand complex predictions. The first problem was how to measure complex levels. Prior methods involved

lysed cells, several days of preparation, and westerns or ELISAs to detect phosphotyrosine levels as an indicator of activated receptor / ligand complexes. A problem with this approach was high noise to signal ratios, not real time, and cell lysing altering cell environment and protein interactions. Thus, it was hypothesized that Molecular Devices Cytosensor measurements of cell metabolic rates could be correlated to receptor / ligand complex levels. As shown in Figures 6.4, 6.5, and 6.6, both  $I^{125}$  EGF binding experiments and Cytosensor response experiments had a dose dependent response to the addition of free EGF. Thus, a correlation could be made equating ECAR to complexes.

Next experiments dealt with Cytosensor sensitivity measurements - could the Cytosensor quantify antibody inhibition of receptor ligand complexes, measuring cellular response to addition of antibody and induction of TGF $\alpha$  expression? The experiment depicted in Figure 6.3 shows that addition of blocking antibody 225 shifted B82R $^{+}$ 's EGF ECAR response rightward. Induction of TGF $\alpha$  expression is a long term event usually requiring long accumulation times before ligand detection. However, the Cytosensor works by continuously flowing medium over cells, washing away accumulation of metabolites and protein. Could the Cytosensor detect TGF $\alpha$  secretion? Uninduced autocrine clone #1 cells were placed on the Cytosensor and induced. After 7 seven hours, a clear difference could be discerned between uninduced and induced cells along with differences upon addition of antibody (Figures 6.16 and 6.17). This experiment was carried one step farther by measuring differences in receptor / ligand complex levels and receptor desensitization as a function of ligand secretion rates (Figure 6.18). Addition of exogenous EGF to cells expressing varying TGF $\alpha$  secretion levels shows that receptor desensitization occurs as receptor downregulation does not account for all of the decrease in receptor signalling (Figure 6.8 and 6.9).

The central tenet of this thesis was that decoy antibodies could not inhibit receptor / ligand complexes as well as blocking antibodies. This hypothesis was tested in Figure 6.20. Induced autocrine clone #1 cells were placed on the Cytosensor and varying concentrations of antibody added. As shown, blocking antibody inhibited receptor / ligand complexes at the expected concentration (1 nM) and inhibited these complexes over a thousand (1000x) times better than decoy antibodies. Proving that these results are not artifacts: addition of IgG did not affect complex levels, addition of antibody 225 does not receptor signalling in B82R $^{+}$  cells (Figure 6.21) and the decoy antibody is a neutralizing antibody (Figure 6.22).

Other researchers observed that blocking antibodies were unable to inhibit cell migration and proliferation upon transfection of sEGF into EGFR positive cells. It was hypothesized that sEGF could intracellularly bind EGFR whereas transmembrane TGF $\alpha$  could not. Thus, in sEGF cells, receptors were secreted as ligand / receptor complexes whereas TGF $\alpha$  positive cells



had to first cleave the protein before it diffused to EGFR and bound, allowing inhibition by addition of blocking antibodies. This hypothesis was tested by addition of blocking antibody 225 to B82R<sup>+</sup> / sEGF cells placed on the Cytosensor. As expected, inhibition of signalling in autocrine sEGF cells was not achieved. In fact, it took about ten thousand (10,000x) times more antibody to achieve the same, barely perceptible, decrease in signalling compared to B82R<sup>+</sup> / TGF $\alpha$  cells (Figure 6.23).

### 7.3 Discussion

Our artificial, bioengineered autocrine cell system has been developed, characterized, and used to test several modelling predictions. Important advances from this research have come from three key findings.

The first finding is the necessity for quantitative standards in ligand characterization. When a ligand is found to be expressed in an autocrine fashion, its extracellular concentration is normally reported qualitative as a Western gel band. Further characterization of the autocrine system and ligand expression may quantify that expression by reporting extracellular ligand concentration. However, this experiment is not performed in a standard manner and all of the crucial information not reported in the literature. Variance in protocol usually include large or small volumes, one or several day incubation of conditioned medium, with or without competing antibodies, sub-confluent or over-confluent cells. As predicted by computer modelling and shown experimentally, all of these parameters have important ramifications on extracellular bulk ligand concentrations. Measuring conditioned medium, incubated over cells for several days, leads to the question: what cell density does one use to equate ligand expression on a per cell basis? low or high density? Figures 2.4 and 4.7 proved the necessity of adding competing antibodies to prevent receptor-mediated ligand uptake, especially for a low expressing autocrine cell at high cell density. A second question is: at what plate coverage does cell density become important? At a cell density greater than 100,000 cells / 60 mm dish or a less than 1% cell plate coverage, ligand concentration begins to decrease even in the presence of competing antibodies. A reason for this phenomenon is cells are becoming close enough to interaction with each other and begin to uptake ligand secreted by other cells before the ligand can escape to the extracellular bulk medium. This nonlinearity at which small surface coverage substantial changes global variables has been found before. A cell with 10,000 receptors reaches half maximum ligand diffusive flux at a surface coverage of 0.02% (Lauffenburger and Cozens 1989). Half-maximal probability of autocrine ligand capture occurs at a receptor surface coverage of 0.2%, assuming a 1 nm protein diameter (Forsten and Lauffenburger 1994b).

The second finding is the substantial disparity in effectiveness of blocking versus decoy antibodies on autocrine complexes. Figure 2.3 and 6.20 reveals that decoy antibodies do not inhibit receptor / ligand complexes as effectively as blocking antibodies. It was determined that a thousand times more decoy antibody was required. As monoclonal antibody can cost a dollar / microgram and dosing patients for anti-cancer therapy requires milligrams, a thousand fold increased antibody requirement is significant. For example, three clinical trials have been initiated for anti-tumor therapy, two using antibodies against the receptor (Divgi *et al.* 1991; Modjtahedi and Dean 1994) and one using an antibody against the ligand (Mulshine *et al.* 1992). A technological advance with this research indicates the futile and prohibitive costs in anti-ligand decoy antibody therapy and should not continue without extreme extenuating circumstances.

The third finding is the possibility of an intracrine pathway, which appears to exist in autocrine B82R<sup>+</sup> / sEGF cells, but not in autocrine B82R<sup>+</sup> / TGF $\alpha$  cells. The occurrence of the intracrine signalling pathway is likely due to the lack of a transmembrane tail in sEGF cells which if present would prevent ligand / receptor binding by spatial and steric separation. The intracrine pathway has been proposed and seen experimentally before (Bejcek *et al.* 1989; Dunbar *et al.* 1989; Keating and William 1988). These studies modified endogenous cytokines such as IL-3 and PDGF by adding the endosomal retention signal, KDEL, to the C-terminus. Thus, the protein was unable to be secreted to the extracellular medium and the cells retained high biologic activity in the presence of antibodies. Additional studies in Dr. Wiley's lab (University of Utah) show EGFR positive cells can proliferate and migrate in the presence of blocking antibodies upon transfection of sEGF (personal communications). These cytokines are important cellular regulators of cell pathology and attempts to inhibit receptor / ligand complexes via competing antibodies is useless if intracrine signalling pathway exists.

Thus, it is hoped that elucidating autocrine receptor / ligand interactions with itself and cellular environment by understanding what cellular parameters are important in autocrine ligand / receptor regulation in this and future research will lead to increased understanding in cellular signalling, proliferation and migration regulation in wound healing and cancer therapy.

#### **7.4 Future Work**

How autocrine cells relate to its environment and what signals cells provide to its neighbors is the next logical and important question to ask. An autocrine cell can secrete several different ligands into its extracellular medium, i.e. there are five (5) different ligands in the EGF family which can bind to the same receptor. How does a cell recognize the different ligands and the signal it might represent? EGF and TGF $\alpha$  are enzymatic cleaved into the medium and binds

its receptor (neighbor or same cell) without extracellular matrix interaction. HB-EGF and amphiregulin can interact with and become entrapped in the extracellular matrix before diffusing and binding to its receptor. Plus, HB-EGF remains mostly cell-associated until PKC activation (receptor / ligand binding) promotes enzymatic cleavage (Goishi *et al.* 1995). A further question is: does receptor affinity, down-regulation and / or desensitization play a role in a cell's interaction with its environment? For example, increased A431 cell - cell contact upon formation of multicellular spheroids resulted in decreased receptor levels and activity compared to subconfluent monolayers (Mansbridge *et al.* 1992).

To answer these questions in a systematic and quantitative fashion, there are several existing and potential cell systems and assays available. There are over a hundred different mutated EGFR positive B82 cells created by Dr. Gordon Gill (University of San Diego) which have altered receptor trafficking and ligand affinity parameters. Table 4.3 shows a select list of mutated receptors. A comparison of results obtained with A654 and M721 cells would indicate internalization importance to receptor / cell interaction with its environment, while performing the experiment in the absence or presence of phorbol esters would indicate receptor / ligand affinities importance. Dr. Steve Wiley (University of Utah) has constructed several chimera proteins composed from mature EGF with EGF COOH tail, EGF NH<sub>2</sub>, and HB-EGF ends. These chimeras would indicate how a ligand interactions with its receptor in the absence and presence of competing extracellular matrix. Another level of complexity is incurred by the intermixing of mutated receptors, chimera ligands and "traditional" EGF ligand family, some of which has already been created and listed in Table 4.4.

Several different assays exist to measure how an autocrine cell interactions with its environment. Mixed cell populations of receiver (receptor only positive) cells and donor cells (receptor positive or negative with ligand expression) can be tested on the Cytosensor with or without extracellular matrix. Using these mixed cell populations, differences in ligand capture / escape between paracrine and autocrine cells could be analyzed as a function of receptor trafficking, ligand / receptor affinity, ligand expression, and ligand / extracellular matrix binding. Another readout system is 32D (Pierce *et al.*, 1988) or EP170.7 (Higashiyama *et al.* 1992) which are EGF dependent cells in the absence of IL-3. These cells would function as the receiver cell, plated with mixed autocrine or paracrine cell populations expressing the desired receptor / ligand construction discussed earlier. Increased receptor phosphorylation or <sup>3</sup>H thymidine uptake would indicated amount of ligand escaping from extracellular matrix and / or autocrine receptor to the extracellular medium.

Utilization of these receptor / ligand constructions with Cytosensor or receiver cells would further elucidate what information does an autocrine cell's ligand or ligands / receptor

system provide to that cell and its neighbors about their environment. By increasing our understanding of how this information is presented, recorded, and acted upon by autocrine cells strengthen our ability to design better wound healing and anti-cancer therapies.

## **APPENDIX A**

### Dulbecco's Modification of Eagles's Media (DMEM)

<u>Amino Acid Stock-100X</u>	<u>mg/L media</u>	<u>g/L stock</u>
L-arginine (HCL)	73.00	0.73
L-glutamine	584	5.84
Glycine	30.0	0.30
L-isoleucine	104.8	1.05
L-leucine	104.8	1.05
L-Lysine.HCl	146.2	1.46
L-phenylalanine	66.00	0.66
L-serine	42.00	0.42
L-threonine	95.2	0.95
L-tryptophan	16.00	0.16
L-tyrosine	71	0.71
L-valine	93.6	0.94

<u>CM Stock--100X</u>	<u>mg/L media</u>	<u>g/500 ml stock</u>
L-Cystine	48.00	0.48
L-methionine	30.00	0.60

<u>Vitamin Stock--100X</u>	<u>mg/L media</u>	<u>g/100 ml stock</u>
D-Ca pantothenate	4.00	0.080
Choline chloride	4.00	0.080
Folic acid	4.00	0.080
i-Inositol	7.00	0.140
Nicotinamide	4.00	0.080
Pyridoxal.HCl	4.00	0.080
Riboflavin	0.40	0.008
Thiamin.HCl	4.00	0.080

<u>Ca.Fe.Mg Stock--10X</u>	<u>mg/L media</u>	<u>g/2L stock</u>
CaCl <sub>2</sub> .H <sub>2</sub> O	264.9	5.30
FeCl <sub>3</sub>	0.25 umol	5 umol
MgSO <sub>4</sub> .7H <sub>2</sub> O	200.0	4.00

<u>Main Salt Stock-10X</u>	<u>mg/L media</u>	<u>g/2L stock</u>
KCl	400.0	8.00
NaCl	6400	128
NaHCO <sub>3</sub>	3700	74
NaHPO <sub>4</sub> .2H <sub>2</sub> O	141.3	2.83
D-glucose	4500	90
Phenol Red Sodium Salt	15.00	0.30
Sodium pyruvate	110.0	2.2

**DMEM His minus**

Main Salt Stock	50 mls
CaFeMg Stock	50 mls
Amino Acid Stock	50 mls
CM Stock	25 mls
Vitamin Stock	5 mls
Serum	50 mls
Penicillin/Streptomycin Stock	5 ml
Glutamine Stock	5 ml
<u>Water or Other Additions</u>	<u>260 mls</u>
Total	500 mls

<u>Other Additions:</u>	<u>Stock</u>	<u>Addition/500 ml</u>	<u>Final Conc.</u>
Tetracycline Stock	500 µg/ml	1 ml	1 µg/ml
Histidinol Stock	3 mM	133 µl	800 µMol
G418 Stock	60 mg/ml	5 mls	600 µg/ml

## **Appendix B**



### Comparison of Cytosensor EGF to secreted TGF $\alpha$

Cytosensor EGF:	10 ng / ml
Flow chamber volume:	2.8 $\mu$ l (100 $\mu$ m high, 6 mm ID spacer)
Flowrate:	100 $\mu$ ls / minute
Cell density:	500,000 # / transwell (seeded at 250,000)
Transwell diameter:	12 mm
Transwell area:	113 mm <sup>2</sup>
Spacer diameter:	6 mm
Transwell area:	28.3 mm <sup>2</sup>
Cell # in spacer:	(28.3 / 113) * 500,000 = 125,000 cells

$$(10 \text{ ng / ml}) * (100 \text{ } \mu\text{l / min}) * (\text{nMol / 6045 ng}) * (\text{ml / 1000 } \mu\text{l}) * (\text{mole / 1e9 nmole}) \\ * (6.02\text{e}23 \text{ molecules / mole}) * (1 / 125,000 \text{ cells}) \quad \text{equals}$$

800,000 molecules / cell minute

Autocrine cell at 50 ng / million cells - 24 hours:

$$(50 \text{ ng / 1e6 cells - 24 hours}) * (\text{hr / 60 minutes}) * (\text{nMol / 6045 ng}) * (\text{mole / 1e9 nmole}) \\ * (6.02\text{e}23 \text{ molecules / mole}) \quad \text{equals}$$

3,500 molecules / cell - minute

## **Appendix C**

```

c      Main.f Program for Plated Cells - Blocker Model
c
c
c      implicit real*8 (a-h,o-z)
c      parameter (nvar=10,iliw=20+nvar,ilrw=22+9*nvar+nvar**2)
c
c      dimension iwork(iliw),rwork(ilrw),x(nvar)
c      character*1 tab
c
c      common/bunny/del,gam,sig,chi,alp,z1,z2,theta,theta2
c      common/bunny/ome,beta,xmu,eps,phi,xnu,epsint
c
c
c      external fex,jex
c
c
c      tab = CHAR(9)
c
c
c      sexp = 2.0d0           ! Step Function for Antibody Conc.
c
c      do 15, k = 1,35       ! Do Loop for Antibody Conc. Grad. around LSODE
c      sexp = sexp + 0.5d0
c
c      x(1) = 1.0d0          ! Receptor, r
c      x(2) = 0.0d0          ! Receptor-Ligand Complex, c
c      x(3) = 0.0d0          ! Secretion Layer Ligand Conc., lstar
c      x(4) = 1.0d0          ! Secretion Layer Antibody Conc., bstar
c      x(5) = 0.0d0          ! Bulk Volume Ligand Conc., lbulk
c      x(6) = 1.0d0          ! Bulk Volumn Antibody Conc., bbulk
c      x(7) = 0.0d0          ! Bound Antibody-Receptor #1, sr1
c      x(8) = 0.0d0          ! Bound Receptor-Antibody-Receptor #2, sr2
c      x(9) = 0.0d0          ! Intermed. Ligand Layer, lint
c      x(10) = 1.0d0         ! Intermed. Antibody Layer, bint
c
c
c --- initialize lsode parameters
c
c      itol = 1
c      rtol = 1e-6
c      atol = 1e-6
c      itask = 1
c      istate = 1
c      iopt = 0
c      lrw = ilrw
c      liw = iliw
c      mf = 21
c
c
c      tstart = 0.0          ! Start 0 minutes
c      tend = 1440.0        ! End 24 hours
c      tstep = 3.0          ! Time interval - minutes
c
c
c      xkt = .03d0          ! Constitutive Internalization Rate Constant

```

```

c          value for EGF
c      xkt = .0046d0
c          value for IL2
c          min^-1
c      xkoff = 1.4d-2
c          value for IL2
c          min^-1
c      xkoff = .34d0          ! EGF / EGFR Disassoc. Rate Constant
c          value for EGF kr
c
c      xkoff = .85d0
c      value for koff EGF based on intrinsic kon and KD
c
c      tstart = tstart*xkoff          ! Dimensionalize Time
c      tend   = tend  *xkoff
c      tstep  = tstep *xkoff
c
c --- set parameter values
c      pi = 3.141592653589793d0
c
c      xke = .3d0          ! Receptor-Ligand Induced Internaliz. Rate Constant
c          value for EGF
c      xke = .0462d0
c          value for IL2
c          min^-1
c      xkon = 1.2d-13          ! EGF/EGFR Association Rate Constant
c          cm^3/site*min
c          7.2d7 (value for kf EGF from Cindy) M^-1 min^-1)
c      xkon = 3.0d-13
c          cm^3/site*min
c          value for kon intrinsic for EGF
c
c      xkon = 3.09d-12
c          cm^3/site*min
c          value for IL2 (1.86d9 M^-1 min^-1)
c
c      xkd = xkoff/xkon          ! Receptor-Ligand Equil. Constant
c          sites/ml
c
c      a = 5.0d-4          ! Cell Radius
c          cm
c      xfu = 5.0d-6          ! Cell Boundary Layer =(4*pi*a^2/N)^.5
c          cm
c      xfuint = 25.0d-4          ! Intermed. Layer
c          cm
c      prad = 3.0d0          ! 60 mm cell dish radius
c          cm
c      plvol = 5.0d0          ! Volume of Media added to plate
c          cm^3
c      parea = pi*prad**2          ! cell plate/dish surface area
c          cm^2
c      xheight = plvol / parea          ! Determine Media height in a plate

```

```

c      cm
      sa = 4.0d0*pi*a*a          ! Cell Surface Area
      avago = 6.02d23           ! Avago. #
c      sites/mol
      ro = 100000.0d0           ! Initial # of Receptors
c      site/cell
c      value for B82 cells in paper
c
c      dens = 1.0d5              ! Cell Density
c      cell/plate
c
c      vr = xkt*ro              ! Receptor Synthesis - Based on Receptor Intern.
c      site/cell*min
c
c      q = 5000.0d0             ! Ligand Secretion Rate
c      site/cell*min
c
c      dl = 9.0d-5              ! Ligand Media Diffusion Rate
c      cm^2/min
c      dist = (prad**2 / dens)**0.5 ! 1/2 dist. btwn cells
c      cm
c
c      spacer = pi*dist*dist    ! area for dist calc.
c      cm^2 / cell
c      vcell = 4.0d0*pi*a**3/3.0d0 ! Cell Volume
c      cm^3/cell
c      vstar = 4.0d0*pi*((a+xfu)**3)/3.0d0 - vcell ! Cell Secr. Layer Vol.
c      cm^3/cell
c      vi = spacer * xfuint - vstar - vcell ! Intermed. Volume
c      cm^3/cell
c      vb = spacer * (xheight - xfuint) ! Bulk Media Vol.
c      cm^3/cell
c
c --- Properties of IgG
c
c      db = 2.28d-5             ! Antibody Media Diffusion Rate
c      cm^2/min
c      (3.8d-7 cm^2/s)
c
c -- assume same koffa and kona as cellular receptor
c
c      xkoffa = 0.34d0          ! Antibody-Receptor Dissoc. Rate Constant
c      min^-1
c      xkoffa = xkoff
c      min^-1
c
c      xkona = 1.2d-13          ! Antibody-Receptor Assoc. Rate Constant
c      cm^3/site*min
c      xkona = xkon
c
c      xkda = xkoffa/xkona      ! Antibody-Receptor Equil. Constant
c

```

```

c      xk1 = xkt                      ! Ab-Receptor Internalization Rate Const.
c      rate of single bound antibody-receptor [sr1]
c
c      xk2 = xke                      ! Recept-Ab-Recept Internal. Rate Const.
c      rate of double bound antibody-receptor [sr2]
c
c      xkc = 480d-10                  ! Recept. Cell Diffusion for Ab. Complex
c      cm^2/min*molecule
c
c      xkcoff = 60.0d0                ! Recept. Cell Diffusion for Ab. Complex
c      min^-1
c
c      st = 10.d0**sexp                ! Ab Conc. Added to Media (Sexp=Step fct)
c      site/cm^3 cell
c      (this corresponds with a vb of 9.9d-5 cm^3/cell)
c      (corresponds with 1d9site/cell (200d-6g/ml))
c
c --- Dedimensionaled Variables
c
c      del = ro*xkc/(sa*xkcoff)
c
c      gam = xkt/xkcoff
c
c      sig = q/(vstar*xkd*xkcoff)
c
c      chi = st/xkda
c
c      alp = xkona/xkon
c
c      z1 = xk1/xkt
c
c      z2 = xk2/xkt
c
c      theta = 2.0d0*pi*(a+xfu)*dl/(xkcoff*vstar) ! 2 for plated cells, norm=4
c
c      theta2 = dl*spacer / (xfuint*xkcoff*vstar)
c
c      ome = xke/xkcoff
c
c      beta = xkoffa/xkcoff
c
c      xmu = ro/(vstar*xkd)
c
c      eps = vstar/vb
c
c      epsint = vstar/vi
c
c      phi = db/dl
c
c      xnu = xkcoff/xkcoff
c
c --- Dedimensionalized Variables

```

```

c
c   eta = r/ro
c   rho = c/ro
c   us = lstar/xkd
c   xlams = bstar/st
c   u = lbulk/xkd
c   xlam = bstar/st
c   psis = [sr1]/ro
c   psi = [sr2]/ro
c   uint = lint/xkd
c   xlamint = bint/st
c
c --- begin integration
c
c   do 4, alpha=tstart,tend+1.d-5,tstep
c   call lsode(fex,nvar,x,tstart,alpha,itol,rtol,atol,itask,istate,
1       iopt,rwork,lrw,iwork,liw,jex,mf)
c
c   eta   = x(1)      ! Dimen. Receptor
c   rho   = x(2)      ! Dimen. Recep.-Ligand Complex
c   us    = x(3)      ! Dimen. Secretion Layer Ligand Conc
c   xlams = x(4)      ! Dimen. Secr. Layer Ab Conc.
c   u     = x(5)      ! Dimen. Bulk Media Ligand Conc.
c   xlam  = x(6)      ! Dimen. Bulk Media Ab Conc.
c   psis  = x(7)      ! Dimen. Bound R/Ab #1
c   psi   = x(8)      ! Dimen. Bound R/Ab/R #2
c   uint  = x(9)      ! Dimen. Intermed. Ligand
c   xlamint = x(10)   ! Dimen. Intermed. Ab.
c
c   time = alpha/xkoff
c
c   write(94,21) time,tab,x(1),tab,x(2),tab,x(3),tab,x(4),tab,
c 1       x(5),tab,x(6),tab,x(7),tab,x(8),tab,x(9),tab,x(10)
c 21  format(10(e14.6,a1),e14.6)
c
c   if(istate .lt. 0) then
c       print *, 'istate = ',istate
c       stop
c   end if
c
c 4   continue
c
c   sexpm = sexp -20.2d0    ! Initial Ab Conc. (log)
c       moles/liter
c   write(93,20) sexpm,tab,x(1),tab,x(2),tab,x(3),tab,x(4),tab,
c 1       x(5),tab,x(6),tab,x(7),tab,x(8),tab,x(9),tab,x(10)
c 20  format(10(e14.6,a1),e14.6)
c
c   print *, iwork(11),iwork(12),iwork(13)
c
c 15  continue
c     end

```

```

c      Func.f Program for Plated Cells - Blocker Model
c
c      subroutine fex(nvar,t,x,f)
c
c      implicit real*8 (a-h,o-z)
c      common/bunny/del,gam,sig,chi,alp,z1,z2,theta,theta2
c      common/bunny/ome,beta,xmu,eps,phi,xnu,epsint
c
c      dimension x(nvar),f(nvar)
c
c      --- calculate function residuals
c
c      eta    = x(1)
c      rho    = x(2)
c      us     = x(3)
c      xlams  = x(4)
c      u      = x(5)
c      xlam   = x(6)
c      psis   = x(7)
c      psi    = x(8)
c      uint   = x(9)
c      xlamint = x(10)
c
c      The actual functions
c
c      f(1) = -us*eta + rho -eta*gam -2.0d0*beta*chi*xlams*eta
1          +beta*(psis+2.0d0*psi) - xnu*del*eta*psis + gam
c
c      f(2) = us*eta -rho*(ome+1.0d0)
c
c      f(3) = -xmu*us*eta + xmu*rho +theta*(uint-us) +sig
c
c      f(4) = -2.0d0*alp*xmu*xlams*eta
1          + xmu*alp*psis*(1.0d0/chi)
1          + phi*theta*(xlamint-xlams)
c
c      f(5) = -theta2*eps*(u-uint)
c
c      f(6) = -theta2*eps*phi*(xlam-xlamint)
c
c      f(7) = 2.0d0*beta*chi*xlams*eta -beta*psis +2.0d0*xnu*psi
1          -gam*z1*psis -xnu*del*eta*psis
c
c      f(8) = xnu*del*psis*eta - psi*(2.0d0*xnu + z2*gam)
c
c      f(9) = -theta*epsint*(uint-us)+theta2*epsint*(u-uint)
c
c      f(10) = -theta*phi*epsint*(xlamint-xlams)
1          +theta2*phi*epsint*(xlam-xlamint)
c
c      return
c      end

```



```

c Jacob.f Program for Plated Cells - Blocker Model
c
c subroutine jex(nvar,t,x,ml,mu,dfdx,nrpd)
c
c implicit real*8 (a-h,o-z)
c
c common/bunny/del,gam,sig,chi,alp,z1,z2,theta,theta2
c common/bunny/ome,beta,xmu,eps,phi,xnu,epsint
c
c
c dimension x(nvar),dfdx(nvar,nvar),dgdx(10,10),f(10),g(10)
c
c --- calculate the 10x10 jacobian
c
c eta = x(1)
c rho = x(2)
c us = x(3)
c xlams = x(4)
c u = x(5)
c xlam = x(6)
c psis = x(7)
c psi = x(8)
c uint = x(9)
c xlamint = x(10)
c
c
c
c dfdx(1,1) = -us -gam -2.0d0*beta*chi*xlams -xnu*del*psis
c dfdx(1,2) = 1.0d0
c dfdx(1,3) = - eta
c dfdx(1,4) = - 2.0d0*beta*chi*eta
c dfdx(1,5) = 0.0d0
c dfdx(1,6) = 0.0d0
c dfdx(1,7) = beta - xnu*del*eta
c dfdx(1,8) = 2.0d0*beta
c dfdx(1,9) = 0.0d0
c dfdx(1,10) = 0.0d0
c
c
c dfdx(2,1) = us
c dfdx(2,2) = -(ome + 1.0d0)
c dfdx(2,3) = eta
c dfdx(2,4) = 0.0d0
c dfdx(2,5) = 0.0d0
c dfdx(2,6) = 0.0d0
c dfdx(2,7) = 0.0d0
c dfdx(2,8) = 0.0d0
c dfdx(2,9) = 0.0d0
c dfdx(2,10) = 0.0d0
c
c
c dfdx(3,1) = -xmu*us
c dfdx(3,2) = xmu
c dfdx(3,3) = -xmu*eta - theta

```

dfdx(3,4) = 0.0d0  
dfdx(3,5) = 0.0d0  
dfdx(3,6) = 0.0d0  
dfdx(3,7) = 0.0d0  
dfdx(3,8) = 0.0d0  
dfdx(3,9) = theta  
dfdx(3,10) = 0.0d0

c

dfdx(4,1) = -2.0d0\*alp\*xmu\*xlams  
dfdx(4,2) = 0.0d0  
dfdx(4,3) = 0.0d0  
dfdx(4,4) = -2.0d0\*alp\*xmu\*eta -phi\*theta  
dfdx(4,5) = 0.0d0  
dfdx(4,6) = 0.0d0  
dfdx(4,7) = xmu\*alp/chi  
dfdx(4,8) = 0.0d0  
dfdx(4,9) = 0.0d0  
dfdx(4,10) = phi\*theta

c

dfdx(5,1) = 0.0d0  
dfdx(5,2) = 0.0d0  
dfdx(5,3) = 0.0d0  
dfdx(5,4) = 0.0d0  
dfdx(5,5) = -theta2\*eps  
dfdx(5,6) = 0.0d0  
dfdx(5,7) = 0.0d0  
dfdx(5,8) = 0.0d0  
dfdx(5,9) = theta2\*eps  
dfdx(5,10) = 0.0d0

c

dfdx(6,1) = 0.0d0  
dfdx(6,2) = 0.0d0  
dfdx(6,3) = 0.0d0  
dfdx(6,4) = 0.0d0  
dfdx(6,5) = 0.0d0  
dfdx(6,6) = -theta2\*eps\*phi  
dfdx(6,7) = 0.0d0  
dfdx(6,8) = 0.0d0  
dfdx(6,9) = 0.0d0  
dfdx(6,10) = theta2\*eps\*phi

c

dfdx(7,1) = 2.0d0\*beta\*chi\*xlams - xnu\*del\*psis  
dfdx(7,2) = 0.0d0  
dfdx(7,3) = 0.0d0  
dfdx(7,4) = 2.0d0\*beta\*chi\*eta  
dfdx(7,5) = 0.0d0  
dfdx(7,6) = 0.0d0  
dfdx(7,7) = -beta -gam\*z1 - xnu\*del\*eta  
dfdx(7,8) = 2.0d0\*xnu  
dfdx(7,9) = 0.0d0  
dfdx(7,10) = 0.0d0

c

```

dfdx(8,1) = xnu*del*psis
dfdx(8,2) = 0.0d0
dfdx(8,3) = 0.0d0
dfdx(8,4) = 0.0d0
dfdx(8,5) = 0.0d0
dfdx(8,6) = 0.0d0
dfdx(8,7) = xnu*del*eta
dfdx(8,8) = -2.0d0*xnu -z2*gam
dfdx(8,9) = 0.0d0
dfdx(8,10) = 0.0d0
c
dfdx(9,1) = 0.0d0
dfdx(9,2) = 0.0d0
dfdx(9,3) = theta*epsint
dfdx(9,4) = 0.0d0
dfdx(9,5) = theta2*epsint
dfdx(9,6) = 0.0d0
dfdx(9,7) = 0.0d0
dfdx(9,8) = 0.0d0
dfdx(9,9) = -theta*epsint-theta2*epsint
dfdx(9,10) = 0.0d0
c
dfdx(10,1) = 0.0d0
dfdx(10,2) = 0.0d0
dfdx(10,3) = 0.0d0
dfdx(10,4) = theta*phi*epsint
dfdx(10,5) = 0.0d0
dfdx(10,6) = theta2*phi*epsint
dfdx(10,7) = 0.0d0
dfdx(10,8) = 0.0d0
dfdx(10,9) = 0.0d0
dfdx(10,10) = -theta*phi*epsint-theta2*phi*epsint
c
c - calculate the jacobian
c
c   dx = 1.d-06
c   zero = 1.0d-06
c
c   call fex(nvar,t,x,f)
c
c   do 2, j= 1,nvar
c
c     if (abs(x(j)).lt.zero) then
c       dxx = dx
c     else
c       dxx = dx*x(j)
c     endif
c
c   x(j) = x(j) + dxx
c
c   call fex(nvar,t,x,g)
c

```

```

c      x(j)=x(j) - dxx
c
c      do 1, i = 1,nvar
c      dgdx(i,j) = (g(i)-f(i))/dxx
c 1    continue
c 2    continue
c
c
c      do 4, i=1,nvar
c      write(8,*) (dfdx(i,j), j=1,nvar)
c      write(8,*) (dgdx(i,j), j=1,nvar)
c
c      write(8,*) ' '
c 4    continue
c
c      return
c      end

```

## **Appendix D**

```

c Main.f Program for Plated Cells - Decoy Model
c
c implicit real*8 (a-h,o-z)
c parameter (nvar=13,iliw=20+nvar,ilrw=22+9*nvar+nvar**2)
c
c dimension iwork(iliw),rwork(ilrw),x(nvar)
c character*1 tab
c
c common/bunny/gam,sig,chi,alp,z,theta,ome,beta,xmu,eps
c common/bunny/theta2, epsint
c
c
c external fex,jex
c
c
c tab = CHAR(9)
c
c
c sexp = 2.0d0 ! Step Function for Antibody Conc.
c
c do 15, k = 1,35 ! Do Loop for Antibody Conc. Grad. around LSODE
c sexp = sexp + 0.5d0
c
c
c x(1) = 1.0d0 ! Receptor, r
c x(2) = 0.0d0 ! Receptor-Ligand Complex, c
c x(3) = 0.0d0 ! Secretion Layer Ligand Conc., lstar
c x(4) = 1.0d0 ! Secretion Layer Antibody Conc., sstar
c x(5) = 0.0d0 ! Secretion Layer Lig / Ab, ystar
c x(6) = 0.0d0 ! Secretion Layer Lig / Ab / Lig, xstar
c x(7) = 0.0d0 ! Bulk Layer Ligand Conc., lbulk
c x(8) = 1.0d0 ! Bulk Layer Antibody Conc., sb
c x(9) = 0.0d0 ! Bulk Layer Lig / Ab, yb
c x(10) = 0.0d0 ! Int. Layer Lig Conc., lint
c x(11) = 1.0d0 ! Int. Layer Antibody Conc., sint
c x(12) = 0.0d0 ! Int. Layer Lig / Ab, yint
c x(13) = 0.0d0 ! Int. Layer Lig / Ab / Lig, xint
c
c ! Bulk Layer Lig / Ab / Lig, xb
c
c
c --- initialize lsode parameters
c
c itol = 1
c rtol = 1e-6
c atol = 1e-6
c itask = 1
c istate = 1
c iopt = 0
c lrw = ilrw
c liw = iliw
c mf = 21
c
c
c tstart = 0.0 ! Start 0 minutes
c tend = 1440.0 ! End 24 hours

```

```

tstep = 1.0          ! Time interval - minutes
c
xkt = .03d0         ! Constitutive Internalization Rate Constant
c
c      value for EGF
c
xkt = .0046d0
c
c      value for IL2
c
c      min^-1
c
xkoff = 1.4d-2      ! EGF / EGFR Disassoc. Rate Constant
c
c      value for IL2
c
c      min^-1
c
xkoff = .34d0
c
c      value for EGF kr
c
c
c
xkoff = .85d0
c
c      value for koff EGF based on intrinsic kon and KD
c
c
c
c
tstart = tstart*xkoff ! Dimensionalize Time
tend = tend *xkoff
tstep = tstep *xkoff
c
c --- set parameter values
c
pi = 3.141592653589793d0
c
c
xke = .3d0          ! Receptor-Ligand Induced Internaliz. Rate Constant
c
c      value for EGF
c
c      min^-1
c
c
xkon = 1.2d-13     ! EGF / EGFR Association Rate Constant
c
c      cm^3/site*min
c
c      value for EGF
c
c
xkd = xkoff/xkon   ! Receptor-Ligand Equil. Constant
c
c      sites/ml
c
c
a = 5.0d-4         ! Cell Radius
c
c      cm
c
xfu = 5.0d-6       ! Cell Boundary Layer = (4*pi*a^2/N)^.5
c
c      cm
c
xfuint = 25.0d-4  ! Intermed. Layer Height
c
c      cm
c
c
prad = 3.0d0       ! 60 mm cell dish radius
c
c      cm
c
c
plvol = 5.0d0      ! Volume of media added to plate
c
c      cm^3/plate
c
c
parea = pi*prad**2 ! Cell dish surface area
c
c      cm^2/plate
c
c

```

```

xheight = plvol / parea ! Determine media height in a plate
c      cm
c
ro = 100000.0d0      ! initial # of Receptors
c      site/cell
c      value for EGf
c
dens = 1.0d7         ! Cell Density
c      cell/plate
c
q = 5000.0d0        ! Ligand Synthesis Rate
c      site/cell*min
c
dc = 9.0d-5         ! Ligand Media Diffusion Rate
c      cm^2/min
c
sa = pi*a*a         ! projected cell surface area
c      cm^2/cell
c
dist = (prad**2 / dens)**0.5 ! 1/2 dist. btwn cells
c      cm
c
spacer = pi*dist*dist      ! area of dist.
c      cm^2/cell
c
vcell = 4.0d0*pi*a**3 / 3.0d0      ! Cell Volume
c      cm^3/cell
c
vstar = 4.0d0*pi*((a+xfu)**3)/3.0d0 - vcell
c      cm^3/cell      ! Cell Secr. Layer Volume
c
vi = spacer * xfuint - vstar - vcell      ! Intermed. Volume
c      cm^3/cell
c
vb = spacer * (xheight - xfuint)
c      cm^3/cell      ! Cell Bulk Volume
c
c --- Properties of IgG
c
ds = 2.28d-5         ! Antibody Media Diffusion Rate
c      cm^2/min
c      (3.8d-7 cm^2/s)
c
c -- assume same koffa and kona as cellular receptor
c
xkoffa = .34d0      ! Antibody-Ligand Dissoc. Rate Constant
c      min^-1
c      xkoffa = xkoff
c      min^-1
c
xkona = 1.2d-13     ! Antibody-Ligand Assoc. Rate Constant
c      cm^3/site*min

```



```

xkona = xkon
c
xkda = xkoffa/xkona      ! Antibody-Ligand Equil. Constant
c
st = 10.d0**sexp        ! Ab Conc. Added to Media (Sexp=Step fct)
c      site/cm^3 cell
c      (this corresponds with a vb of 9.9d-5 cm^3/cell)
c      (corresponds with 1d9site/cell (200d-6g/ml))
c
c --- Dedimensionaled Variables
c
gam = xkt/xkoff
c
sig = q/(vstar*xkd*xkoff)
c
chi = st/xkda
c
alp = xkona/xkon
c
z = ds/dc
c
theta = 2.0d0*pi*(a+xfu)*dc/(xkoff*vstar)
c
theta2 = dc*spacer / (xfuint*xkoff*vstar)
c
ome = xke/xkoff
c
beta = xkoffa/xkoff
c
xmu = ro/(vstar*xkd)
c
eps = vstar/vb
c
epsint = vstar / vi
c
c --- Dedimensionalized Variables
c
eta = r/ro
c
rho = c/ro
c
us = lstar/xkd
c
xlams = sstar/st
c
phis = ystar/st
c
psis = xstar/st
c
u = lbulk/xkd
c
xlam = sb/st
c
phi = yb/st
c
psi = xb/st
c
uint = lint/xkd
c
xlamint = sint/st
c
phint = yint/st
c
psint = xint/st
c

```

```

c --- begin integration
c
do 4, r=tstart,tend+1.d-5,tstep
    call lsode(fex,nvar,x,tstart,r,itol,rtol,atol,itask,istate,
1    iopt,rwork,lrw,iwork,liw,jex,mf)
c
c
eta    = x(1)
rho    = x(2)
us     = x(3)
xlams  = x(4)
phis   = x(5)
psis   = x(6)
u      = x(7)
xlam   = x(8)
phi    = x(9)
uint   = x(10)
xlamint= x(11)
phint  = x(12)
psint  = x(13)
c
psi = eps+1.0d0+eps/epsint-eps*(xlams+psis+phis)-eps/epsint
1    *(xlamint+psint+phint) - (xlam+phi)
c
time = r/xkoff
c
c write(94,21) time,tab,x(1),tab,x(2),tab,x(3),tab,x(4),tab,
c 1    x(5),tab,x(6),tab,x(7),tab,x(8)
c 21 format(8(e14.6,a1),e14.6)
c
if(istate .lt. 0) then
print *, 'istate = ',istate
stop
end if
c
4 continue
c
sexpm = sexp -20.2d0
c    moles/liter
write(93,20) sexpm,tab,x(1),tab,x(2),tab,x(3),tab,x(4),tab,
1    x(5),tab,x(6),tab,x(7),tab,x(8),tab,x(9),tab,
1    psi
20 format(10(e14.6,a1),e14.6)
c
c
c print *, iwork(11),iwork(12),iwork(13)
c
c --- format statements
c
c
15 continue
end

```

```

c Func.f Program for Plated Cells - Decoy Model
c
c subroutine fex(nvar,t,x,f)
c
c implicit real*8 (a-h,o-z)
c
c common/bunny/gam,sig,chi,alp,z,theta,ome,beta,xmu,eps
c common/bunny/theta2,epsint
c
c dimension x(nvar),f(nvar)
c
c --- calculate function residuals
c
c eta = x(1)
c rho = x(2)
c us = x(3)
c xlams = x(4)
c phis = x(5)
c psis = x(6)
c u = x(7)
c xlam = x(8)
c phi = x(9)
c uint = x(10)
c xlamint = x(11)
c phint = x(12)
c psint = x(13)
c
c psi = eps+1.0d0+eps/epsint-eps*(xlams+psis+phis)-eps/epsint
1 * (xlamint+psint+phint) - (xlam+phi)
c
c The actual functions
c
c f(1) = -us*eta + rho -gam*eta + gam
c
c f(2) = us*eta -rho*(ome+1.0d0)
c
c f(3) = -xmu*us*eta + xmu*rho +2.0d0*chi*beta*beta*psis/alp
1 -2.0d0*chi*beta*us*xlams - beta*chi*phis*us
1 +chi*beta*beta*phis/alp + theta*(uint-us) +sig
c
c f(4) = -2.0d0*alp*xlams*us +beta*phis +z*theta*(xlamint-xlams)
c
c f(5) = 2.0d0*alp*xlams*us - beta*phis -alp*phis*us
1 +2.0d0*beta*psis +z*theta*(phint-phis)
c
c f(6) = alp*phis*us-2.0d0*beta*psis +z*theta*(psint-psis)
c
c f(7) = -2.0d0*beta*chi*xlam*u + beta*chi*beta*phi/alp
1 +2.0d0*beta*beta*chi*psi/alp-beta*chi*phi*u
1 -theta2*eps*(u-uint)
c
c f(8) = -2.0d0*alp*xlam*u +beta*phi -z*eps*theta2*

```

```

1      (xlam -xlamint)
c
f(9) = 2.0d0*alp*xlam*u - beta*phi -alp*phi*u
1      + 2.0d0*beta*psi-z*eps*theta2*(phi-phint)
c
f(10) = 2.0d0*beta*chi*beta*psint/alp - 2.0d0*uint*xlamint
1      *beta*chi-uint*phint*beta*chi+beta*chi*beta*phint/alp
1      - theta*epsint*(uint-us) + theta2*epsint*(u-uint)
c
f(11) = -2.0d0*alp*uint*xlamint + beta*phint - epsint*theta
1      *z*(xlamint-xlams) + epsint*theta2*z*(xlam-xlamint)
c
f(12) = 2.0d0*alp*uint*xlamint - beta*phint - alp*phint*uint
1      + 2.0d0*beta*psint - theta*epsint*z*(phint-phis)
1      + theta2*epsint*z*(phi-phint)
c
f(13) = alp*uint*phint - 2.0d0*beta*psint - theta*epsint*z
1      *(psint-psis) + theta2*epsint*z*(psi-psint)
c
c
return
end

```

```

c Jacob.f Program for Plated Cells - Decoy Model
c
c subroutine jex(nvar,t,x,ml,mu,dfdx,nrpd)
c
c implicit real*8 (a-h,o-z)
c
c common/bunny/gam,sig,chi,alp,z,theta,ome,beta,xmu,eps
c common/bunny/theta2, epsint
c
c dimension x(nvar),dfdx(nvar,nvar),dgdxd(13,13),f(13),g(13)
c
c --- calculate the 13x13 jacobian
c
c eta = x(1)
c rho = x(2)
c us = x(3)
c xlams = x(4)
c phis = x(5)
c psis = x(6)
c u = x(7)
c xlam = x(8)
c phi = x(9)
c uint = x(10)
c xlamint= x(11)
c phint = x(12)
c psint = x(13)
c
c psi = eps+1.0d0+eps/epsint-eps*(xlams+psis+phis)-eps/epsint
c 1 *(xlamint+psint+phint) - (xlam+phi)
c
c
c dfdx(1,1) = -us -gam
c dfdx(1,2) = 1.0d0
c dfdx(1,3) = - eta
c dfdx(1,4) = 0.0d0
c dfdx(1,5) = 0.0d0
c dfdx(1,6) = 0.0d0
c dfdx(1,7) = 0.0d0
c dfdx(1,8) = 0.0d0
c dfdx(1,9) = 0.0d0
c dfdx(1,10)= 0.0d0
c dfdx(1,11)= 0.0d0
c dfdx(1,12)= 0.0d0
c dfdx(1,13)= 0.0d0
c
c dfdx(2,1) = us
c dfdx(2,2) = -ome - 1.0d0
c dfdx(2,3) = eta
c dfdx(2,4) = 0.0d0
c dfdx(2,5) = 0.0d0
c dfdx(2,6) = 0.0d0
c dfdx(2,7) = 0.0d0

```

dfdx(2,8) = 0.0d0  
dfdx(2,9) = 0.0d0  
dfdx(2,10)= 0.0d0  
dfdx(2,11)= 0.0d0  
dfdx(2,12)= 0.0d0  
dfdx(2,13)= 0.0d0

c

dfdx(3,1) = -xmu\*us  
dfdx(3,2) = xmu  
dfdx(3,3) = -xmu\*eta-2.0d0\*chi\*beta\*xlams-theta-beta\*chi\*phis  
dfdx(3,4) = -2.0d0\*chi\*beta\*us  
dfdx(3,5) = -beta\*chi\*us +chi\*beta\*beta/alp  
dfdx(3,6) = 2.0d0\*chi\*beta\*beta/alp  
dfdx(3,7) = 0.0d0  
dfdx(3,8) = 0.0d0  
dfdx(3,9) = 0.0d0  
dfdx(3,10)= theta  
dfdx(3,11)= 0.0d0  
dfdx(3,12)= 0.0d0  
dfdx(3,13)= 0.0d0

c

dfdx(4,1) = 0.0d0  
dfdx(4,2) = 0.0d0  
dfdx(4,3) = -2.0d0\*alp\*xlams  
dfdx(4,4) = -2.0d0\*alp\*us - z\*theta  
dfdx(4,5) = beta  
dfdx(4,6) = 0.0d0  
dfdx(4,7) = 0.0d0  
dfdx(4,8) = 0.0d0  
dfdx(4,9) = 0.0d0  
dfdx(4,10)= 0.0d0  
dfdx(4,11)= z\*theta  
dfdx(4,12)= 0.0d0  
dfdx(4,13)= 0.0d0

c

dfdx(5,1) = 0.0d0  
dfdx(5,2) = 0.0d0  
dfdx(5,3) = 2.0d0\*alp\*xlams - alp\*phis  
dfdx(5,4) = 2.0d0\*alp\*us  
dfdx(5,5) = -beta -alp\*us -z\*theta  
dfdx(5,6) = 2.0d0\*beta  
dfdx(5,7) = 0.0d0  
dfdx(5,8) = 0.0d0  
dfdx(5,9) = 0.0d0  
dfdx(5,10)= 0.0d0  
dfdx(5,11)= 0.0d0  
dfdx(5,12)= z\*theta  
dfdx(5,13)= 0.0d0

c

dfdx(6,1) = 0.0d0  
dfdx(6,2) = 0.0d0  
dfdx(6,3) = alp\*phis

$dfdx(6,4) = 0.0d0$   
 $dfdx(6,5) = alp*us$   
 $dfdx(6,6) = -2.0d0*beta - z*theta$   
 $dfdx(6,7) = 0.0d0$   
 $dfdx(6,8) = 0.0d0$   
 $dfdx(6,9) = 0.0d0$   
 $dfdx(6,10) = 0.0d0$   
 $dfdx(6,11) = 0.0d0$   
 $dfdx(6,12) = 0.0d0$   
 $dfdx(6,13) = z*theta$

c

$dfdx(7,1) = 0.0d0$   
 $dfdx(7,2) = 0.0d0$   
 $dfdx(7,3) = 0.0d0$   
 $dfdx(7,4) = -eps*2.0d0*beta*beta*chi/alp$   
 $dfdx(7,5) = -eps*2.0d0*beta*beta*chi/alp$   
 $dfdx(7,6) = -eps*2.0d0*beta*beta*chi/alp$   
 $dfdx(7,7) = -2.0d0*beta*chi*xlam - beta*chi*phi-theta2*eps$   
 $dfdx(7,8) = -2.0d0*beta*chi*u - 2.0d0*beta*chi*beta/alp$   
 $dfdx(7,9) = -1.0d0*beta*chi*beta/alp - beta*chi*u$   
 $dfdx(7,10) = theta2*eps$   
 $dfdx(7,11) = -2.0d0*eps*beta*beta*chi/(alp*epsint)$   
 $dfdx(7,12) = -2.0d0*eps*beta*beta*chi/(alp*epsint)$   
 $dfdx(7,13) = -2.0d0*eps*beta*beta*chi/(alp*epsint)$

c

$dfdx(8,1) = 0.0d0$   
 $dfdx(8,2) = 0.0d0$   
 $dfdx(8,3) = 0.0d0$   
 $dfdx(8,4) = 0.0d0$   
 $dfdx(8,5) = 0.0d0$   
 $dfdx(8,6) = 0.0d0$   
 $dfdx(8,7) = -2.0d0*alp*xlam$   
 $dfdx(8,8) = -2.0d0*alp*u - z*eps*theta2$   
 $dfdx(8,9) = beta$   
 $dfdx(8,10) = 0.0d0$   
 $dfdx(8,11) = z*eps*theta2$   
 $dfdx(8,12) = 0.0d0$   
 $dfdx(8,13) = 0.0d0$

c

$dfdx(9,1) = 0.0d0$   
 $dfdx(9,2) = 0.0d0$   
 $dfdx(9,3) = 0.0d0$   
 $dfdx(9,4) = -2.0d0*beta*eps$   
 $dfdx(9,5) = -2.0d0*beta*eps$   
 $dfdx(9,6) = -2.0d0*beta*eps$   
 $dfdx(9,7) = 2.0d0*alp*xlam - alp*phi$   
 $dfdx(9,8) = 2.0d0*alp*u - 2.0d0*beta$   
 $dfdx(9,9) = -beta - alp*u - 2.0d0*beta - z*eps*theta2$   
 $dfdx(9,10) = 0.0d0$   
 $dfdx(9,11) = -2.0d0*beta*eps/epsint$   
 $dfdx(9,12) = z*eps*theta2 - 2*beta*eps/epsint$   
 $dfdx(9,13) = -2.0d0*beta*eps/epsint$

c

```
dfdx(10,1) = 0.0d0
dfdx(10,2) = 0.0d0
dfdx(10,3) = theta*epsint
dfdx(10,4) = 0.0d0
dfdx(10,5) = 0.0d0
dfdx(10,6) = 0.0d0
dfdx(10,7) = theta2*epsint
dfdx(10,8) = 0.0d0
dfdx(10,9) = 0.0d0
dfdx(10,10) = -theta*epsint - theta2*epsint-2*xlamint*beta*chi-phint*beta*chi
dfdx(10,11) = -2.0d0*uint*beta*chi
dfdx(10,12) = -uint*beta*chi + beta*chi*beta/alp
dfdx(10,13) = 2.0d0*beta*chi*beta/alp
```

c

```
dfdx(11,1) = 0.0d0
dfdx(11,2) = 0.0d0
dfdx(11,3) = 0.0d0
dfdx(11,4) = epsint*theta*z
dfdx(11,5) = 0.0d0
dfdx(11,6) = 0.0d0
dfdx(11,7) = 0.0d0
dfdx(11,8) = epsint*theta2*z
dfdx(11,9) = 0.0d0
dfdx(11,10) = -2.0d0*alp*xlamint
dfdx(11,11) = -2.0d0*alp*uint -epsint*theta*z -epsint*theta2*z
dfdx(11,12) = beta
dfdx(11,13) = 0.0d0
```

c

```
dfdx(12,1) = 0.0d0
dfdx(12,2) = 0.0d0
dfdx(12,3) = 0.0d0
dfdx(12,4) = 0.0d0
dfdx(12,5) = theta*epsint*z
dfdx(12,6) = 0.0d0
dfdx(12,7) = 0.0d0
dfdx(12,8) = 0.0d0
dfdx(12,9) = theta2*epsint*z
dfdx(12,10) = 2.0d0*alp*xlamint - alp*phint
dfdx(12,11) = 2.0d0*alp*uint
dfdx(12,12) = -beta - alp*uint-theta*epsint*z-theta2*epsint*z
dfdx(12,13) = 2.0d0*beta
```

c

```
dfdx(13,1) = 0.0d0
dfdx(13,2) = 0.0d0
dfdx(13,3) = 0.0d0
dfdx(13,4) = -theta2*epsint*z*eps
dfdx(13,5) = -theta2*epsint*z*eps
dfdx(13,6) = -theta2*epsint*z*eps + theta*epsint*z
dfdx(13,7) = 0.0d0
dfdx(13,8) = -theta2*epsint*z
dfdx(13,9) = -theta2*epsint*z
```



```

dfdx(13,10) = alp*phint
dfdx(13,11) = -eps*theta2*z*epsint/epsint
dfdx(13,12) = alp*uint - eps*theta2*epsint*z/epsint
dfdx(13,13) = -2.0d0*beta-theta*epsint*z-theta2*epsint*z
1      -eps*theta2*epsint*z/epsint
c
c - calculate the jacobian
c
c      dx = 1.d-06
c      zero = 1.0d-06
c
c      call fex(nvar,t,x,f)
c
c      do 2, j= 1,nvar
c
c      if (abs(x(j)).lt.zero) then
c          dxx = dx
c      else
c          dxx = dx*x(j)
c      endif
c
c      x(j) = x(j) + dxx
c
c      call fex(nvar,t,x,g)
c
c      x(j)=x(j) - dxx
c
c      do 1, i = 1,nvar
c          dgdx(i,j) = (g(i)-f(i))/dxx
c 1      continue
c 2      continue
c
c
c      do 4, i=1,nvar
c          write(8,*) (dfdx(i,j), j=1,nvar)
c          write(8,*) (dgdx(i,j), j=1,nvar)
c
c          write(8,*) ' '
c 4      continue
c
c      return
c      end

```

## References

- Alberts, B., Bray, D., Lewis, J., Raff, M., Roberts, K., and Watson, J. D. (1994). *Molecular Biology of the Cell*, Garland Press, New York.
- Anzano, M. A., Roberts, A. B., Meyers, C. A., Komoriya, A., Lamb, L. C., Smith, J. M., and Sporn, M. B. (1982). "Synergistic Interaction of Two Classes of Transforming Growth Factors from Murine Sarcoma Cells." *Cancer Research*, **42**: 4776-4778.
- Banerji, J., Rusconi, S., and Schaffner, W. (1981). "Expression of a beta-Globulin Gene is Enhanced by Remote SV40 DNA Sequences." *Cell*, **27**: 299-308.
- Barrandon, Y., and Green, H. (1987). "Cell Migration is Essential for Sustained Growth of Keratinocyte Colonies: The Roles of Transforming Growth Factor- $\alpha$  and Epidermal Growth Factor." *Cell*, **50**: 1131-1138.
- Baulida, J., Kraus, M. H., Alimandi, M., Di Fiore, P. P., and Carpenter, G. (1996). "All ErbB Receptors other than the Epidermal Growth Factor Receptor are Endocytosis Impaired." *J. Biol. Chem.*, **271**: 5251-5257.
- Beauchamp, R. D., Barnard, J. A., McCutchen, C. M., Cherner, J. A., and Coffey, R. J. (1989). "Localization of Transforming Growth Factor alpha and Its Receptor in Gastric Mucosal Cells." *J. Clin. Invest.*, **84**: 1017-1023.
- Bejcek, B. E., Li, D. Y., and Deuel, T. F. (1989). "Transformation by v-sis Occurs by an Internal Auto-activation Mechanism." *Science*, **245**: 1496-1498.
- Bell, G. I., Fong, N. M., Wornstead, M. A., Caput, D. F., Ku, L., Urdea, M. S., Rall, L. B., and Sanchez-Pescador, R. (1986). "Human Epidermal Growth Factor Precursor: cDNA Sequence, Expression *in vitro* and Gene Organization." *Nucleic Acids*, **14**: 8427-8446.
- Bennett, N. T., and Schultz, G. S. (1993). "Growth Factors and Wound Healing: Biochemical Properties of Growth Factors and Their Receptors." *American Journal of Surgery*, **165**: 728-737.
- Berg, H. C. (1983). *Random Walks in Biology*, Princeton University Press, Princeton.
- Bertics, P. J., and Gill, G. N. (1985). "Self-Phosphorylation Enhances the Protein-Tyrosine Kinase Activity of the Epidermal Growth Factor Receptor." *J. Biol. Chem.*, **260**(27): 14642-14647.
- Boonstra, J., Rijken, P., Humbel, B., Cremers, F., Verkleij, A., and van Bergen en Henegouwen, P. (1995). "The Epidermal Growth Factor." *Cell Biology International*, **19**(5): 413-430.
- Boshart, M., Weber, F., Jahn, G., Dorsch-Hasler, K., Fleckenstein, B., and Schaffner, W. (1985). "A Very Strong Enhancer is Located Upstream of an Immediate Early Gene of Human Cytomegalovirus." *Cell*, **41**: 521-530.

- Boyfield, I., Winn, F., and Coldwell, M. (1996). "Comparison of Agonist Potencies at Human Dopamine D2 and D3 Receptors, expressed in the Same Cell line, using the Cytosensor Microphysiometer." *Biochem. Soc. Trans.*, **24**: 57S.
- Brenner, D. A., Koch, K. S., and Leffert, H. L. (1989). "Transforming Growth Factor- $\alpha$  Stimulates Proto-Oncogenes c-jun Expression and a Mitogenic Program in Primary Cultures of Adult Rat Hepatocytes." *DNA*, **8**: 279-285.
- Bringman, T. S., Lindquist, P. B., and Derynck, R. (1987). "Different Transforming Growth Factor- $\alpha$  Species Are Derived from a Glycosylated and Palmitoylated Transmembrane Precursor." *Cell*, **48**: 429-440.
- Campbell, I. D., Baron, M., Cooke, R. M., Dudgeon, T. J., Fallon, A., Harvey, T. S., and Tappin, M. J. (1990). "Structure-Function Relationships in Epidermal Growth Factor (EGF) and Transforming Growth Factor-Alpha (TGF $\alpha$ )." *Biochemical Pharmacology*, **40**(1): 35-40.
- Carpenter, G., and Wahl, M. I. (1990). "The Epidermal Growth Factor Family." *Peptide Growth Factors and Their Receptors I*, M. B. Sporn and A. B. Roberts, eds., Springer-Verlag, New York, 69-172.
- Carraway, K. L., and Cerione, R. A. (1993). "Inhibition of Epidermal Growth Factor Receptor Aggregation by an Antibody Directed against the Epidermal Growth Factor Receptor Extracellular Domain." *Journal of Biological Chemistry*, **268**(32): 23860-23867.
- Carraway, K. L., and Cantley, L. C. (1994). "A Neu Acquaintance for ErbB3 and ErbB4: A Role for Receptor Heterodimerization in Growth Signalling." *Cell*, **78**: 5-8.
- Carraway, K. L., Soltoff, S. P., Diamonti, A. J., and Cantley, L. C. (1995). "Heregulin Stimulates Mitogenesis and Phosphatidylinositol 3-Kinase in Mouse Fibroblasts Transfected with erbB2/neu and erbB3." *Journal of Biological Chemistry*, **270**(13): 7111-7116.
- Chan, S. D., Antoniucci, D. M., Fok, K. S., Alajoki, M. L., Harkins, R. N., Thompson, S. A., and Wada, H. G. (1995). "Heregulin Activation of Extracellular Acidification in Mammary Carcinoma Cells is Associated with Expression of HER2 and HER3." *J. Biol. Chem.*, **270**: 22608-22613.
- Chang, C.-P., Lazar, C. S., Walsh, B. J., Komuro, M., Collawn, J. F., Kuhn, L. A., Tainer, J. A., Trowbridge, I. S., Farquhar, M. F., Rosenfeld, M. G., Wiley, H. S., and Gill, G. N. (1993). "Ligand-induced Internalization of the Epidermal Growth Factor Receptor is Mediated by Multiple Endocytic Codes Analogous to the Tyrosine Motif Found in Constitutively Internalized Receptors." *Journal of Biological Chemistry*, **268**(26): 19312-19320.
- Chen, W. S., Lazar, C. S., Lund, K. A., Welsh, J. B., Chang, C.-P., Walton, G. M., Der, C. J., Wiley, H. S., Gill, G. N., and Rosenfeld, M. G. (1989). "Functional Independence of the Epidermal Growth Factor Receptor from a Domain Required for Ligand-Induced Internalization and Calcium Regulation." *Cell*, **59**: 33-43.

- Claret, E., Renversez, J. C., Zheng, X., Bonnefoix, T., and Sotto, J. J. (1992). "Valid Estimation of IL-2 Secretion by PHA-stimulated T-cell Clones Absolutely Requires the Use of anti-CD25 Monoclonal Antibodies to Prevent IL-2 Consumption." *Immunol. Lett.*, **33**: 179-186.
- Cohen, S. (1962). "Isolation of a Mouse Submaxillary Gland Protein Accelerating Incisor Eruption and Eyelid Opening in the New-born Animal." *Journal of Biological Chemistry*, **237**(5): 1555-1562.
- Cohen, S., and Ushiro, H. (1980). "Identification of Phosphotyrosine as a Product of Epidermal Growth Factor-activated Protein Kinase in A-431 Cell Membranes." *J. Biol. Chem.*, **255**: 8363-8365.
- Cohen, S., Ushiro, H., Stoschek, C., and Chinkers, M. (1982). "A Native 170,000 Epidermal Growth Factor Receptor-Kinase Complex from Shed Plasma Membrane Vesicles." *J. Biol. Chem.*, **257**: 1523-1531.
- Czech, M. P., Clairmont, D. B., Yagaloff, K. A., and Corvera, S. (1990). "Properties and Regulation of Receptors for Growth Factors." *Peptide Growth Factors and Their Receptors I*, M. B. Sporn and A. B. Roberts, eds., Springer-Verlag, New York, 69-171.
- Davis, R. J. (1988). "Independent Mechanisms Account for the Regulation by Protein Kinase C of the Epidermal Growth Factor Receptor Affinity and Tyrosine-Protein Kinase Activity." *Journal of Biological Chemistry*, **263**(19): 9462-9469.
- DeLarco, J. E., and Todaro, G. (1978). "Growth Factors from Murine Sarcoma Virus-Transformed Cells." *Proc. Natl. Acad. Sci. USA* **75** (8): 4001-4005
- Dempsey, P. J., and Coffey, R. J. (1994). "Basolateral Targeting and Efficient Consumption of Transforming Growth Factor- $\alpha$  When Expressed in Madin-Darby Canine Kidney Cells." *J. Biol. Chem.*, **269**: 16878-16889.
- den Hartigh, J. C., van Bergen en Henegouwen, P. M. P., Verkleij, A. J., and Boonstra, J. (1992). "The EGF Receptor is an Actin-binding Protein." *Journal of Cell Biology*, **119**(2): 349-355.
- Derynck, R., Goeddel, D. V., Ullrich, A., Gutterman, J. U., William, R. D., Bringman, T. S., and Berger, W. H. (1987). "Synthesis of Messenger RNAs for Transforming Growth Factor  $\alpha$  and  $\beta$  and the Epidermal Growth Factor Receptor by Human Tumours." *Cancer Research*, **47**: 707-712.
- Derynck, R. (1992). "The Physiology of Transforming Growth Factor- $\alpha$ ." *Advances in Cancer Research*, **58**: 27-52.
- Divgi, C. R., Welt, S., Kris, M., Real, F. X., Yeh, S. D. J., Gralla, R., Merchant, B., Schweighart, S., Unger, M., Larson, S. M., and Mendelsohn, J. (1991). "Phase I and Imaging Trial of Indium 111-Labeled Anti-Epidermal Growth Factor Receptor Monoclonal Antibody 225 in Patients with Squamous Cell Lung Carcinoma." *J. Natl. Cancer Inst.*, **83**(2): 97-104.
- Downward, J., Parker, P., and Waterfield, M. D. (1984). "Autophosphorylation Sites on the Epidermal Growth Factor Receptor." *Nature*, **311**: 483-485.

- Dunbar, C. E., Browder, T. M., Abrams, J. S., and Nienhuis, A. W. (1989). "COOH-Terminal-Modified Interleukin-3 is Retained Intracellularly and Stimulates Autocrine Growth." *Science*, **245**: 1493-1496.
- Duprez, V., Lenoir, G., and Dautry-Varsat, A. (1985). "Autocrine Growth Stimulation of a Human T-cell Lymphoma Line by Interleukin 2." *Proc. Natl. Acad. Sci. USA*, **82**: 6932-6936.
- Dvorak, H. F. (1986). "Tumors: Wounds That Do Not Heal." *N. Engl. J. Med.*, **315**: 1650-1659.
- Ebner, R., and Derynck, R. (1991). "Epidermal Growth Factor and Transforming Growth Factor- $\alpha$ : Differential Intracellular Routing and Processing of Ligand-Receptor Complexes." *Cell Regulation*, **2**: 599-612.
- Eming, S. A., Snow, R. G., Yarmush, M. L., and Morgan, J. R. (1996). "Targeted Expression of Insulin-like Growth Factor to Human Keratinocytes: Modification of the Autocrine Control of Keratinocyte Proliferation." *J. Invest. Dermatol.*, **107**: 113-120.
- Engler, D. A., Matsunami, R. K., Campion, S. R., Stringer, C. D., Stevens, A., and Niyogi, S. K. (1988). "Cloning of Authentic Human Epidermal Growth Factor as a Bacterial Secretory Protein and Its Initial Structure-Function Analysis by Site-directed Mutagenesis." *Journal of Biological Chemistry*, **263**(25): 12384-12390.
- Ennis, B. W., Valverius, E. M., Bates, S. E., Lippman, M. E., Bellot, F., Kris, R., Schlessinger, J., Masui, H., Goldenberg, A., Mendelsohn, J., and Dickson, R. B. (1989). "Anti-Epidermal Growth Factor Receptor Antibodies Inhibit the Autocrine-Stimulated Growth of MDA-468 Human Breast Cancer Cells." *Mol. Endocrinol.*, **3**: 1830-1838.
- Fabricant, R. N., DeLarco, J. E., and Todaro, G. J. (1977). "Nerve Growth Factor Receptors on Human Melanoma Cells in Culture." *Proc. Natl. Acad. Sci. USA*, **74**(2): 565-569.
- Feild, J. A., Reid, R. H., Rieman, D. J., Kline, T. P., Sathe, G., Greig, R. G., and Anzano, M. A. (1992). "Structure-Function Analysis of Human Transforming Growth Factor- $\alpha$  by Site-Directed Mutagenesis." *Biochem. J.*, **283**: 91-98.
- Filmus, J., Pollak, M. N., Cailleau, R., and Buick, R. N. (1985). "MDA-468, A Human Breast Cancer Cell Line with a High Number of Epidermal Growth Factor (EGF) Receptors, has an Amplified EGF Receptor Gene and is Growth Inhibited by EGF." *Biochemical and Biophysical Research Communications*, **128**(2): 898-905.
- Fontana, J. A., Nervi, C., Shao, Z.-M., and Jetten, A. M. (1992). "Retinoid Antagonism of Estrogen-responsive Transforming Growth Factor alpha and pS2 Gene Expression in Breast Carcinoma Cells." *Cancer Research*, **52**: 3938-3945.
- Forsten, K. E., and Lauffenburger, D. A. (1992a). "Autocrine Ligand Binding to Cell Receptors: Mathematical Analysis of Competition by Solution "decoys"." *Biophys. Journal*, **61**: 518-529.

- Forsten, K. E., and Lauffenburger, D. A. (1992b). "Interrupting Autocrine Ligand-Receptor Binding: Comparison Between Receptor Blockers and Ligand Decoys." *Biophysical Journal*, **63**: 857-861.
- Forsten, K. E., and Lauffenburger, D. A. (1994a). "The Role of Low-Affinity Interleukin-2 Receptors in Autocrine Ligand Binding: Alternative Mechanisms for Enhanced Binding Effect." *Molecular Immunology*, **31**(10): 739-751.
- Forsten, K. E., and Lauffenburger, D. A. (1994b). "Probability of Autocrine Ligand Capture by Cell-Surface Receptors: Implications for Ligand Secretion Measurements." *Journal of Computational Biology*, **1**: 15-23.
- Fowler, K. J., Walker, F., Alexander, W., Hibbs, M. L., Nice, E. C., Bohmer, R. M., Mann, G. B., Thumwood, C., Maglito, R., Danks, J. A., Chetty, R., Burgess, A. W., and Dunn, A. R. (1995). "A Mutation in the Epidermal Growth Factor Receptor in Waved-2 Mice has a Profound Effect on Receptor Biochemistry that Results in Impaired Lactation." *Proc. Natl. Acad. Sci. USA*, **92**: 1465-1469.
- French, A. R., Tadaki, D. K., Niyogi, S. K., and Lauffenburger, D. A. (1995). "Intracellular Trafficking of Epidermal Growth Factor Family Ligands is Directly Influenced by the pH Sensitivity of the Receptor/Ligand Interactions." *J. Biol. Chem.*, **270**(9): 4334-4340.
- Gan, B. S., Hollenberg, M. D., MacCannell, D. L., Lederis, K., Winkler, M. E., and Derynck, R. (1987). "Distinct Vascular Actions of Epidermal Growth Factor-Urogastrone and Transforming Growth Factor- $\alpha$ ." *J. Pharmacol. Exp.*, **242**: 331-337.
- Gill, G. N., and Lazar, C. S. (1981). "Increased Phosphotyrosine Content and Inhibition of Proliferation in EGF-treated A431 Cells." *Nature*, **293**: 305-307.
- Gill, G. N., Bertics, P. J., and Santon, J. B. (1987). "Epidermal Growth Factor and Its Receptor." *Molecular and Cellular Endocrinology*, **51**: 169-186.
- Goishi, K., Higashiyama, S., Klagsbrun, M., Nakano, N., Umata, T., Ishikawa, M., Mekada, E., and Taniguchi, N. (1995). "Phorbol Ester Induces the Rapid Processing of the Cell Surface Heparin-binding EGF-like Growth Factor: Conversion from Juxtacrine to Paracrine Growth Factor Activity." *MBC*, **6**: 967-980.
- Goldstein, B., Posner, R. G., Torney, D. C., Erickson, J., Holowka, D., and Baird, B. (1989). "Competition Between Solution and Cell Surface Receptors for Ligand: Dissociation of Hapten Bound to Surface Antibody in the Presence of Solution Antibody." *Biophysical Journal*, **56**: 955-966.
- Gong, Y., Ballejo, G., Murphy, L. C., and Murphy, L. J. (1992). "Differential Effects of Estrogen and Anti-estrogen on Transforming Growth Factor Gene Expression in Endometrial Adenocarcinoma Cells." *Cancer Research*, **52**: 1704-1709.
- Gossen, M., and Bujard, H. (1992). "Tight Control of Gene Expression in Mammalian Cells by Tetracycline-responsive Promoters." *Proc. Natl. Acad. Sci.*, **89**: 5547-5551.

- Guarnier, F. G., Arterburn, L. M., Penno, M. B., Cha, Y., and August, J. T. (1993). "The Motif Tyr-X-X-hydrophobic Residue Mediates Lysosomal Membrane Targeting of Lysosome-associated Membrane Protein 1." *Journal of Biological Chemistry*, **268**(3): 1941-1946.
- Haddow, A. (1972). "Molecular Repair, Wound Healing, and Carcinogenesis: Tumor Production a Possible Overhealing?" *Adv Cancer Res.*, **16**: 181-234.
- Hamburger, A. W., and Pinnamaneni, G. (1992). "Interferon-Induced Enhancement of Transforming Growth Factor- $\alpha$  Expression in a Human Breast Cancer Cell Line." *Proc. Soc. Exp. Biology Medicine*, **202**: 64-68.
- Heldin, C. H., and Westermark, B. (1990). "Platelet-derived Growth Factor: Mechanism of Action and Possible *in vivo* Function." *Cell Regulation*, **1**: 555-566.
- Hendler, F. J., Richards, C. S., Shum, A., Burns, D., Schaefer, S., and Ozanne, B. (1985). "Nuclear Mechanisms for the Increase of Epidermal Growth Factor Receptor in Squamous Cell Carcinoma." *Trans. Assoc. Am. Phys.*, **98**: 189-197.
- Higashiyama, S., Lau, K., Besner, G. E., Abraham, J. A., and Klagsbrun, M. (1992). "Structure of Heparin-binding EGF-like Growth Factor." *Journal of Biological Chemistry*, **267**(9): 6205-6212.
- Hoeprich, P. D., Langton, B. C., Zhang, J.-w., and Tam, J. P. (1989). "Identification of Immunodominant Regions of Transforming Growth Factor alpha." *Journal of Biological Chemistry*, **264**(32): 19086-19091.
- Holmes, W. E., Sliwkowski, M. X., Akita, R. W., Henzel, W. J., Lee, J., Park, J. W., Yansura, D., Abadi, N., Raab, H., Lewis, G. D., Shepard, H. M., Kuang, W.-J., Wood, W. I., Goeddel, D. V., and Vandlen, R. L. (1992). "Identification of Heregulin, a specific Activator of p185<sup>erbB2</sup>." *Science*, **258**: 1205-1210.
- Honegger, A. M., Dull, T. J., Felder, S., Obberghen, E. V., Bellot, F., Szapary, D., Schmidt, A., Ullrich, A., and Schlessinger, J. (1987). "Point Mutation at the ATP Binding Site of EGF Receptor Abolishes Protein-Tyrosine Kinase Activity and Alters Cellular Routing." *Cell*, **51**: 199-209.
- Huang, A. L., Ostrowski, M. C., Berard, D., and Hagar, G. L. (1981). "Glucocorticoid Regulation of the Ha-MuSV p21 Gene Conferred by Sequences from Mouse Mammary Tumor Virus." *Cell*, **27**: 245-255.
- Kawano, M., Hirano, T., Matsuda, T., Taga, T., Horii, Y., Iwato, K., Asaoku, H., Tang, B., Tanabe, O., Tanaka, H., Kuramoto, A., and Kishimoto, T. (1988). "Autocrine Generation and Requirement of BSF-2/IL-6 for Human Multiple Myelomas." *Nature*, **332**: 83-85.
- Keating, M. T., and Williams, L. T. (1988). "Autocrine Stimulation of Intracellular PDGF Receptors in v-sis-transformed Cells." *Science*, **239**: 914-916.
- Kern, J. A., Schwartz, D. A., Nordberg, J. E., Weiner, D. B., Greene, M. I., Torney, L., and Robinson, R. A. (1990). "p185<sup>neu</sup> Expression in Human Lung Adenocarcinomas Predicts Shortened Survival." *Cancer Res.*, **50**: 5184-5187.

- King, C. R., Kraus, M. H., and Aaronson, S. A. (1985). "Amplification of a Novel v-erbB-related Gene in a Human Mammary Carcinoma." *Science*, **229**: 974-976.
- Knauer, D. J., Wiley, H. S., and Cunningham, D. D. (1984). "Relationship between Epidermal Growth Factor Receptor Occupancy and Mitogenic Response." *Journal of Biological Chemistry*, **259**(2): 5623-5631.
- Kobrin, M. S., Samsodar, J., and Kudow, J. E. (1988). "Transforming Growth Factor- $\alpha$  Secreted by Untransformed Bovine Anterior Pituitary Cells in Culture: Identification Using a Sequence-Specific Monoclonal Antibody." *Cancer Res.*, **50**: 5184-5187.
- Kraus, M. H., Popescu, N. C., Amsbaugh, S. C., and King, R. C. (1987). "Overexpression of the EGF Receptor-Related Proto-Oncogene erbB-2 in Human Mammary Tumor Cell Lines by Different Molecular Mechanisms." *EMBO*, **8**(3): 167-172.
- Kraus, M. H., Issing, W., Miki, T., Popescu, N. C., and Aaronson, S. A. (1989). "Isolation and Characterization of ErbB3, a Third Member of the ErbB/Epidermal Growth Factor Receptor Family: Evidence for Overexpression in a Subset of Human Mammary Tumors." *Proc. Natl. Acad. Sci. USA*, **86**: 9193-9197.
- Kriegler, M. (1990). *Gene Transfer and Expression - A Laboratory Manual*, W.H. Freeman and Company, New York.
- Kumar, V., Cotran, R. S., and Robbins, S. L. (1992). *Basic Pathology*, W.B. Saunders Co., Philadelphia.
- Kurten, R. C., Cadena, D. L., and Gill, G. N. (1996). "Enhanced Degradation of EGF Receptors by a Sorting Nexin, SNX1." *Science*, **272**: 1008-1010.
- Lauffenburger, D., and Cozens, C. (1989). "Regulation of Mammalian Cell Growth by Autocrine Growth Factors: Analysis of Consequences for Inoculum Cell Density Effects." *Biotechnology and Bioengineering*, **33**: 1365-1378.
- Lax, I., Johnson, A., Hawk, R., Snap, J., Bellot, F., Winkler, M., Ullrich, A., Vennstrom, B., Schlessinger, J., and Givol, D. (1988a). "Chicken Epidermal Growth Factor (EGF) Receptor: cDNA Cloning, Expression in Mouse Cells, and Differential Binding of EGF and Transforming Growth Factor Alpha." *Mol. Cell. Biol.*, **8**: 1970-1978.
- Lee, F., Mulligan, R., Berg, P., and Ringold, G. (1981). "Glucocorticoids Regulate Expression of Dihydrofolate Reductase cDNA in Mouse Mammary Tumor Virus Chimeric Plasmids." *Nature* **294**: 228-232.
- Luetkeke, N. C., Phillips, H. K., Qui, T. H., Copeland, N. G., Earp, H. S., Henkins, N. A., and Lee, D. C. (1994). "The Mouse waved-2 Phenotype Results from a Point Mutation in the EGF Receptor Tyrosine Kinase." *Genes and Development*, **8**: 399-413.
- Lund, K. A., Lazar, C. S., Chen, W. S., Walsh, B. J., Welsh, J. B., Herbst, J. J., Walton, G. M., Rosenfeld, M. G., Gill, G. N., and Wiley, H. S. (1990). "Phosphorylation of the Epidermal Growth Factor Receptor at Threonine 654 Inhibits Ligand-induced Internalization and Down-regulation." *Journal of Biological Chemistry*, **265**(33): 20517-20523.



- Madtes, D. K., Raines, E. W., Sakariassen, K. S., Assoian, R. K., Sporn, M. B., Bell, G. I., and Ross, R. (1988). "Induction of Transforming Growth Factor- $\alpha$  in Activated Human Alveolar Macrophages." *Cell*, **53**: 285-293.
- Mansbridge, J. N., Knuchel, R., Knapp, A. M., and Sutherland, R. M. (1992). "Importance of Tyrosine Phosphatase in the Effects of Cell-Cell Contact and Microenvironments on EGF-Stimulated Tyrosine Phosphorylation." *Journal of Cellular Physiology*, **151**: 433-442.
- McConnell, H. M., Owicki, J. C., Parce, J. W., Miller, D. L., Baxter, G. T., Wada, H. G., and Pitchford, S. (1992). "The Cytosensor Microphysiometer: Biological Applications of Silicon Technology." *Science*, **257**: 1906-1912.
- McNeill, J., Sanchez, A., Gray, P. P., Chesterman, C. N., and Sleigh, M. J. (1989). "Hyper-inducible Gene Expression from a Metallothionein Promoter Containing Additional Metal-Responsive Elements." *Gene*, **76**: 81-88.
- Mendelsohn, J., Masui, H., and Goldenberg, A. (1987). "Anti-Epidermal Growth Factor Receptor Monoclonal Antibodies May Inhibit A431 Tumor Cell Proliferation by Blocking an Autocrine Pathway." *Transactions of the Association of American Physicians*, **100**: 173-178.
- Meyer-Ingold, W. (1993). "Wound Therapy: Growth Factors as Agents to Promote Healing." *TIBTECH*, **11**: 387-392.
- Modjtahedi, H., Eccles, S. A., Box, G., Styles, J., and Dean, C. J. (1993a). "Antitumor Activity of Combinations of Antibodies Directed Against Different Epitopes on the Extracellular Domain of the Human EGF Receptor." *Cell Biophysics*, **22**: 129-146.
- Modjtahedi, H., Styles, J., and Dean, C. (1993b). "The Growth Response of Human Tumour Cells Lines Expressing the EGF receptor to Treatment with EGF and / or Mabs that Block Ligand Binding." *International Journal of Oncology*, **3**: 237-243.
- Modjtahedi, H., and Dean, C. (1994). "The Receptor for EGF and its Ligands: Expression, Prognostic Value and Target for Therapy in Cancer." *International Journal of Oncology*, **4**: 277-296.
- Molecular Devices Corp. (1994). "Using the Cytosensor Microphysiometer for Signal Transduction." *0120-1016A*.
- Moolenaar, W. H., Bierman, A. J., Tilly, B. C., Verlaan, I., Defize, L. H. K., Honegger, A. M., Ullrich, A., and Schlessinger, J. (1988). "A Point Mutation at the ATP-binding Site of the EGF-receptor Abolishes Signal Transduction." *EMBO*, **7**(3): 707-710.
- Moreau, P., Hen, R., Wasyluk, B., Everett, R., Gaub, M. P., and Chambon, P. (1981). "The SV40 Base-Repair Repeat has a Striking Effect on Gene Expression both in SV40 and Other Chimeric Recombinants." *Nucl. Acids Res.*, **9** (22): 6047-6068.
- Morishige, K.-i., Kurachi, H., Amemiya, K., Adachi, H., Inoue, M., Miyake, A., Tanizawa, O., and Sakoyama, Y. (1991). "Involvement of Transforming Growth Factor  $\alpha$  / Epidermal Growth Factor Receptor Autocrine Growth Mechanism in an Ovarian Cancer Cell Line in Vitro." *Cancer Research*, **51**: 5951-5955.

- Mulshine, J. L., Shuke, N., Daghighian, F., Carrasquillo, J., Ghosh, B., Walsh, T., Avis, I., Reynolds, J. C., Cuttitta, F., and Larson, S. M. (1992). "The Correct Dose: Pharmacologically Guided End Point for Anti-Growth Factor Therapy." *Cancer Research*, **52**: 2743s-2746s.
- Niitsu, Y., Urushizaki, Y., Koshida, Y., Terui, K., Mahara, K., Kohgo, Y., and Urushizaki, I. (1988). "Expression of TGF-beta Gene in Adult T Cell Leukemia." *Blood*, **71**: 263-266.
- Okunji, C. O., Iwu, M. M., Jackson, J. E., and Tally, J. D. (1996). "Biological Activity of Saponins from Two *Dracaena* Species." *Adv. Exp. Med. Biol.*, **404**: 415-428.
- Opresko, L. K., Chang, C.-P., Will, B. H., Burke, P. M., Gill, G. N., and Wiley, H. S. (1995). "Endocytosis and Lysosomal Targeting of Epidermal Growth Factor Receptors Are Mediated by Distinct Sequences Independent of the Tyrosine Kinase Domain." *Journal of Biological Chemistry*, **270**(9): 4325-4333.
- Owicki, J. C., Parce, J. W., Kersco, K. M., Sigal, G. B., Muir, V. C., Venter, J. C., Fraser, C. M., and McConnell, H. M. (1990). "Continuous Monitoring of Receptor-mediated Changes in the Metabolic Rates of Living Cells." *Proc. Natl. Acad. Sci. USA*, **87**: 4007-4011.
- Palmiter, R. D., Chen, H. Y., and Brinster, R. L. (1982). "Differential Regulation of Metallothionein-Thymidine Kinase Fusion Genes in Transgenic Mice and Their Offspring." *Cell*, **29**: 701-710.
- Pandiella, A., Bosenberg, M. W., Huang, E. J., Besmer, P., and Massague, J. (1992). "Cleavage of Membrane-anchored Growth Factors Involves Distinct Protease Activities Regulated through Common Mechanisms." *Journal of Biological Chemistry*, **267**(33): 24028-24033.
- Parce, J. W., Owicki, J. C., Kercso, K. M., Sigal, G. B., Wada, H. G., Muir, V. C., Bousse, L. J., Ross, K. L., Sikic, B. I., and McConnell, H. M. (1989). "Detection of Cell-Affecting Agents with a Silicon Biosensor." *Science*, **246**: 243-247.
- Pawson, T., and Schlessinger, J. (1993). "SH2 and SH3 Domains." *Current Biology*, **3**(7): 434-444.
- Pierce, J. H., Ruggiero, M., Fleming, T. P., Di Fiore, P. P., Greenberger, J. S., Varticovski, L., Schlessinger, J., Rovera, G., and Aaronson, S. A. (1988). "Signal Transduction through the EGF Receptor Transfected in IL-3-dependent Hematopoietic Cells." *Science*, **239**: 628-631.
- Pitchford, S., Moor, K. D., and Glaeser, B. S. (1995). "Nerve Growth Factor Stimulates Rapid Metabolic Responses in PC12 Cells." *Am. J. Physiol.*, **268**(Cell Physiol. 37): c936-c943.
- Plowman, G. D., Culouscou, J. M., Whitney, G. S., Green, J. M., Carlton, G. W., Foy, L., Neubauer, M. G., and Shoyab, M. (1993a). "Ligand-Specific Activation of HER4/p180<sup>erbB4</sup>, a Fourth Member of the Epidermal Growth Factor Receptor Family." *Proc. Natl. Acad. Sci. USA*, **90**: 1746-1750.

- Plowman, G. D., Green, J. M., Culouscou, J.-M., Carlton, G. W., Rothwell, V. M., and Buckley, S. (1993b). "Heregulin Induces Tyrosine Phosphorylation of HER4/p180<sup>erbB4</sup>." *Nature*, **366**: 473-475.
- Puddicombe, S. M., Chamberlain, S. G., MacGarvie, J., Richter, A., Drummond, D. R., Collins, J., Woods, L., and Davies, D. E. (1996). "The Significance of Valine 33 as a Ligand-specific Epitope of Transforming Growth Factor Alpha." *J. Biol. Chem.*, **271**: 15367-15372.
- Rappolee, D. A., Mark, D., Banda, M. J., and Werb, Z. (1988a). "Wound Macrophages Express TGF $\alpha$  and Other Growth Factors *in vivo*: Analysis by mRNA Phenotyping." *Science*, **241**: 708-712.
- Reddy, C. C., Niyogi, S. K., Wells, A., Wiley, H. S., and Lauffenburger, D. A. (1996). "Engineering Epidermal Growth Factor for Enhanced Mitogenic Potency." *Nature Biotechnology*, **14**: 1696-1699.
- Reiss, M., Stash, E. B., Vellucci, V. F., and Zhou, Z.-l. (1991). "Activation of the Autocrine Transforming Growth Factor  $\alpha$  Pathway in Human Squamous Carcinoma Cells." *Cancer Research*, **51**: 6254-6262.
- Renschler, M. F., Wada, H. G., Fok, K. S., and Levy, R. (1995). "B-lymphoma Cells are Activated by Peptide Ligands of the Antigen Binding Receptor or by Anti-Idiotypic Antibody to Induce Extracellular Acidification." *Cancer Res.*, **55**: 5642-5647.
- Richter, A., Drummond, D. R., MacGarvie, J., Puddicombe, S. M., Chamberlain, S. G., and Davies, D. E. (1995). "Contribution of the Transforming Growth Factor  $\alpha$  B-loop  $\beta$ -sheet to Binding and Activation of the Epidermal Growth Factor Receptor." *Journal of Biological Chemistry*, **270**(4): 1612-1616.
- Roberts, A. B. "Progress in Basic Research of Wound Repair and Its Application to Clinical Management of Problematic Wounds." *Keystone Symposium*, Breckenridge, Co.
- Rodeck, U., Williams, N., Murthy, U., and Herlyn, M. (1990). "Monoclonal Antibody 425 Inhibits Growth Stimulation of Carcinoma Cells by Exogenous EGF and Tumor-Derived EGF/TGF $\alpha$ ." *Journal of Cellular Biochemistry*, **44**: 69-79.
- Scatchard, G. (1949). "The Attractions of Proteins for Small Molecules and Ions." *Ann. N. Y. Acad. Sci.*, **53**: 660-672.
- Scott, J., Urdea, M., Quiroga, M., Sanchez-Pescador, R., Fong, N., Selby, M., Rutter, W. J., and Bell, G. I. (1983). "Structure of a Mouse Submaxillary Messenger RNA Encoding Epidermal Growth Factor and Seven Related Proteins." *Science*, **221**: 236-240.
- Sellheyer, K. J., Bickenbach, J. R., Rothnagel, J. A., Bundman, D., Longley, M. A., Krieg, T., Roche, N. S., Roberts, A. B., and Roop, D. R. (1993). "Inhibition of Skin Development by Overexpression of Transforming Growth Factor  $\beta$ 1 in the Epidermis of Transgenic Mice." *Proc. Natl. Acad. Sci. USA*, **90**: 5237-5241.
- Shing, T., Christofori, G., Hanahan, D., Ono, Y., Sasada, R., Igarashi, K., and Folkman, J. (1993). "Betacellulin: A Mitogen from Pancreatic B Cell Tumors." *Science*, **259**: 1604-1607.

- Shoyab, M., Plowman, G. D., McDonald, V. L., Bradley, J. G., and Todaro, G. J. (1989). "Structure and Function of Human Amphiregulin: A Member of the Epidermal Growth Factor Family." *Science*, **243**: 1074-1076.
- Slamon, D. J., Clark, G. M., Wong, S. G., Levin, W. J., Ullrich, A., and McGuire, R. L. (1987). "Human Breast Cancer: Correlation of Relapse and Survival with Amplification of the HER-2/neu Oncogene." *Science*, **244**(4785): 177-182.
- Slamon, D. J., Godolphin, W., Jones, L. A., Holt, J. A., Wong, S. C., Keith, D. E., Levin, W. J., and Stuart, S. G. (1989). "Studies of the HER-2/neu Proto-Oncogene in Human Breast and Ovarian Cancer." *Science*, **244**(4905): 707-712.
- Smith, K. A. (1990). "Interleukin-2." *Scientific American*(March): 50-57.
- Sporn, M. B., and Todaro, G. J. (1980). "Autocrine Secretion and Malignant Transformation of Cells." *New England Journal of Medicine*, **303**(15): 878-880.
- Sporn, M. B., and Roberts, A. B. (1986). "Peptide Growth Factors and Inflammations, Tissue Repair, and Cancer." *J. Clin. Invest.*, **78**: 329-332.
- Sporn, M. B., and Roberts, A. B. (1992). "Autocrine Secretion - 10 Years Later." *Annals of Internal Medicine*, **117**(5): 408-414.
- Stern, P. H., Krieger, N. S., Nissenson, R. A., Williams, R. D., Winkler, M. E., Derynck, R., and Strewler, G. J. (1985). "Human Transforming Growth Factor-alpha Stimulated Bone Resorption *in vitro*." *J. Clin. Invest.*, **76**: 2016-2019.
- Sun, L. Z., Wu, S. P., Ziober, B. L., and Brattain, M. B. (1994). "Role of Autocrine Growth Factors in Cancer Cells." *Biochemical and Molecular Aspects of Selected Cancers*, **2**: 495-519.
- Technical Support. (1995). "Anti-human TGF $\alpha$  Neutralizing Antibody." R&D Systems, Minneapolis, MN. *Support Specifications*, 12/12/95
- ten Dijke, P., and Iwata, K. K. (1989). "Growth Factors for Wound Healing." *Bio/Technology*, **7**: 793-798.
- Threadgill, D. W., Dlugosz, A. A., Hansen, L. A., Tennenbaum, T., Lichti, U., Yee, D., LaMantia, C., Mourton, T., Herrup, K., Harris, R. C., Barnard, J. A., Yuspa, S. H., Coffey, R. J., and Magnuson, T. (1995). "Targeted Disruption of Mouse EGF Receptor: Effect of Genetic Background on Mutant Phenotype." *Science*, **269**: 230-234.
- Todaro, G. J., Fryling, C., and DeLarco, J. E. (1980). "Transforming Growth Factors Produced by Certain Human Tumor Cells: Polypeptides that Interact with Epidermal Growth Factor Receptors." *Proc. Natl. Acad. Sci. USA*, **77**(9): 5258-5262.
- Tsao, M.-S., Zhu, H., and Viallet, J. (1996). "Autocrine Growth Loop of the Epidermal Growth Factor Receptor in Normal and Immortalized Human Bronchial Epithelial Cells." *Experimental Cell Research*, **223**: 268-273.

- Ullrich, A., Coussens, L., Hayflick, J. S., Dull, T. J., Gray, A., Tam, A. W., Lee, J., Yarden, Y., Libermann, T. A., Schlessinger, J., Downward, J., Mayes, E. L. V., Whittle, N., Waterfield, M. D., and Seeburg, P. H. (1984). "Human Epidermal Growth Factor Receptor cDNA Sequence and Aberrant Expression of the Amplified Gene in A431 Epidermoid Carcinoma Cells." *Nature*, **309**: 418-425.
- Valverius, E. M., Bates, S. E., Stampfer, M. R., Clark, R., McCormick, F., Salomon, D. S., Lippman, M. E., and Dickson, R. B. (1989). "Transforming Growth Factor alpha Production and Epidermal Growth Factor Receptor Expression in Normal and Oncogene Transformed Human Mammary Epithelial Cells." *Molecular Endocrinology*, **3**(1): 203-214.
- van der Vijver, M. J., van der Bersselaar, R., Devilee, P., Cornelisse, C., Peterse, J., and Nusse, R. (1987). "Amplification of the Neu(c-erbB-2) Oncogene in Human Mammary Tumors is Relatively Frequent and is often Accompanied by Amplification of the Linked c-erbA Oncogene." *Mol. Cell. Biol.*, **7**(5): 2019-2023.
- van der Vijver, M. J., Kumar, R., and Mendelsohn, J. (1991). "Ligand-induced Activation of A431 Cell Epidermal Growth Factor Receptors Occurs Primarily by an Autocrine Pathway that acts upon Receptors on the Surface rather than Intracellularly." *Journal of Biological Chemistry*, **266**(12): 7503-7508.
- Wang, H. M., and Smith, K. A. (1987). "The Interleukin 2 Receptor Functional Consequences of its Biomolecular Structure." *J. Exp. Med.*, **166**: 1055-1069.
- Varley, J. M., Swallow, J. E., Brammar, W. J., Whittaker, J. L., and Walker, R. A. (1987). "Alterations to Either c-erbB-2(Neu) or c-Myc Proto-Oncogenes in Breast Carcinomas Correlate with Poor Short-term Prognosis." *Oncogene*, **1**(3): 423-430.
- Vassar, R., and Fuchs, E. (1991). "Transgenic Mice Provide New Insights into the Role of TGF- $\alpha$  During Epidermal Development and Differentiation." *Genes and Development*, **5**: 714-727.
- Wen, D., Peles, E., Cupples, R., Suggs, S. V., Bacus, S. S., Luo, Y., Trail, G., Hu, S., Silbiger, S. M., Levy, R. B., Koski, R. A., Lu, H. S., and Yarden, Y. (1992). "Neu Differentiation Factor: A Transmembrane Glycoprotein Containing an EGF Domain and an Immunoglobulin Homology Unit." *Cell*, **69**: 559-572.
- Wigler, M., Pellicer, A., Silverstein, S., Axel, R., Urlaub, G., and Chasin, L. (1979). "DNA-mediated Transfer of the Adenine Phosphoribosyltransferase Locus into Mammalian Cells." *Proc. Natl. Acad. Sci. USA*, **76**(3): 1373-1376.
- Wilcox, J. N., and Derynck, R. (1988b). "Localization of Cells Synthesizing Transforming Growth Factor-alpha mRNA in the Mouse Brain." *J. Neurosci.*, **8**: 1901-1904.
- Wiley, H. S., Herbst, J. J., Walsh, B. J., Lauffenburger, D. A., Rosenfeld, M. G., and Gill, G. N. (1991). "The Role of Tyrosine Kinase Activity in Endocytosis Compartmentation, and Down-regulation of the Epidermal Growth Factor Receptor." *Journal of Biological Chemistry*, **266**(17): 11083-11094.
- Wiley, L. M., Adamson, E. D., and Tsark, E. C. (1995). "Epidermal Growth Factor Receptor Function in Early Mammalian Development." *BioEssays*, **17**(10): 839-846.

- Will, B. H., Lauffenburger, D. A., and Wiley, H. S. (1995). "Studies on Engineered Autocrine Systems: Requirements for Ligand Release from Cells Producing an Artificial Growth Factor." *Tissue Engineering*, **1**(1): 81-95.
- Wong, H. L., and Wahl, S. M. (1991). "Inflammation and Repair." *Peptide Growth Factors and Their Receptors I*, M. B. Sporn and A. B. Roberts, eds., Springer-Verlag, New York, 509-548.
- Yamada, Y., and Serrero, G. (1988). "Autocrine Growth Induced by the Insulin-related Factor in the Insulin-independent Teratoma Cell Line 1246-3A." *Proc. Natl. Acad. Sci. USA*, **85**: 5936-5940.
- Yarden, Y., and Schlessinger, J. (1987). "Self-Phosphorylation of Epidermal Growth Factor Receptor: Evidence for a Model of Intermolecular Allosteric Activation." *Biochemistry*, **26**: 1434-1442.
- Yoshida, K., Kyo, E., Tsuda, T., Tsujino, T., Ito, M., Niimoto, M., and Tahara, E. (1990). "EGF and TGF $\alpha$ , the Ligands of Hyperproduced EGFR in Human Esophageal Carcinoma Cells, act as Autocrine Growth Factors." *Int. J. Cancer*, **45**: 131-135.
- Zhang, K., Sun, J., Liu, N., Wen, D., Chang, D., Thomason, A., and Yoshinaga, S. K. (1996). "Transformation of NIH 3T3 Cells by HER3 or HER4 Receptors requires the Presence of HER1 or HER2." *J. Biol. Chem.*, **271**: 3884-3890.